2011

AN INVESTIGATION INTO USE OF THE FRESHWATER GASTROPOD VIVIPARUS AS A RECORDER OF PAST CLIMATIC CHANGE

BUGLER, MELANIE JANE

AN INVESTIGATION INTO USE OF THE FRESHWATER GASTROPOD *VIVIPARUS* AS A RECORDER OF PAST CLIMATIC CHANGE

By

MELANIE JANE BUGLER

A thesis submitted to the University of Plymouth

in partial fulfilment for the degree of

DOCTOR OF PHILOSOPHY

School of Geography, Earth, & Environmental Sciences,

Faculty of Science

JANUARY 2011

ABSTRACT:

AN INVESTIGATION INTO USE OF THE FRESHWATER GASTROPOD *VIVIPARUS* AS A RECORDER OF PAST CLIMATIC CHANGE

MELANIE JANE BUGLER

Through isotopic analysis of *Viviparus lentus* (*V. lentus*) a high resolution record of stepwise changes in $\delta^{18}O$ and $\delta^{13}C$ across the Eocene / Oligocene transition and Oi-1 glacial maximum has been produced for the continental Solent Group strata, Isle of Wight (UK). Comparison of this *V. lentus* $\delta^{18}O_{carb.}$ record with high resolution marine $\delta^{18}O_{carb.}$ records shows that similar isotopic shifts exist in the near coastal continental and marine realms. In order to calculate palaeotemperatures from this new continental record an investigation into the biology of modern *Viviparus* and its effect on the isotopic composition of its shell carbonate was undertaken. Experimental measurements of the $^{18}O/^{16}O$ isotope fractionation between the biogenic aragonite of *Viviparus* and its host freshwater were undertaken on samples derived from the Somerset Levels in order to generate a genus specific thermometry equation. The results from using this new *Viviparus* equation on fossil *V. lentus* shell fragments suggests that aquatic and terrestrial biota were being affected by climate change associated with the Late Eocene Event. This coincides with a decrease in mammal species richness in the Osborne Member, reaching its climax at the end of the Osborne / Seagrove Bay Members. This event is followed by a brief warming in the Bembridge Limestone which was marked by a within-Europe mammal turnover involving dispersal from the south and an increase in species richness, concurrent with this is an increase in size of *Harrisichara* gyrogonites.

An additional investigation into seasonal isotopic variability using whole well preserved *V. lentus* specimens has also revealed a shift from tropical /subtropical to temperate climatic zones occurring before the Eocene /Oligocene boundary and Oi-1 glacial maximum. Overall the evidence provided by these investigations would suggest that climatic change was already in progress prior to the build up of glacial ice on Antarctica.

LIST OF CONTENTS

LIST OF FIGURES

LIST OF TABLES

List of Equations

ACKNOWLEDGEMENTS

Firstly I would like to thank my supervisors Dr Stephen Grimes, Dr Gregory Price, Dr Jerry Hooker, and Prof. Margaret Collinson for their help, supervision, advice, criticism and discussion over the past three years.

I would like to thank the National Trust for access and permission to collect samples from various locations on the Isle of Wight and to Mr and Mrs Cool for parking and access to Hamstead Ledge. For his help, advice and assistance in running the IRMS I would like to thank Dr Paul Sutton. For their assistance and advice I would like to thank the Geology technicians at the University of Plymouth. For assistance with field collection for the modern gastropod specimens I am grateful to Dr Stephen Grimes, Dr Simon Rundle, Dr Charu Sharma, Dr Timothy Kearsey and Dr Laura Domingo Martıńez. For help with setting up of culturing tanks, we would like to thank Dr Simon Rundle and the Ecology technicians at Plymouth University. For their help and assistance in the analysis of isotopic samples, I would also like to thank Prof. Melanie Leng and the technical staff at NIGL. For their assistance and advice on XRD analysis I would like to thank Dr Dave Alderton from RHUL and Peter Davis from the University of Plymouth. I would like to thank Dr Mathieu Daëron and Prof. John Eiler for their assistance and analysis of the clumped isotope analysis.

I would also like to thank the University of Plymouth for funding my PhD, the NERC Isotope Geosciences Facilities Steering Committee (NIGFSC) for providing analytical training and the isotopic analysis of modern gastropod samples, and the Natural Environment Research Council (NERC) IODP for funding my attendance to the Past Global Change Reconstruction and Modelling Techniques / Summer School in Paleoclimatology.

AUTHORS DECLARATION

At no time during the registration for the degree of Doctor of Philosophy had the author been registered for any other University award without prior agreement of the Graduate Committee.

This study was financed with the aid of a studentship from the University of Plymouth. Analytical training and the isotopic analysis of modern gastropod samples was funded by the NERC Isotope Geosciences Facilities Steering Committee (NIGFSC) (November 2007).

Relevant scientific seminars and conferences were attended at which work was often presented; external institutions were visited for consultation purposes and papers prepared for publication. A grant from the Natural Environment Research Council (NERC) IODP directed programme was awarded to the author for attendance to the Past Global Change Reconstruction and Modelling Techniques / Summer School in Paleoclimatology. July 18th to August 3rd, 2007, Urbino, Italy.

Publications:

- Bugler, M., Grimes, S.T., Leng, M.J., Rundle, S.D., Price, G.D., Hooker, J.J. & Collinson, M.E. 2009. Experimental determination of a *Viviparus contectus* thermometry equation. Rapid Communication in Mass Spectrometry 23(18):2939-51.

Presentations and conferences attended:

- Bugler, M.J., Grimes, S.T., Price, G.D., Smart, C.W., Hooker, J.J. & Collinson, M.E., 2010. An investigation into the use of the freshwater gastropod *Viviparus* as a recorder of past climatic change. Ussher Society Conference, 2010.

- Bugler, M.J., Grimes, S.T., Hooker, J. J., Collinson, M.E., Price, G.D. & Smart, C.W. 2009. The first high resolution continental $\delta^{18}O$ isotopic record demonstrating a 'stepwise' transition into Oligocene icehouse conditions. Vol. 11, EGU2009-1117-5, EGU General Assembly 2009.
- Bugler, M.J., Grimes, S.T., Price, G.D., Smart, C.W., Hooker, J.J. & Collinson, M.E. 2008. A palaeoclimatic study of the Eocene/Oligocene transition on the Isle of Wight, Hampshire Basin, UK Geophysical Research Abstract, Vol. 10, EGU2008-A-00000, EGU General Assembly 2008.
- Bugler, M., Grimes, S.T., Price, G.D., Smart, C.W., Hooker, J.J., Collinson, M.E., 2007. A palaeoclimatic study of the Eocene/Oligocene transition on the Isle of Wight, Hampshire Basin, UK. BSRG, University of Birmingham, 2007.
- Bugler. M. 2007. Is seasonal climate variability a key factor in biotic extinctions? (Departmental seminar).
- Bugler. M. 2006. 'Sedimentation and sea-level history of the Avon Estuary, Devon' at the Young Geoscientist Presentation 2006, (South west Regional Group of the Geological Society).

Word count of main body of thesis: 65,328 words

Signed...M. Bugler.....

Date .29/.3/..2011.

CHAPTER 1 : INTRODUCTION

1.1 Why is it important to study climate change?

Over the last decade 'climate change' has become an important topic, particularly significant in political and economical terms. Our understanding of past climates has moved forward considerably in recent years, propelled by significant advancements in our knowledge, aided by pioneering techniques in the assessment of palaeoclimatic data and climate reconstructions. Although uncertainties remain, the constant addition of new and revised palaeoclimatic data allows us to re-examine and refine how the climate system has responded to large changes in climate forcing in the past.

An important source of information about past climatic change is preserved within the calcium carbonate remains of organisms which geochemically record climate induced changes (e.g. foraminifera (Shackleton, & Opdyke, 1973; Coxall *et al.*, 2005; Lear *et al.*, 2008), molluscs (Kobashi *et al.*, 2001; Hansen *et al.*, 2004), and nanoplankton (Villa *et al.*, 2008)). These proxy data can be incorporated into or used to test how well climate model simulations can reconstruct changes in the climate system over inter-annual to millennial time scales. They can also be used to test physical hypotheses quantitatively in order to understand the mechanisms involved in past and potentially future climate change. Developing a quantitative understanding of the mechanisms involved is the most effective way to learn from past climates (Jansen *et al.*, 2007). These continual improvements are useful in assessing how the same climate system might respond to the large anticipated changes in the future (Jansen *et al.*, 2007).

Current predictions from the Intergovernmental Panel on Climate Change (IPCC) (Solomon, 2007) suggest that:

- Global mean surface temperatures will continue to rise (0.2°C per decade). This warming will show the greatest temperature increase at high northern latitudes and over land.
- Precipitation will generally increase in the tropical precipitation maxima, decrease in the subtropics and increase at high latitudes as a consequence of a general intensification of the global hydrological cycle. Estimates suggest a high latitude increase of 20% (including Eastern Africa, Central Asia and Equatorial Pacific Ocean). Heavy precipitation events will become more common.
- Snow cover and sea ice extent will decrease; glaciers and ice caps lose mass and contribute to sea level rise. Sea ice extent will decrease in the 21st Century in both the Arctic and Antarctic. For example by the end of the 21st Century annual Northern Hemisphere snow cover will be reduced by 9 to 17% with a shortened snow cover season. Snow cover reduction will be accelerated in the Arctic by positive feedbacks and widespread increases in thaw depth occurring over much of the permafrost regions.
- Heat waves will become more frequent and longer lasting in a future warmer climate. The greatest intensity increase will occur in Western Europe, Mediterranean region and southeast and western USA. Decreases in frost days are projected to occur almost everywhere in the mid-high latitudes, with an increase in growing season length. There is a tendency for summer drying of the mid-continental areas during summer, indicating a greater risk of droughts in those regions.
- Sea level will continue to rise in the 21st century because of thermal expansion and loss of land ice. Estimates in the range of 0.18 to 0.59 m increase by the end of the 21st Century (average rise of 3.8 mm/yr).

A full understanding of both cooling and warming events and their associated mechanisms and feedbacks is required in order to produce reliable models for future climatic predictions. Abrupt climate change is a rapidly advancing area of climate research. These changes are where a forced or unforced climatic change involves crossing a threshold into a new climate regime (e.g. new mean state or character of variability), often where the transition time to the new regime is short relative to the duration of the regime (Rahmstorf, 2001; Alley *et al.*, 2003; Overpeck and Trenberth, 2004). A geological example of abrupt climate change is the first Oligocene glacial maximum (Oi-1), occurring just after the Eocene / Oligocene (E/O) boundary (~33.7Ma). Although the build up to this event was gradual the final transition from a greenhouse to icehouse world is thought to be relatively abrupt in nature. This event provides a suitable example of climate change between two distinct climatic regimes.

To produce a robust investigation into climate changes across the E/O transition and Oi-1 glaciation an investigation into both modern and fossil specimens of the freshwater gastropod *Viviparus* (the carbonate proxy chosen for the study) has been undertaken.

Therefore, the thesis structure has been divided into two parts:

- Part 1 (Chapters 2 to 5):
  - A modern investigation into the biology of *Viviparus* and its effect on the isotopic composition of its shell carbonate. Including experimental analysis of the methods used to calculate palaeotemperatures.
- Part 2 (Chapters 6 and 7):
  - Using the information gained from Part 1 a high resolution isotopic and temperature record has been produced from the analysis of *Viviparus lentus* (Solander) shell fragments across the E/O transition and Oi-1 glaciation from the Solent Group strata, Isle of Wight (Hampshire Basin, U.K).

- An investigation into seasonal isotopic variability has been carried out to investigate whether variability in the seasonal isotopic record obtained was responsible for the observed shift in the isotopic record produced in Part 2.

1.2 Oi-1 Glaciation

During the Cenozoic conditions existed that allowed the formation of permanent continental scale ice caps on Antarctica (Miller *et al.*, 1991; Zachos *et al.*, 1996; Zachos *et al.*, 2001). Long-term cooling commenced after the Early Eocene Climatic Optimum (EECO)(55 to 50 Ma), culminating in the Oi-1 glacial maximum (~33.7 Ma) (Miller *et al.*, 1991; Zachos *et al.*, 1996, 2001; Lear *et al.*, 2000; Bohaty and Zachos, 2003). This rapid build up of ice has been associated with a dramatic transition from a greenhouse to an icehouse world. The long-term climatic deterioration prior to the Oi-1 glacial event was a culmination of rapid climatic changes fluctuating between warming and cooling events. Initial ice formation on Antarctica during the late Eocene and early Oligocene (~33.7 Ma) had a wide and lasting impact on global climate regimes. This fundamental turning point in the Earth's climate history is coincidental with a significant turnover event in both the marine and terrestrial record.

1.3 Marine record

A significantly large proportion of the research carried out in relation to the E/O transition and Oi-1 glacial maximum has been derived from marine sediments. Evidence for glacial conditions was initially provided through the recovery of glaciomarine sediments from on and near Antarctica, indicating the presence of grounded ice sheet by the earliest Oligocene (e.g. site 751 southern Kerguelen plateau (Breza *et al.*, 1992)). These sedimentary deposits were shown by pioneering investigations such as those carried out by Shackleton and

Kennett, 1975; Kennett and Shackleton, 1976; Poore and Mathews, 1984; Miller *et al.* (1987) and Zachos *et al.* (1992), to be consistent with a positive excursion of >1‰ in the benthic foraminiferal oxygen isotope records. Misinterpretation in particular of Miller *et al.* (1991) terminology of the isotopic record has lead to confusion over the naming of these isotopic events. The rapid increase in resolution of the $\delta^{18}O$ record in the last few decades had also attributed to the multiple naming of potentially equivalent events. Coxall and Pearson (2007) have attempted to redefine the nomenclature of this time period to eliminate confusion during correlation. Although much of this is based on the author's interpretation of the isotopic data, particularly when dating is poorly constrained, as it is unlikely that these events are synchronous in time.

In recent years a range of sedimentological, palaeoecological and geochemical records have revealed information on the impacts and possible causes relating to the abrupt climatic change associated with the build up of glacial ice on Antarctica.

1.3.1 Sedimentological evidence

In the late 1980's the Ocean Drilling Programme (ODP) carried out an intensive drill program in deep sea sediments off Antarctica, searching for evidence of ice sheets in the earliest Oligocene (summaries on these are provided by Miller *et al.*, 1991; Zachos *et al.*, 1992). These cores located grounded tills and ice rafted debris (IRD) relating to the build up of glacial ice on Antarctica. A summary diagram of this evidence and more recent data can be found in Miller *et al.* (2008, fig. 1). Sedimentological evidence suggests that 33.5 Ma was probably the first time that ice sheets reached the coast, allowing large ice bergs to calve and reach distal locations, for example the Kerguelen Plateau (e.g. ODP Site 748

(Zachos *et al.*, 1992)). Once the Antarctica ice sheet reached the coastline it became a driver of, not just a response to, climate change (Miller *et al.*, 2008).

1.3.2 Palaeoecological evidence

Many of the biotic groups (e.g. foraminifera (Boersma and Premoli Silva, 1986; Keller *et al.*, 1992) and molluscs (Hickman, 2003 and Nesbitt, 2003)) show evidence of minor extinction events of those species adapted to warm water conditions throughout the E/O transition (e.g. Keller *et al.*, 1992; Pearson *et al.*, 2008), allowing cold water species to fill their ecological niche. The late Eocene experienced a general cooling over a time interval of 10^6 years and this cooling is generally held responsible for the waves of extinction among marine and terrestrial organisms that occurred at this time (e.g. Keller *et al.*, 1992; Ivany *et al.*, 2000, 2008; Hansen *et al.*, 2004; Villa *et al.*, 2008; Pearson *et al.*, 2008; Rabosky and Sorhannus, 2009).

1.3.2.1 Foraminifera: Planktonic

The E/O boundary is defined by the last occurrence of the planktonic foraminiferal Family Hantkeninidae at the Global Stratotype Section and point at Massignano (Italy), (Nocchi *et al.*, 1988; Premoli Silva & Jenkins 1993). All five species of Hantkeninidae simultaneously become extinct at the E/O boundary (Coxall and Pearson, 2006). The boundary tie point is fixed onto the timescale of Cande and Kent (1995) at 33.7 Ma. It is considered by several authors that astronomical tuning of the section will undoubtedly redefine this in time (Coxall *et al.*, 2005; Gale *et al.*, 2006; Jovane *et al.*, 2006). Predating the extinction of *Hantkenina* at both Massignano and Tanzania (Pearson *et al.*, 2008) is another major extinction in planktonic foraminifera, the *Turborotalia cerroazulensis* group. Evidence suggests that both of these extinctions are related to a prolonged phase of environmental disruption (Coxall and Pearson, 2007). Over this time period planktonic foraminiferal tests

show evidence for a long-term trend in the form of an evolutionary turnover, involving extinctions of the warm water tropical surface dwelling species e.g. *Hantkenina* and *Turborotalia cerroazulensis* (Boersma & Premoli Silva, 1986; Keller *et al.*, 1992). Coxall and Pearson (2007) suggest that this could have been brought about by a rapid environmental change and cooling, influenced by changes in water mass stratification and the pattern of biological productivity.

Multiple extinctions and species turnovers at the E/O boundary make it one of the best defined biostratigraphic levels of the Cenozoic for planktonic foraminifera (Coxall and Pearson, 2007). However, the use of Hantkeninidae as the E/O boundary marker has been criticised, as the extinction of *Hantkenina* is considered to be diachronous in nature, representing an isolated event that may not be suitable for global correlation (van Mourik and Brinkhuis, 2005). Further evidence from Poore and Matthews (1984), who located the *Hantkenina* extinction at ODP site 522 (Walvis Ridge in the South Atlantic), showed that this extinction event coincided with a $\delta^{18}O$ shift preceding the most positive $\delta^{18}O$ values. Recently, the *Hantkenina* extinction event in Tanzania has also been shown to occur between two positive isotopic shifts in carbonate $\delta^{18}O$ (Pearson *et al.*, 2008) (Fig. 1.1). Data from Pearson *et al.* (2008) and Poore (1984) indicate that the period between the two $\delta^{18}O$ isotopic steps has the potential to be used to identify the E/O boundary. If correct this may provide the opportunity to place the E/O boundary using the $\delta^{18}O$ profiles in areas where *Hantkenina* are not preserved or do not exist e.g. polar regions or in the terrestrial realm.

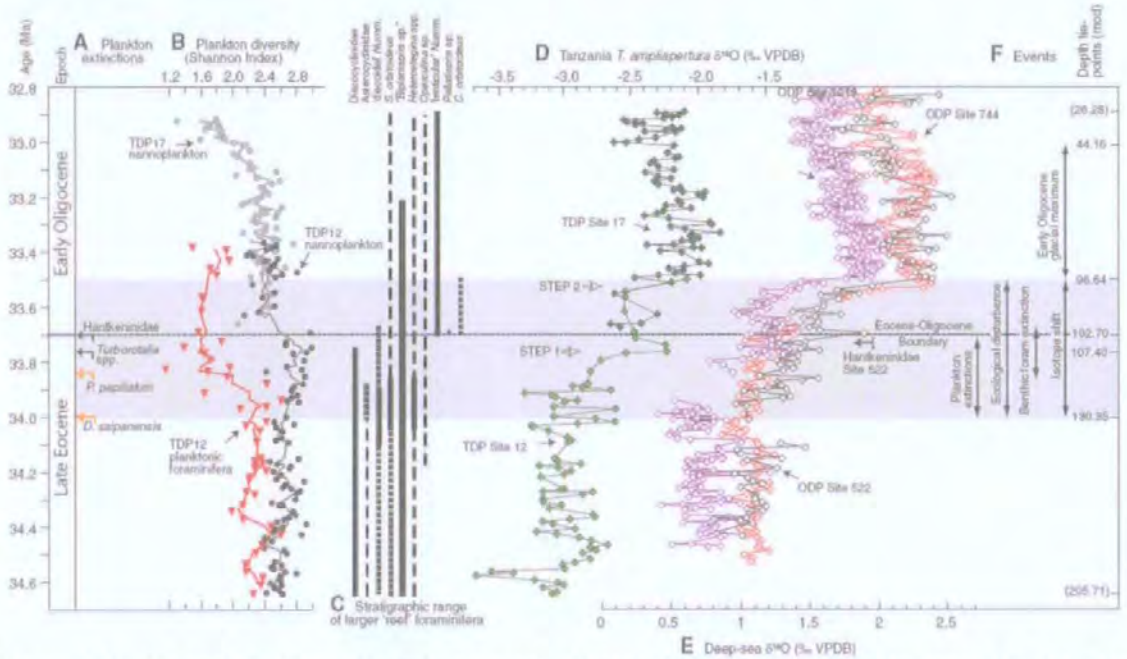

Figure 1.1 Biotic and geochemical events across the Eocene-Oligocene boundary compared to deep-sea records. Of interest are part A: Plankton extinction levels. D: Planktonic foraminifer oxygen isotope record from *Turborotalia ampliapertura*, 212–150 µm (light-green diamonds, TDP Site 12; dark-green diamonds, TDP Site 17).VPDB—Vienna Peedee belemnite. E: Deep-sea benthic foraminifer isotope records (purple diamonds, Ocean Drilling Program [ODP] Site 1218 from Coxall *et al.* [2005]; red diamonds, ODP Site 744 from Zachos *et al.* [1994]; black diamonds ODP Site 522 from Zachos *et al.* [1994]. *Hantkenina* extinction with sampling bracket is from Poore (1984). Figure taken from Pearson *et al.* (2008)

1.3.3 The isotopic record

It was recognised in the 1950's that the oxygen and carbon isotopic composition of organisms that precipitate calcium carbonate shells were potential archives of palaeoenvironmental and palaeotemperature information (McCrea, 1950; Urey *et al.*, 1951; Epstein *et al.*, 1953). A multitude of organisms both marine and terrestrial utilise calcium carbonate from their surrounding environments in the formation of their skeletal structure (see Chapter 2 for more detailed information). The preserved calcium carbonate remains of these organisms can be found within sedimentological deposits extending throughout the Cenozoic. However, preservation issues are paramount, as only well preserved specimens that have not undergone post depositional alteration can be used in the determination of isotopic ratio and in turn palaeotemperatures.

Benthic foraminiferal oxygen isotope records were shown by pioneering investigations to have a positive $\delta^{18}O$ excursion of >1‰ coinciding with E/O glaciomarine deposits (Shackleton and Kennett, 1975; Kennett and Shackleton, 1976; Poore and Mathews, 1984; Miller *et al.*, 1987 and Zachos *et al.*, 1992). Miller *et al.* (1991) introduced zones Oi-1 (circa 35.8 Ma) and Oi-2 (circa 32.5 Ma) based on the benthic foraminiferal $\delta^{18}O$ increases which could be linked with $\delta^{18}O$ increases in subtropical planktonic foraminifera and with intervals of glacial sedimentation on or near Antarctica. Zachos *et al.* (1996) re-used the term Oi-1 to identify the climax of the early Oligocene $\delta^{18}O$ excursion that lasted ca. 400 kyr.

Zachos *et al.* (2001) global benthic oxygen and carbon isotope curves (Fig. 1.2) are inescapable when describing climate change during the Cenozoic. This record is compiled from more than 40 DSDP and ODP sites, utilising the $\delta^{18}O$ and $\delta^{13}C$ values obtained from the analysis of benthic foraminifera. The culmination of this work produced the first high resolution global record of isotopic changes in the deep ocean for the last 70 Ma (Fig. 1.2). The Oi-1 glacial maximum is defined by a positive $\delta^{18}O$ shift of ~1.8‰ at ~33.7 Ma. This positive $\delta^{18}O$ isotopic excursion coincides with the first appearance of permanent ice on Antarctica (~33.7 Ma) (Kennett and Schackleton, 1976; Miller *et al.*, 1991; Zachos *et al.*, 1996; Lear *et al.*, 2000) in the Cenozoic.

The resolution of the isotopic records encompassing the E/O transition and Oi-1 glaciation has advanced rapidly in recent years. Several investigations have now shown this transition to be stepwise in nature (Coxall *et al.*, 2005; Lear *et al.*, 2008; Katz *et al.*, 2008) (Fig. 1.3). Coxall *et al.* (2005) were the first to produce a detailed isotopic record across the E/O transition, from sedimentary cores taken from the Pacific. The isotopic excursion relating to the E/O transition and Oi-1 glaciation will be discussed in more detail in the following sections.

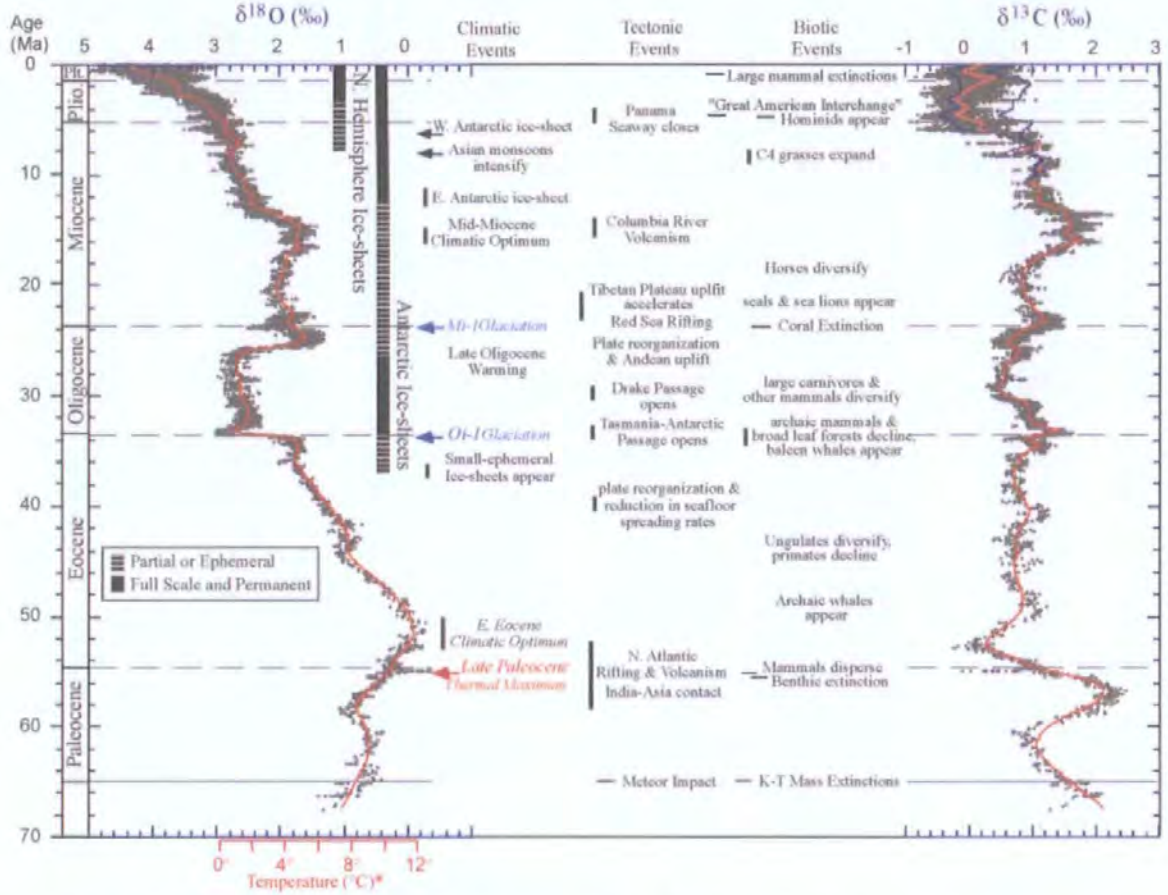

Figure 1.2 Deep-sea oxygen and carbon isotope records based on data compiled from more than 40 DSDP and ODP sites (36) correlate with climatic, tectonic and biotic event in the 70 Ma (taken from Zachos *et al.*, 2001).

1.3.4 Temperature or ice volume?

The way in which $\delta^{18}O$ is incorporated into the calcium carbonate shell of an organism has two main influences; temperature and the isotopic composition of the water ($\delta^{18}O_{water}$) in which the organism inhabits. Trying to decouple this combined temperature and $\delta^{18}O_{water}$ signal has become increasingly important, especially concerning the use of $\delta^{18}O_{carb.}$ data to calculate palaeotemperatures. However, this does rely on being able to determine the $\delta^{18}O$ of the host water in which the carbonate proxy lived. Details concerning palaeotemperature calculations are discussed further in Chapters 2 to 5.

Within the marine realm deconvolution of the $\delta^{18}O$ isotopic record has been achieved through the use of magnesium/calcium ratios (Mg/Ca ratios) (Lear *et al.*, 2000). This ratio

has been brought to the forefront of climate change studies as it has, for the first time, determined the amount of cooling and ice volume change across the Oi-1 glaciation. When calculating deep sea temperatures from the Mg/Ca ratio of benthic foraminiferal calcite, Lear *et al.* (2000) argued for a higher proportion of the Oi-1 positive $\delta^{18}O$ shift being related to ice volume changes. They implied that 1‰ to 1.5 ‰ of the marine benthic $\delta^{18}O$ signal represents changes in ice volume, with a very small temperature component.

However, the $\delta^{18}O$ isotopic signal could not be explained by ice volume change alone, therefore it was considered that there was a problem with the Mg/Ca ratio methodology. Lear *et al.* (2004) suggested that something was masking the cooling signal in the Mg/Ca records taken from deep sea deposits. They attributed this to either the increase of seawater pH and/or CO_3^{2-} associated with the carbon compensation depth (CCD) or the Mg partitioning into the foraminifera calcite. Contemporaneous with the $\delta^{18}O$ isotopic shift across the E/O transition was a deepening of the CCD to greater than 1km (Coxall *et al.*, 2005; Rea and Lyle, 2005). The partitioning of Mg into the calcite shell of the benthic foraminifera are likely to have been affected by the carbonate saturation state of the deep ocean altered by the increasing depth of the CCD (Lear *et al.*, 2004; Elderfield *et al.*, 2006).

Recent publications of foraminiferal isotope profiles across the E/O transition from Tanzania have shown that the $\delta^{18}O$ and $\delta^{13}C$ records are similar to the most complete deep-sea benthic foraminifer isotope records (e.g. Oberhänsli *et al.*, 1984; Zachos *et al.*, 1996; Coxall *et al.*, 2005). These isotope records show two main steps, with a total increase of ~1.5‰ in formainiferal $\delta^{18}O$ (Coxall *et al.*, 2005).

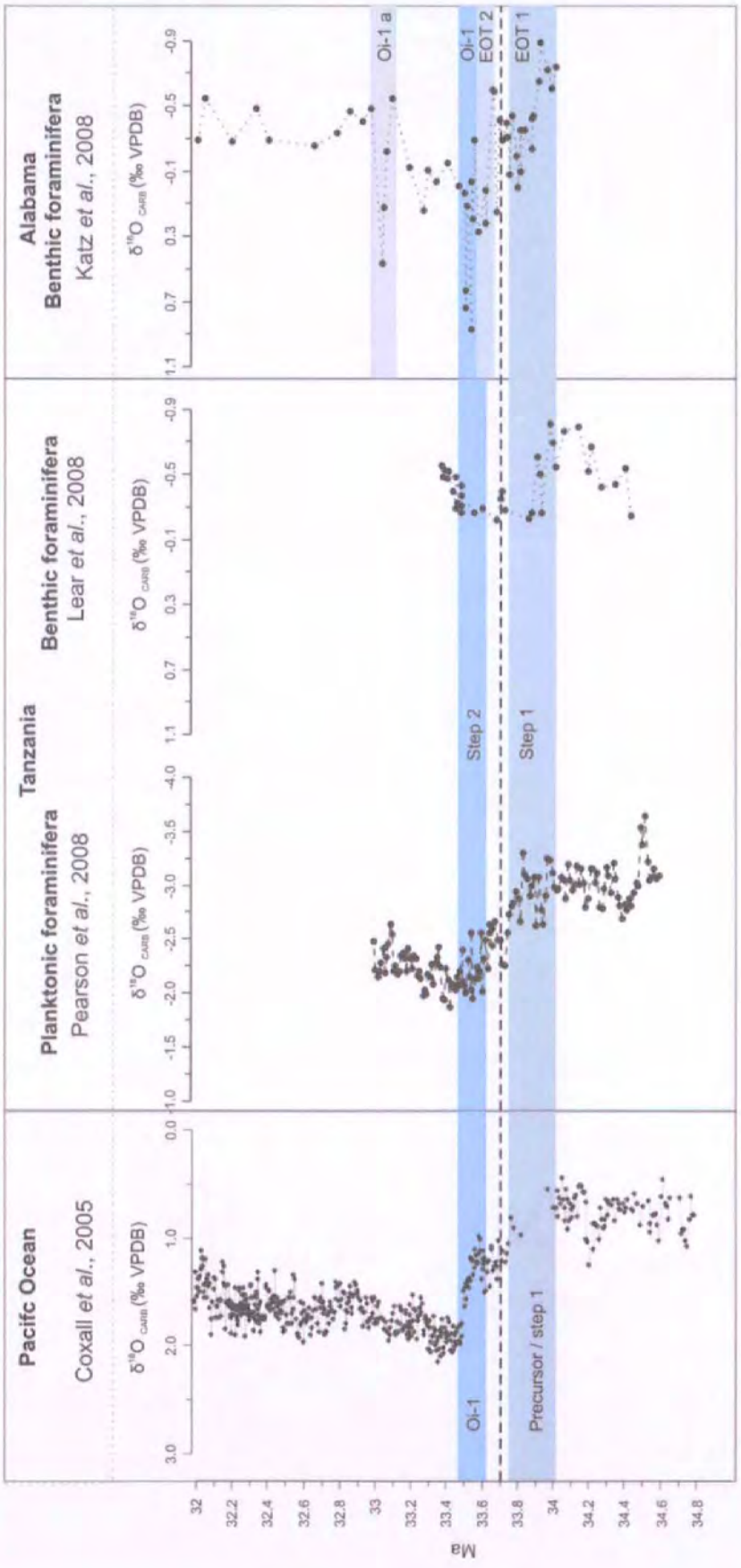

Figure 1.3 Four marine isotopic records (Coxall *et al.*, 2005; Lear *et al.*, 2008; Pearson *et al.*, 2008; Katz *et al.*, 2008) show a stepwise transition into the Oi-1 glacial maximum. A comparison diagram was constructed to compare the $\delta^{18}O$ isotopic profiles from different locations.

The analysis of shallow continental shelf deposits from above the CCD in Tanzania (Lear *et al.*, 2008) and the Gulf of Mexico (Katz *et al.*, 2008) provided Mg/Ca ratio temperatures indicating a cooling of ~2.5 °C during the first step of the E/O transition. However, the two records disagree on the temperature change across the Oi-1 glacial maximum with Lear *et al.* (2008) indicating no temperature change where Katz *et al.* (2008) suggest a decrease of ~2°C. When these temperatures are used in combination with the $\delta^{18}O$ record changes in the $\delta^{18}O_{water}$ can be determined. Each positive excursion event will be discussed in detail in the following sections.

1.3.5 Vonhof *et al.* (2000) Cooling Event (35.5 Ma)

Extraterrestrial impact events in the early late Eocene have been linked to accelerated climatic cooling, as evident from ODP site 689 (Maund Rise, Southern Ocean). It was considered by Vonhof *et al.* (2000) that two closely spaced impact events introduced large quantities of dust particles into the atmosphere leading to a 100 k.y cooling through feedback mechanisms, e.g. a global albedo increase due to snow and ice cover. These feedbacks were recorded within the bulk carbonate and benthic foraminiferal $\delta^{18}O$ isotopic record as a + 0.5 ‰ shift. Part of this shift is related to changes in ice volume therefore, cooling across this event was estimates as less than 2 °C (Vonhof *et al.*, 2000). Concurrent with the $\delta^{18}O$ isotopic shift within the fine fraction is an increase of 0.5 ‰ in $\delta^{13}C$ suggesting an increase in surface water productivity (Vonhof *et al.*, 2000). Evidence for this event has also been recorded by a strong increase in the abundance of *Thalassiphora pelagica* in the Massignano section (Italy) (Brinkhuis and Coccioni, 1995). Further north De Man (2004) implies that the increase in cool water taxa seen in the North Sea Basin benthic foraminiferal assemblages and the demise of *Nummulites* spp. at the top of the Bassevelde 1 submember (36.8 to 35.5 Ma) could have been related to the Vonhof cooling

event. The spread of evidence from various locations throughout north-western Europe suggests that the cause of this event may have had a regional rather than a global impact.

1.3.6 Late Eocene Event (~34.1 Ma)

Little information regarding the positive $\delta^{18}O$ excursion termed the Late Eocene Event has been published. Katz *et al.* (2008) re-interpretation of the isotopic data presented by Zachos *et al.* (1996) and Coxall *et al.* (2005), indicates a ~0.5‰ increase in the $\delta^{18}O$ of benthic foraminifera coinciding with this event. Post the Late Eocene Event values return to pre-excursion $\delta^{18}O$ values. The Late Eocene Event has been associated with glacial ice melt and sea level rise, recorded by a decrease of ~0.7 ‰ at Saint Stevens Quarry (SSQ) (Katz *et al.*, 2008) and ~0.5 ‰ at site 522 and 1218 (Zachos *et al.*, 1996; Coxall *et al.*, 2005) in $\delta^{18}O_{water}$ to more negative values. The Mg/Ca records of Lear *et al.* (2004) indicate that the isotopic response to this event is primarily related to ice volume change. However, potential changes in the calcite compensation depth at this time (Coxall *et al.*, 2005) may have caused alterations in carbonate ion activity masking cooling in the Mg/Ca record (Lear *et al.*, 2004). Katz *et al.* (2008) considered the event to be consistent with the hiatus in their SSQ record, representing a sea-level fall of ~40 m. Current evidence would suggest that the Late Eocene Event within the marine records is not associated with a decrease in temperature but entirely due to changes in ice volume.

1.3.7 Eocene-Oligocene Transition event 1 (EOT-1 of Katz *et al.*, 2008) (~33.8 Ma)

This precursor event, first recognised by Coxall *et al.* (2005), forms the initial part of the stepwise $\delta^{18}O$ transition which leads into the Oi-1 Glacial Maximum. Although this event can be observed in Zachos *et al.* (1996) $\delta^{18}O$ record, they did not refer to this isotopic

event specifically. Katz *et al.* (2008) re-interpreted Zachos *et al.* (1996) data and concluded that there was a 2.0 °C cooling associated with this event.

Planktonic foraminifera extracted from the Tanzanian cores shows that $\delta^{18}O$ increases by ~0.7‰ across the first step in the E/O transition (Lear *et al.*, 2008). Coinciding with this isotopic change is a decrease in the planktonic Mg/Ca ratio, equivalent to ~2.5 °C cooling of tropical near-surface and bottom waters. Lear *et al.* (2008) indicate that ~0.5‰ of the shift in $\delta^{18}O$ associated with the first step represents cooling, with the remaining ~0.2‰ available to accommodate an increase in continental ice volume. Katz *et al.* (2008) isotopic analysis of benthic foraminifera from Saint Stephens Quarry (SSQ) (Alabama) indicates an increase of 0.9‰ in $\delta^{18}O$ across this event, with the Mg/Ca ratio suggesting a cooling of 2.5 °C. Therefore, a change of 0.4‰ in the $\delta^{18}O$ of the water was attributed to a sea level fall of ~30m, associated with an ice volume change. However, Miller *et al.* (2008) suggest that this precursor event is not associated with an observable sea level change (no greater than 15-20 m) suggesting that it was caused by cooling, not ice sheet growth. This event is preceded by a return to more negative $\delta^{18}O$ values (0.7 ‰) and a 0.4 ‰ $\delta^{18}O_{water}$ increase, which according to Katz *et al.* (2008) suggests a sea level rise.

	Site / author	Late Eocene (34.1 Ma)			EOT-1/Step 1 (33.8 Ma)			EOT-2 (33.63 Ma)			Oi-1/Step 2 (33.545 Ma)			Overall isotopic shift (‰)	Overall Temp. shift (°C)	Change in δ_w (‰)	Sea level fall (m)
		$\delta^{18}O$ (‰)	Temp (°C)	Ice volume (‰)	$\delta^{18}O$ (‰)	Temp (°C)	Ice volume (‰)	$\delta^{18}O$ (‰)	Temp (°C)	Ice volume (‰)	$\delta^{18}O$ (‰)	Temp (°C)	Ice volume (‰)				
MARINE	Zachos *et al.* (1996) Site 552	0.5	-	-	-	-	-	-	-	-	1.5	-3 to -4	0.6	1.5	-3 to -4	1.5 (corrected by Katz *et al.*, 2008)	-
	Zacho *et al.* (2001)	-	-	-	-	-	-	-	-	-	>1.0	-	0.6	>1.0	-	-	-
	Bohaty and Zachos, (2003)	0.45	-	-	0.3	-	-	-	-	-	1.28	-	-	1.59	-	-	-
	Coxall *et al.* (2005) Site 1218	0.5	0	0.5	1.25	0	1.25	-	-	-	1.90	0	1.90	3.15	-	1.2 (corrected by Katz *et al.*, 2008)	70
	Lear *et al.* (2008) Tanzania	-	-	-	0.7	-2.5	0.2	-	-	-	0.4	0	0.4	0.8	-2.5	0.6	70
	Katz *et al.* (2008) Site SSQ	0.5	0	0.5	0.9	-2.5	0.4	0.8	No data	>0	1.0	-2	0.5	2.7	-5.0	1.2	67
TERRESTRIAL	This study Hampshire Basin	1.87	-7.0	-	1.11	-4	-	1.54	-6	-	-	-	-	2.28	-14.0	-	-
	Grimes *et al.* (2005) Hampshire Basin	0.77 to 1.13	-2.0 to -5.2	-	-	-	-	-	-	-	-	-	-	0.99	-1.0	-	-
	Zanazzi *et al.* (2007) North America	-	-	-	-	-	-	-	-	-	-	-	-	1.7	-8.2	-	-

Table 1.1 Information from terrestrial and marine records showing the $\delta^{18}O$ shifts and how this shift has been apportioned to temperature and ice volume for each of the isotopic shifts. An overall $\delta^{18}O$,

temperature, $\delta^{18}O_{water}$ and estimates of sea level fall are given for the E/O transition.

1.3.8 Eocene-Oligocene Transition event 2 (EOT-2) (~33.6 Ma)

Katz *et al.* (2008) revealed a previously unidentified positive $\delta^{18}O$ excursion of 0.8 ‰ in-between the two $\delta^{18}O$ steps of Coxall *et al.* (2005) and Lear *et al.* (2008). As the benthic foraminifers were rare within this section of core it was impossible to carry out Mg/Ca ratios to decouple the isotopic record and calculate temperature and ice volume changes (Katz *et al.*, 2008).

1.3.9 Oi-1glacial maximum / EOT 2 / Step 2 (33.5 Ma)

Prior to the discovery of the precursor steps which, are now known to lead into the Oi-1 glacial maximum, it was suggested that the build up of glacial ice was accompanied by a decrease in temperature (e.g. Zachos *et al.*, 1996). Higher resolution studies focusing on the E/O transition indicate that the second shift known as Oi-1 is marked by ~1 ‰ shift in $\delta^{18}O$ (Coxall *et al.*, 2005; Lear *et al.*, 2008 and Katz *et al.*, 2008). However, the proportion of this isotopic shift attributed to temperature change appears to vary between different data sets from different regions (Table 1.1).

1.3.10 Sea level fall

The formation of the permanent continental scale ice cap on Antarctica led to a significant sea level fall, with estimates ranging from 30–90 m (Pekar *et al.*, 2002; Kominz and Pekar, 2001; Miller *et al.*, 1991) and modelled more conservatively at 40–50 m (Deconto & Pollard, 2003). Wade and Pälike (2004) record indicates that they can match third-order eustatic sea level variations with high resolution oxygen isotope records, and that major

glaciation cycles are indeed driven by the confluence of eccentricity cycles and longer-term obliquity amplitude variations.

Many high-resolution $\delta^{18}O$ records (e.g. Lear *et al.*, 2008; Katz *et al.*, 2008) suggest that the proportion of the $\delta^{18}O$ record attributed to ice volume and in turn sea level fall is much smaller than that apportioned to temperature for the first (precursor) step in $\delta^{18}O$ but that the second step is associated with a major sea-level fall (Coxall *et al* 2005; Lear *et al.*, 2008; Katz *et al.*, 2008). This isotopic excursion represents the point in time when the Antarctic ice sheet reached the coastline during the Cenozoic, changing from a response to a driver of climate change (Miller *et al.*, 2008).

1.3.11 Atmospheric and oceanic circulation

Permanent ice formation on the poles had a dramatic effect on the structure of the ocean and atmospheric circulation. This reorganization is thought to have led to the development of the modern ocean structure (Allen and Armstrong, 2008). The presence of permanent ice cover on Antarctica and the Arctic Ocean produces stable and persistent high pressure systems at the Polar Regions, allowing the development of well defined frontal systems (Hay *et al.*, 2005). These frontal systems act as barriers to heat transport and in combination with positive albedo feedbacks on incoming solar radiation, increases the latitudinal temperature gradient (Hay *et al.*, 2005). Palaeobiogeographical evidence from marine calcareous plankton and land plants (Miao *et al.*, 2008) indicate that the subtropical and polar frontal systems were not persistent features during the Eocene. It was speculated by Hay (2000) that these barriers came into permanent existence in the early Oligocene prior to which inconsistent winds that varied in strength and direction generated mesoscale eddies that transported heat to the poles more efficiently (Hay *et al.*, 2005). In relation to this study (north western Europe), it is important to note that in the modern atmospheric

and oceanic circulation scheme the wind direction is dominantly from a westerly direction, where in the Eocene schematic the atmospheric currents are from the east and are significantly weaker (Fig. 1.4). If correct this would have a significant impact on the isotopic composition of meteoric water in north Western Europe.

Ocean circulation plays a critical role in transporting the signals and feedbacks associated with climate change around the globe. Recent studies have suggested that the initiation of deepwater overflowing the Greenland – Scotland Ridge (GSR) occurred in the early Oligocene (~35 Ma) (Davies *et al.*, 2001; Via and Thomas, 2006). The abrupt suppression of the Iceland plume triggered the rapid deepening of the GSR, which moderated the deep water circulation between the Nordic sea and the North Atlantic (Abelson *et al.*, 2008). This allowed the Nordic sea water, with relatively high $\delta^{18}O$ values (as high-latitude water are usually colder and there is evidence for ice sheets formation on Greenland ~38 Ma (Eldrett *et al.*, 2007; 2009)), to kick start the Atlantic Thermohaline Circulation (ATC) and in turn the Global Thermohaline Circulation (GTC). Evidence from Nd isotopes studies from the Southern Ocean and the Southeast Atlantic also indicate the initiation of North Atlantic Deep Water at the E/O boundary (Scher and Martin, 2004; Via and Thomas, 2006).

1.3.12 Calcite compensation depth

Permanent deepening of the global CCD by 1200-1500m (Van Andel and Moore 1974; Delaney and Boyle, 1988; Peterson *et al.*, 1992) occurred rapidly, synchronized with the glaciation of Antarctica (Coxall *et al.*, 2005). Coxall *et al.* (2005) record a decrease in the CCD taking place in two steps (~40 kyr each) separated by an intermediate plateau (~200 kyr). This stepped change in the CCD is synchronised with the stepped increases in $\delta^{18}O$ and $\delta^{13}C$ of benthic foraminifera and development of major permanent Cenozoic Antarctic

ice sheets (Coxall *et al.*, 2005). During the Oi-1 glacial maximum there was geographically extensive carbonate burial as much as 10° N of the equator, which is twice the distance from the equator than modern carbonate deposition (Leg 199 shipboard scientific party, 2002). Berger and Winterer (1974) investigations and Merico *et al.* (2008) modelling indicates that the deepening of the CCD was initially driven by a shift from shelf to deep sea deposition associated with falling sea level. This glaciation affected weathering rates and carbon fluxes with riverine inputs of bicarbonate ions and terrestrial productivity decreasing carbonate ion concentrations and $\delta^{13}C$.

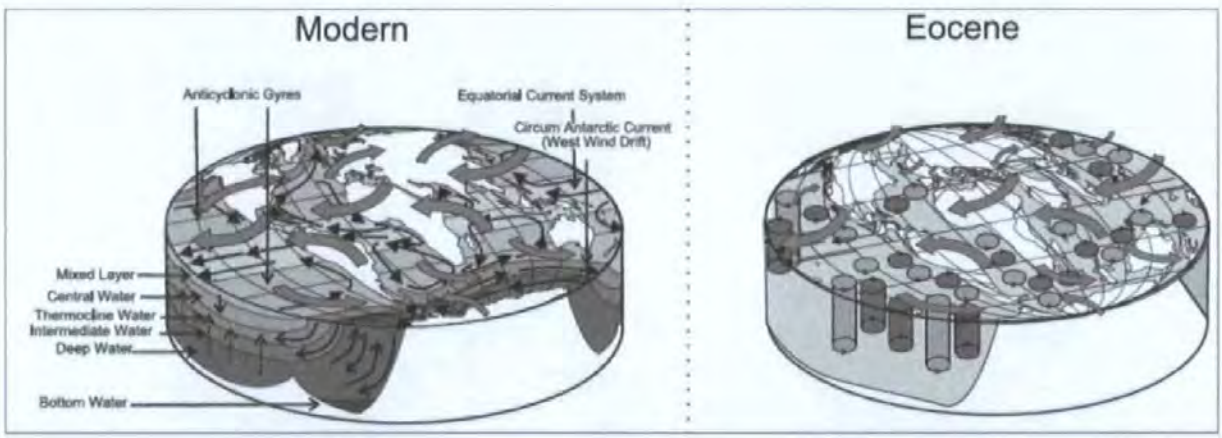

Figure 1.4 A. The general scheme of modern atmospheric and oceanic circulation. Winds associated with atmospheric cells are shown as large grey arrows. Ocean currents are shown by black arrows. Vertical motions in the ocean interior are shown by solid arrows representing general flows and dotted arrows representing the diffuse upwelling by which deep water return to the surface. B. Hypothetical circulation of the Eocene oceans in Northern Hemisphere summer. The ocean circulation is dominated by eddies rather than gyres. Light grey cylinders and circles represent anticyclonic eddies that pump water downward; dark grey cylinders and circles represent cyclonic eddies that pump water upward. Winds associated with atmospheric cells are shown as large grey arrows. Equatorial ocean currents are shown by black arrows. Taken from Hay *et al.* (2005)

1.4 Terrestrial record

How biota dealt with the rapid shifts in climate related to changes in ice volume and temperature across the E/O transition is important in understanding how modern terrestrial

environments would cope with such an event. A summary of the recorded changes taking place in relation to the E/O transition and Oi-1 glacial maximum is given in the following sections.

1.4.1 America

A large proportion of published investigations covering the E/O transition and the Oi-1 glaciation have been undertaken on the North American continent. The majority of these investigations show evidence for long-term environmental deterioration and increased seasonality across the E/O transition (e.g. Prothero and Heaton, 1996; Wolfe, 1978; 1992; Sheldon and Retallack 2004; Zanazzi *et al.*, 2007; Sheldon *et al.*, 2009). Calculated mean annual temperatures imply a decline in temperature of 13 °C in less than a million years, while the mean annual range of temperature increased dramatically from 5 °C to almost 25°C (Wolfe, 1978). In contrast, the warm monthly mean temperature changed little (Wolfe, 1994). Botanically most of North America changed from subtropical vegetation typical of central America today to highly seasonal deciduous vegetation typical of present day north-eastern United States (Prothero and Heaton, 1996). Evidence from mammal remains suggests that a major faunal turnover occurred prior to the major climatic changes associated with the Oi-1. However, Prothero and Heaton (1996) results show that there is a complete lack of response by mammals to the changing climate over the E/O transition, with little migration taking place. Although, Hunt (2004) suggests a moderate mammalian faunal shift occurred across the Oi-1 glacial maximum (~33.7 Ma). Palaeoprecipitation and palaeotemperature estimates based on paleosols indicate that changes occurring at the E-O transition are a smaller part of a long-term decline rather than a sudden climatic shift (Sheldon, 2009). The majority of data from North America suggests the long-term climatic deterioration (over ~6 Ma) was accompanied by aridification (Sheldon and Retallack, 2004) and fluctuating but generally declining biodiversity, beginning with the early

Oligocene (33.5 Ma) and reaching a new equilibrium by the middle Oligocene (29 Ma) (Retallack, 2004).

Recent isotopic analysis of fossil tooth enamel and fossil bone from sediment crossing the E/O transition in central North America indicate a controversial large drop in annual mean temperature (8.2 ± 3.1 °C) and a small increase in seasonality (Zanazzi *et al.*, 2007). This large drop in temperature is much greater than those implied by the marine temperature records (e.g. Lear *et al.*, 2008; Katz *et al.*, 2008 (see Table 1.1)). Their inference of little change in seasonality is also contrary to other studies (Wolfe, 1978, 1994); Prothero and Heaton, 1996; Ivany *et al.*, 2000; Grimes *et al.*, 2005) (See Chapter 7 for more information). Furthermore, Kohn *et al.* (2004) analysed fossil mammal teeth from southern Argentina crossing the E/O transition. Their results showed no resolvable change in the oxygen isotope composition of meteoric water during this period. This evidence in combination with the paleoflora and geographical positioning of Patagonia suggested to them that despite evidence elsewhere for mid to high latitude cooling (Wolfe, 1978, 1994; Prothero and Heaton, 1996) no appreciable change in the climate occurred in South America. Kohn *et al.* (2004) suggest that an increase in latitudinal temperature gradients and strengthening of ocean circulation gyres may have increased heat transport to the western Atlantic, producing near constant temperatures in southern Argentina, or that the paradigm of major global cooling at the E/O transition is largely false.

1.4.2 Asia

Investigations carried out by Dupont-Nivet *et al.* (2007) and Wang *et al.* (1990) showed that significant aridification and cooling of the Asian continent was associated with the E/O transition. In the north of the Tibetan Plateau a mammalian faunal turnover has been linked to these climatic changes, indicated by a decrease in mammal size and the evolution

of mammal tooth patterns from the Eocene to Oligocene species (Meng and McKenna, 1998). The isotopic ($\delta^{18}O$ and $\delta^{13}C$) record from these sediments also showed a large positive $\delta^{18}O$ shift across the E/O transition (Graham *et al.* 2005). Dupont-Nivet *et al.* (2007) concluded that the most likely cause of this large positive shift was climate cooling across the E/O transition coinciding with the uplift of the Tibetan Plateau. These two processes enhanced continental aridification along with the intensification of the monsoon and increased regional erosion. If the timing of the Tibetan Plateau uplift coincides with the E/O boundary, then questions can be raised as to whether this increased weathering brought about a drawdown of atmospheric CO_2 (Bowen, 2007).

1.4.3 Greenland

Recent evidence of terrestrial climate change during the E/ O transition suggests that a 5°C cooling in the cold months (winter) mean temperatures was responsible for a decrease in the mean annual temperature (Eldrett *et al.*, 2009). The cooling of winter temperatures is consistent with other northern high latitude temperature records like that of Grimes *et al.* (2005) and Zanazzi *et al.* (2007). Concomitant with this temperature decrease is an increase in seasonality. This is represented by a shift towards a more extreme temperature range which was greater in magnitude than the mean annual temperature change (Eldrett *et al.*, 2009). However, this cooling and change in vegetation occurs much earlier than the E/O transition and is thought to be contemporaneous with the first ice build up on Greenland ~38 Ma (Eldrett *et al.*, 2007).

1.4.4 Europe

1.4.4.1 Biotic extinctions

In Western Europe the Oi-1 glaciation is associated with a major mammalian faunal turnover known as the 'Grande Coupure' (H.G. Stehlin, 1909) or 'Big Break'. This event

has been recorded throughout Europe (Barbera *et al.*, 2001; Hooker *et al.*, 2004; Smith, 2004) and shows contrasting evidence to North America (Prothero and Heaton, 1996). Two physical changes have been proposed as possible causes of this turnover event:

1. Climate change associated with the E/O transition and the Oi-1 glacial maximum is thought to be a key forcing mechanism for global biotic change.

2. The absence of land bridges between landmasses. This has been shown to prevent or inhibit geographical range extensions and cause widespread endemism. During a large part of the Eocene, Europe was an archipelago of large and small islands (Auge and Smith, 2009). By the late Eocene the terrestrial records shows that the E/O transition is accompanied by a major eustatic sea level fall (Gély and Lorenz, 1991; Steubaut, 1992; Hooker *et al.*, 2004). Dispersal of new mammals faunas from Asia were facilitated by this fall in sea level, which allowed migration along the newly formed land bridges.

Other biota have also been influenced by the changes associated with the Oi-1 glaciation and E/O transition. Lizard assemblages from Belgium show a marked decrease in diversity between MP20 and MP21 across the E/O transition (Auge and Smith, 2009). It has been estimated that between 66% and 80% of the lizard and snake species in Europe may have been lost across this event (Rage and Augé, 1993), representing the most critical turnover in the Cenozoic history of lizards. Lizards are vertebrate ectotherms (cold blooded) and therefore require warm temperatures as part of their physical requirements, consequently they are considered to be good climatic indicators (Markwick, 1998; Böhme, 2003). Other reptile species were also affected. Numerous extinction of crocodylia occurred at the end of the Eocene (Buffetaut, 1982), and only small snakes survived as the large Boidae present during the middle and late Eocene became extinct at the Grande Coupure Event (Ivanov *et al.*, 2000; Szyndlar and Rage, 2003).

Other biota affected by the E/O transition and Oi-1 glaciation are discussed in greater detail in Chapters 6 and 7.

1.4.4.2 Isotope and temperature records

On the IOW a terrestrial $\delta^{18}O$ record encompassing the E/O transition and Oi-1 glacial maximum was achieved though the analysis of various proxies throughout the Solent Group stratigraphy, including rodent (*Thalerimys fordi, Theridomys bonduelli* and *Isoptychus* sp. of the extinct rodent family Theridomyidae) cheek tooth enamel, gastropod shells (*Lymnaea* sp.), charophyte gyrogonites, fish otoliths, and fish scale ganoine (Grimes *et al.*, 2005). Their analysis recorded isotopic snap shots throughout the Eocene, with a single (charophyte gyrogonites) data point above Hooker *et al.* (2004, 2009) placement of the Oi-1 glacial maximum. Grimes *et al.* (2005) calculated palaeotemperatures indicates a temperature change prior to the E/O transition and Oi-1 glacial maximum. However, their results indicate no significant temperature change across the Oi-1 glacial maximum itself.

Temperature calculations for central Europe over the last 45 Ma were also reconstructed using the 'coexistence intervals' of stratigraphically well constrained megafloras (fruits, seeds and leaves) from locations in Germany (Mosbrugger *et al.*, 2005). This continental record (Fig. 1.5) suggests a long-term cooling trend from the Early Eocene Climate Optimum (EECO) to the Pleistocene glaciation (Mosbrugger *et al.*, 2005). As would be expected the degree of continental cooling (14°C) is 4 °C greater than the marine global record (10 °C) due to greater extremes in temperature variability. Mosbrugger *et al.* (2005) considered an overall decrease in Mean Annual Temperature (MAT) of 11% over the last 45 Ma when it is assumed that a decrease of 0.4°C per degree of MAT for the European latitudinal shift.

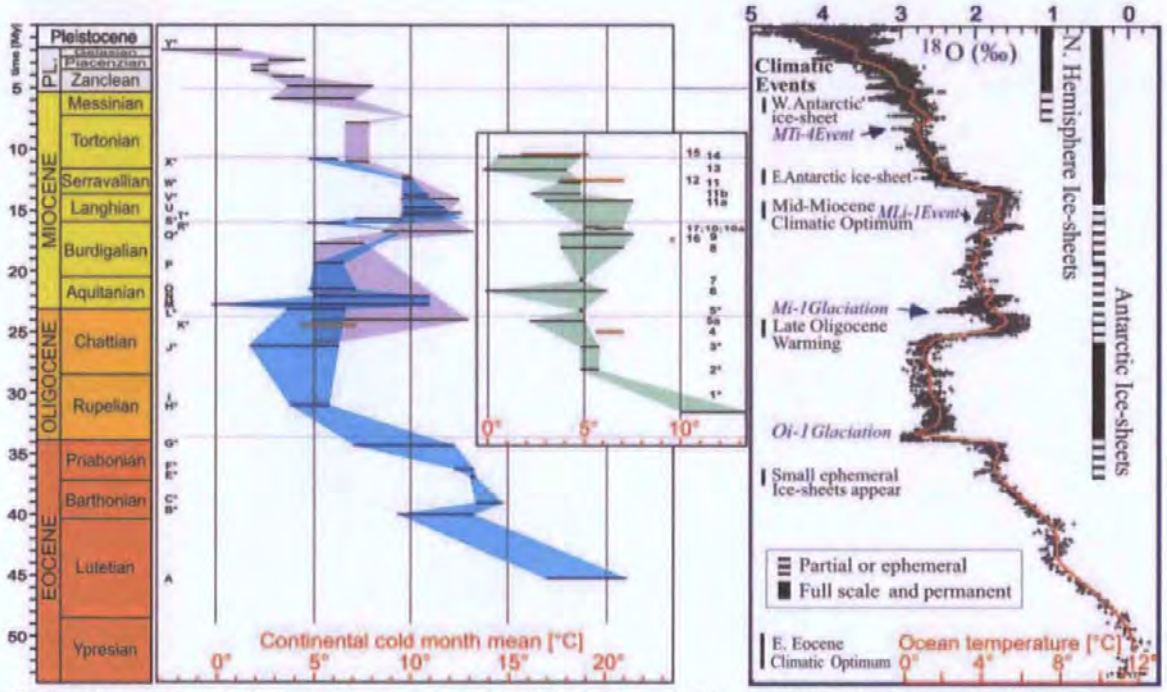

Figure 1.5 Continental temperature curves (CMM) for Central Europe during the last 45 Ma (blue curve = Weisselster and Lausitz Basins; green curve = Molasses Basin; purple curve = Lower Rhine Basin) in comparison with the global marine oxygen isotope record of Zachos *et al.* (2001) adapted to the International Commission on Stratigraphy 2004 time scale (Gradstein *et al.*, 2004). Taken from Mosbrugger *et al.* (2005).

For the period encompassed by this investigation the middle Eocene represents the warmest climate throughout the last 45 Ma with MAT between 23 °C to 25 °C, Mean Annual Precipitation (MAP) between 1,000 mm to 1600 mm and the Cold Monthly Mean (CMM) between 17 °C to 21 °C (Mosbrugger *et al.*, 2005). These climatic parameters, particularly the MAT, indicate a tropical climate existed during the middle Eocene (Mosbrugger *et al.*, 2005). By the late Eocene the MAT had reduced significantly to between 9 °C and 12 °C which is more characteristic of warm temperate climates (Mosbrugger *et al.*, 2005). This decrease in MAT is synchronized with a 5 °C cooling in the CMM, but the Warm Monthly Mean (WMM) remains at relatively high temperatures. Divergence by the CMM would indicate that the primary cause of cooler MAT is the increase in seasonality (Mosbrugger *et al.*, 2005). Minimum temperatures become cooler, with extreme temperature variation occurring at higher frequency.

1.5 Causes and mechanisms of the E/O transition and Oi-1 glaciation

The Oi-1glaciation marks a period in time when permanent continental scale ice-sheets first formed on Antarctica, but the causes and mechanisms behind this glacial ice build up are widely debated. Several mechanisms have been put forward as possible causes, these include: tectonic forcing (opening of oceanic gateways and mountain building); biogeochemical process (drawdown of atmospheric CO_2 and changes to ocean and atmospheric circulation); and orbital forcing.

1.5.1 Tectonic forcing

1.5.1.1 Oceanic Gateways- the thermal isolation of Antarctica?

It was initially suggested that the thermal isolation of Antarctic, caused by the widening of oceanic passages, lead to the initial appearance of the continental ice sheets on Antarctica (Kennet and Shackleton, 1976). The opening of the Southern Ocean Gateways is thought to have caused the thermal isolation of Antarctica by the creation of the Antarctic Circumpolar Current (ACC) (Kennet, 1977; Berggren and Holister, 1977). This process changed the configuration of the ocean circulation between Australia and Antarctica, initiating alterations to the global ocean and atmosphere circulations. For complete isolation of Antarctica both the Tasmanian gateway and Drake Passage must have opened. Timing of the Tasmanian gateway opening is relatively well constrained, with Australia breaking away from Antarctica in the late Cretaceous, with final separation in the late Eocene (~33.5 Ma) (Shipboard scientific party, 2003). The opening of this gateway provided a ~50 m deep connection into the northward flowing limb of the Eocene Antarctic subpolar gyre (Huber *et al.*, 2004; Stickley *et al.*, 2004), with continued deepening to 2000 m by 32 Ma (Lawver and Gahagan, 2003). The opening of Drake Passage has been widely debated with evidence indicating an early Oligocene opening that

is older than 30.5 Ma (Lawver and Gahagan, 1998; Livermore *et al.*, 2005) or an early Miocene opening between 22 and 17 Ma (Barker and Burrell, 1977; Barker, 2001). Livermore *et al.* (2005) indicate that a partial opening forming a shallow passage may have occurred through crustal extension between 50 and 33 Ma. Changes in Nd isotope values place the initial opening of Drake Passage at ~41 Ma, intermediate depths by ~37 Ma (Scher and Martin, 2004) with the establishment of a deeper Pacific- Atlantic connection at ~34 Ma (Scher and Martin, 2006). Drake Passage is thought to have opened before the Tasmanian gateway, implying a late Eocene establishment of a complete circum-Antarctic pathway (Scher and Martin, 2006) and Antarctic Circumpolar Current. Thomas *et al.* (2003) concluded that during the late Eocene no warm current flowed southwards along eastern Australia due to a counter clockwise gyre in the southern Pacific (Haq, 1981), thus preventing warm waters from reaching Antarctica. Scher and Martin (2006) suggest that the cooling immediately following the Middle Eocene Climatic Optimum (MECO) is coincidental with the opening of Drake Passage, associated changes in circulation and productivity leading to the drawdown of CO_2 that may have accelerated cooling.

Huber *et al.* (2004) models do not support changes in the thermal isolation of Antarctica as a primary force of the Oi-1 glaciation as the change in meridional heat transport associated with the onset of the ACC was insignificant. Lyle *et al.* (2008) findings agree with Huber *et al.* (2004) models, indicating that the development of the ACC occurred after the E/O boundary. Deconto and Pollard (2003) modelled the draw down of atmospheric CO_2 from four times the modern levels to two times over a 10 Ma period. Outputs from these models suggested that ice caps would form whether or not the gateway was open or closed. However, the CO_2 levels required to cause ice cap glaciation were much lower when the gateways (Drakes Passage and Tasmanian gateway) was closed. Overall, the evidence suggests that although the thermal isolation of Antarctica may not be the primary driving

force for Antarctic glaciation, it provided an important link in the chain of events occurring at this time.

1.5.1.2 Effects on the regional climate of Europe and global ocean circulation

The timing of tectonic closure of the southern Neotethys Ocean gateway by the Arabia–Eurasia collision is controversial (Allen, 2009; Bea *et al.*, 2009). It is currently thought to have occurred between 40.4 Ma and 23.03 Ma (Boulton, 2009), with Allen and Armstrong (2008) giving a more precise date of ~35 Ma. Allen and Armstrong (2008) suggest that global cooling was forced by processes associated with the initial collision via reduction in atmospheric CO_2. One of the stated processes leading to this cooling is a shift towards modern patterns of ocean currents. They show that during the Eocene a westerly transport of warm Indian Ocean water entered the Atlantic via the Tethys Ocean. By the Early Oligocene the connection between the Indian and Atlantic Oceans was impeded by the Arabian – Eurasian collision zone causing this warm water transport to cease. Closure of this ocean gateway may have been responsible for regional changes in heat transport in North Western Europe and partly responsible for the shift toward modern ocean circulation.

1.5.1.3 Orogenic activity

The uplift of the Tibetan Plateau is thought to have caused a long-term drawdown of atmospheric CO_2 by weathering processes (Raymo *et al.*, 1988; Dupont-Nivet *et al.* (2007; 2008). Orogenesis increases rock weathering, organic carbon burial, changes alkalinity and the major elemental composition of the oceans, enhancing the consumption of atmospheric CO_2, and leading to global cooling (Raymo *et al.*, 1988; Zachos and Kump, 2005). Dupont-Nivet *et al.* (2007; 2008) and Pei *et al.* (2009) have suggested that significant

regional uplift throughout the Tibetan region began prior to the E/O transition, initiating at ~38 Ma. This regional uplift initiated at least 4 Ma before the E/O transition and is consistent with the idea that the associated increase in rock weathering and erosion contributed to the lowering of atmospheric CO_2 (Dupont-Nivet *et al.*, 2007; 2008). Kump and Arthur (1997) showed that the increase in $^{87}Sr/^{86}Sr$ values in the marine carbonate record started at 40-38 Ma, indicating enhanced silicate weathering associated with the uplift of the Himalayas and Tibetan Plateau. It is currently believed that this mechanism lead to the initiation of ice formation on Antarctica (Deconto and Pollard 2003).

1.5.2 Biogeochemical processes: Atmospheric CO_2 drawdown

Royer (2006) compared 490 published proxy records of atmospheric CO_2 spanning the Ordovician to Neogene with records of global cooling events to evaluate the strength of CO_2 –temperature coupling over the Phanerozoic. Her results indicate a tight correlation between CO_2 and temperature indicating that CO_2, operating in combination with many other factors such as solar luminosity and palaeogeography, has imparted a strong control over global temperatures for much of the Phanerozoic (Royer, 2006).

Decreasing atmospheric pCO_2 concentrations during the E/O transition and Oi-1 glaciation have been indicated by a variety of proxy indicators (e.g. Diester-Haas and Zahn, 1996; 2001; Retallack, 2001; 2002; Roth-Nebelsick *et al.*, 2004; Pagani *et al.*, 2005). A recent high resolution investigation suggests that a reduction in pCO_2 occurred before the main phase of ice growth (Oi-1 glacial maximum), followed by a sharp recovery to pre-transition values and then a more gradual decline into the early Oligocene (Pearson *et al.*, 2009) (Fig. 1.6). This implies that declining pCO_2 had a central role in the development of the Antarctic ice sheet.

Deconto and Pollard (2003) and Deconto *et al.* (2008) modelled the threshold response of long-term Cenozoic decline in atmospheric CO_2 levels and idealised orbital forcing. Their model outputs infer that this decline caused the initiation of ice-sheet height and mass balance feedbacks, causing the ice sheets to expand rapidly, pulsating in size with orbital variations (particularly with the 41 kyr obliquity cycles and 110kyr and 405 kyr eccentricity cycles). Antarctic ice sheets grew suddenly once pCO_2 reached the critical threshold values of 2.8 to 2.6 times 'pre-industrial' atmospheric levels (~750 p.p.m.v) (Deconto *et al.*, 2008) (Fig. 1.7), causing the coalescence of individual ice caps to form the continental scale Antarctic ice-sheets. The model output showed that two rapid jumps in ice formation occurred as a response to height/mass balance and albedo feedbacks when the snowline intersected high plateaux's during orbital periods producing cold austral summers (Deconto and Pollard, 2003). These two jumps are comparable to the two steps seen in the foraminiferal $\delta^{18}O$ isotope records (Coxall *et al.*, 2005; Lear *et al.*, 2008).

Throughout the E/O the carbon cycle and global climate are thought to have been linked until the Neogene when the decoupling of climate and atmospheric pCO_2 appears to take place (Pagani *et al.*, 2005). Variation in pCO_2 concentrations caused a variety of feedbacks including; changes in radiative forcing, atmospheric circulation patterns and humidity (Pagani *et al.*, 2005), all in turn having their own feedback mechanisms. Other feedbacks could be accelerated by pCO_2 draw down such as increased sea ice, upwelling in the southern ocean (Zachos and Kump, 2005; Deconto *et al.*, 2007) and falling sea levels (Merico *et al.*, 2008). Model scenarios indicate that a pCO_2 decrease across the E/O transition is more important than the opening of oceanic gateways (Deconto and Pollard, 2003; Huber and Norf, 2006; Deconto *et al.*, 2008) when it comes to the build up of glacial ice on Antarctica.

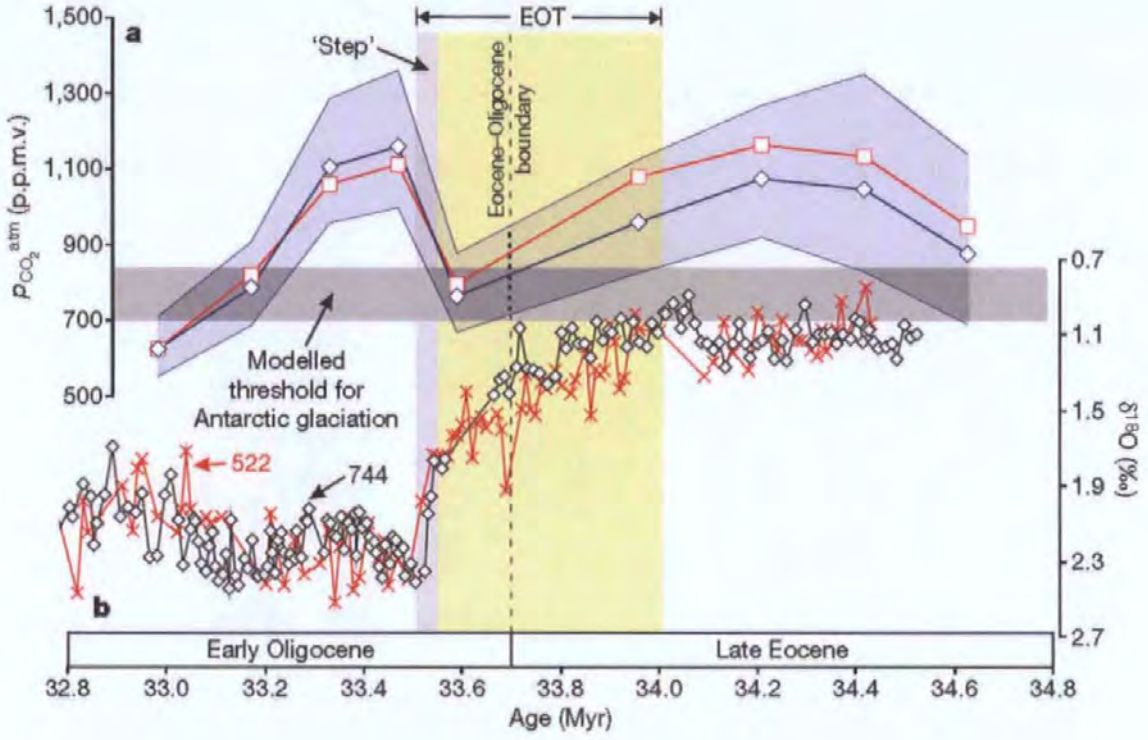

Figure 1.6 Reconstructed pCO_2 compared with the deep-sea benthic foraminiferal stable isotope record. A, pCO_2 (uncertainty from $\delta^{11}B$ measurements at 95% confidence). Blue symbols are calculated using modelled $[CO_3^{2-}]$ changes based on varying calcite compensation depth; red symbols are for constant $[CO_3^{2-}]$. The grey band is the threshold for Antarctic glaciation (Deconto and Pollard, 2003; Deconto *et al.*, 2008). B, Deep-sea oxygen isotopes from DSDP site 522 (red crosses) and ODP site 744 (black diamonds; Zachos *et al.*, 1996). Figure taken from Pearson *et al.* (2009).

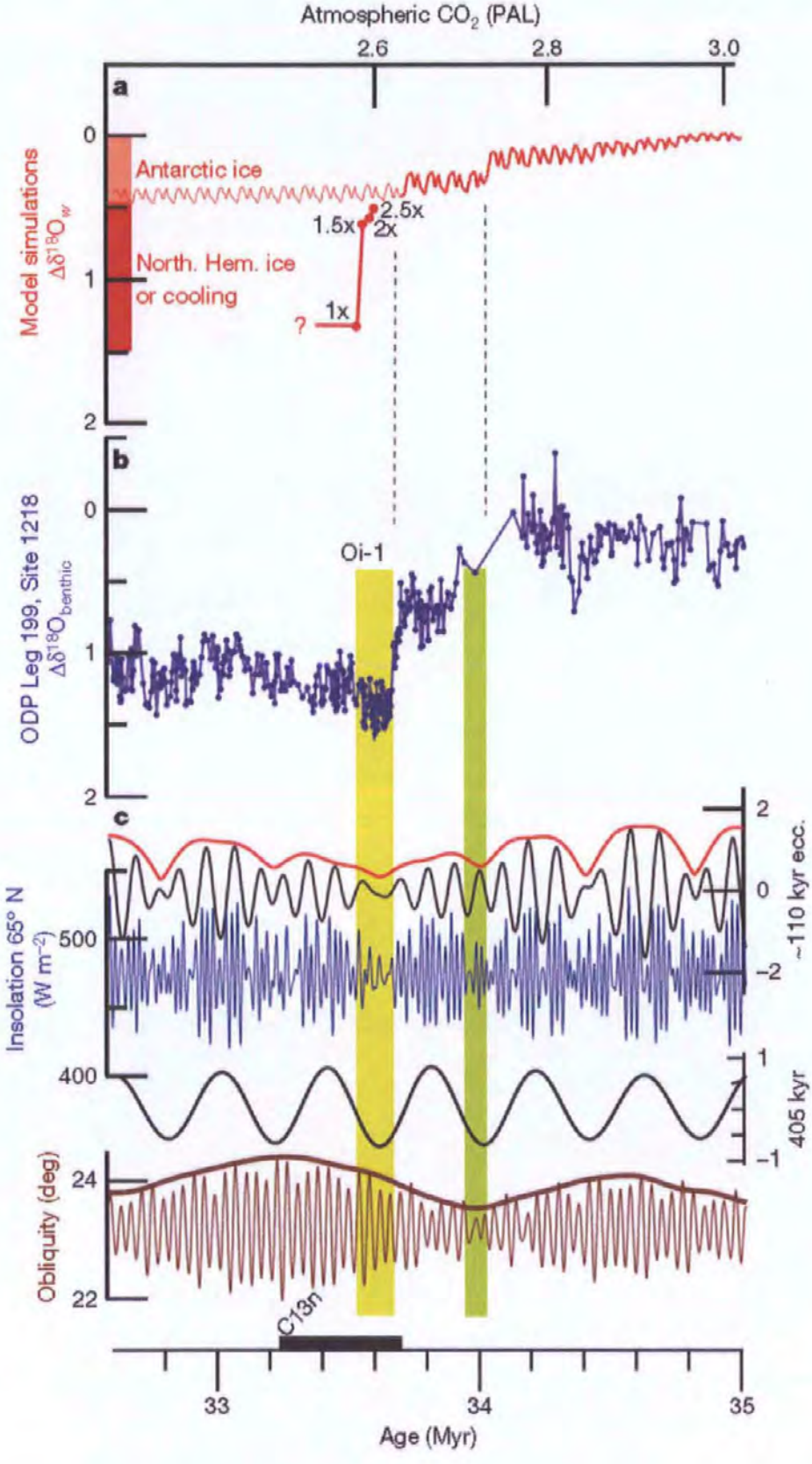

Figure 1.7 Changes in the isotopic composition of the ocean across the Eocene/Oligocene transition. Isotopic, orbital and model time series are shown on the same astronomically tuned timescale 4, with the simulated and observed stepwise timing of glaciation aligned (dashed lines) for comparison. (Taken from Deconto *et al.*, 2008).

1.5.3 Orbital forcing

Orbital forcing has a dominant effect on the extent of the ice caps, as shown by Deconto and Pollard (2003) and Deconto *et al.* (2008) models. Coxall *et al.* (2005) indicates that the Earth's own orbital configuration can be considered as a trigger for the initiation of the Oi-1 and the pacemaker for ice sheet growth. Pälike *et al.* (2006) indicate that this 'heart beat' consist of 405,000, 127,000 and 96,000 eccentricity cycles and 1.2 ma obliquity cycles. Pälike *et al.* (2006) indicates that glaciation is triggered by astronomical forcing as soon as pCO_2 levels are close to a key threshold value. Coxall *et al.* (2005) detailed investigation indicates that the initial isotopic shift (precursor) occurred during a period of minimum obliquity orbital forcing. This preconditioning lead to the prolonged absence of warm summers, inhibiting summer snow melt, allowing ice accumulation and ultimately the development of continental sized ice sheets.

1.5.4 Summary

The shift from a Greenhouse to an Icehouse world appears to be controlled by a series of tectonic, atmospheric and orbital events controlling global climate with a variety of positive and negative feedback mechanisms finely tuning its regional impacts. Tectonic forcing appears to initiate a long-term cooling trend and the reorganise of the world's continental configuration providing the perfect template for glaciation. The uplift of continental landmass (e.g. the Himalayas) kick started pCO_2 drawdown through weathering processes. Orbital preconditioning and the crossing of pCO_2 threshold then lead to a dramatic increase in ice accumulation on Antarctica.

1.6 Bipolar glaciation?

Evidence has been put forward for the existence of continental ice sheet within the greenhouse world of the late Cretaceous to Eocene (Stoll and Schrag, 2000; Kominz *et al.*, 2008; Miller *et al.*, 2005; Van Sickel *et al.*, 2004) based on large changes in sea level that could not be attributed to temperature fluctuation alone. There are questions over whether the ice volumes predicted by the $\delta^{18}O$ and Mg/ Ca ratios for the Oi-1 glaciation is achievable solely through the glaciation of Antarctica or whether Northern Hemisphere glaciation played a part. Coxall *et al.* (2005) indicted that if the isotopic composition of the Antarctic ice was less extreme than today (e.g. -30 ‰), with the implied global ice budget and apparent sea level fall for the E/O transition are correspondingly greater (-2.7 times) and impossibly large for Antarctica alone to accommodate. However, Lear *et al.* (2008) suggest that translating their~0.6 ‰ increase in $^{TM}{}_{18}O_{w}$ across the climate transition into the early Oligocene glacial maximum into an ice-volume equivalent requires estimation of the isotopic composition of ancient ice sheets (ice sheets in warmer climates could have had heavier $^{TM}{}_{18}O$ than today), but most likely represents an increase in ice volume approximately equivalent to the modern-day Antarctic ice sheet. They indicate that the ~70 m of apparent sea-level fall estimated from sequence stratigraphy (Pekar et al., 2002) is consistent with the growth of an ice sheet of this size (Lear *et al.*, 2008).

The exact timing of the initial glaciation in the Northern Hemisphere related to the Oi-1 glaciation is controversial. pCO_2 thresholds required to initiate Northern Hemisphere glaciation are significantly lower than those associated with Antarctic glaciation (Deconto *et al.*, 2008). If both were to occur during the Oi-1 transition ice sheet formation in the Northern Hemisphere would require rapid draw-down of pCO_2 by 400 p.p.m.v (to ~280 p.p.m.v) within 200 kyr (Deconto *et al.*, 2008) (Fig. 1.7). Palaeoproxies indicate a decrease in pCO_2 across this transition but both geochemical proxy data (Pearson and Palmer, 2000;

Pagani *et al.*, 2005; Pearson *et al.*, 2009) and carbon cycle models (Zachos and Kump, 2005; Merico *et al.*, 2008) predict values significantly higher than those required for Northern Hemisphere glaciation. The proxies estimate that pCO_2 remained above 290 p.p.m.v until 25 Ma and has remained near or below those values ever since (Pagani *et al.*, 2005; Pearson and Palmer, 2000). This would imply that permanent Northern Hemisphere glaciation was not achievable until the late Oligocene / early Miocene (Edgar *et al.*, 2007).

To test whether Antarctic glaciation alone was responsible for the Oi-1 transition Deconto *et al.* (2008) used GCM's to generate a similar isotopic record to those produced by palaeoproxy analysis (e.g. Coxall *et al.*, 2005; Lear *et al.*, 2008; Katz *et al.*, 2008). In order to produced a similar $\delta^{18}O$ record a deep sea cooling of 4°C was necessary and Antarctic ice was required to be less isotopically depleted (-30 to -35 ‰) than previously indicated by the palaeoproxies. Deconto *et al.* (2008) conclude that major bipolar glaciation at the E/O transition is unlikely and that the estimates of deep sea temperatures across the boundary are unreliable (e.g. Lear *et al.*, 2004).

Evidence in the form of Ice-Rafted Debris (IRD) found in sediments from the Greenland Sea (Moran *et al.*, 2006; Eldrett *et al.*, 2007; Tripati *et al.*, 2008) and the Arctic Ocean (John, 2008) have been associated with glacial ice in the Northern Hemisphere. However, the IRD could be sourced from small valley glaciers, which would be consistent with Deconto *et al.* (2008). The amount of ice responsible remains controversial as the source may be small isolated ice caps and high elevation alpine outlet glaciers (e.g. Browning *et al.*, 1996), therefore not related to full scale continental glaciations (Eldrett *et al.*, 2007). Winter temperatures calculated by Eldrett *et al.* (2009) suggests the presence of extensive Arctic Ocean winter sea-ice. It is thought that this may have increased deep convection and been responsible for the apparent initiation of Northern Component Water formation prior to the Oi-1 glacial maximum (Via and Thomas, 2006).

1.7 Summary

Understanding the events and effects of the rapid build up of continental ice on Antarctica has improved significantly in recent years, particularly through high resolution investigations from the marine realm. However, information relating to this event is particularly deficient and currently at a lower resolution in terrestrial deposits. In order to understand how this transition from a Greenhouse to Icehouse world affected terrestrial climate and biota, gaps within our understanding of the E/O transition and Oi-1 glaciation, particularly referring to Northern Hemisphere need further investigation.

Part 1: Modern Gastropods

CHAPTER 2 AN INVESTIGATION INTO THE BIOLOGY OF *VIVIPARUS CONTECTUS* (MILLLET, 1813) AND ITS EFFECT ON THE ISOTOPIC COMPOSITION OF ITS SHELL CARBONATE

2.1 Introduction

Reconstruction of palaeoclimates from proxy isotopic data requires a full understanding of the chain of processes involved in the formation of the carbonate material secreted by a freshwater proxy. Working through the various steps, even in their basic form, requires assumptions particularly when applying modern day examples to ancient systems. The chain of events leading to the ultimate isotopic composition of the freshwater that a proxy inhabits involves the isotopic composition of the host water; ground/soil/surface waters; precipitation and finally climate (see Darling *et al.*, 2005). The most important factors affecting the final isotopic composition of a carbonate freshwater proxy (e.g. freshwater gastropods) are temperature and the $\delta^{18}O$ of the water (Fritz & Poplawski, 1974; Abell, 1985; Abell & Williams, 1989; Abell *et al.*, 1995; Leng *et al.*, 1999; White *et al.*, 1999; Shanahan *et al.*, 2005), although other processes may be influential under certain circumstances. In many cases it is impossible to account for the influence that these individual processes impart on the final isotopic composition of the host water and shell carbonate, due to inherent uncertainties produced by the complex factors involved. However, it may be possible to draw basic conclusions about the climate from the more dominant processes influencing the preserved isotopic signal (Darling *et al.*, 2005).

2.1.1 Freshwater gastropods and isotopes

Fossil freshwater gastropods have been widely utilised as recorders of palaeoclimatic change (Schmitz and Andreasson, 2001; Kobashi *et al.*, 2001 Jones *et al.*, 2002; Grimes *et al.*, 2005; Harzhauser *et al.*, 2007) as their shell carbonate $\delta^{18}O$ value is generally thought to have been precipitated in isotopic equilibrium with their host water (Fritz and Poplawski

1974; Grossman and Ku, 1986; White *et al.*, 1999). In order to reconstruct past climates the relationship between the equilibrium $\delta^{18}O$ value of carbonate and the temperature of the precipitation must be well constrained (Shanahan *et al.*, 2005). The calculated fractionation factors differ significantly between different proposed relationships depending upon the method used in their determination, such as those produced using experimental measurements (e.g. Kim *et al.*, 2006; 2007); theoretical calculations (e.g. Chacko and Deines, 2008) and biological specimens from natural settings (e.g. Grossman and Ku, 1986; White *et al.*, 1999). Within the literature it is unclear which of these temperature – $\delta^{18}O$ relationships should be applied to a particular organism for a valid interpretation of the $\delta^{18}O$ data. This is further complicated by non-equilibrium isotopic effects which are generally attributed to either vital and/or non-vital kinetic effects.

Non-equilibrium vital effects are problematic when applying thermometry equations to the oxygen isotopic composition obtained from fossil shell carbonates. Taking such genus or species specific 'vital and /or non-vital kinetic effects' into account could be critical for the interpretation of temperature records calculated from proxy isotope data using current thermometry equations (Grossman and Ku, 1986; White *et al.*, 1999). The influence of vital effects on oxygen isotope fractionation is directly related to the metabolic processes of a host organism or the differential composition of internal fluids from which the mineral is precipitated (Kim *et al.*, 2006). Direction and magnitude of the fractionation varies from species to species as each organism has a unique calcification physiology (Kim *et al.*, 2006). External influences include changes in the microenvironment (Leng *et al.*, 2005) which may also impact on the isotopic fractionation.

When the oxygen isotopic composition of the host water remains constant, temperature is the most important factor affecting the sign and magnitude of equilibrium isotope fractionation (Kim *et al.*, 2006). Zeebe (1999) proposed a non-equilibrium effect on the

oxygen isotope composition of biogenic carbonates. He suggested that the oxygen isotopic composition is also dependent on the relative abundance of the isotopically distinct carbonic acid species in solution or on pH at the time of precipitation. He hypothesised that calcium carbonate precipitated from a higher pH solution would have a lower $\delta^{18}O$ value because of a greater contribution from the isotopically lighter CO_3^{2-} ion among the carbonate acid species. Conversely, experimental analysis of synthetic aragonite indicates that statistically indistinguishable oxygen isotope fractionation factors were determined under distinctly different pH conditions (Kim *et al.*, 2006).

The effect of carbonate precipitation rate on the oxygen isotope composition is also referred to as a non-vital kinetic effect. Experimental evidence concerning non-vital kinetic effects provides contradictory results. Kim *et al.* (2006) suggest that a lack of re-equilibration as a result of quick precipitation as well as preferential deprotonation of isotopically light HCO_3^- ions and the incorporation of light CO_3^{2-} isotopologues into a growing carbonate mineral could account for the kinetic isotope effects observed during carbonate mineral precipitation. However, Kim *et al.* (2007) show that no apparent kinetic isotope effects are involved during the precipitation of inorganic aragonite under the experimental conditions of their study. A detailed description of the proposed mechanisms for these offsets can be found in McConnaughey (2003).

2.2 Aims and Objectives

The causes of disequilibrium or vital effects are often systematic and can be accounted for by detailed studies of the particular genus or species in question. The aim of this study is to improve our understanding of gastropod aragonite palaeothermometry equations by calibrating the fractionation between water and biogenic carbonate (aragonite) of *Viviparus contectus* (Millet, 1813) (Fig. 2.1). A species of the genus *Viviparus* has been chosen specifically to complement the main part of this research, which focuses on palaeoclimatic

change across the E/O transition and Oi-1 glaciation (~33 Ma) in the Hampshire Basin, UK (51°41.570'N 1°19.003'W).

For a reliable interpretation of the results and formulation of the thermometry equation a clear understanding of the genus or species under investigation is necessary. This includes their biology, shell morphology, ontogeny and fecundity. Particularly relevant to isotopic investigations are the processes of shell secretion and how ontogeny and environmental stresses can affect this.

2.3 *Viviparus* Biology

The Family Viviparidea name means "live-bearing" and is derived from the Latin vivus ("alive") and parere ("to beget"). The name refers to the ovoviviparous nature of these molluscs.

The genus *Viviparus* colonises a wide range of habitats including rivers, streams, ponds, lakes, pools and marshes (Gray, 1847) and is found in parts of North America, Australia, Asia, Africa and Europe, but does not extend to Polar Regions (Boycott, 1936). The widespread distribution of species of *Viviparus* since the Eocene (~50 Ma) makes them an important geological proxy. They are gill breathers and therefore are found in permanent water bodies ranging between 0-20 m water depths (Boss, 1978). Their dependence on dissolved oxygen for respiration makes them intolerant of polluted water (Harman, 1974; Strayer, 1990); therefore, they are rarely found in stagnant water bodies e.g. shallow ponds, where oxygen levels are low at night or when temperatures are high (Jokinen, 1983). All freshwater gastropods that use gills to breathe are placed under the generalised term of prosobranch. These prosobranch species are rare in ponds and common in lakes, as they are vulnerable to hypoxic conditions common in ponds (Brown, 1991). Their thick shells, relative to the thin-shelled pulmonates (air breathing species), provide protection against shell crushing fish which are often found in lakes or large water bodies. For short periods

of time *Viviparus* can exist out of water by withdrawing into their shell and sealing their aperture with the operculum (Preshad, 1928). Annual reproduction occurs in spring with *Viviparus* occurring in large unevenly distributed aggradations (Cheatum, 1934; Jokinen, 1982). Primarily they are detritus feeders usually grazing on stones etc. They also have the ability to filter feed by collecting suspended particles via the ctenidium, which transfers them to the pallial groove and they are then raked into the mouth by the radular (Cook, 1949).

2.3.1 Reproduction

Viviparus has separate females and male individuals (gonochoristic or dioecious), unlike many other gastropod genera (e.g. *Lymnaea*) which are hermaphrodite. Within the majority of *Viviparus* species sexual dimorphism occurs, with females reaching a larger size and having longer life expectancies (Browne, 1978; Stanczykowska *et al.*, 1971) than their male equivalents. This however is not true for *V. ater* which shows no size difference or extended life expectancy between the two sexes (Staub and Ribi, 1995). Males can be easily identified by their enlarged right tentacle, which is used as a copulatory organ (Fretter and Graham, 1962).

Jakubik (2007) observed large unevenly distributed aggradations of *V. viviparus* generally occurring in the same place every year within the littoral zone of Zegrzyński Reservoir during the summer months. Similar aggradations have been observed between April and November in *V. ater* (Staub and Ribi, 1995) and *V. georgianus* (Jokinen *et al.*, 1982). During this period copulation occurs within a proportion of the active population, for example, females and males that have reached sexual maturity. This reproductive age interval for females of *V. ater* appears to be between 2 to 6 years (Ribi, 1986).

Jakubik (2007) noted during these reproductive aggradation periods:

- the highest rates of reproduction occurred;
- females contained the greatest number of embryos;
- presence of the largest number of fertile females; and
- the highest index of reproductive effort.

Several species of gastropods have been shown to follow mucus trails in search of a mate (Peters, 1964; Trott and Dimock, 1978; Mcfarlaine, 1981; Ribi and Katoh, 1998) and it has been speculated that *Viviparus* uses these chemical cues to distinguish potential mates (Dillon, 2000; Ribi and Katoh, 1998). Staub and Ribi (1995) observed that individuals of *V. ater* copulated on average 60 times between April and November. It is thought that multiple copulations throughout the aggregation period can be both beneficial and a disadvantage to *Viviparus*. Males may benefit from frequent copulation as it can increase their fitness, and enables them to transfer larger amounts of sperm to the females, increasing the offspring's chances of containing their genetic material (Trivers, 1972). The chance of the offspring produced containing the genes of a male can also be increased by optimal timing of copulation (Cheng and Burns, 1988; Drickeimer, 1992). Copulation has a large energy consumption and can take from 30 minutes (Ribi and Katoh, 1998) to 36 hours (Lind, 1988; Tischler, 1973), with multiple copulation events throughout the reproductive period which may reduce the life span of the male (Jakubik, 2006). Younger, fitter males may be more successful in competing to fertilise females. According to Jakubik (2006), the ratio of females to males in the spring is 2:1. Therefore, competition for females may not be an important factor. The energetic cost of mating is greater for males than for females (Ribi and Katoh, 1998), as females continue to feed during copulation whilst males do not. Males would therefore have limited time for feeding and are generally more active in this period (Browne, 1978). This would result in low growth and limited storage of energy reserve leading to a smaller chance of prolonged life (Browne, 1978).

Females in theory have an optimum number of times that copulation is required, as they have a limited number of eggs that they can produce in one year requiring fertilisation. Caged experiments showed that fertile *V. ater* females, which were separated from males, continued to produce offspring after being isolated for 2 years (Trub, 1990). In another cage unfertile females isolated from males did not produce any offspring. For females the cost of additional copulation may exceed any possible benefits, for example:

- interference with feeding;
- increased predation risk (Simmons, 1986; Pollard, 1975);
- physical damage by the act of copulation (Ward *et al.*, 1992) and;
- parasite infections (Armstrong, 1977; Morand, 1988).

Although there are disadvantages, some advantages have been considered. *Viviparus* males are capable of producing two types of sperm (Meves, 1902; Fretter and Graham, 1994):

- Eupyrene sperm – full chromosome set capable of fertilizing an egg; and
- Oligopyrene sperm – reduced chromosome set, sterile but large and energy rich.

Females of *V. contectus* which have been observed mating with several males in one day, have been shown to incorporate identifiable particles of both sperm types into the uterine wall and the follicle cells (Dembski, 1986). This additional ejaculate may provide the female and / or embryos with additional energetic resources (Boggs and Gilbert, 1979). Therefore, multiple copulations may be beneficial, as the total energy output may be neutral if not positive (Ribi and Katoh, 1998). Older females tend to have much higher maintenance costs (Browne, 1978) therefore multiple copulations maybe more common.

Multiple copulations may also benefit the female by:

- increasing the chance of finding better quality sperm (Curtsinger, 1991); and
- increasing genetic variation of the offspring, e.g. sperm from multiple males (Williams, 1975).

Once copulation has been completed *Viviparus* migrates back to the bottom mud. Seasonal migrations are common in lakes, with snails moving to deeper water in the autumn and back to shallower littoral areas in the spring (Cheatum, 1934). Jokinen *et al.* (1982) observed that they migrate to depths of at least 2 m. Prosobranchs very rarely have two generations per year and much more commonly show generation times of two or even three years (Dillon, 2000).

The fertilised ova are brooded in a modified pallial oviduct, sometimes called the uterus (Vail, 1977); this method of gestation is termed ovoviviparity. While the embryos develop they are fed via secretions from a protein gland, consisting of galaktogen, proteins, glycoproteins, free amino acids and calcium (Fretter and Graham, 1978; D'Asoro, 1988; Rawlings, 1994, 1999; Miloslavich, 1996). The oxygen and carbon isotope composition of the shell produced by the developing embryo has not currently been investigated. It is hypothesised that owing to the allocation of energy resources by the female to reproduction the calcium within the secretions from the protein gland will represent $\delta^{18}O$ and $\delta^{13}C$ values similar to the female's shell and in turn host water. It is unknown whether the secretions are continuous or formed in a batch. However, Alakrinskaja (1969) indicates that the secretions are gradually used up by the embryo, implying that the secretion is formed in a batch. If the secretion is continuously produced then the growth achieved by the female should have a similar $\delta^{18}O$ and $\delta^{13}C$ if not the same composition as the developing embryos. This assumes that fractionation is not taking place within the oviduct and protein gland.

As the embryo develops within the oviduct three growth stages can be recognised (Jakubik, 2007):

1. Oval , transparent egg capsule;
2. Egg capsule with visible shell contour; and finally
3. Snails with a shell.

Embryo development has a gestation time of several months (e.g. *V. ater* for 3 to 9 months (Staub and Ribi, 1995) and 9 months for *V. georgianus* (Jokinen *et al.*, 1982)). Gestation occurs during autumn and winter, when the females have migrated to deeper water and submerge themselves in the bottom mud. This migration may affect the isotopic composition of the host water. Burial within the bottom mud is likely to affect the adults shell isotopic compositions, buffering the effect of temperature changes. As the embryos are developing during this period it is likely that their isotopic composition will also represent this change. Release of the juveniles occurs during spring once favourable conditions are achieved for *Viviparus* to translocate to shallower water. The juveniles are released individually, protected by a protein shield which breaks away soon after birth (Jakubik, 2007). Giving birth to fully developed young is a relatively rare phenomenon among gastropods. Reproduction the following year can only take place once the developed juveniles have been released, generally occurring during April or when conditions are suitable. Once released the juveniles tend to prefer living at depth. This behaviour is interpreted by Keller and Ribi (1993) as predator avoidance, due to the relatively thin shells of juveniles. Dillon (2007) suspects that the environment may play a role in the determination of prosobranch sex, although the theory on the evolution of environmentally determined sex does not seem to fit the particulars of prosobranch natural history (Charnov and Bull, 1977).

Development of ovoviviparity is an evolutionary response for the need to increase offspring survival rates. When comparisons are made between *Lymnaea elodes* (Brown *et al.*, 1988) and *Viviparus georgianus* (Jokinen *et al.*, 1982), survival to maturity is much less for the pulmonate populations (1%) than for the ovoviviparous prosobranchs (40%) (Brown, 1991). Pulmonate species lay multiple egg batches throughout the breeding season. These egg batches are more vulnerable to attack and changes in environmental conditions, whereas, the ovoviviparous prosobranch eggs are contained in the ovaries until they reach a size at which they have a greater chance of surviving in the natural environment. *Viviparus* gastropods therefore place all its efforts into a single brood per year, often containing a small number of juveniles, but these juveniles have a greater chance of reaching maturity.

This method of reproduction gives some indication that their development stages have strict physiological requirements; therefore species of prosobranchs may have a greater tendency to remain in their home areas, that is, to be philopatric (Boss, 1978).

2.3.2 Growth rates

According to Fretter and Graham (1976) *V. viviparus* has the ability to grow throughout the year, with the only limits on growth caused by the cold and lack of food. An all year round growth cycle, without a distinctive winter break, was noted by Young (1975) in *V. viviparus* from the Worcester - Birmingham Canal in England, also in *V. ater* (Italy) (De. Bernardi *et al.*, 1976) and *V. georgianus* (USA) (Browne, 1978).

Growth rates vary due to both the behaviour of the species and changes to its environment. Conditions affecting growth rates are:

- Ontogeny;
- Reproductive phase;

- Seasonality and temperature;
- Food availability / diet;
- Water chemistry; and
- Dissolved calcium concentrations.

2.3.2.1 Ontogeny

As with the majority of organisms juveniles allow more energy for growth, where adults use more energy for reproduction. Growth rates can also vary due to the sex of the gastropod, as females tend to be larger in size due to longer life expectancies and faster growth (Browne, 1978). Browne (1978) showed that on average females of *V. ater* are 9% larger than males after the first 12 months.

2.3.2.2 Reproductive phase

The proportion of energy allocated to growth varies with age, as a greater percentage is utilised for reproduction later in life (Brownie and Russell-Hunter, 1978; Tashiro, 1982; Russell Hunter and Buckley, 1983). Shell growth continues throughout life (Heller & Farsley, 1990; Pointier *et al.*, 1992) with a greater investment in widening the shell after sexual maturity. An example from Lake Tully (USA) indicates that *V. georgianus* allocates 5.3 % of their energy as a 2 year old and 79.6 % of their energy as a 4 year old towards reproduction (Buckley, 1986). This alteration in energy expenditure exists as fecundity increases with increasing shell height. The larger size of the females allows for the accumulation of energy reserves and the appropriate space within the shell for the snail's body and an oviduct filled with embryos. A larger number of embryos are able to exist within the reproductive tract and the embryo size and growth stage are generally more advanced (Jakubik, 2007). In *V. ater* it has been observed that the larger females tend to

increase the size of their offspring rather than the number of offspring (Ribi and Gebhartdz, 1986) most likely to increase juvenile survivorship.

Differences in biomass accumulation and growth rates can be ascribed to differences in habitats. For example, Gebhardt and Ribi, (1987) investigated two lakes with different climatic regimes that contained *V. ater*. In Lake Zürich *V. ater* showed high initial growth rates for the first two years after which energy requirements were re-directed into reproduction. In Lake Maggiore the size of the 1-2 years old *V. ater* were considerably smaller than in Lake Zürich, due to the low $CaCO_3$ concentration, limited food supply and stony bed. This abnormal environment induced stresses in the form of pitting, dissolution and abrasion weakening the shell.

2.3.2.3 Seasonality and temperature

Growth bands indicate changes in mantle secretary activity and alterations in the ratio of matrix to crystalline deposition. When growth ceases a band is formed by a slightly raised part of the shell, deep groove or a different colour. Conditions that bring about ring formation within gastropods are:

- Winter or annuli bands, formed during the winter when temperatures fall below the species cold temperature threshold;
- Summer bands - inhibition of growth at high temperatures (less common in temperate regions);
- Lack of food / starvation; and
- Physical disturbances, e.g. predation or human intervention.

Growth bands have been used to reconstruct and model the life history of gastropods (Gebhardt and Ribi, 1987) and have been successfully applied to freshwater bivalves (Detterman *et al.*, 1999). It may therefore be possible for age reconstruction to be carried

out by using isotopic data and the positioning of growth lines on the shell. Seasonal and disturbance cessation marks can be distinguished by the combination of the two methods. Firstly, for gastropods, the deeper, well defined cessation marks represent seasonal changes, whereas on bivalves these cessations are represented by ridges that stand proud of the normal shell level (Detterman *et al.*, 1999). Secondly, micro-milling of the shell carbonate for isotopic analysis can provide information on whether the seasonal cessation marks coincide with the most positive isotopic values (e.g. Schmitz and Andreasson, 2001). If they coincided they are likely to be due to changes in temperature, as disturbance marks tend to be less obvious and are less likely to occur in winter, particularly as *Viviparus* migrates to the bottom mud over winter. Complication may arise where the cessation threshold temperature is not exceeded during a particular winter, therefore cessation may not occur. If the winter temperature fluctuates around the threshold value several cessations may be produced. In temperate zones temperatures falling below cold threshold values are more likely than those exceeding hot threshold values, therefore cessation marks are more likely to be caused by winter cold.

Jokinen *et al.* (1982) determined ages in *V. georgianus* using the mean shell width and number of opercula rings, thought to be related to winter cessation (Fig. 2.1). According to Jokinen *et al.* (1982) *V. georgianus* had a life span of 3 years for females and 2 years for males. Schmitz and Andreasson (2001) showed that *Viviparus* shells from temperate to subtropical zones had the most positive $\delta^{18}O$ values associated with a zone of thickened and irregular growth layers, reflecting decreased growth rates in connection with winter hibernation. As *Viviparus* tends to grow rapidly for the first 2 years, a clear seasonal cycle (assuming there is one) will be seen in the isotopic data. As the specimen gets older the growth rate slows causing the isotopic signal to become compressed if displayed against growth rather than time.

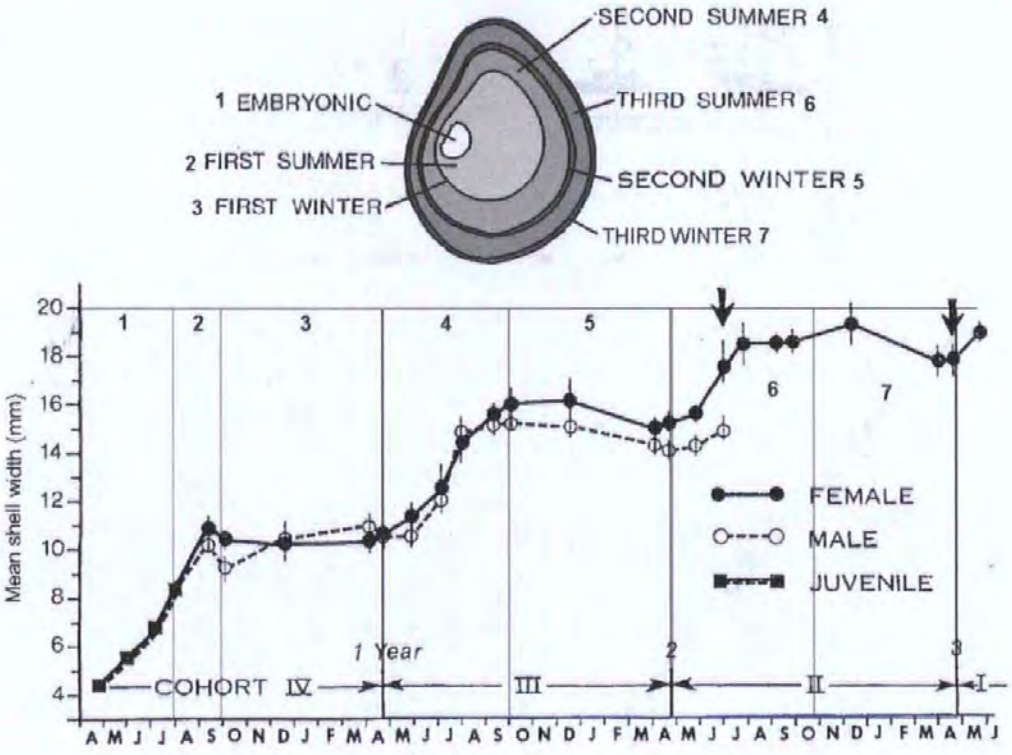

Figure 2.1 Two diagrams showing the structure of an operculum from a 36 month old female *V. georgianus* from Lake Waramaug Connecticut, USA. Each cessation of growth is marked by two bands close together, in this case representing winter growth cessation. The operculum is compared with the shell growth for the entire life cycle of this species. The time period between the dark arrows represents the time period the female is carrying maturing eggs / embryos. (Diagrams modified from Jokinen *et al.*, 1982).

The first formal classification of freshwater gastropod life cycles (Russell-Hunter, 1961, 1964, 1978) is based on the number of generations per year and survival after egg laying (based on pulmonates). The classification was expanded and modified by Calow (1978):

- One generation a year, reproducing semelparously in spring / late summer.
- Two generations per year, the spring born iteroparous and the late summer born semelparous.
- Two generations a year both semelparous
- Three generations a year, spring, summer generation's iteroparous, autumn generations semelparous.

- Three generations per year, spring generation's semelparous, summer iteroparous, and autumn semelparous.
- One generation per year reproducing interoparously per a two year generation time.
- Three semelparous generation per year.

Dillon (2000) additionally added:

Hi. Populations that required 24 – 35 months to mature and reproduce interoparously.

Hs. Those reproducing semelparously at age 24 – 35 months.

From this classification *Viviparus* would fit into the Hi category.

Semelparity and iteroparity refer to the reproductive stage of an organism. A specie is considered semelparous if it is characterised by a single reproductive episode before death and iteroparous if it is characterised by multiple reproductive cycles over the course of its lifetime.

2.3.2.4 Food availability / diet

Snails are able to exert control the materials entering their mouths, therefore are ecologically specialised (Dillon, 2000). Each species may have special adaptations and dietary preferences. The following are some of the substrate preferences of gastropods in general:

- Suspended particles;
- Detritus;
- Bacteria;
- Algal filaments;

- Diatoms;
- Macrophytes; and
- Carrion e.g. fish eggs or dead fish etc.

Viviparus are unusual in that they have two feeding habits, filter feeding and grazing. Most Viviparids are detritivores, utilising the bacteria associated with detritus. However, *Viviparus* prefers filter feeding in muds and silts as their dietary preferences are associated with this particular substrate (Studier and Pace, 1978). In the absence of silts and muds they have retained their ability to graze (Dillon, 2000), the method for which is outlined in Figure 2.2. In the case of *Viviparus* the method of feeding depends on the abundance of algal growth and diatoms. The gills of *Viviparus* are characterised by unusually large triangular lamellae whose tips hang over a ciliated gutter or 'food groove' running across the floor of the mantle cavity (Cook, 1949).The cilia propel water currents through the mantle cavity, with particles becoming entrapped onto the mucus covered gill filaments. A mucus food string forms in the food groove which is carried forward and collected into a ball or sausage. Periodically the snail will turn its head to collect the food. To complete the food digestion, follow the flow diagram (Fig. 2.2) from box 6.

An example of the different feeding habits comes from *V. georgianus,* which has been documented as a micro-algivore (Duch, 1976; Jokinen *et al.*, 1982) and a detritivore on fine particulate organic matter (Pace and Szuch, 1985). During macrophyte decomposition nitrogen levels rise increasing the value of the food source (Brown, 1991). This can produce high density accumulation of *Viviparus*, which has been observed in *V. georgianus* (Pace and Szuch, 1985) and *V. subpurpureus* (Brown *et al.*, 1989).

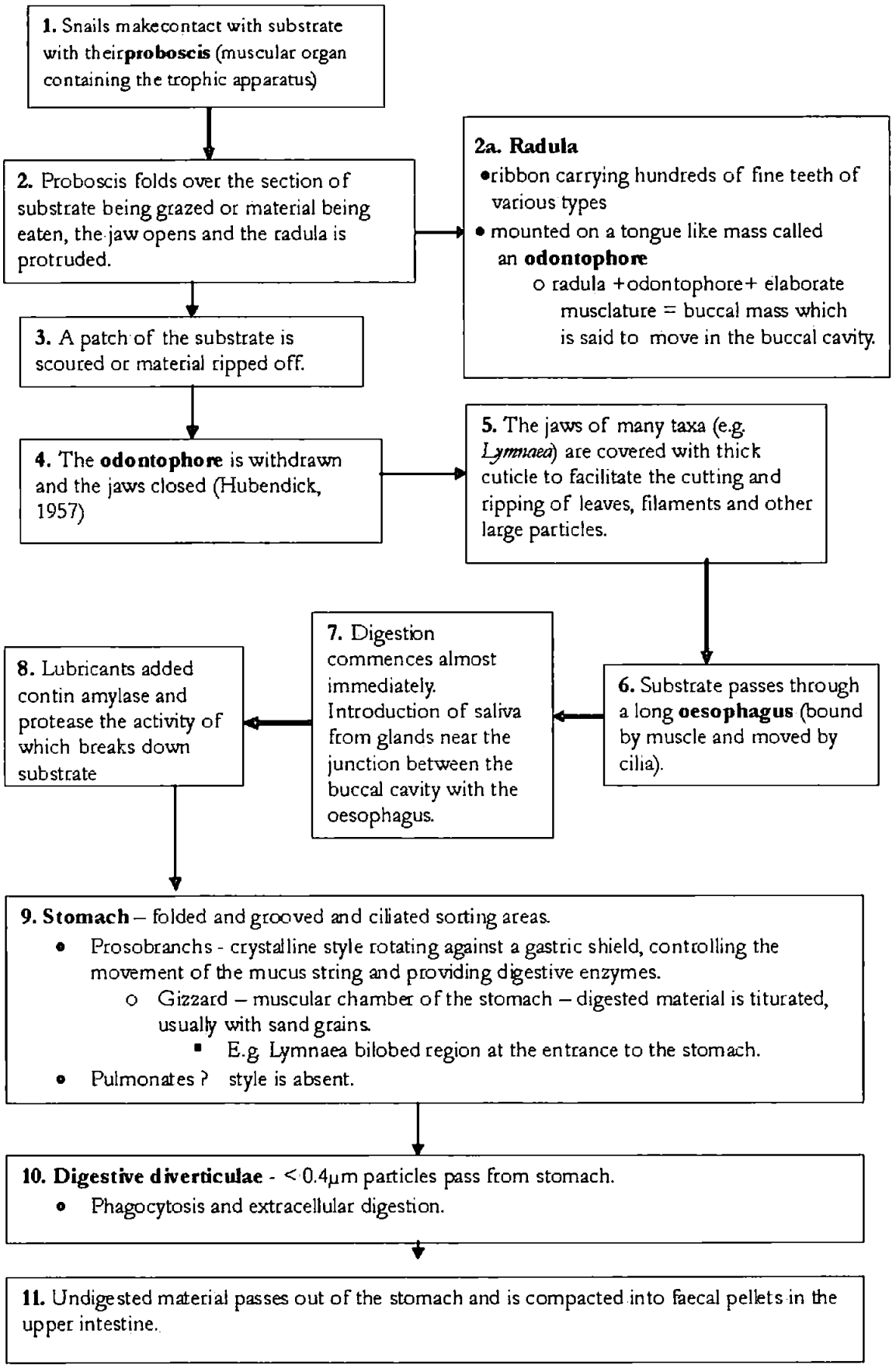

Figure 2.2 A flow diagram showing the feeding processes for grazing freshwater gastropods.

2.3.2.5 Water Chemistry

There are six water chemistry factors that influence freshwater gastropods growth:

- Water temperature;
- pH, a limnological factor of importance which is intricately entangled in the complex biological system of a body of water and affects at least indirectly the snail fauna (Hubendick, 1958). Below pH 6 gastropods are not normally found (Perera and Yono, 1984; Brown, 1980; Hall-Spencer *et al.*, 2009);
- Dissolved oxygen;
- Chloride concentrations; and
- Water hardness PO_4^{3-}.

2.3.2.6 Calcium concentrations

Freshwater gastropods have a fundamental physiological requirement for calcium in order to complete development successfully (Russell-Hunter, 1964; McMahon, 1983; Dillon, 2000; Briers, 2003). Decalcification of the shell can occur if there is a carbonate deficiency in the water (Ribi *et al.*, 1986). Variation in environmental calcium levels influence taken from Dillon (2000):

- Growth;
- Survivorship (Harrison *et al.*, 1970; Young, 1975; Dussart, 1976; McMahon, 1983; Dillon, 2000);
- Fecundity; and
- Distribution of gastropods.

Approximately 45 % of all freshwater gastropods are restricted to waters with calcium concentration greater than 25 mg / litre and 95 % to levels greater than 3 mg / litre (Brown, 1991). It may be energetically costly to secrete calcium into the shell against an electrochemical gradient (Dillon, 2000).

2.3.3 Shell Formation

Understanding the shell formation process is vital when selecting shell material for analysis and the realistic interpretation of isotopic data. The mantle tissue, a thin organ lining the inside of the aperture, is responsible for the secretion of carbonate (either in the form of calcite or aragonite) and crystal formation. Between the mantle and the shell is a thin zone of extrapallial fluid (EPF) which is directly responsible for carbonate secretion (Shanahan *et al.*, 2005). Calcium and other ions are supplied by direct uptake from the surrounding environment at the external body surface, the gills and in some cases such as with *Lymnaea stagnalis,* by digestion in the form of metabolic carbon (Wilbur and Saleuddin, 1983). According to McConnaughey *et al.* (1997) metabolic carbon can account for < 6 - 10 % of the total carbon used in shell formation. Carbon dioxide is converted into bicarbonate then to carbonate within the EPF, where it is catalysed by carbonic anhydrase (Wilbur and Younge, 1964). In general there are two phases of shell formation (Wilbur and Saleuddin, 1983):

- Cellular processes of ion transport, protein synthesis and secretion.
- A series of physicochemical processes in which crystals of $CaCO_3$ are nucleated, orientated and grow in intimate association with a secreted organic matrix.

See Figure 2.3 for diagrammatical explanation of the process by which shell secretion takes place.

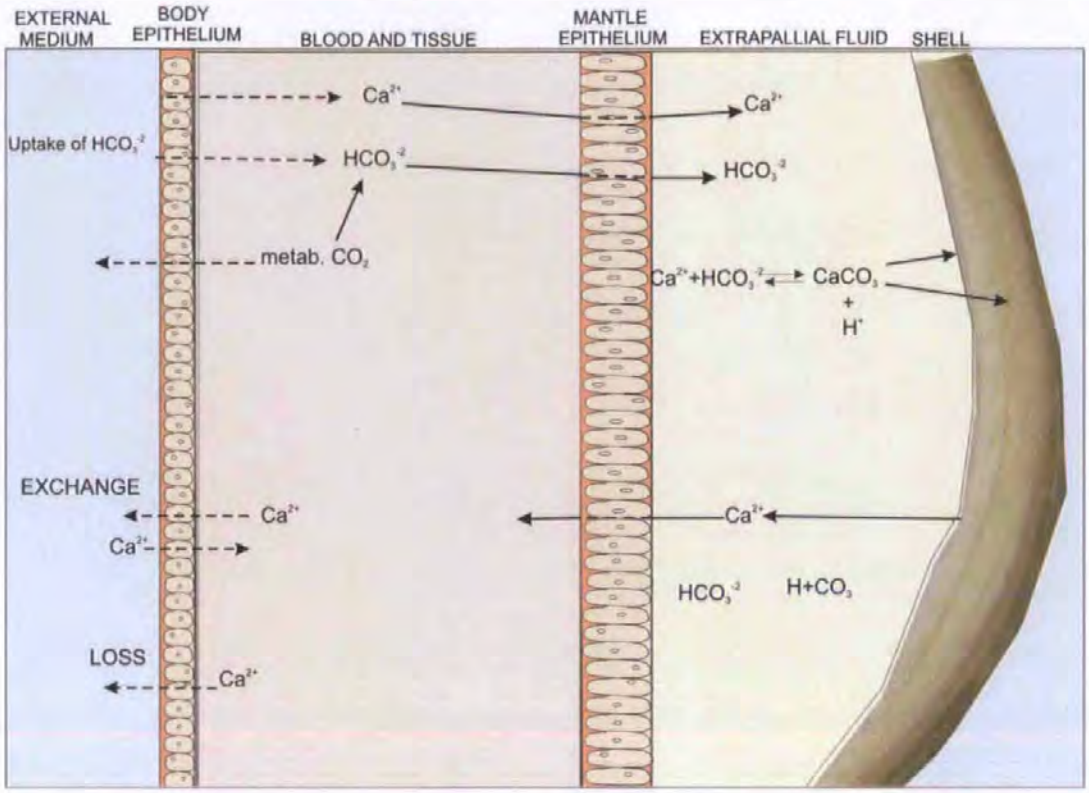

Figure 2.3 A schematic representation of the process by which mollusc shell mineralization takes place, re-drawn from Wilbur and Saleuddin (1983).

The shell formed by this process results in a thin outer layer, the organic protein periostracum (generally absent in fossil shells), with the main part of the shell constituting 2-3 calcareous layers:

- Outer prismatic layer.
- Middle lamellate layer.
- Inner nacreous layer (the hypostracum).

All three layers consist of calcium carbonate (either aragonite or calcite) and can be distinguished by the different growth structures. For example, the prismatic layer has vertical crystals which are bound together by organic proteins. This crystal structure

produces the growth banding observed on the outer shell surface. The nacreous layer on the other hand forms rounded flattened crystals producing conical stacks (Wilbur and Saleuddin, 1983; Mutvei, 1978).

Aragonite or calcite forms between 96.6 % and 98 % of the total amount of inorganic constituents in a gastropod shell (Cox, 1964). Small quantities of silica, aluminium and oxides of iron also occur in most shells and in some there is a small amount of magnesium carbonate (Cox, 1964).

2.3.4 Population Dynamics

The reproductive pattern adopted by *V. viviparus* is the most influential factor on population dynamics with females appearing to be dominant (Jakubik, 2003, 2006, 2007). Jakubik (2006) observed that the ratios varied seasonally, with the ratio of females to males being 2:1 in spring and 1:1 in autumn. He proposed that these ratios altered due to either males dying off in winter or earlier migration to deeper water than females. It may also be linked to the increase in reproductive effort which may weaken the male and shorten its life span.

Jakubik (2006) assigned different sized *V. viviparus* into four classes:

I - ≤8.0 mm long and have hair characteristics of young snails.

II – 8.1 to 12.0 mm width and height

III – 12.1 to 25.0 mm width and 12.1 – 20.0 mm height

IV – 25.1 to 35 mm width and 20.1 to 35.0 mm height.

The results showed that in spring females of classes III and IV and males of classes II and III were dominant, with fertile females making up 50 to 90% of the population.

2.3.5 Life Expectancies

Estimates on the life span of the genus *Viviparus* vary with species (Table 2.1). Life expectancies may be different between males and females for example *V. georgianus* female life expectancies were more variable then males (Browne, 1978).

Species	Age estimate	Author
V. viviparus	5-10 years	Piechocki, 1979
	4 years	Samachwalenko and Stonczykowska, 1972
	2 years	Young, 1975
V. contectus	4 years	Samachwalenko and Stonczykowska, 1972
V. georgianus	2 to 3 years	Jokinen *et al.*, 1982
	Males = 2 years Females = 2 to 3 years	Browne, 1978
V. ater	6 years	Gebhardz and Ribi, 1987
	>10 years	Ribi, 1986
V. malleatus	4 years	Stanczykowska *et al.*, 1971

Table 2.1 Estimated life expectancies taken from the literature for several species of *Viviparus*.

2.4 Methods

South Drain Canal on the Somerset Levels (Somerset, UK) was chosen based upon the known occurrence of *Viviparus contectus (V. contectus)* (Fig. 2.4) and because large flowing water bodies (river or canal), as opposed to standing waters such as lakes, have been shown in previous studies (White *et al.*, 1999) to have hydrological conditions that

allow the isotope composition of the water to remain relatively constant throughout the year.

Figure 2.4 Example specimen of *V. contectus* from South Drain Canal.

The methods used in the production of the *V. contectus* thermometry equation were modified from those techniques outlined by White *et al.* (1999).

2.4.1 Field based method

South Drain Canal forms part of a man made drainage system, initially constructed to drain the Somerset Levels for agricultural use in response to the Brue Drainage Act of 1801 (Dunning, 2004). The sampling site is located between the villages of Chilton Polden and Burtle, where the Chilton Road crosses South Drain Canal (51°10.839'N 2°52.815'W).

An I-button data logger was installed to record water temperatures every two hours throughout the 12 month sampling period. The I-button was placed inside a mesh and nailed to a post which was hammered in just beneath the bridge so that it was safe from dredging but still within the main channel. The post was put in place at 12.10 pm on the 31/10/2007. As a backup on every sampling trip temperature, pH and salinity of the water (at the same location and approximate water depth) were collected using a Yellow Springs Incorporated (YSI) model 63, pH, Conductivity, Salinity and Temperature probe. During each sampling visit (approximately once per month) water samples were collected and

analysed for $^{18}O/^{16}O$ ratios and the $^{13}C/^{12}C$ ratios of total dissolved organic carbon (TDIC) (see full methods in Appendix 2). The collected water samples were filtered in the field through a series of filters (1.2 mm, 11 μm and 0.2 μm) to remove any particulate matter. Samples for oxygen isotope analysis were refrigerated in 30 mL Nalgene Narrow-Mouth Low-Density Polyethylene (LDPE) Bottles (Rochester, NY) until analysed. Temperature (±1°C), pH (± 0.2) and salinity (±0.5) measurements were also measured on site.

2.4.1.1 Field based methods for the collections of *V. contectus*

A minimum of 5-10 *V. contectus* specimens were collected from the bottom sediments of South Drain canal (~4 m in depth) using a drag net, approximately once a month between 30/8/2007 and 13/8/2008. Upon return to the laboratory the *V. contectus* samples were ethically euthanized by cryogenesis. Their bodies were removed from the shells, sexed (males have a deformed fattened left tentacle forming the penis) and when eggs / juveniles occurred these were also counted. The shells were soaked overnight in dilute (2%) NaOCl to remove organic material including the periostracum. The shells were then rinsed in ultra pure water and oven dried at 25°C. Using a small Dremel drill and a 0.4 mm tungsten carbide spade drill bit, approximately the last millimetre of shell growth was removed by milling the growth bands parallel to the aperture edge. A minimal number of growth bands were removed to produce a powdered sample at the weight required (~0.30 to 0.50 mg) for the $^{18}O/^{16}O$ and $^{13}C/^{12}C$ ratios to be analysed.

2.4.1.2 Outline of the field cage method

Development in the understanding of growth rates in *Viviparus* and the need for more reliable data for the production of the genus specific thermometry equation, lead to the

addition of two cages submerged into South Drain on the Somerset Levels (Fig. 2.5). On 29th February 2008 at the South Drain canal site, two cages were submerged to a depth of ~4 m, embedding approximately 5 cm of the bottom part of the cage into the canal bed sediment. The first cage consisted of a cylindrical metal structure (height 30 cm, diameter 13 cm), encased in a 15 mm^2 metal mesh (Fig. 2.6A). The second cage was a plastic box (height 23 cm, width 24 cm) encased in 2 mm^2 plastic mesh (Fig. 2.6B). Each cage contained 10 *V. contectus* specimens of varying sizes (ranging from 1.4 mm in height and 1.3 mm in width to 3.6 mm in height and 2.8 mm in width) that had been collected that day. Each specimen was numbered and the aperture (growing edge) was marked with white paint so that any subsequent growth could be identified. During each monthly sampling visit the cages were removed for inspection. Any specimens exhibiting new growth along their aperture edge were measured (using a tape measure) from the white line marking the previous location of the aperture to the present aperture edge (Fig. 2.7A). Samples exhibiting more than 0.5 mm of growth were taken back to the laboratory for analysis. The remaining specimens and replacements for those taken were remarked and returned to the cage. In general the smaller (spire height < 2 cm) specimens (approximately 6 to 12 months old) acquired more shell growth per month than the larger specimens, which led to smaller specimens being preferentially chosen as replacements.

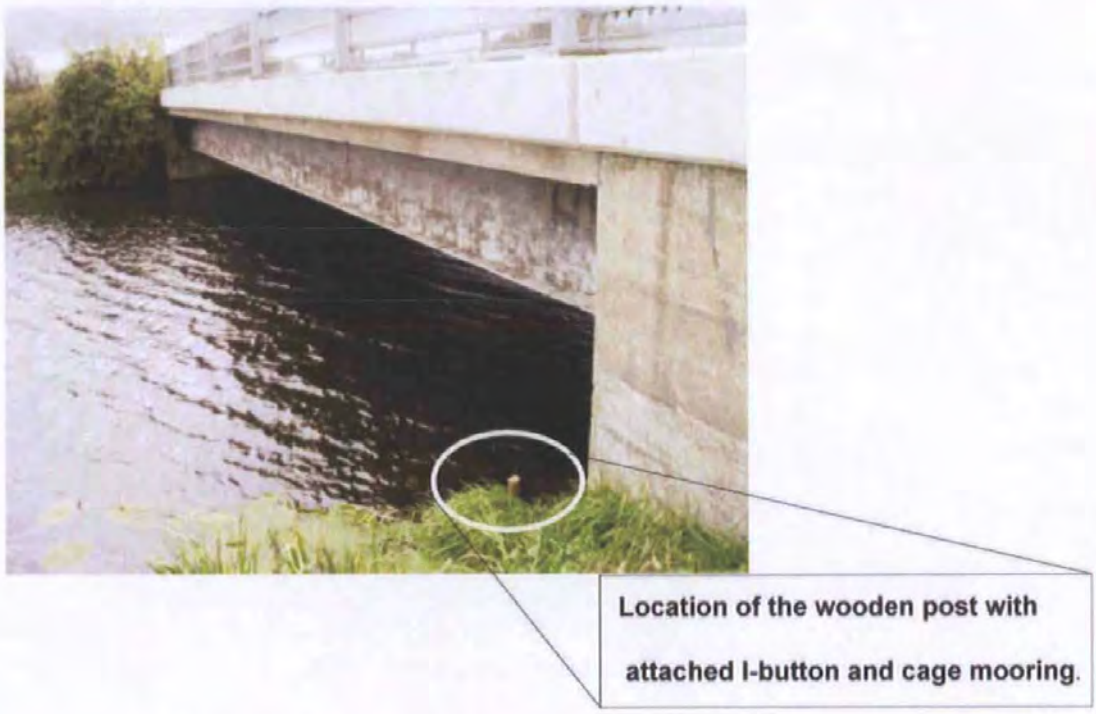

Figure 2.5 South Drain Canal on the Somerset Levels, showing the location of the cages and I-button.

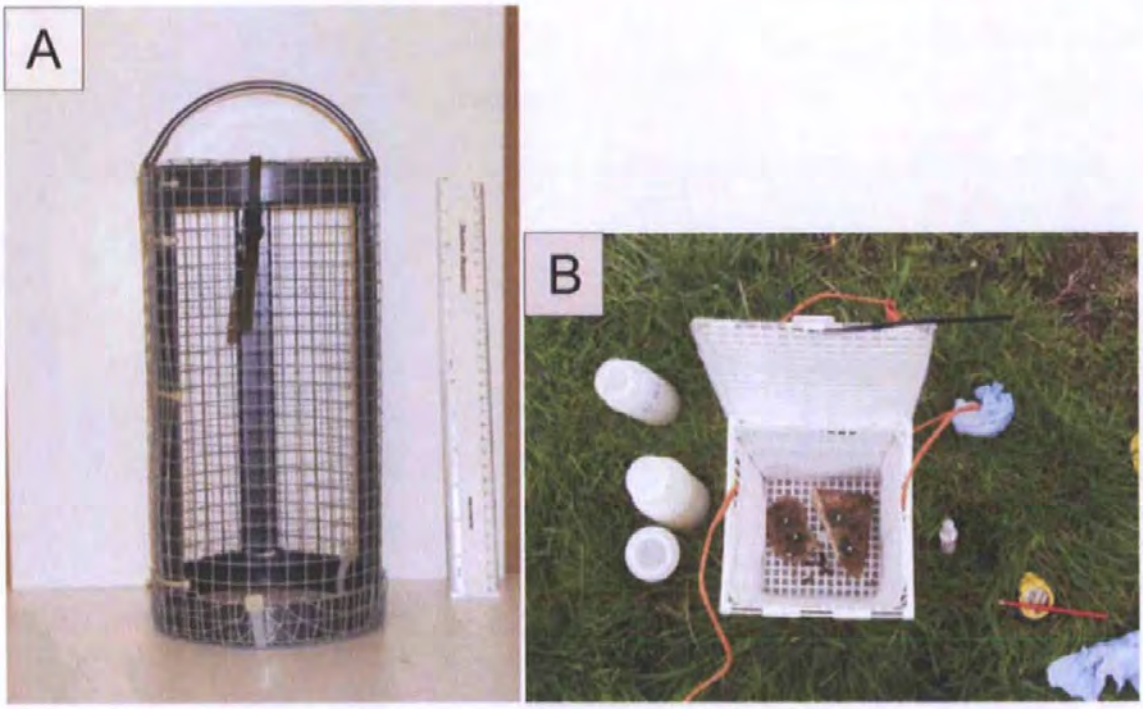

Figure 2.6 Photographs showing the metal and plastic cages used in the field cage experiments.

On return to the laboratory the specimens from the cage experiment were treated as stated for the 'field based *V. contectus* sample collection' with an additional preparation step. A small hole (~0.3 mm in diameter) was drilled into the shell marking the position of the white paint lines (Fig. 2.7B/C), as during the removal of the residual organic material by NaOCl, the white paint was also removed. Growth while within the cage dictated the number of drill lines taken for isotopic analysis, i.e. each drill line was c. 0.4 mm in width and therefore if growth exceeded 0.4 mm then a greater number of samples could be taken. Each drill line followed the growth banding parallel to the aperture, incorporating a minimal number of growth bands without compromising sample size. In an attempt to reduce errors the drill lines were located close to the position of the white line, as this growth was secreted closest to the collection of $\delta^{18}O_{water}$ samples and temperature readings. Shell stabilisation for drilling purposes depended on the amount of growth secreted by the specimen. Infilling of the shell with resin was necessary when growth was greater than 2-3 mm.

Two specimens that had remained within the cage from February to July 2008 and one other specimen that had remained within the cage for the whole experiment (February to August 2008), were chosen to determine isotopic variation in growth secreted during spring to summer. To investigate whether sexual dimorphism or fecundity affect oxygen isotope fractionation the three specimens sampled were: a male (VC 8), a female containing 16 eggs (stage 1 of the embryonic development) (VC 9), and a female containing 21 juveniles (stage 3 of the embryonic development) (VC 5) (Table 2.2). As the mean growth achieved by the three specimens was 24 mm, infilling with resin was necessary for shell stabilisation. Each shell was in-filled with blue resin so a clear comparison between the resin and shell could be seen to prevent any resin from being incorporated into the carbonate sample. For each specimen an average of 11 drill lines of c. 0. 4 mm width were sampled from growth bands parallel to the aperture. As continuous

monitoring was not possible dates for the intervening samples (between the monthly collections, e.g. the white lines) were calculated by dividing the total amount of growth secreted within a specific time period, e.g. 19 mm over 42 days, giving an average daily growth rate of 0.45 mm per day. The position of the drill line was measured from the beginning of the specific sampling period (position of the white line) and was used in combination with the average growth rate to calculate an approximate date at which the growth bands encompassed by the drill line were secreted. Therefore, a constant growth rate was assumed throughout any given time period.

	Specimen	Tank temp. (°C)	Sex	Egg/ juveniles	Shell		Aperture		Total aperture growth (mm)	Duration in Tank/Cage (days)	Growth rate per day(mm)
					Height (mm)	Width (mm)	Height (mm)	Width (mm)			
Cage	VC 5		Female	21 juv's	3.1	2.5	1.6	1.2	24.0	167	0.144
	VC 8		Male	-	2.5	2.0	1.3	1.1	21.0	126	0.167
	VC 9		Female	16 eggs	3.0	2.4	1.6	1.3	26.5	126	0.210
	VC 14		Male	-	1.9	1.8	1.1	0.9	3.0	110	0.027
	VC 26		Female	-	1.5	1.3	0.8	0.7	2.0	28	0.071
	VC 27		Female	-	1.5	1.4	0.9	0.8	3.0	28	0.107
Laboratory	VC 3	15	Male	-	1.7	1.5	1.0	0.8	0.9	48	0.019
	VC 7		Male	-	1.4	1.2	0.8	0.7	0.5	48	0.010
	VC 6	20	Female	-	1.3	1.3	0.9	0.8	0.9	48	0.019
	VC 3		Female	-	1.7	1.5	1.0	0.8	0.8	48	0.017
	VC 5	25	Female	-	1.8	1.6	1.1	0.9	1.2	48	0.025
	VC 6		Female	-	1.5	1.4	0.9	0.8	2.0	48	0.042

Table 2.2 Information on *V. contectus* regarding the sex, whether the specimens contained eggs or juveniles and shell measurements. The measurements indicate shell secretion rates for six specimens taken from the cage experiment and six specimens from the laboratory experiments.

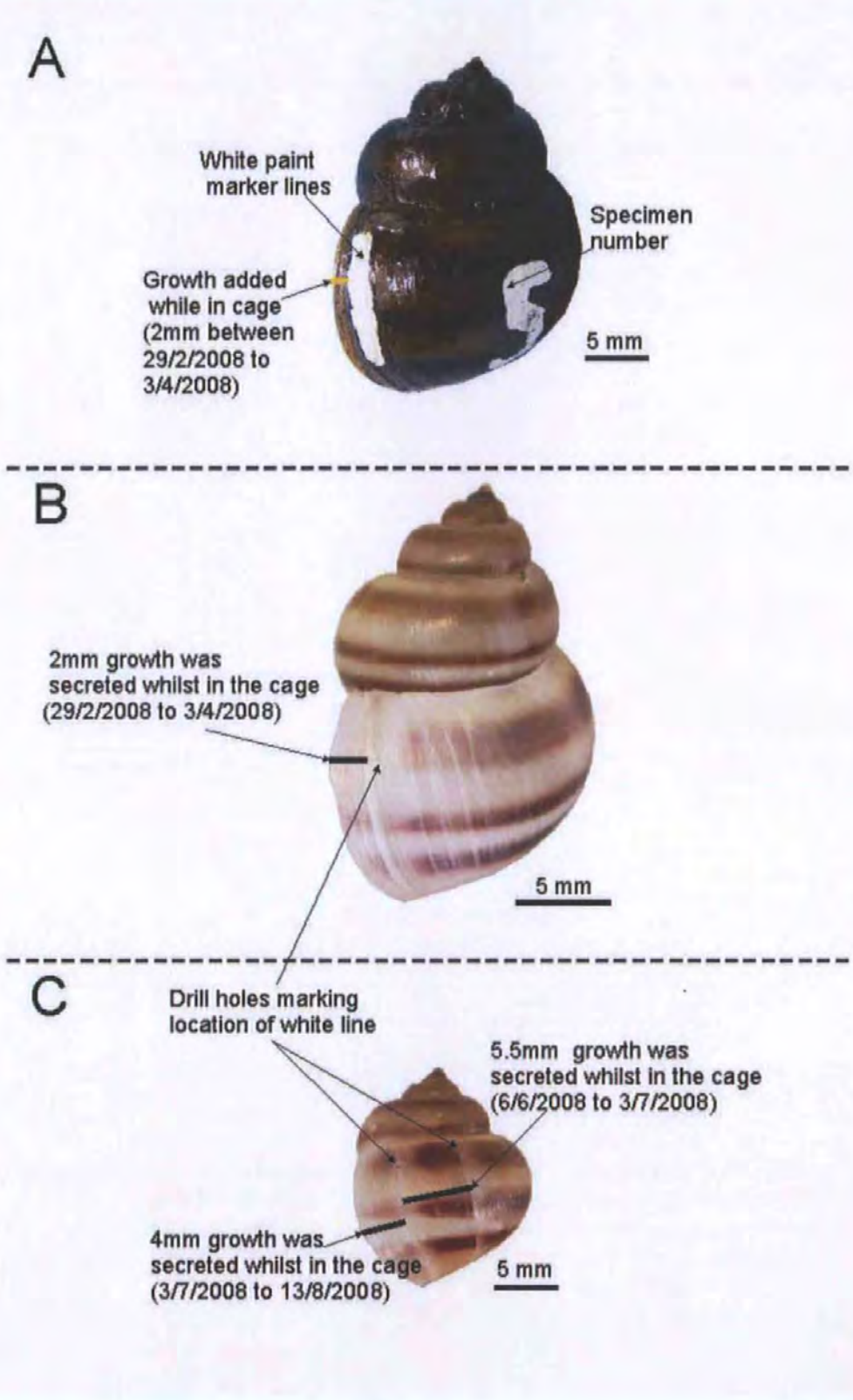

Figure 2.7 Three specimens from the field cage experiment. A) A specimen before being treated with NaOCl showing the white line marking the location of the aperture at the previous time of collection. B) and C) two specimens after they had been cleaned with NaOCl showing the drill holes marking the position of the white lines. Associated with these white lines are disturbance cessation marks.

2.4.2 Laboratory culturing method

V. contectus samples were collected from South Drain during the first sampling trip (August 2007) with additional specimens added during February 2008. These specimens (~10 per controlled temperature) were cultured thereafter in tanks in the laboratory at controlled temperatures (15°C, 20°C and 25°C) for a period of approximately two months, or until each specimen had added enough new shell growth for sampling. The growing edge (aperture) of the *V. contectus* shells was marked with white paint before being added to the culturing tanks to ensure that new growth could be identified. The specimens were kept in deionised water containing 14.7 g of $MgSO_4$, 11.7 g of $NaHCO_3$, 0.48 g of KCl and 5.4 g of $CaSO_4$ (for every 60 litres), to maintain suitable water quality for the gastropods to live comfortably (Rundle *et al.*, 2004). The isotopic composition, temperature, pH and salinity of the water were measured weekly during the culturing period. Samples were collected for isotopic analysis, while temperature, pH and salinity measurements were collected using a Yellow Springs Incorporated (YSI) model 63, pH, Conductivity, Salinity and Temperature probe. The waters isotopic content was monitored through weekly collections each sample was passed through a 0.2 μm filter and collected in 30 mL Nalgene Narrow-Mouth Low-Density Polyethylene (LDPE) Bottles. Care was taken to remove air bubbles produced when the cap was tightened, as these may fractionate the water samples altering the isotopic composition during refrigerated storage. Initial isotopic analysis of the collected water samples revealed that evaporation was taking place particularly within the warmer tanks. To minimise evaporation, particularly in the 25°C tank, each tank was sealed with cling film causing most of the vapour to condense and be recycled back into the tank. Minimal aeration ensured that the water was well mixed and oxygen levels were sufficient to sustain the gastropod specimens. Lettuce was provided as food and green algal growth was retained on the tank surfaces as an additional food source.

2.4.3 Oxygen and carbon isotope analysis

The majority of the oxygen and carbon isotopic analyse were carried out at the NERC Isotope Geosciences Laboratory. One exception are the samples discussed in Section 2.4.6 which, were analysed at the University of Plymouth (see Section 2.4.6 for the method). The waters were equilibrated with CO_2 using an Isoprep 18 device for oxygen isotope analysis with mass spectrometry performed on a stable isotope ratio analyser. For hydrogen isotope analysis an on-line Cr reduction method was used with a EuroPyrOH-3110 system coupled to an Isoprime mass spectrometer. Isotopic ratios ($^{18}O/^{16}O$ and $^{2}H/^{1}H$) and $\delta^{18}O$ and $\delta^{2}H$ (‰, parts per mil), are defined in relation to the international standard Vienna Standard Mean Ocean Water (VSMOW) by comparison with laboratory standards calibrated using NBS standards. Analytical precision is typically ±0.05‰ for $\delta^{18}O$ and ±1.0‰ for $\delta^{2}H$.

Total dissolved inorganic carbon (TDIC) from the water samples was precipitated in the field as $BaCO_3$ by addition of a solution of barium chloride and sodium hydroxide. In the laboratory CO_2 was generated by the reaction of the $BaCO_3$ with 100% phosphoric acid. The CO_2 was analysed for $^{13}C/^{12}C$ ratio using an Optima dual inlet mass spectrometer. Analytical precision (1 Standard Deviation (SD)) based on laboratory standard is < 0.1‰.

For the shell carbonate $^{13}C/^{12}C$ and $^{18}O/^{16}O$, approximately 30 to 100 µg of carbonate was analysed using the IsoPrime dual inlet mass spectrometer plus Multiprep device. Analytical precision (1SD) is typically < 0.07‰ for both ratios. Carbonate and TDIC isotopic ratios are reported in the per mil notation (‰) relative to the international standard Vienna Pee Dee Belemnite (VPDB) by comparison with laboratory standards calibrated using NBS standards. An aragonite fractionation factor (1.01034 taken from Friedman and O'Neil, 1977), was applied to convert the measured isotope compositions of CO_2 generated by the reaction of aragonite with ortho-phosphoric acid to the isotope compositions of aragonite.

2.4.4 Formulation of equation

Shell $\delta^{18}O_{carb.}$ values were used in conjunction with temperature and water $\delta^{18}O$ to derive values of 1000lnα and $\Delta\delta^{18}O$ ($\delta^{18}O_{carb.}$ – $\delta^{18}O_{water}$). This information was then plotted against $1/T$ (T in Kelvin) and T (°C), respectively, to give the relationships described below. The temperature dependence of the fractionation factor (α) is given by the linear relationship (Eq. 1):

$$1000\ln \alpha = M\,(1000T^{-1}) - C \quad (1)$$

Where:

$\alpha = ((\delta^{18}O_{carb.}\ \text{VSMOW}) + 1000) / ((\delta^{18}O_{water}\ \text{VSMOW}) + 1000)$

M = gradient of the linear trend

C = y-axis intercept

T = temperature in Kelvin

The thermometry equations for both the laboratory and field based studies were generated by plotting the dependent variable, $\Delta\delta^{18}O$ ($\delta^{18}O_{carb.}$ (VPDB) – average $\delta^{18}O_{water}$ (VSMOW)), against the independent variable, average recorded water temperature (°C). A linear regression was calculated to determine the relationship between the $\Delta\delta^{18}O$ and temperature, producing a thermometry equation (Eq.2 and 3) in the form of:

$$\Delta\delta^{18}O = M\ (2\ S.E)^{*}\ Temp. + C\ (2\ S.E) \quad (2)$$

This was then rearranged to give:

$$Temp.\ (°C) = -\ M\ (2\ S.E)^{*}\Delta\delta^{18}O + C\ (2\ S.E) \quad (3)$$

Where:

C = y-axis intercept

M = gradient of linear trend

2 S.E = 2 times standard error

2.4.5 Shell structure of *V. contectus*

Understanding the shell formation process is vital for the removal of shell material and the realistic interpretation of isotopic data. Several specimens collected during the first sampling trip to South Drain Canal (30/8/2007) were selected for thin sectioning. Preparation of the specimens once they were returned to the laboratory follows the methodology outline in Section 2.4.1.1. Once the shells had been cleaned shell dimensions of each of the specimens was measured including the maximum height and width of the shell and the maximum height and width of the aperture. The shells were in-filled with resin and left until the resin had hardened so that they could be dissected for thin sectioning. The shells were then cut in half along the columella from the apex to the left hand side of the aperture (Fig. 2.8A). Each of the shell halves were then dissected into sections so that the cut surface was parallel to the growth banding for each of the whorls (Fig. 2.8B). Each section was numbered in order from the aperture to the apex. To prevent the shell from dislodging during the thin sectioning process and for ease of handling the smaller sections near the apex, each of the sections was once again embedded in resin. A thin section was made from each of the sections showing the cut surface parallel to the growth bands. One of the *V. contectus* specimens had each section highly polished rather than cut to produce a thin section so that it could be observed using reflective light microscopy (Fig. 2.8C).

2.4.6 Bulk fragments versus high resolution drilling

In order to compare the micromilled and fragmented gastropods a modern *V. contectus* specimen was subjected to both high resolution sampling and randomly selected bulk fragments which were analysed for $\delta^{18}O$ and $\delta^{13}C$. Prior to isotopic sampling the selected shell had been subjected to the cleaning protocol stated in Section 2.2.5. Once cleaned the shell was in-filled with blue resin so a clear comparison between the resin and shell could be seen to prevent any resin from being incorporated into the carbonate samples. The shell was then drilled at high resolution from aperture to the apex. Each of the 92 drill lines (~0.4 mm in width) followed the growth banding parallel to the aperture, incorporating a minimal number of growth bands without compromising sample size. The high resolution sampling concentrated on the central part of the whorl so, that bulk fragments could also be taken from above or blow the drill lines. From the same specimen 17 different sized fragments were removed randomly from the gastropod shell. These fragments were crushed to a fine powder using an agate pestle and mortar and isotopically analysed.

Isotopic analysis was carried out at the University of Plymouth. The carbonate powder samples from the bulk fragments and high resolution drill lines were reacted with 100 % phosphoric acid at 90 °C. The CO_2 produced was analysed on a GV Instruments Isoprime Mass Spectrometer with a Gilson Multiflow carbonate auto-sampler. Any isotopic results below 1.2 nA were removed from the dataset and rerun if material was available. The results were calibrated against Peedee Belemnite (PDB) using the international standard NBS-19 (National Bureau of Standards 19; $\delta^{13}C$ = 1.95 ‰; $\delta^{18}O$= -2.20 ‰).

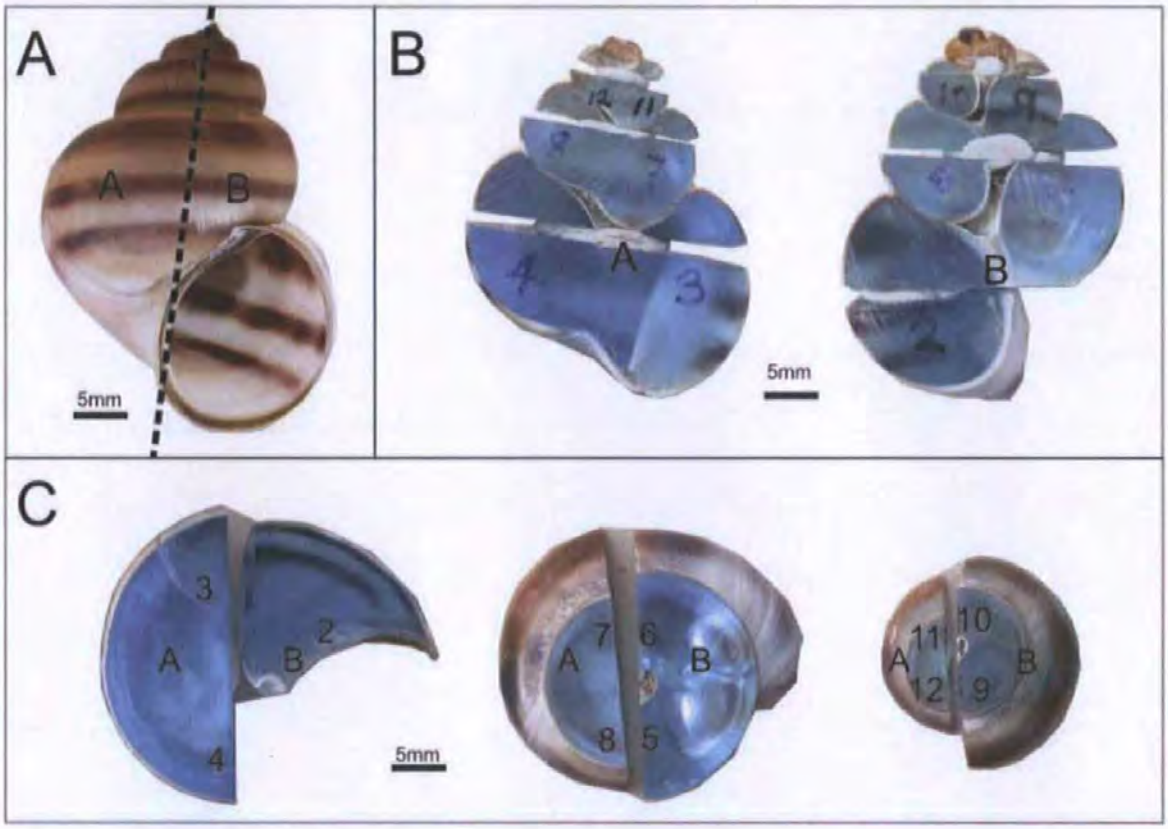

Figure 2.8 The procedure followed for the preparation of a whole gastropod shell for thin section. A) Shows the whole shell prior to being in-filled with resin. The dashed line show the path of the cut line used to halve the shell. B) The two shell halves have been dissected into sections so that the cut surface cross cuts the growth banding. C) Shows the cut surfaces which have been highly polished, so that they could be observed using reflected light.

2.5 Results

The results for the laboratory culturing experiment, field cage experiment and field collection experiments are given in Tables 2.3, 2.4 and 2.5 respectively.

2.5.1 Laboratory culturing experiment

For the duration of the laboratory experiment temperatures, with minor deviation from the controlled temperatures, were 15°C mean = 15.1°C (± 0.4 °C); 20°C mean =19.6°C (± 0.2°C); 25°C mean = 25.0°C (± 0.1°C). The measured $\delta^{18}O_{water}$ shows minimal variation from the mean, 15°C mean = − 5.2‰ (± 0.2‰); 20°C mean = −5.1‰ (± 0.3‰); 25°C mean = −4.9‰ (± 0.3‰) however, deviation from the average $\delta^{18}O_{water}$ values increases with

higher temperatures, suggesting some minor evaporation with increasing water temperature.

For the laboratory culturing experiment the temperature dependence of the fractionation factor (α), between 15 and 25°C is given by (Eq. 4):

$$1000\ln \alpha = 8.59(\pm 0.1)*(1000T^{-1}) \; 0.64\ (\pm 0.28) \qquad (r^2 = 0.92) \qquad 4)$$

Where T is in Kelvin, and the relationship between $\Delta\delta^{18}O$ and temperature is given by (Eq. 5 and 6):

$$\Delta\delta^{18}O = -10.0\ (\pm 0.04)*\text{Temp} + 1.98(\pm 0.72) \qquad (5)$$

This rearranges to:

$$\text{Temp. (°C)} = -10.09(+1.73, -4.24)*\ \Delta\delta^{18}O + 20.4(\pm 7.20) \qquad \text{(Fig. 2.10A)} \qquad (6)$$

The relationship between $\Delta\delta^{18}O$ and temperature shows a good statistical regression (r^2 = 0.91).

	Mean pH	Mean Salinity (ppt)	Mean Temp. (°C)	Mean $\delta^{18}O_{water}$ (‰ VSMOW)	$\delta^{18}O_{carb.}$ (‰ VPDB)	$\Delta\delta^{18}O$ ($\delta^{18}O_{carb.}$ ‰ (VPDB) – $\delta^{18}O_{water}$ ‰ (VSMOW))
Laboratory culturing data	7.6 (±0.3 std) (n=24)	0.3 (±0.1 std) (n=24)	15.1 (±0.4 std) (n=24)	-5.2 (±0.2 std) (n=2)	-4.9	0.3
					-4.5	0.7
					-4.8	0.4
					-4.7	0.6
	7.5 (±0.2 std) (n=24)	0.3 (±0.2 std) (n=24)	19.6 (±0.2 std) (n=24)	-5.1 (±0.3 std) (n=2)	-5.0	0.1
					-5.1	0.0
					-5.4	-0.2
					-5.1	0.0
					-5.1	0.1
	7.3 (±0.3 std) (n=9)	0.3 (±0.0 std) (n=9)	25.0 (±0.3 std) (n=9)	-4.9 (±0.3 std) (n=2)	-5.5	-0.6
					-5.3	-0.3
					-5.4	-0.4
					-5.5	-0.6
					-5.5	-0.6

Table 2.3 Laboratory culturing data (probe result and water analysis) and the results from the analysis of carbonate material from *V. contectus* cultured within the laboratory culturing experiments.

2.5.2 Field experiments

Due to the failure of the I-button, which was placed in the cage experiment to collect water temperatures every 2 hours throughout the experiment, we were limited to temperature data collected using the temperature probe. The Exeter Canal I-button data was used in an attempt to improve the temperature record, however as shown by Fig. 2.9 the regression was more robust using the probe data. It was assumed that the probe temperatures between known collection dates was linear and that an average temperature would provide an average for the material grown during the equivalent period.

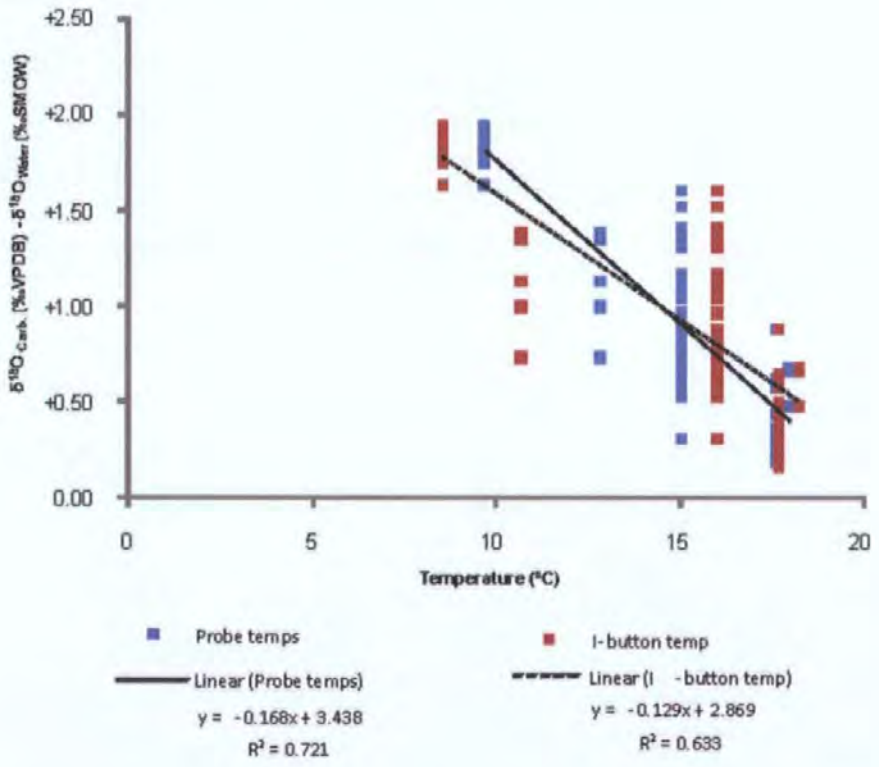

Figure 2.9 The relationships between temperature and $\Delta\delta^{18}O$ ($\delta^{18}O_{carb.} - \delta^{18}O_{water}$) for *V. contectus* specimens from the tank the cage experiment at South Drain Canal on the Somerset Levels. The data show the different regression when plotted against the probe temperatures and the average temperature from Exeter Canal I-button data logger.

In the field experiment the temperature (August 2007 to 2008) reached a maximum of 19.9°C and a minimum of 7.4°C, indicating a range of ~12.5°C for the sampling period. The range in temperature between successive sampling collections was determined by

calculating the difference between the monthly probe readings. Evidence suggests that the longer a time interval spans a wider range of temperatures are recorded. For example, between 25/4/2008 to 6/6/2008 (42 days) temperature was measured as 12.9°C and 15.1°C giving a ~2°C difference. Whereas between 3/4/2008 to 25/4/2008 (22 days) temperature varied between 12.0°C and 13.7°C, a difference of 1.7°C.

South Drain canal had a range of $\delta^{18}O_{water}$ over the entire sampling period of 1.9‰. The longer a time interval spans a wider range of $\delta^{18}O_{water}$ values are recorded. For example, between 25/4/2008 to 6/6/2008 (42 days) $\delta^{18}O_{water}$ varied between −4.8 ‰ to −5.7‰ a difference of 0.9‰, whereas between 3/4/2008 to 25/4/2008 (22 days) $\delta^{18}O_{water}$ varied between −5.0‰ and −4.8‰ a difference of 0.2‰. These two parameters (temperature and $\delta^{18}O_{water}$) are important for the formulation of the thermometry equation. Owing to variability within the natural environment, temperature and $\delta^{18}O_{water}$ are not as well constrained as those obtained for the laboratory culturing method. Production of the field based *V. contectus* thermometry equation involved estimating average probe temperatures and $\delta^{18}O_{water}$ values between successive sampling trips (for example between 6/6/2008 to 3/7/2008 and 3/7/2008 to 13/8/2008).

	Date	pH	Salinity (ppt)	Probe temp. (°C)	$\delta^{18}O_{water}$ (‰ VSMOW)	$\delta^{18}O_{carb.}$ (‰ VPDB)
Cage data	03/04/2008	7.8	0.4	11.6	-5.2	-3.6
						-3.4
						-3.4
						-3.4
						-3.5
						-3.4
						-3.5
						-3.3
						-3.3
	25/04/2008	8.1	0.4	13.5	-4.9	-4.0
						-3.9
						-3.6
						-3.6
						-4.3
	06/06/2008	7.6	0.3	17.4	-5.2	-3.7
						-4.8
						-4.5
						-4.5
						-4.7
						-4.0
						-4.3
						-4.4
						-4.0
						-4.8
						-4.2
						-4.4
						-4.5
						-4.6
						-3.9
						-5.0
						-4.4
						-4.3
						-4.6
						-4.4
						-4.6
						-3.7
						-4.8
						-4.2
						-4.8
						-3.8
						-4.0
						-4.0
						-4.5
						-4.5
						-4.6
						-4.7
						-4.5
						-4.7
						-4.7
						-4.5
						-4.2
	03/07/2008	7.7	0.3	19.6	-5.2	-4.9
						-5.0
						-4.9
						-5.0
						-4.9
						-5.0
						-5.1
						-5.1
						-5.2
						-4.9
						-5.1
						-5.0
						-4.9
						-5.0
						-4.8
						-4.8
						-4.7
						-4.8
						-4.7
						-4.9
						-4.4
						-5.0
						-5.0
						-5.0
	13/08/2008	7.3	0.3	16.9	-4.2	-3.6
						-3.7
						-3.8
						-3.6
						-3.8

Table 2.4 Field data (probe result and water analysis) from South Drain canal and the results from the analysis of carbonate material from *V. contectus* collected from the cage experiments.

2.5.2.1 Field cage experiment

For the field cage experiment the temperature dependence of the fractionation factor (α), between 8.2 and 19.6°C is given by (Eq.7):

$$1000\ln \alpha = 13.29(\pm 1.06)*(1000T^{-1}) - 15.35\ (\pm 3.69) \qquad (r^2 = 0.67) \qquad (7)$$

Where T is in Kelvin, and the relationship between $\Delta\delta^{18}O$ and temperature is given by (Eq. 8 and 9)

$$\Delta\delta^{18}O = -0.16(\pm 0.02)*\text{Temp.} + 3.25(\pm 0.40) \qquad (8)$$

This rearranges to:

$$\text{Temp. (°C)} = -6.22(+0.86, -1.18)*\Delta\delta^{18}O + 20.75(\pm 2.47) \qquad \text{(Fig. 2.10B)} \qquad (9)$$

The relationship between $\Delta\delta^{18}O$ and temperature shows a good statistical regression (r^2 = 0.67) (Fig. 2.10B).

2.5.2.2 Field collection

For the field collection experiment the temperature dependence of the fractionation factor (α), between 8.2 and 19.6°C is given by (Eq. 10):

$$1000\ln \alpha = 9.72\ (\pm 1.73)*(1000T^{-1}) - 3.01\ (\pm 6.04) \qquad (r^2 = 0.44) \qquad (10)$$

Where T is in Kelvin, and the relationship between $\Delta\delta^{18}O$ and temperature is given by (Eq. 11 and 12):

$$\Delta\delta^{18}O = -0.12(\pm 0.04)*\text{Temp.} + 2.55(\pm 0.60) \qquad (11)$$

This rearranges to:

$$\text{Temp. (°C)} = -8.48(+2.22, -4.67)^{*} \Delta\delta^{18}O + 22.00\ (\pm 5.15) \qquad \text{(Fig. 2.10C)} \qquad (12)$$

The equation produced by the field collection method shows a relatively poor statistical regression (r^2 =0.44) in contrast to the tank and field cage experiments (Fig. 2.10C).

	Date	pH	Salinity (ppt)	Probe temp. (°C)	$\delta^{18}O_{water}$ (‰ VSMOW)	$\delta^{18}O_{carb.}$ (‰ VPDB)
Field data	03/08/2007	7.9	0.2	19.9	-3.9	-4.0
						-4.2
						-4.1
						-3.6
	31/10/2007	7.8	0.4	11.1	-4.3	-3.8
						-4.1
						-4.2
						-3.7
	22/01/2008	7.6	0.3	8.2	-5.8	-3.6
						-3.1
						-3.1
						-4.3
	02/09/2008	7.9	0.4	8.6	-5.3	-5.1
						-4.8
						-3.4
						-3.8
						-3.8
	03/04/2008	7.8	0.4	11.6	-5.0	-4.1
						-3.6
						-3.5
						-4.4
						-3.2
	25/04/2008	8.1	0.4	13.5	-4.8	-3.2
						-3.3
						-3.1
						-3.5
						-3.1
	06/06/2008	7.6	0.3	17.4	-5.7	-4.9
						-5.3
						-3.9
						-5.2
						-4.8
	03/07/2008	7.7	0.3	19.6	-4.8	-4.4
						-4.5
						-4.6
						-4.6
						-4.7
	13/08/2008	7.3	0.3	17.1	-4.2	-4.1
						-3.5
						-3.6
						-3.6
						-3.6

Table 2.5 Field data (probe result and water analysis) from South Drain canal and the results from the analysis of carbonate material from *V. contectus* collected from the field.

2.5.3 Combined equation

The regression analysis indicates that the gradient for all three experiments lies within 2 standard error of each other therefore, a correlation using all three datasets is justifiable. For the combined dataset (laboratory, field cage and field collection) the temperature dependence of the fractionation factor (α), between 8.2 and 25.0°C is given by (Eq. 13):

$$1000\ln\alpha = 9.72\ (\pm 1.73)*(1000T^{-1}) - 3.01\ (\pm 6.04) \quad (r^2 = 0.63) \qquad (13)$$

Where T is in Kelvin, and the relationship between $\Delta\delta^{18}O$ and temperature is given by (Eq. 14 and 15):

$$\Delta\delta^{18}O = -0.13(\pm 0.02)*\text{Temp.} + 2.81(\pm 0.28) \qquad (14)$$

This rearranges to:

$$\text{Temp.}\ (°C) = -7.43(+0.87,-1.13)*\ \Delta\delta^{18}O + 20.89(\pm 2.09) \qquad \text{(Fig. 2.10D)} \qquad (15)$$

The relationship between $\Delta\delta^{18}O$ and temperature shows relatively good statistical regression ($r^2 = 0.63$) (Fig. 2.10D).

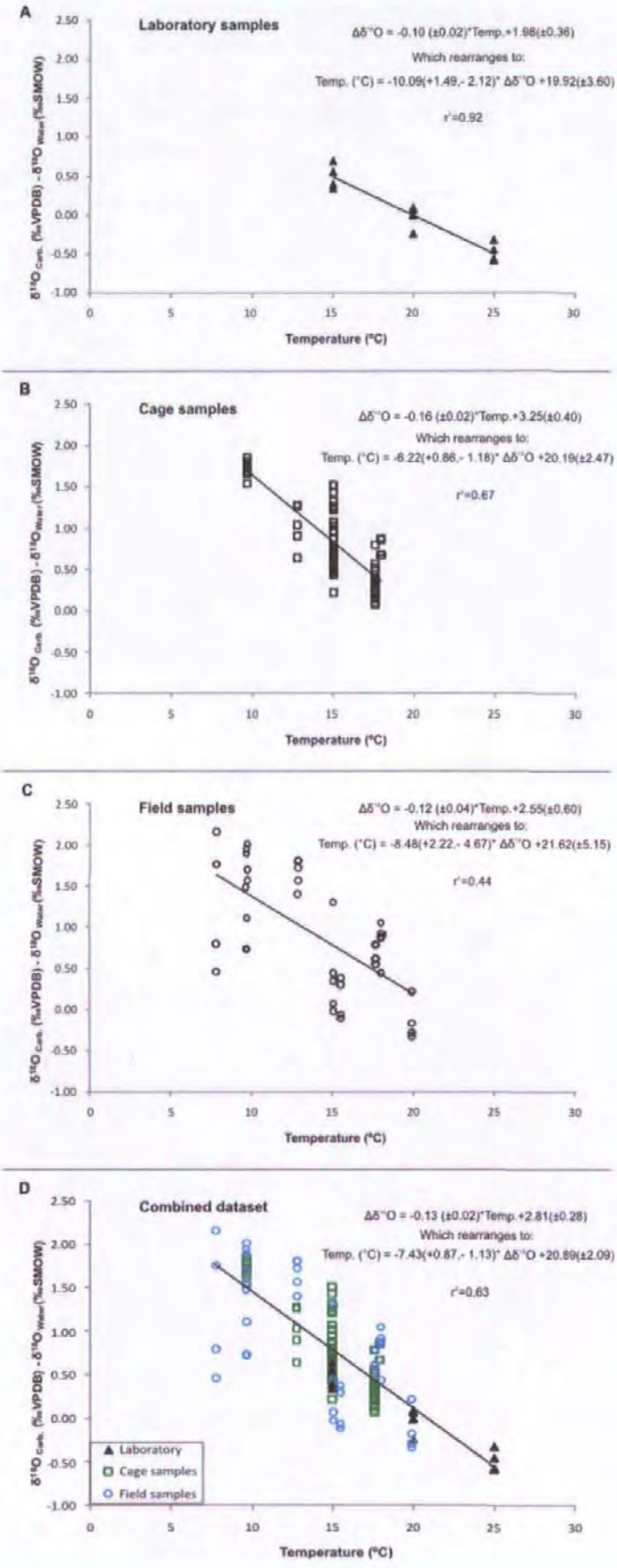

Figure 2.10 The relationships between temperature and $\Delta\delta^{18}O$ ($\delta^{18}O_{carb.} - \delta^{18}O_{water}$) for *V. contectus* specimens from the tank (2A) experiments and specimens from the cage (2B) and field (2C) experiments at South Drain Canal on the Somerset Levels. Figure 2D shows the relationship between temperature and $\Delta\delta^{18}O$ ($\delta^{18}O_{carb.} - \delta^{18}O_{water}$) for the combined dataset (laboratory, field cage and field collection).

2.5.4 Temperature vs. $\delta^{18}O$ water

The $\delta^{18}O_{water}$ and $\delta^{2}H_{water}$ results from the analysis of water samples collected from South Drain Canal plot along a local evaporation line (LEL), which deviates away from the global meteoric water line (GMWL) (Fig. 2.11). The data points exhibiting the greatest deviation are not associated with the warmest temperatures nor do they change with seasonal temperature variation (Fig. 2.12 and Table 2.6). Comparisons made with the monthly precipitation records from Yeovilton (51°0.529'N 2°38.275'W) (Fig. 2.12), the closest Meteorological Office monitoring station to our field site, illustrates that the samples deviating furthest from the global meteoric water line were collected after a period of low average monthly precipitation (Fig. 2.12). In particular, reference is made to the samples collected on the 29/2/2008 and the 6/6/2008.

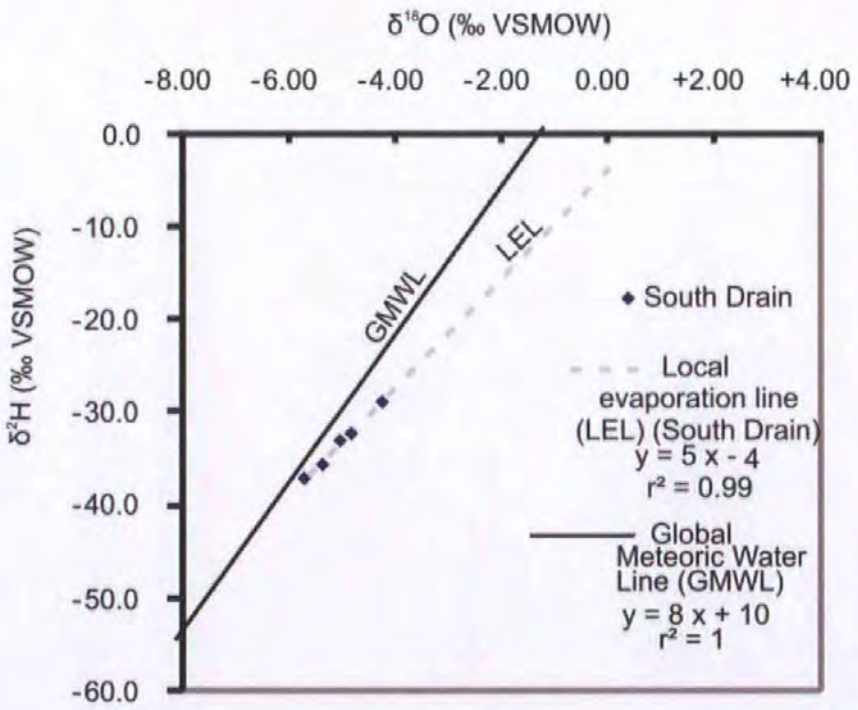

Figure 2.11 A graph showing $\delta^{18}O$ (VSMOW) plotted against $\delta^{2}H$ (VSMOW) which were measured from the water samples collected from South Drain Canal. This is compared with the global meteoric water line of Craig (1961).

Location	Date	$\delta^{13}C_{TDIC}$ (‰)	$\delta^{18}O_{water}$ (‰ VSMOW)	Temp (°C)	$\delta^{13}C_{carb.}$ (‰ VPDB)	$\delta^{18}O_{carb.}$ (‰ VPDB)
South Drain	30/08/2007		-3.9	19.9	-12.5	-3.9
South Drain	31/10/2007		-4.3	11.1	-12.0	-3.9
South Drain	22/01/2008		-5.8	8.2	-12.2	-3.4
South Drain	29/02/2008	-11.9	-5.3	7.4	-12.0	-4.1
South Drain	03/04/2008	-12.9	-5.0	12.0	-12.5	-3.7
South Drain	25/04/2008	-11.1	-4.8	13.7	-14.6	-3.1
South Drain	06/06/2008	-14.1	-5.7	16.4	-12.7	-4.7
South Drain	03/07/2008	-12.2	-4.8	18.9	-11.8	-4.5
South Drain	13/08/2008	-13.5	-4.2	17.1	-12.6	-3.6

Table 2.6 $\delta^{18}O$ water, $\delta^{13}C_{TDIC}$ and temperature for each visit to the South Drain Canal site along side the average $\delta^{18}O_{carb.}$ and $\delta^{13}C_{carb.}$ from the analysis of *V. contectus* specimens collected during those time periods.

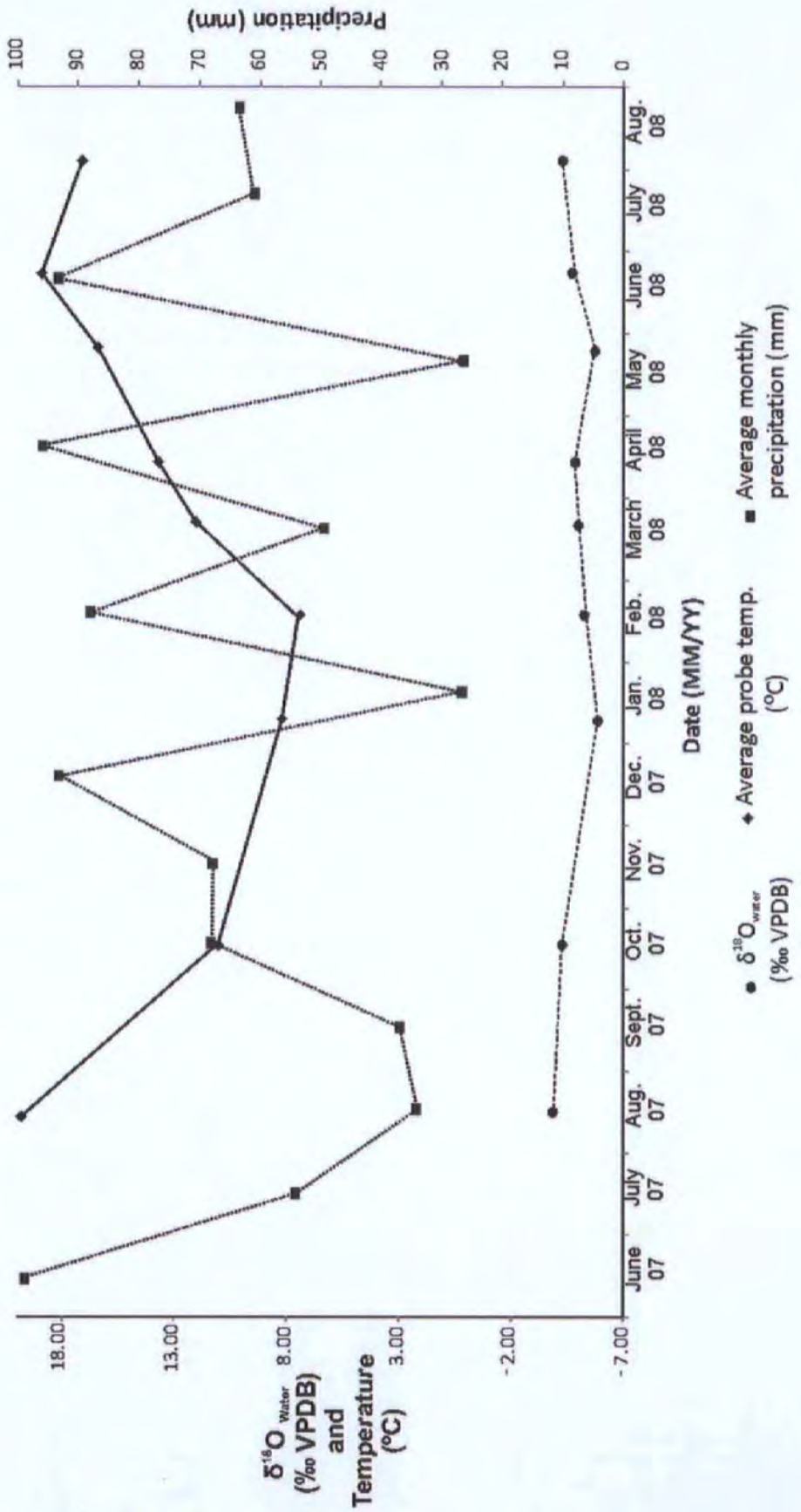

Figure 2.12 A comparison between the water temperatures and $\delta^{18}O$ of the canal water taken from South Drain Canal with the average monthly precipitation record from Yeovilton for 6/2007 to 9/2008.

2.5.5 Seasonal profiles

Three *V. contectus* specimens grown within the field cage experiment were drilled at high resolution to produce a detailed record of the shell $\delta^{18}O_{carb.}$ between February and August 2008 (Fig. 2.13A). A date was attributed to each drill line by calculating the average daily growth rate, using the total growth secreted during a given sampling period (as stated in the outline of field cage methods). Temperature and $\delta^{18}O_{water}$ averages were used for the individual drills lines between known sample collections.

A comparison of the $\delta^{18}O_{carb.}$ seasonality profiles from the three *V. contectus* specimens indicates that there is good isotopic reproducibility, with $\delta^{18}O_{carb.}$ co-varying throughout the experiment (Fig. 2.13A). In general, the $\delta^{18}O_{carb.}$ of the *V. contectus* profiles becomes progressively more negative over the duration of the experiment (-3.3‰ in February to -4.9 ‰ in July), indicating a total $\delta^{18}O_{carb.}$ shift of 1.7‰ between February to July 2008. However, the last two $\delta^{18}O_{carb.}$ data points of VC5 show a return to relatively positive values during August. Throughout the field cage experiment the average monthly temperatures increased from 7.4°C to 18.9°C, an overall increase of 11.5°C. The average $\delta^{18}O_{water}$ of the canal water was recorded as fluctuating between -5.6‰ to -4.5‰, a difference of 1.1‰.

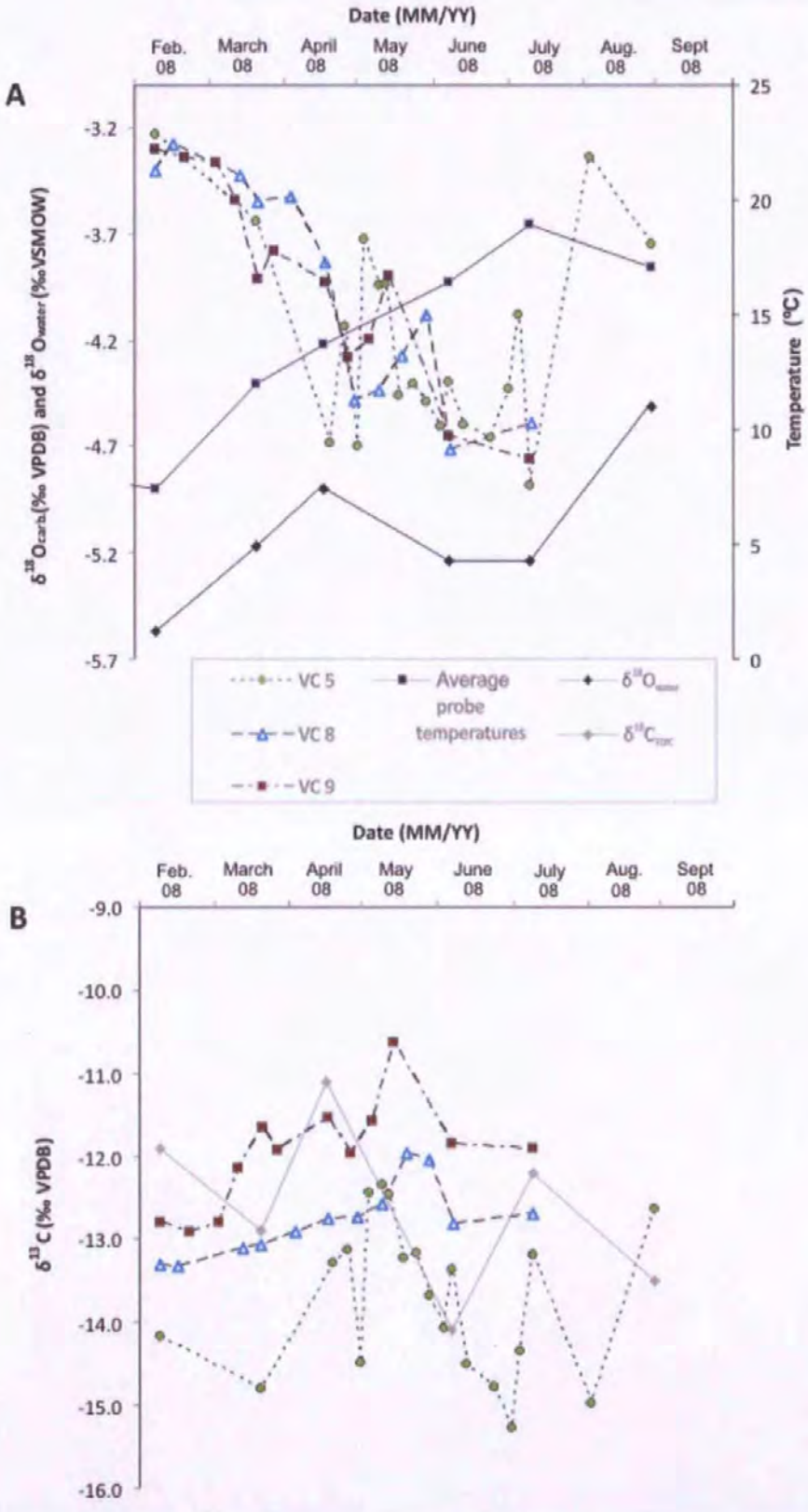

Figure 2.13 Graph A shows the co-varying $\delta^{18}O_{carb}$. relationship between the three cage specimens drilled at high resolution related to the $\delta^{18}O_{water}$ and probe temperature record from South Drain Canal site over time. Graph B shows how the $\delta^{13}C_{carb}$. profiles from the three cage specimens compared with the $\delta^{13}C_{TDIC}$ of the water samples over time from the South Drain Canal site. For graphs A and B the open symbols for the *V. contectus* (VC) indicates that the specimen is a male and the closed symbols indicate the specimen is a female.

2.5.6 Carbon ($\delta^{13}C$) uptake

Three *V. contectus* specimens grown within the field cage experiment were drilled at high resolution to produce a detailed record of the shell $\delta^{13}C_{carb.}$ between February and August 2008 (Fig. 2.13B). When the resulting $\delta^{13}C_{carb.}$ profiles from the three *V. contectus* specimens are plotted against the $\delta^{13}C_{TDIC}$ record, the observed fluctuation appear to not co-vary (Fig. 2.13B). The $\delta^{13}C$ in the *V. contectus* specimens have an overall range of 5‰, which is significantly larger than the 3‰ range of the $\delta^{13}C_{TDIC.}$ Actual values indicate that the $\delta^{13}C$ of the TDIC is within the range of the values obtained from the *V. contectus* specimens. Therefore, the sources of $\delta^{13}C$ for the secreted shell carbonate cannot be solely related to $\delta^{13}C$ of TDIC within the water column. However, $\delta^{13}C$ profiles of the *V. contectus* specimens show some covariance, i.e. generally increasing between February and June with a small decrease from June to August. This would suggest that the methods of uptake and / or sources of carbon influencing the final $\delta^{13}C_{carb.}$ of the shell are relatively consistent between specimens.

2.5.7 Shell structure of *Viviparus contectus*

A thin section showing a cross section of a *V. contectus* shell which was observed under crossed polarised light (Fig. 2.14), clearly shows three distinct layers. The upper layer consists of vertical crystals with faint brown coloration at the base of the layer and a thinner brown band in the middle of this layer. Figure 2.15 shows a cross section of another *V. contectus* shell observed under reflected light. This shows more clearly that the bands of brown coloration are restricted to the upper layer. This layer makes up greater than half of the shell thickness (~108μm); however the thickness of this layer was observed to vary throughout the shell. The middle lamellate layer (~40μm thick) consists of obliquely crossed crystals, forming a herring bone pattern (Fig. 2.14). The inner nacreous

layer is significantly thinner (~10μm thick) and does not show a distinctive crystal structure (Fig. 2.14).

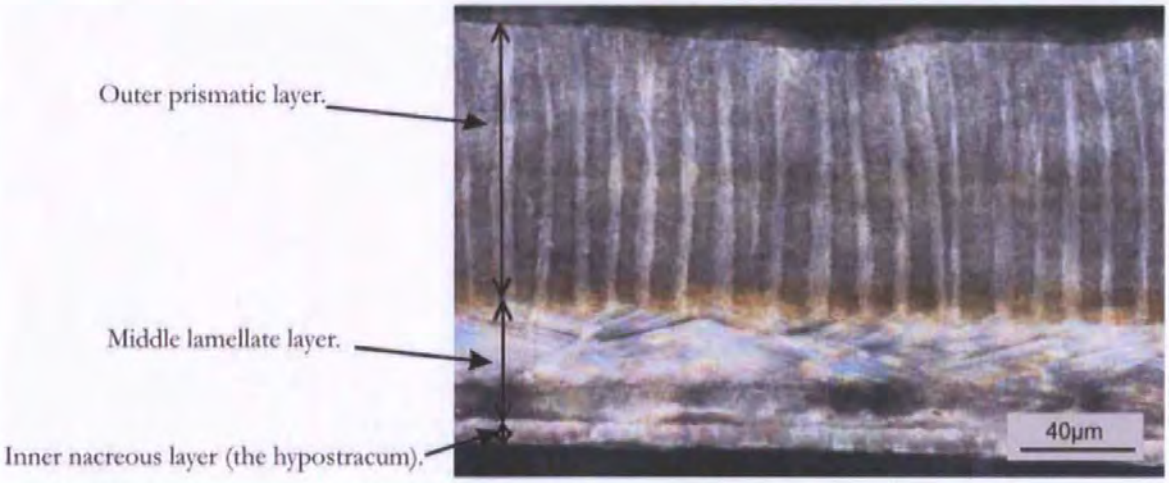

Figure 2.14 A thin section of a modern *V. contectus* shell observed under cross polarised light, clearly showing the three calcareous layers with their individual crystal structure. The periostracum has been removed using NaClO.

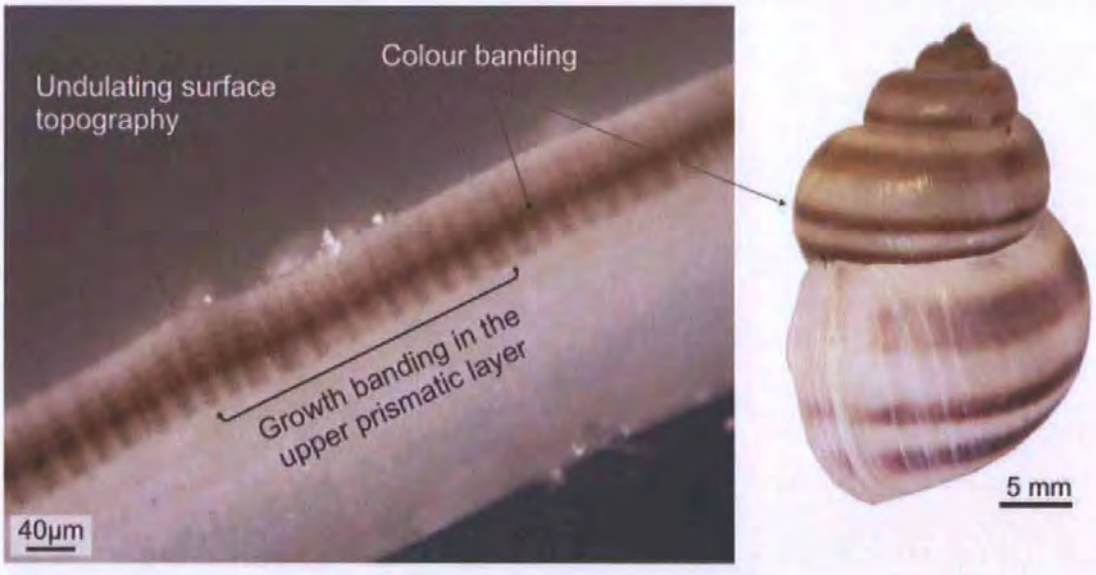

Figure 2.15 Cross section of a *V. contectus* shell showing the prismatic layer containing growth banding which is coloured brown by one of the three coloured bands decorating the shell. This coloration does not penetrate in to the middle lamellate layer or inner nacreous layer (the hypostracum).

The crystal structure of the prismatic layer appears to become deformed just prior to the point of growth cessation (Fig. 2.16). The uniform crystal structure becomes erratic with the crystal form becoming inconsistent, some are curved, others branch and some do not

extend across the width of the layer (Fig. 2.16 and 2.17). This deformation appears to affect the crystalline structure to a greater extent when growth is continued at a reduced rate (Fig. 2.17) rather than when cessation occurs (Fig. 2.16).

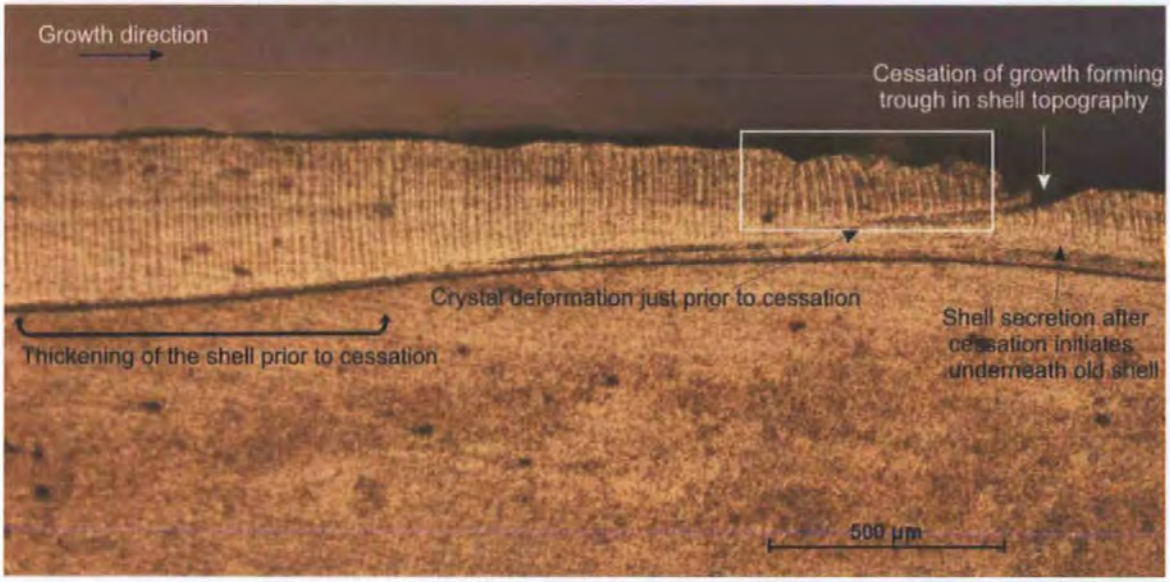

Figure 2.16 A polished cross section observed under reflected light shows that the thicker shell section thins towards the point of cessation. The crystal structure in the thinner shell just prior to cessation has a erratic crystal structure. A topographic low occurs due to the newly secreted shell initiating underneath the old shell.

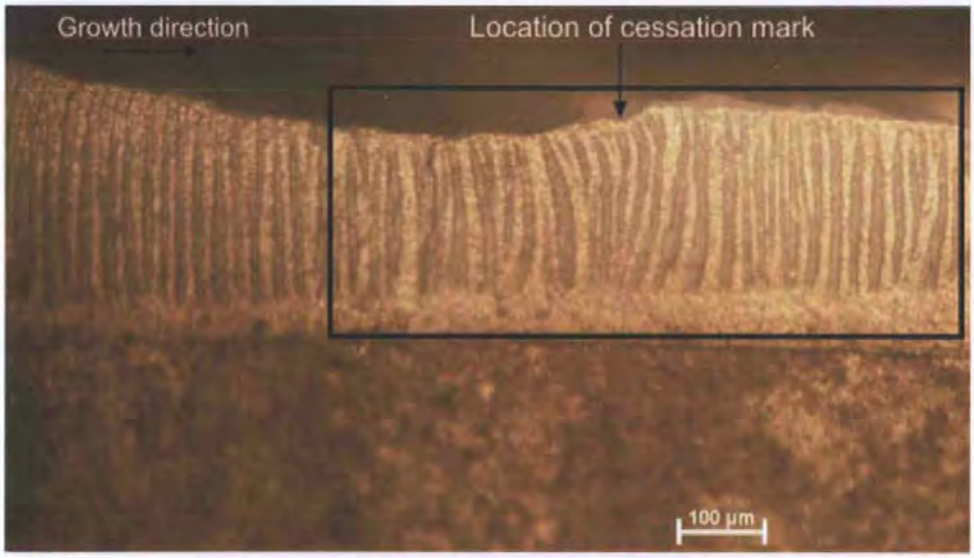

Figure 2.17 The area highlighted by the box shows the effect of growth cessation on the crystal structure of the prismatic layer when looking at a polished cross section with reflected light. The crystals appear to lose their uniform appearance and, show a greater and more inconsistent range in width and length. Some of the crystals show branching and do not extend across the full width of the prismatic layer. The surface topography of the shell also becomes jagged and uneven.

Observations suggest that the thickness of these vertical crystals in the upper layer alter with the overall thickness of the shell. A section of 'thick' and 'thin' shell from the same specimen, observed at the same magnification and area of coverage was used to investigate this observed difference. The crystals appear to alternate with the more prominent crystals termed 'ridges' and the area between these termed 'troughs'. The length and width of each ridge and trough was measured using a Nikon eclipse LV100POL with NIS-Elements BR-2.30 software package. The two graphs in Figure 2.18, plot width against length for both the ridge and troughs for the thick and thin shell sections. Measurements of the ridges and troughs taken from the thin shell section suggest that the crystals are horizontally thicker and vertically shorter when compared to the thicker shell section.

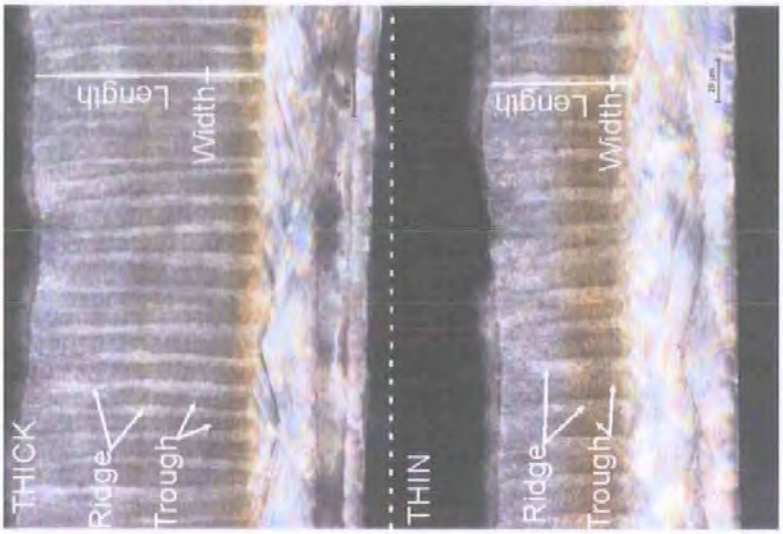

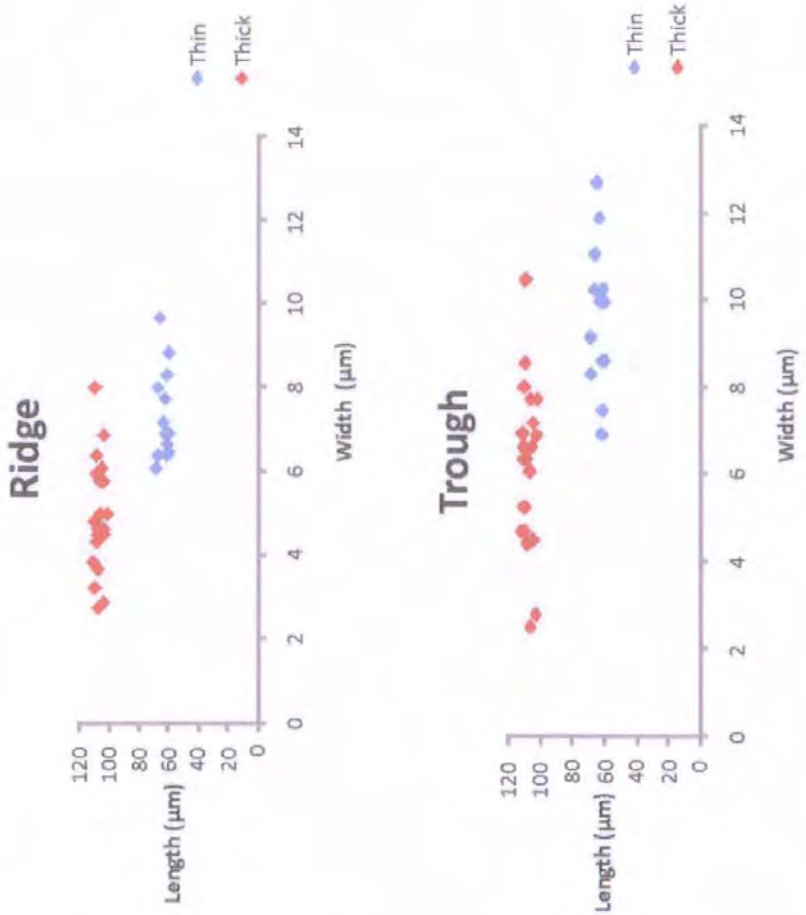

Figure 2.18 Thin sections of a modern *V. contectus* shell were used to investigate the shell structure. These diagrams compare the observed growth banding from a thin and thick piece of the same shell. It suggests that in the thicker part of the shell the growth banding in the outer prismatic layer produces thinner and more elongated crystals where in the thinner shell the crystals are squat and thicker.

2.5.8 *V. contectus* shell fragments.

A modern *V. contectus* was firstly drilled and analysed at high resolution for $\delta^{18}O$ and $\delta^{13}C$, and from these results average isotopic values were calculated. Subsequently, randomly picked fragments were removed from the same shell and analysed for $\delta^{18}O$ and $\delta^{13}C$ from which average isotopic values were also calculated. Firstly, results from the high resolution drilling suggest that the $\delta^{18}O$ isotopic record changes with seasonal temperature change. This is indicated by the cyclic shifts from negative to positive $\delta^{18}O$ values (Fig. 2.19). The $\delta^{18}O$ values at the apex are relatively negative (-4.7‰) and become progressively negative towards section 11 (–5.6‰). Between sections 11 and 8 a return to more positive $\delta^{18}O$ values (-2.9‰) occurs after which the overall trend of $\delta^{18}O$ is to become more negative (-4.8‰) again until section 2. Between section 2 and 1 the values rapidly become more positive (-3.0‰) after which they return to negative values (-3.8) at the aperture. Cessation marks on the shell tend to coincide with the most positive $\delta^{18}O$ values. One exception is at the boundary between sections 2 and 1 (11.7mm) where, although these values are relatively negative, the cessation coincides with a positive peak in $\delta^{18}O$ (Fig. 2.19).

The high resolution $\delta^{18}O$ profile has a range of isotopic values between –2.9‰ to –5.7‰ (range of 2.8‰) whereas the *V. contectus* shell fragments have a minimum of –4.0 and a maximum of –2.7‰ (range of 1.3‰) (Fig. 2.19 right hand graph). Three of the fragments taken from sections 6, 7 and 8 have $\delta^{18}O$ values that plot more positive than the range of values from the high resolution sampling. Overall, the majority of fragments plot more positively than the equivalent high resolution samples

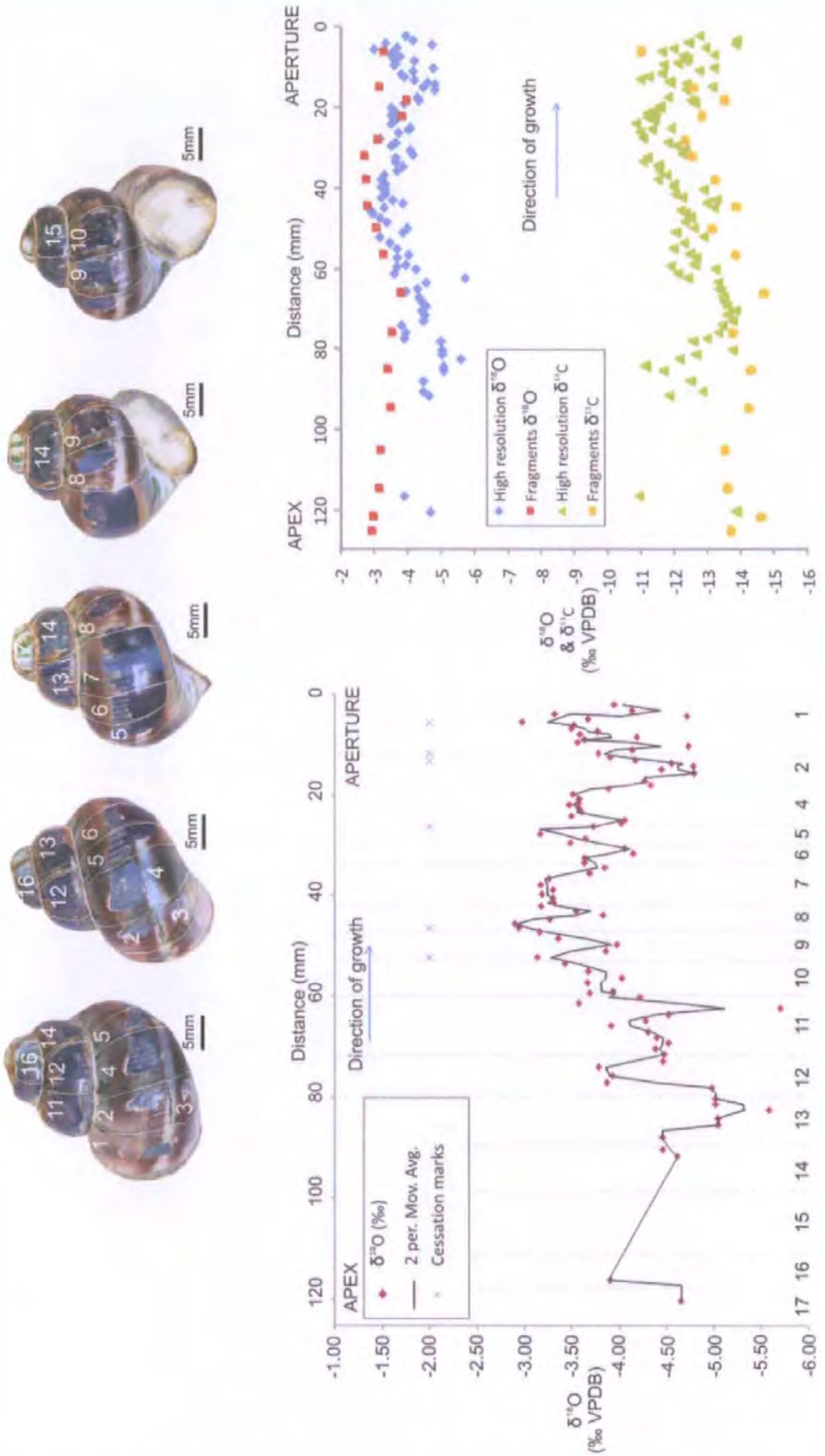

Figure 2.19 A modern *V. contectus* which has been drilled at high resolution to show seasonal changes in $\delta^{18}O$ throughout its lifetime. Bulk fragments (numbered along the X axis on the left hand graph) were then removed and analysed for $\delta^{18}O$ to see how representative the fragments were when compared with the high resolution drilling averages from the same shell section.

2.6 Discussion

2.6.1 Laboratory culturing experiment

The linear regression (r^2 =0.91) calculated for the relationship between $\Delta\delta^{18}O$ and temperature indicates that the laboratory equation is statistically the most robust of all the *V. contectus* results. This is owing to all three known variables being well constrained. However, it should be noted that specimen growth rates were significantly slower than those within the natural environment. Specimens of a comparable size and age (e.g. those released as juveniles at the start of the experiments) in the field cage experiment secreted up to five times more carbonate per day than the laboratory specimens (Table 2.2). The proportion of energy allocated to growth varies with age, as a greater percentage is utilised for reproduction later in life (Browne and Russell-Hunter, 1978; Tashiro, 1982; Russell-Hunter and Buckely, 1983). Therefore, comparisons between specimens of the same age are necessary. This observed difference in growth rates could be related to a number of factors unique to the laboratory experiments including: lack of seasonal change in temperature; poor or incorrect food source; insufficient quantities of dissolved calcium carbonate; disturbance and light intensities. *V. contectus* uses a single unipectinate gill which is the principal site of oxygen uptake, so the influence of oxygen concentration on its density in its natural environment may be related to its gill-based mode of respiration (Aldridge, 1983; McMahon, 1983; Eleutheriadis and Laxaedou-Dimitiadou, 1995). If the population density within the tanks was not balanced with the concentration of dissolved oxygen the specimens may have experienced stress inhibiting shell growth. Aeration of the tanks was maintained at a minimum to reduce the effect of isotopic fractionation, but not to inhibit the oxygen concentration of the water. The pH of the water is also important in maintaining shell secretion, comparisons made between the field and laboratory

experiments show that the pH of the tanks was within error of the field values (Tables 2.2 and 2.4). Although the dissolved calcium concentrations in the tank experiments were controlled, population density and variation in the length of time between water changes may have resulted in a calcium deficiency within the water. These inconsistencies in dissolved calcium concentration may have result in reduced calcium carbonate secretion rates.

2.6.2 Field cage experiment

The linear regression applied to determine the relationship between $\Delta\delta^{18}O$ and temperature for the field cage experiment produced a regression ($r^2 = 0.67$) that is not considered to be as statistically robust as the laboratory tank experiment ($r^2 = 0.92$). This is probably related to the spread of temperature and $\delta^{18}O_{water}$ data. These data could not be as well constrained owing to natural variation between sample collections. The amount of carbonate secreted by individual specimens between sampling trips was well constrained, but it was impossible to know when during the period between successive sampling trips the carbonate was secreted.

2.6.3 Field collection

The poor linear regression produced by the field collection experiment ($r^2 = 0.44$) was, in hindsight, inevitable. It was presumed that growth had occurred at some time within the time interval between collections. However, the cage experiment highlighted differential growth rates between specimens. This could account for the spread of data obtained. It is probable that some specimens exhibited no carbonate secretion during the time period between sampling trips.

2.6.4 Combined dataset

As the linear regression output shows that the gradients of all three experiments lie within error (± 2 S.E) of each other, it is possible to combine all of the datasets. A linear regression was therefore applied to the entire dataset (laboratory, field cage and field collection) in order to determine the relationship between $\Delta\delta^{18}O$ and temperature. A combined regression of 0.63 indicates a good statistical relationship between the two variables. However, this combined dataset should be treated with some caution as there is a strong overlap between the laboratory and field samples towards higher temperatures. This is likely to be related to how well the variables used to construct the correlations are constrained. Greater variability in the $\delta^{18}O_{carb.}$ values obtained from *V. contectus* specimens from the field cage and collection experiments could account for this overlap. However, it has been previously stated that the growth rates of specimens in the tank experiments were significantly lower than those from the natural environment therefore could imply that some of this overlap may be due to the slower growth rates.

2.6.5 Temperature versus $\delta^{18}O$ water

Several of the $\delta^{18}O_{water}$ values obtained from samples collected from South Drain Canal appear to have been affected by the amount of precipitation and / or variation in the $\delta^{18}O$ of precipitation within the local area. Although unclear from the $\delta^{18}O$ of the canal water, some of this variation may be related to seasonal changes in the $\delta^{18}O$ of precipitation. Other influential factors are wind (e.g. high winds enhance evaporation) and humidity (high humidity would reduce evaporation); these two factors are regarded to be two of the biggest drivers of evaporation. However, there is also a land management issue. The highly managed drainage system of the Somerset Levels is likely to be responsible in part for periods of enhanced evaporation. Owing to the low elevation of the Somerset Levels, water is diverted or pumped out to sea during periods of high rainfall to prevent flooding of

agricultural land. This allows a rapid recycling of water causing the isotopic composition to be close to the global meteoric water line. However, in periods of low rainfall pumping ceases and water is retained to prevent the Somerset Levels from drying out. This increases the water residence times and, in turn, enables greater evaporative effects on the waters isotopic composition. This suggested effect of land management is, however, speculative as no data can be presented to test this hypothesis.

The scatter of data points is most likely down to the methodology used. The frequency of $\delta^{18}O_{water}$ measurements needs to be increased and targeted at specific meteorological events. For example, during periods of drought, prolonged precipitation and heat waves. This would provide information on extremes during the experimental periods. In additions to this, the time period over which the shell material is sampled needs to be targeted during specific meteorological events, so long as the amount of growth is sufficient for the analytical procedures.

Nevertheless, when periods of low precipitation and relatively high temperature coincide, as for the period prior to water sampling on the 6/6/2008, the isotopic composition of the South Drain Canal water deviates furthest from the GMWL. This deviation is thought to be concealed by time averaging within the carbonate shell material at the achievable sampling resolution, but could be the source of some error.

2.6.6 Seasonality profiles

The seasonal profiles demonstrate the relationship between the $\delta^{18}O$ of the shell carbonate and water temperature, with $\delta^{18}O$ of the shell carbonate becoming negative with increasing temperature (Fig. 2.13A). It would therefore appear that the $\delta^{18}O$ of the shell carbonate is in equilibrium with the $\delta^{18}O$ of the host water. Over the time period encompassed by the

cage experiments, temperature varied between 7°C to 20°C and $\delta^{18}O_{carb.}$ between −3.3‰ to −4.9‰ (1.7‰ difference) indicating a ~ 0.1‰ change per °C. In the majority of samples temperature appears to be the dominant factor determining $\delta^{18}O_{carb.}$ of the shell carbonate. This does not, however, apply to the penultimate data point (13/8/2008) analysed for V/C 5, where the isotopic composition of the water appears to have a greater influence on $\delta^{18}O$ of the shell carbonate (Fig. 2.13A).

2.6.7 Does sexual dimorphism or fecundity affect the oxygen isotope fractionation?

The genus *Viviparus* has separate male and female forms, whereas many other gastropods are hermaphrodite, which could have implications for carbonate secretion. However, sex can only be determined by the snail's soft part anatomy, which could only be preserved in cases of exceptional preservation within the fossil record. Sexual dimorphism also exists, with females tending to be larger than males after sexual maturity. Nevertheless, neither of these diagnostic features can easily be determined in the fossil record. Reproductive activity in modern specimens is determined by the presence of juveniles or eggs (which also would only be found in exceptionally preserved fossil specimens), which would be hard to determine in incomplete or compacted fossils or where soft part decay and transport has resulted in the loss of juveniles from the adult shell. However, the isotopic profiles of the cage specimens appear to indicated that $\delta^{18}O$ of the shell carbonate secretion appears not to be influenced by sex or whether females contain eggs or juveniles (Fig. 2.13A). Although, the data from only three specimens of similar sizes is not conclusive. As these potential vital effects appear to have no influence on oxygen isotope fractionation, the *V. contectus* thermometry equation can readily be applied to the fossil record.

2.6.8 Factors influencing $\delta^{13}C$ values

The range of $\delta^{13}C_{carb.}$ obtained from the three *V. contectus* specimens is larger than the range of $\delta^{13}C_{TDIC}$ values. However, the low sampling resolution of the $\delta^{13}C_{TDIC}$ may not provide sufficient information on the natural variability within the South Drain Canal system. Therefore, it is impossible to determine whether the shell $\delta^{13}C_{carb.}$ and $\delta^{13}C_{TDIC}$ are in equilibrium. Controls on $\delta^{13}C_{TDIC}$ of the host water in lakes include changes in; lake residence time, catchments vegetation cover and lake productivity (Leng *et al.*, 2005). Observations indicate a substantial increase in vegetation cover while the cage experiment was taking place. This seasonal increase in aquatic macrophyte coverage would have enriched the waters in ^{13}C, as photosynthesis preferentially uptakes ^{12}C, producing higher $\delta^{13}C_{TDIC}$. If we assume that $\delta^{13}C_{TDIC}$ is the dominant source for $\delta^{13}C_{carb.}$ then the generally increasing $\delta^{13}C$ of the shell carbonate for the time period encompassed by the cage experiment would represent the removal of ^{12}C by photosynthesis. However, the available data suggest that metabolised carbon and the availability of carbon as a food source has some influence on $\delta^{13}C$ of the shell carbonate. Furthermore, most viviparids are detritivores, preferentially filter feeding on bacteria found within detritus contained in the bottom silts and mud (Cook, 1949; Studier and Pace, 1978). In the absence of this food source, they have retained their ability to graze on algae and macrophytes (Dillon, 2000). The method of feeding depends on the abundance of algal growth, diatoms or bacteria which will change seasonally. Therefore, the proportion of $\delta^{13}C_{TDIC}$ and metabolic $\delta^{13}C$ may change seasonally or be related to the species' life cycle, e.g. reproduction and associated migration. *Viviparus* seasonally migrates to deeper water in the autumn and back to shallower littoral areas in the spring (Jokinen, 1982; Cheatum, 1934). This migration may influence the food sources on offer and perhaps provide a valid reason for this genus retaining a variety of feeding mechanisms. Finally, during Spring the energetic cost of reproduction is greater for males than for females (Ribi and Katoh, 1998), as

females continue to feed during copulation where males do not. This would result in low growth rates during this period and therefore may not affect the $\delta^{13}C_{carb.}$ of the shell.

Interestingly, $\delta^{13}C$ of shell carbonate from the tank experiments are similar to $\delta^{13}C_{TDIC}$ values measured from the field and field cage specimens. It was observed that the *V. contectus* specimens preferred to graze the tank sides, which were rapidly colonised by green algae, whereas they were rarely observed filter feeding or grazing on the provided food source (lettuce). It is probable that the green algal layers on the tank walls were seeded by propagules attached to the gastropod shells when initially introduced to the tanks. The $\delta^{13}C$ of TDIC and in turn the algae may have been influenced by the addition of $NaHCO_3$, maintaining the TDIC values similar to those of the natural environment.

Grossman and Ku (1986) concluded that carbon isotope fractionation between *Hoeglundina* and DIC, and between the molluscs and DIC, showed significant temperature dependences of -0.108 and -0.131‰ °C, respectively. They suggested that the temperature dependences were large enough to warrant consideration by researchers using the carbon isotopic compositions of aragonitic fossils as paleoenvironmental indicators. Further research by Romanek *et al.* (1992) for calcite and aragonite, found that the fractionation factor between shell carbonate and aqueous HCO_3, or $CaCO_3$-HCO_3, is 1.0027 ± 0.0006, and is only weakly dependent on temperature.

Although there is insufficient evidence to make a sound conclusion on whether the shell $\delta^{13}C_{carb.}$ and $\delta^{13}C_{TDIC}$ are in equilibrium, there is indirect evidence to suggest that carbon equilibrium may exist. Covariance between the *V. contectus* specimens $\delta^{13}C_{carb.}$ profiles would suggest that the carbon incorporated into the shell was not substantially derived from metabolic carbon, but from the $\delta^{13}C_{TDIC}$ of the canal water (Jones *et al.*, 2002). McConnaughey *et al.* (1997) also noted that fully aquatic, gill-breathing gastropods (such as *V. contectus*) produced shells with $\delta^{13}C$ values similar to $\delta^{13}C_{TDIC}$. They suggest that the

CO_2:O_2 values are much higher in aquatic systems resulting in greater amounts of environmental carbon being incorporated into their skeletons when compared with air breathing species. This assumes that CO_2 accompanies O_2 during exchange within the gills. Fritz and Poplawski (1974) showed that aquatic gastropods reared under differing TDIC conditions had $\delta^{13}C$ values that closely resembled the isotopic composition of the TDIC rather than the food they ingested. However, the range of $\delta^{13}C$ values obtained from the shell carbonate and TDIC imply that metabolic carbon has a greater influence.

2.6.9 Equation comparison

In order to validate the use of the combined *V. contectus* thermometry equation a comparison was made with already established palaeothermometry equations (Fig. 2.20). Our combined equation shows good agreement in the absolute magnitude of the oxygen isotope fractionation, particularly at higher temperatures, when compared to the laboratory study of White *et al.* (1999) and the field samples of Grossman and Ku (1986). Deviation in the cooler temperatures can be attributed to the data obtained from the field collection experiment. This portion of the data has a larger associated error due to poor constraints on temperature, $\delta^{18}O$ of the canal water and growth of the specimens. Care must also be taken when comparing this study to others due to possible difference in the fractionation factors (fractionation caused by the addition of hot acid during isotopic analysis) used to produce these equations. To be fully compatible, the same aragonitic fractionation factor must have been used in all three studies. Grossman and Ku (1986) used the calcite fractionation factor where White *et al.* (1999) provide no information on the value of the aragonite fractionation factor that they used.

This study appears to be in within error of other studies of isotope fractionation between biogenic aragonite and water covering a wide range of phyla e.g. marine and freshwater fish otoliths, gastropoda, scaphopoda, foraminifera, bivalves etc. (e.g. Epstein *et al.*, 1953;

Grossman and Ku, 1986; Patterson *et al.*, 1993; White *et al.*, 1999). This would imply that any of the aragonitic equations (this study, White *et al.* (1999) or Grossman and Ku (1986)) could be applied to fossil specimens of the genus *Viviparus*. Application of the combined thermometry equation will be used to calculate palaeotemperatures in the fossil part of this thesis. It is also recommended that the *V. contectus* combined thermometry equation should be used if fossil specimens of the genus *Viviparus* can be identified and that the $\delta^{18}O$ of the host water can be determined.

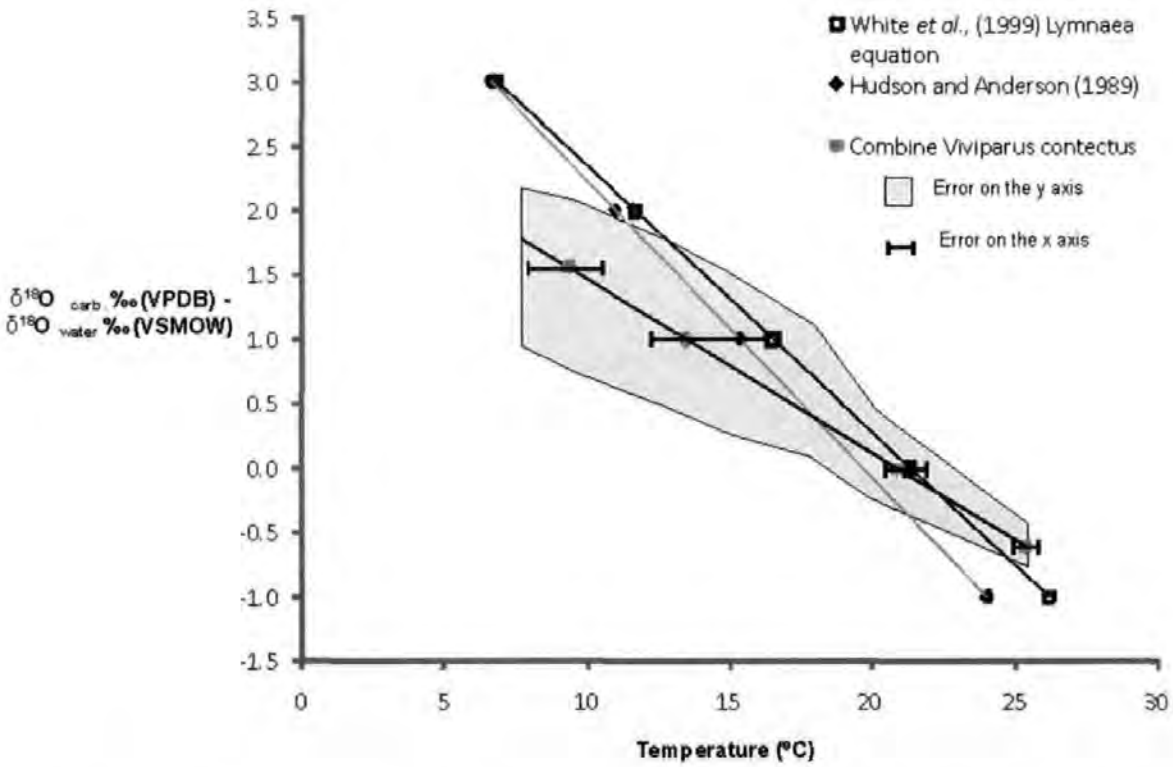

Figure 2.20 Graph showing the *V. contectus* equations in comparison with White *et al.* (1999) *Lymnaea* equation and Hudson and Anderson (1989) which is based on Grossman and Ku (1986) general aragonite equation with water $\delta^{18}O$ values cast in terms of SMOW. The solid lines represent the temperature range used in the determination of the linear regression.

2.6.10 Shell structure of *V. contectus*

The cross section of the *V. contectus* shell shows that the shell structure is similar to other gastropod species, consisting of three main layers, the upper or outer prismatic layer, the middle lamellate layer and the inner nacreous layer (Fig. 2.14). The crystalline structure of these layers is described by Wilbur and Saleuddin (1983) for the generalised gastropod shell structure. The different shell layers have distinct crystals types which are directly related to the different cell types in the mantle epithelium which overlies them. These specific epithelial regions control crystal form (Wilbur and Saleuddin, 1983). Analysis of a *V. contectus* shell using XRD showed that the calcium carbonate was aragonite.

Many of the *Viviparus* species decorate their shells with coloured banding (Fig. 2.15). A cross section of a *V. contectus* specimen (Fig. 2.15) shows that the colour is only present in the prismatic layer and does not extend into the middle lamellate layer or inner nacreous layer (the hypostracum) (Fig. 2.14 and 2.15). It is thought that the secretion of pigment is primarily a means of disposing of the waste products of metabolism, although colour patterns may play their part in natural selection (Cox, 1960). Field observations (by the author) indicate that the colour banding can be seen through the periostracum, unless obscured by algal growth as in Figure 2.7A.

Investigation into the shell structure of *V. contectus* using thin sections revealed that the thinner and thicker portions of the shell viewed in cross section were constructed differently. In the thinner parts of the shell the alternating crystals in the prismatic layer (ridges and troughs) were much thicker and squatter than those crystals in the thicker shell sections (Fig. 2.18). It is thought that the thinner shell material was secreted during the winter months when food resources were limited and temperatures were cooler causing the crystals to be secreted over a longer time period (slower growth rate). This would suggest that the rate of crystal growth is influenced by environmental conditions e.g. seasonality.

Figures 2.16 and 2.17 confirm this, as the shell appears to thin just prior to cessation. The erratic nature of the crystal structure also indicates that the condition for shell secretion is inconsistent. Wada (1957) found that the size and shape of the nacreous crystals were different in seasons of fast and slow growth.

Although further testing would be required, the troughs are thought to consist of organic proteins binding together the ridges or $CaCO_3$ crystals. These $CaCO_3$ crystals are composed of an inorganic substance which is derived primarily from the hemolymph in the mantle after diffusion and active transport across the outer mantle epithelium (Wilbur and Saleuddin, 1983). The organic proteins are secreted from cells of the epithelium and serve to separate individual crystals and to bind the crystals and individual crystal layers into a unified structure (Wilbur and Saleuddin, 1983). These matrix proteins are thought to make up less than 5% of the shell weight (Zhang and Zhang, 2006).

2.6.11 Ontogeny and bulk fragments in comparison with high resolution drilling

2.6.11.1 $\delta^{18}O$

The isotopic composition of the shell follows a cyclic pattern, with values shifting from negative to positive values. The $\delta^{18}O$ signature of the shell carbonate is predominantly controlled by temperature and it has been shown by the seasonality profiles (section 2.3.1.5.) that the positive $\delta^{18}O$ values are associated with cooler temperatures where the more negative $\delta^{18}O$ values are related to warmer temperatures. As the UK has clear seasonal cycles it may be possible to determine from the specimens' isotopic record how long it had lived. The high resolution $\delta^{18}O$ record appears to shows that the *V. contectus* specimen in Figure 2.19, lived for ~2+ years. These shifts in the high resolution $\delta^{18}O$

record appear to become more condensed closer to the aperture (Fig. 2.19). As juveniles are released from the parent during April, $\delta^{18}O$ values close to the apex are thought to relate to spring temperatures. The $\delta^{18}O$ values become more negative in section11 (–5.6‰) and return to more positive values by section 8 (–2.9‰). This yearly isotopic shift covers the first 74.8 mm (120.35 mm to 45.55 mm), the oldest part of the shell. The second isotopic cycle occurs between 45.55 mm and 5.5 mm, total shell growth of 40.05 mm. During this period $\delta^{18}O$ reached a minimum value of –4.8‰ and a maximum value of –3.0. The specimen was collected from the field at the end of August 2007. Just prior to this at 5.5 mm the values start to return to more negative values. It would therefore suggest that this part of the shell represents half of another seasonal cycle. Sexual maturity occurs when *V. contectus* reaches approximately 2 years old. This would explain the drop in growth rate as the proportion of energy allocated for growth is reduced. Fast growth rate in the first year is particularly important for females as they require room within the shell for juvenile growth while within the pallial oviduct.

The cessation marks on the shell tend to coincide with the most positive $\delta^{18}O$ values indicating that they are related to cooler temperatures. This would suggest that temperature fell below the 3°C growth threshold. However there is one exception, occurring at 11.7 mm on the boundary between section 2 and 1. Although these values are relatively negative the cessation mark coincides with a positive peak in $\delta^{18}O$. Therefore, this growth cessation may have brought about by a rapid change in temperature rather than the crossing of a growth temperature threshold.

A comparison of the average values for each section shows that the *V. contectus* fragments produced more positive $\delta^{18}O$ averages than the $\delta^{18}O$ record of the high resolution drilling (Fig. 2.19). The large isotopic offset between the micromilled samples and the fragments is

greatest between 120mm and 82mm. Several reasons could be put forward to explain this difference:

1. Analytical error. Samples between 120mm and 82mm were analysed during 2009, where the remaining samples were analysed at the end of 2007 beginning of 2008. Calibration differences on the GV Instruments Isoprime Mass Spectrometer may be responsible for some of the isotopic offset between 120mm and 82mm.
2. Sampling procedure. The bulk fragments consist of the entire shell (all three shell layers) where during the micromilling procedure there is potential for part of the inner nacrecous layer to be missed during the drilling process. There is evidence that the nacrecous layer in bivalves may consist of re-deposited and / or isotopically heavy calcite (e.g. Cusack *et al.*, 2008). If this is true for *Viviparus* then this may explain the observed offset seen in Fig. 2.19.

This offset has implications for obtaining an isotopic seasonality profile and the calculation of palaeotemperatures. To test this several *Viviparus* shells could be sectioned into the individual shell layers, with each layer analysed for $\delta^{18}O$ and $\delta^{13}C$. This would potentially prove or disprove the theory of different shell layers having different isotopic compositions. This offset has implications for obtaining an isotopic seasonality profile and the calculation of palaeotemperatures from such data. This will be further discussed in Chapter 7.

2.6.11.2 $\delta^{13}C$

A comparison of the average values for each section shows that the *V. contectus* fragments produced more negative $\delta^{13}C$ averages than the $\delta^{13}C$ record of the high resolution drilling (Fig. 2.19). The isotopic offset is similar to that seen in the $\delta^{18}O$. This is likely to be caused by the reasons stated in Section 2.6.11.1.

2.7 Summary

Experimental measurements of the $^{18}O/^{16}O$ isotope fractionation between the biogenic aragonite of *V. contectus* (Gastropoda) and its host freshwater was undertaken to generate a species specific thermometry equation. The temperature dependence of the fractionation factor and the relationship between $\Delta\delta^{18}O$ ($\delta^{18}O_{carb.} - \delta^{18}O_{water}$) and temperature, were calculated from specimens maintained under laboratory and field (collection and cage) conditions. The field specimens were grown (Somerset, UK) between August 2007 and August 2008, with water samples and temperature measurements taken monthly. Specimens grown in the laboratory experiment were maintained under constant temperatures (15°C, 20°C and 25°C) with water samples collected weekly. Application of a linear regression to the datasets indicated that the gradients of all three experiments were within experimental error of each other (±two times standard error) therefore, a combined (laboratory and field data) correlation could be applied. The relationship between $\Delta\delta^{18}O$ ($\delta^{18}O_{carb.} - \delta^{18}O_{water}$) and temperature (T) for this combined dataset is given by:

$$T = -7.43(+0.87, -1.13) * \Delta\delta^{18}O + 22.89(\pm 2.09)$$

(T is in °C, $\delta^{18}O_{carb.}$ is with respect to Vienna Pee Dee Belemnite (VPDB) and $\delta^{18}O_{water}$ is with respect to Vienna Standard Mean Ocean Water (VSMOW). Quoted errors are 2 times standard error).

The results from this study indicate that *V. contectus* appears to not exhibit any significant species specific vital effects when secreting shell carbonate. This species appears to precipitate its shell in oxygen isotopic equilibrium with the host water, as the equation produced is within error of the previously published aragonitic equations. This confirms that this species is capable of recording the combined signal of temperature and the oxygen isotope composition of the host water. The isotope signal of the secreted shell carbonate is dominated by temperature when the $\delta^{18}O$ of the host water remains relatively constant, as

indicated by the laboratory experiment and cage specimens. Seasonal isotopic profiles indicate that the uptake of $\delta^{18}O$ during shell secretion is not influenced by size, sex or whether females contain eggs or juveniles.

An understanding of the crystalline shell structure of modern *Viviparus* can aid in the determining the preservation of fossil specimens. The investigation into the shell structure of *V. contectus* has also revealed interruptions in shell secretion activity termed growth cessations. These areas are particularly important when sampling the shell material at high resolution for seasonality investigations. Prior to the point of cessation the crystal structure become irregular with the amount of calcium carbonate secreted reduced. New shell growth initiated behind the older shell material producing an overlap. This is important as sampling of these areas may produce averaging of isotopic values due to incorporating shell material secreted before and after the cessation in growth. High resolution sampling in comparison with bulk fragment samples has suggested that there may be an issue concerning the isotopic composition of individual shell layers. This requires further investigation.

CHAPTER 3 EXPERIMENTAL DETERMINATION OF A *VIVIPARUS*

3.1 Introduction

In order to reconstruct past climates the relationship between the equilibrium $\delta^{18}O$ value of carbonate and the temperature of the precipitation must be well constrained (Shanahan *et al.*, 2005). The calculated fractionation factors differ significantly between different proposed relationships depending upon the method used in their determination, such as those produced using experimental measurements (e.g. Kim *et al.*, 2006, 2007); theoretical calculations (e.g. Chacko and Deines, 2008) and biological specimens from natural settings (e.g. Grossman and Ku, 1986; White *et al.*, 1999). Within the literature it is unclear which of these temperature – $\delta^{18}O$ relationships should be applied to a particular organism for a correct interpretation of the $\delta^{18}O$ data. This is further complicated by non-equilibrium isotopic effects which are generally attributed to either vital and/or non-vital kinetic effects. The causes of disequilibrium or vital effects are often systematic and can be accounted for by detailed studies of the particular genera or species in question. This is discussed further in Chapter 2 Section 2.1.2.

A general introduction to the gastropod genus *Viviparus* can be found in Chapter 2 Section 2.1.

The aim of this study is to improve our understanding of gastropod aragonite palaeothermometry equations by calibrating the fractionation between water and biogenic carbonate (aragonite) of *Viviparus viviparus* (Linnaeus, 1758) (Fig. 3.1). A species of the genus *Viviparus* has been chosen specifically to complement the other part of this research, which focuses on palaeoclimatic change across the E/O transition and Oi-1 glaciation (~33 Ma). *Viviparus viviparus* was also chosen on the basis that the closest living relative of *Viviparus lentus* (the species chosen for the fossil study see Chapter 6) is the European

species *Viviparus viviparus* and the North American species *Viviparus georgianus* (Preshad, 1928).

3.2 Methods

Exeter Canal (Devon, UK) was chosen as a study site based upon the known occurrence of *Viviparus viviparus* (*V. viviparus*) (Fig. 3.1) and because large flowing water bodies (river or canal), as opposed to standing waters such as lakes, have been shown in previous studies (White *et al.*, 1999) to have hydrological conditions that allow the isotope composition of the water to remain relatively constant throughout the year.

Figure 3.1 Example specimen of *V. viviparus* from Exeter Canal.

The methods used in the production of the *V. viviparus* thermometry equation were modified from those techniques outlined by White *et al.* (1999).

Exeter Canal was initially constructed in 1566 to encourage the development of trade routes with other UK ports and Europe. Extension, deepening and widening of the canal occurred in several stage (1676, 1698, 1830), allowing access for sea going vessels of up to 150 tonnes to Exeter quay to supply the increasing demand for the wool trade (Blair, 2007). By 1844 the railway line had reached Exeter, reducing the shipping trade which eventually caused the canal to deteriorate and fall into disuse. Renovation of the quay area

and improvements to the lock system has encouraged recreational use of the canal in recent years.

The sampling site used in this study is located near to the Alphington Industrial Estate on the outskirts of Exeter (50°42.387'N 3°31.228'W). On the initial site visit an I-button data-loggers was installed to record water temperatures every two hours throughout the 12 month sampling period. The I-button was sealed in a square plastic mesh pouch and attached using nails to the underside of the sleeper forming the basal part of a fisherman's pontoon.

During each sampling visit (approximately once per month) water samples were collected and analysed for $^{18}O/^{16}O$ ratios and the $^{13}C/^{12}C$ ratios of total dissolved organic carbon (TDIC) (see full methods in Appendix 2). Temperature (±1°C), pH (± 0.2) and salinity (±0.5) measurements were also measured on site using a Yellow Springs Incorporated (YSI) model 63, pH, Conductivity, Salinity and Temperature probe.

3.2.1 Field based methods *V. viviparus* collection

On each visit between 5 and 10 *V. viviparus* specimens were collected from the bottom sediments of Exeter Canal (~3 m in depth) using a drag net, approximately once a month between 30/8/2007 and 13/8/2008. As *Viviparus* is a bottom dweller (particularly during the winter months) a specially designed net was made that was heavy enough to sink into the muds in the bottom of the canal. During spring and summer specimens were collected by hand, removed from the canal edge or off rocks within wade depth. Upon return to the laboratory the *V. viviparus* samples were ethically euthanized by cryogenesis. Their bodies were removed from the shells, sexed and when eggs / juveniles occurred these were counted. The shells were soaked overnight in dilute (2%) NaOCl to remove organic material including the periostracum. The shells were then rinsed in ultra pure water and oven dried at 25°C. Shell measurements were taken, including shell height and width;

aperture height and width and the number of cessation marks observed on the shell. Using a small Dremel drill and a 0.4 mm tungsten carbide spade drill bit, approximately the last millimetre of shell growth was removed by milling the growth bands parallel to the aperture edge. A minimal number of growth bands were removed to produce a powdered sample at the weight (~0.30 to 0.50 mg) require for the $^{18}O/^{16}O$ and $^{13}C/^{12}C$ ratios to be analysed.

A field cage experiment, like that described in Chapter 2, was not undertaken at Exeter Canal as a suitable location could not be found.

3.2.2 Laboratory culturing method

V. viviparus samples were collected for culturing from Exeter Canal during the first sampling trip (August 2007) with additional specimens added during February 2008. These specimens (~10 per controlled temperature) were cultured thereafter in tanks in the laboratory at controlled temperatures (15°C, 20°C and 25°C) for a period of approximately two months, or until each specimen had added enough new shell growth for sampling. The growing edge (aperture) of the *V. viviparus* shells was marked with white paint before placing shells in culturing tanks to ensure that new growth could be identified. The specimens were kept in deionised water containing 14.7 g of $MgSO_4$, 11.7 g of $NaHCO_3$, 0.48 g of KCl and 5.4 g of $CaSO_4$ (for every 60 litres), to maintain suitable water quality for the gastropods to live comfortably (Rundle *et al.*, 2004). The isotopic composition, temperature, pH and salinity of the water were measured weekly during the culturing period. To minimise evaporation, particularly in the 25°C tank, each tank was sealed with cling film causing most of the vapour to condense and be recycled back into the tank. Minimal aeration ensured that the water was well mixed and oxygen levels were sufficient to sustain the gastropod specimens.

For full details on the laboratory culturing method see Chapter 2 Section 2.2.2.

3.2.3 Oxygen and carbon isotope analysis

All of the oxygen and carbon isotopic analysis was carried out at the NERC Isotope Geosciences Laboratory. The waters were equilibrated with CO_2 using an Isoprep 18 device for oxygen isotope analysis with mass spectrometry performed on a SIRA. For hydrogen isotope analysis an on-line Cr reduction method was used with a EuroPyrOH-3110 system coupled to an Isoprime mass spectrometer. Isotopic ratios ($^{18}O/^{16}O$ and $^{2}H/^{1}H$) and $\delta^{18}O$ and $\delta^{2}H$ (‰, parts per mil), are defined in relation to the international standard Vienna Standard Mean Ocean Water (VSMOW) by comparison with laboratory standards calibrated using NBS standards. Analytical precision is typically ±0.05‰ for $\delta^{18}O$ and ±1.0‰ for $\delta^{2}H$.

Total dissolved inorganic carbon (TDIC) from the water samples was precipitated in the field as $BaCO_3$ by addition of a solution of barium chloride and sodium hydroxide. In the laboratory CO_2 was generated by the reaction of the $BaCO_3$ with 100% phosphoric acid. The CO_2 was analysed for $^{13}C/^{12}C$ ratio using an Optima dual inlet mass spectrometer. Analytical precision (1 Standard Deviation (SD)) based on laboratory standard is < 0.1‰.

For the shell carbonate $^{13}C/^{12}C$ and $^{18}O/^{16}O$, approximately 30 to 100 μg of carbonate was analysed using the IsoPrime dual inlet mass spectrometer plus Multiprep device. Analytical precision (1SD) is typically < 0.07‰ for both ratios. Carbonate and TDIC isotopic ratios are reported in the per mil notation (‰) relative to the international standard Vienna Pee Dee Belemnite (VPDB) by comparison with laboratory standards calibrated using NBS standards. An aragonite fractionation factor (1.01034 taken from Friedman and O'Neil, 1977), was applied to convert the measured isotope compositions of CO_2 generated by the reaction of aragonite with ortho-phosphoric acid to the isotope compositions of aragonite.

3.2.4 Formulation of equation

Shell $\delta^{18}O_{carb.}$ values were used in conjunction with temperature and water $\delta^{18}O$ to derive values of $1000\ln\alpha$ and $\Delta\delta^{18}O$ ($\delta^{18}O_{carb.} - \delta^{18}O_{water}$). This information was then plotted against $1/T$ (T in Kelvin) and T (°C), respectively, to give the relationships described below. The temperature dependence of the fractionation factor (α) is given by the linear relationship (Eq. 1):

$$1000\ln\alpha = M\,(1000T^{-1}) - C \quad (1)$$

Where:

$\alpha = ((\delta^{18}O_{carb.}\ VSMOW) + 1000) / ((\delta^{18}O_{water}\ VSMOW) + 1000)$

M = gradient of the linear trend

C = y-axis intercept

T = temperature in Kelvin

The thermometry equations for both the laboratory and field based studies were generated by plotting the dependent variable, $\Delta\delta^{18}O$ ($\delta^{18}O_{carb.}$ (VPDB) − average $\delta^{18}O_{water}$ (VSMOW)), against the independent variable, average recorded water temperature (°C). A linear regression was calculated to determine the relationship between the $\Delta\delta^{18}O$ and temperature, producing a thermometry equation (Eq.2 and 3) in the form of:

$$\Delta\delta^{18}O = M\ (2\ S.E)^{*}\ Temp. + C\ (2\ S.E) \quad (2)$$

This was then rearranged to give:

$$Temp.\ (°C) = -\ M\ (2\ S.E)^{*}\Delta\delta^{18}O + C\ (2\ S.E) \quad (3)$$

Where:

C = y-axis intercept

M = gradient of linear trend

2 S.E = 2 times standard error

3.3 Results

The results for the laboratory culturing experiment and field collection experiment are given in Tables 3.1 and 3.2.

3.3.1 Laboratory culturing experiment

For the laboratory culturing experiment the temperature dependence of the fractionation factor (α), between 15 and 25°C is given by (Eq. 4):

$$1000\ln \alpha = 11.48(\pm 0.1)*(1000T^{-1}) - 8.12\ (\pm 0.28) \qquad (r^2 = 0.42) \qquad (4)$$

Where T is in Kelvin, and the relationship between $\Delta\delta^{18}O$ and temperature is given by (Eq. 5 and 6):

$$\Delta\delta^{18}O = -0.12\ (\pm 0.10)*\text{Temp} + 2.82(\pm 1.78) \qquad (5)$$

This rearranges to:

$$\text{Temp. (°C)} = -8.03(+3.53, -29.19)*\ \Delta\delta^{18}O + 22.62(\pm 14.24) \qquad \text{(Fig. 3.2A)} \qquad (6)$$

The equation produced by the laboratory culturing experiment shows a very poor statistical regression (r^2 =0.42) in contrast to the *V. contectus* tank and field experiments (Fig. 2.10).

	Mean pH	Mean Salinity (ppt)	Mean Temp. (°C)	$\delta^{18}O_{water}$ (‰ VSMOW)	$\delta^{18}O_{carb.}$ (‰ VPDB)	$\Delta\delta^{18}O$ ($\delta^{18}O_{carb.}$ ‰ (VPDB) – $\delta^{18}O_{water}$ ‰ (VSMOW))
Laboratory culturing data	7.6 (±0.3 std) (n=24)	0.3 (±0.1 std) (n=24)	15.1 (±0.4 std) (n=24)	-5.3	-4.6	0.7
					-4.6	0.7
					-5.1	0.2
					-3.2	2.0
				-5.2	-3.5	1.7
					-4.0	1.1
					-4.7	0.5
	7.5 (±0.2 std) (n=24)	0.3 (±0.2 std) (n=24)	19.6 (±0.2 std) (n=24)	-4.7	-4.5	0.2
					-5.1	-0.4
	7.3 (±0.3 std) (n=9)	0.3 (±0.0 std) (n=9)	25.0 (±0.3 std) (n=9)	-5.5	-5.6	-0.1
					-5.6	-0.1

Table 3.1 Laboratory culturing data (probe result and water analysis) and the results from the analysis of carbonate material from *V. viviparus* cultured within the laboratory culturing experiments.

3.3.2 Exeter Canal field collection experiment

The I-button data provides a temperature record from August 2007 to August 2008, showing a seasonal profile overprinted by daily fluctuations (Fig. 3.2).Temperature is therefore well constrained for each sampling collection interval. During the field experiment (August 2007 to August 2008) temperatures reached a maximum of 20.8°C and a minimum of 3.4°C (a range of ~17.5°C) and a mean of ~11.5°C for the entire sampling period. An average temperature between the known collection dates was calculated for the regression analysis (Table 3.3). Water samples were collected on every sampling trip and analysed for $\delta^{18}O$. Over the entire collection period the range of recorded $\delta^{18}O_{water}$ values was 1.3 ‰ for Exeter Canal whereas the samples collected for the same time period from South Drain Canal showed greater variation (range of 1.9‰). Production of the field based *V. viviparus* thermometry equation involved establishing average $\delta^{18}O_{water}$ values between successive sampling trips (for example between 6/6/2008 to 3/7/2008 and 3/7/2008 to 13/8/2008) (Tables 3.2 and 3.3).

For the field collection experiment the temperature dependence of the fractionation factor (α), between 7.7 and 18.2 °C is given by (Eq. 7):

$$1000\ln \alpha = 4.05\ (\pm 1.19)*(1000T^{-1})\ 16.54\ (\pm 6.04) \quad (r^2 = 0.29) \tag{7}$$

Where T is in Kelvin, and the relationship between $\Delta\delta^{18}O$ and temperature is given by (Eq. 8 and 9):

$$\Delta\delta^{18}O = -0.05(\pm 0.02)*\text{Temp.} + 1.17(\pm 0.35) \tag{8}$$

This rearranges to:

$$\text{Temp. (°C)} = -20.55(+7.42, -24.53)*\ \Delta\delta^{18}O + 24.03\ (\pm 7.43) \quad \text{(Fig.3.3)} \tag{9}$$

The equation produced by the field collection method shows a relatively poor statistical regression (r^2 =0.29) in contrast to the *V. viviparus* tank experiment (r^2 =0.42) (Fig. 3.3B) and the *V. contectus* tank (r^2 =0.92) and field experiments (field cage (r^2 =0.67 and field collection (r^2 =0.44)).

	Date	pH	Salinity (ppt)	I- button Av. temp. (°C)	$\delta^{18}O_{water}$ (‰ VSMOW)	$\delta^{18}O_{carb.}$ (‰ VPDB)
Field data	03/08/2007	7.9	0.1	14.7 (±2.4)	-5.9	-5.3
						-5.5
						-5.4
						-5.6
						-5.2
	31/10/2007	7.5	0.1	7.6 (±2.0)	-5.9	-5.3
						-5.1
						-3.7
						-5.3
						-4.8
	22/01/2008	7.7	0.1	7.5 (±1.2)	-5.3	-5.2
						-4.3
						-5.0
						-5.3
						-4.9
	02/09/2008	8.2	0.1	8.5 (±1.0)	-5.0	-5.3
						-5.2
						-5.1
						-5.0
						-4.9
	03/04/2008	7.8.	0.1	16.0 (±3.2)	-5.7	-5.9
						-5.4
						-6.1
						-5.8
						-5.3
	25/04/2008	7.7	0.1	17.7 (±1.1)	-4.8	-5.2
						-6.2
						-5.4
						-5.4
						-5.3
	06/06/2008	7.2	0.1	18.2 (±1.2)	-5.4	-5.1
						-5.1
						-5.3
						-5.3
						-5.2

Table 3.2 Field data (probe result and water analysis) from Exeter Canal and the results from the analysis of carbonate material from *V. viviparus* collected from the field.

Sampling period	No. of days	Av. Temp. (°C)	Stdev (°C)	Min. (°C)	MaX. (°C)	Range (°C)
30/8/07 to 31/10/07	62	14.7	2.4	9.9	18.8	8.9
31/10/07 to 22/1/08	83	7.5	1.9	3.4	11.6	8.2
22/1/08 to 29/2/08	38	7.5	1.2	5.4	9.6	4.2
29/2/08 to 3/4/08	34	8.5	1.0	7.4	12.2	4.8
3/4/08 to 25/4/08	22	10.7	1.4	9.0	13.6	4.6
25/4/08 to 6/6/08	42	16.0	2.1	9.0	20.1	7.9
6/6/08 to 3/7/08	27	17.8	1.1	16.1	19.0	3.1
03/07/08 to 13/8/08	41	18.2	1.2	16.6	20.9	4.3

Table 3.3 I- button temperature data summary for the periods between known collections dates, giving average temperature (±) minimum and maximum temperatures and the range of temperatures for that period.

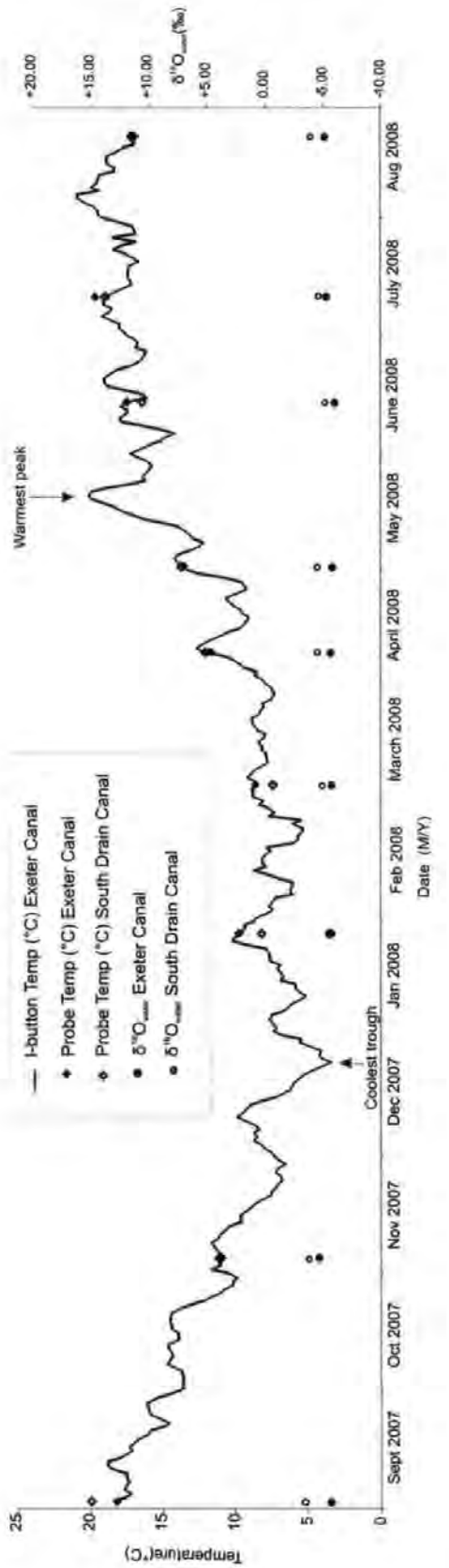

Figure 3.2 I-button temperature record from Exeter Canal is compared with the probe temperature readings from Exeter Canal and South Drain Canal. These results indicate that the probe temperatures are, in general, close to those recorded by the I-button. The $\delta^{18}O$ of the local water from Exeter Canal and South Drain Canal show that South Drain Canal has consistently more positive $\delta^{18}O_{water}$ values than Exeter Canal and that these values do not co-vary with temperature.

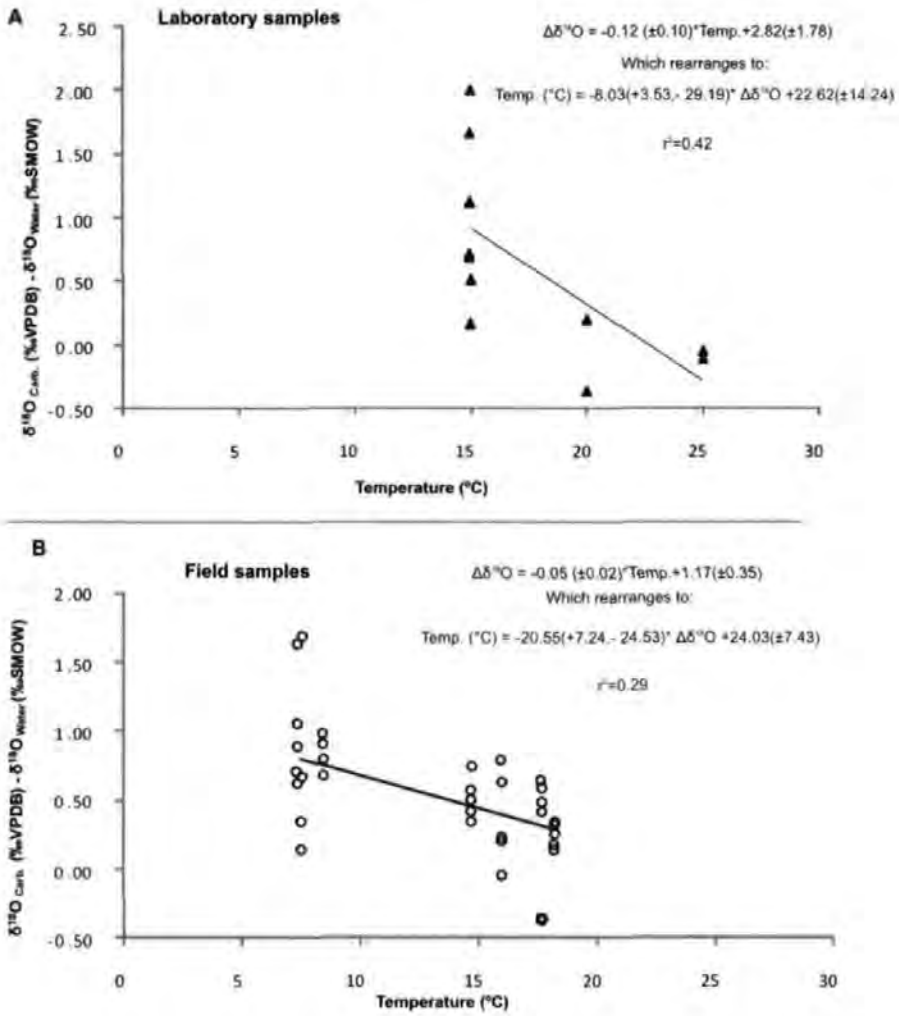

Figure 3.3 The relationships between $\Delta\delta^{18}O$ ($\delta^{18}O_{carb.} - \delta^{18}O_{water}$) and temperature for *V. viviparus* specimens from the tank experiments (A) and specimens from the field collection experiment (B) at Exeter Canal. A lack of data between 9 and 15°C in graph B was caused by the author not being able to collect *V. viviparus* specimens during the site visit on the 31/10/2007. Leading to the introduction of the net collection method.

3.3.3 Temperature vs. $\delta^{18}O$ water

A comparison of the I-button temperature record from Exeter Canal with the probe readings from both Exeter Canal and South Drain Canal (Fig. 3.2) indicates that the probe temperatures are, in general, close to those recorded by the I-button for that particular day. As expected, the South Drain Canal probe temperatures are further displaced from the I-button temperature record than Exeter Canal due to the difference in site location. The $\delta^{18}O$

of the local water from Exeter Canal and South Drain Canal suggests that the latter has consistently more positive $\delta^{18}O_{water}$ values. The $\delta^{18}O_{water}$ and $\delta^{2}D_{water}$ results from the analysis of the water samples collected from South Drain Canal and Exeter Canal plot along local evaporation lines (LEL), which deviates from the global meteoric water line (GMWL) (Fig. 3.4). The majority of Exeter Canal's data points plot along the GMWL. Therefore, Exeter Canal's LEL deviates to a lesser extent than the South Drain Canal LEL.

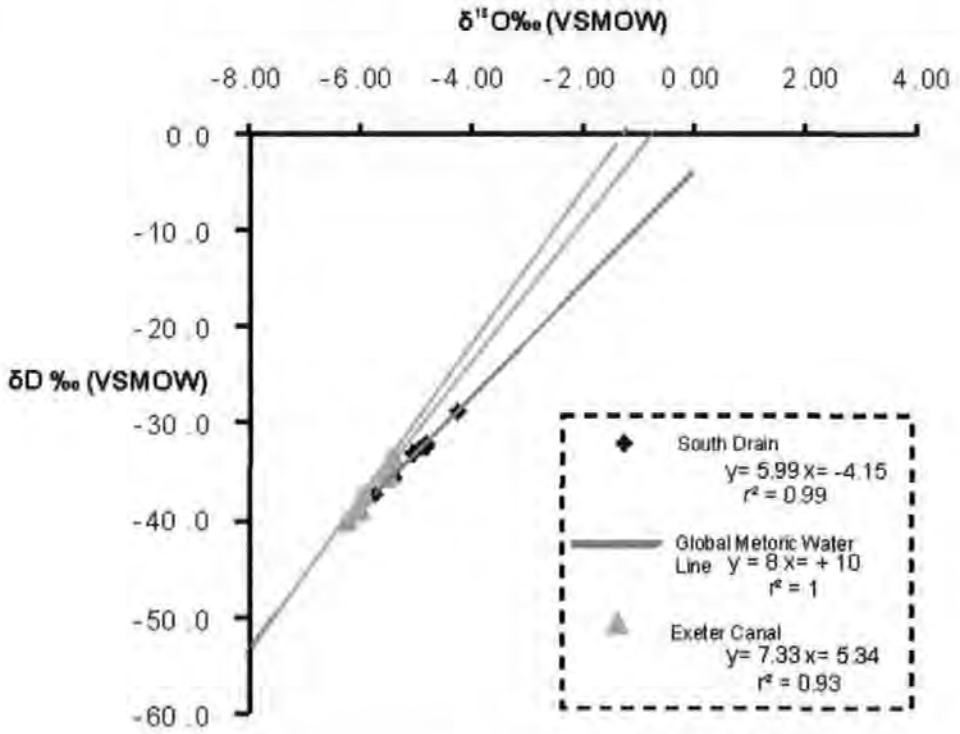

Figure 3.4 $\delta^{18}O_{water}$ values obtained from Exeter Canal and South Drain Canal in comparison with the global meteoric water line.

3.4 Discussion

3.4.1 Laboratory culturing experiments

The linear regression ($r^2 = 0.42$) calculated for the relationship between $\Delta\delta^{18}O$ and temperature indicates that the laboratory equation is statistically the most robust of the *V. viviparus* results. However, the linear regression for *V. viviparus* is poor in comparison with the linear regressions obtained from the *V. contectus* laboratory culturing experiment

($r^2 = 0.91$). Part of the spread in seen in specimen cultured at 15°C within the laboratory experiments represents the likely genuine variation in samples. However, growth rates of *V. viviparus* were significantly less than those recorded for *V. contectus*. In some cases *V. viviparus* specimens achieved no growth while within the laboratory experiment. The size of the *V. viviparus* specimens indicates that they were too large to be juveniles; therefore it is likely that they had already reached sexual maturity prior to being placed into the laboratory experiment. The proportion of energy these specimens allocate for growth would be significantly reduced and could explain the slower growth rates. The observed difference in growth rates could also be related to a number of factors unique to the laboratory experiments including: lack of seasonal change in temperature; poor or incorrect food source; insufficient quantities of dissolved calcium carbonate; disturbance; light intensities and pH (although weekly measurements have shown this to remain within the tolerance levels (Table 3.2). Therefore the *V. viviparus* cultured at 20 and 25 °C had more specimens showing no growth.

3.4.2 Field collection

In comparison with the linear regression of *V. contectus* field collection experiment ($r^2 = 0.44$) the linear regression produced by the field collection experiment was poor. Variable growth rates of the *V. viviparus* are thought to be responsible for this poor linear regression, as it was presumed that the shell material nearest the aperture would have been secreted at some time between sampling collections. It is probable that some of the specimens exhibited no carbonate secretion during the time period between sampling.

3.4.3 Shell condition

The condition of the *V. viviparus* shells was an issue in regards to the preservation of their shells isotopic composition. Evidence of chemical corrosion and mechanical breakage of the *V. viviparus* shells while the specimens were alive is clearly shown in Figure 3.5.

Chemical corrosion is concentrated around the spire and in places penetrates deep into the shell structure. On occasions there is evidence for the erosion forming a hole through the entire shell. Colouration of the shell in these locations had also been lost due to the removal of the prismatic layer (discussed further in Chapter 2 Section 2.4.7). The location of this type of erosion would suggest that the speed at which this process takes place is slow, as the shell nearest the aperture shows no significant erosion of this kind, or that this particular method of erosion attacks the juvenile part of the shell only (that formed while the juvenile was retained within the female). However, areas of weakness such as cessation marks also tend to be picked out by this method of shell erosion. Decalcification of the shell can occur if there is a carbonate deficiency within the water (Ribi *et al.*, 1986). Re-adsorption of the shell carbonate can occur, with the calcium carbonate obtained potentially being re-deposited along the aperture. This could have a significant impact on the relationship between the equilibrium $\delta^{18}O$ value of carbonate and the temperature of the precipitation. Further work is required to determine whether this affects the resulting calcite or whether it is re-precipitated according to fractionation of the temperature at the time of re-precipitation.

In some cases cessation marks situated close to the aperture are jagged (reflecting a former angular aperture margin) suggesting that the shell has been damaged by a mechanical process. With both mechanically induced cessation marks and those produced by natural stimuli (e.g. cold temperature) the new shell growth begins underneath the old shell material. Exeter Canal is used heavily for recreational activates which may cause the shells to become mechanically damaged. Although this does not directly impact on the isotopic composition of the shell, the pattern of re-growth needs to be taken into account when high resolution sampling is undertaken.

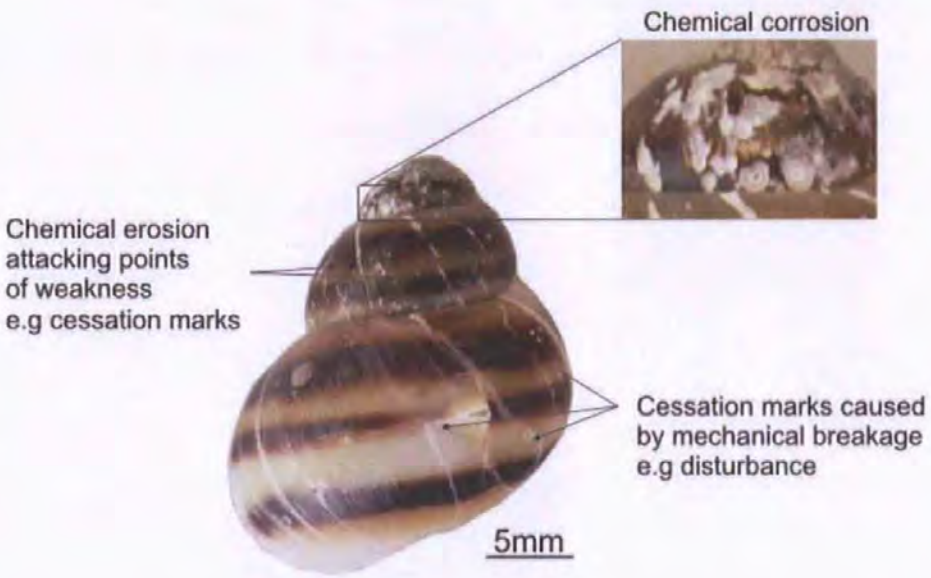

Figure 3.5 A typical example of *V. viviparus* shell showing evidence of chemical corrosion and mechanical erosion. The chemical erosion is concentrated around the shell spire with the mechanical breakage of the shells forming distinctive cessation marks on the section of shell nearest the aperture and within the last whorl.

3.4.4 Temperature versus $\delta^{18}O$ water

Exeter Canal provides one of the best examples of an open fluvial system as the $\delta^{18}O_{water}$ values obtained do not significantly deviate from the 'Global Meteoric Water Line' (McCrea, 1950) (Fig. 3.4). Deviation from the global meteoric line indicates that the water body involved has experienced kinetic fractionation (evaporation) producing a local evaporation line. Exeter Canal appears to plot very close to the global meteoric water line indicating that the canal water is very nearly in isotopic equilibrium with precipitation. The Exeter Canal catchment area is not as highly managed, in term of water management, as South Drain Canal. Therefore, Exeter Canal does not experience long residence times which would potentially lead to significant evaporation.

3.4.5 Comparison of the *V. viviparus* thermometry equation with the *V. contectus* thermometry equation

Although the *V. viviparus* combined regression experiences a greater spread in the dataset which, produces a poor r^2 value, a comparison can still be made with the combined *V. contectus* thermometry equations (outlined in Chapter 2) and already established palaeothermometry equations (Fig. 3.6). The *V. viviparus* combined equation shows good agreement in the absolute magnitude of the oxygen isotope fractionation, particularly at higher temperatures, when compared to the other palaeothermometry equations. Deviation from White *et al.* (1999) and Grossman and Ku (1986) in the cooler temperatures is smaller than that of the *V. contectus* thermometry equation. This portion of the data has a larger associated error due to poor constraints on temperature, $\delta^{18}O$ of the canal water and growth of the *V. viviparus* specimens.

Care must also be taken when comparing this study to others due to possible difference in the fractionation factors used to produce these equations. To be fully compatible, the same aragonitic fractionation factor must have been used in all three studies. Both White *et al.* (1999) and Grossman and Ku (1986) provide no information on the value of the aragonite fractionation factor they used.

Due to the poor regression it is not possible to determine whether *V. viviparus* shows a strong species specific vital effect. Confirmation of this is needed through experimental analysis on the same species from a different location where the condition of the shell is not an issue. The addition of a cage experiment would provide tighter constraints on the parameters affecting carbonate secretion, potentially reducing the scatter of data. Without further experimental analysis it would be unwise to produce a genus specific thermometry equation by combining the *V. viviparus* and *V. contectus* datasets.

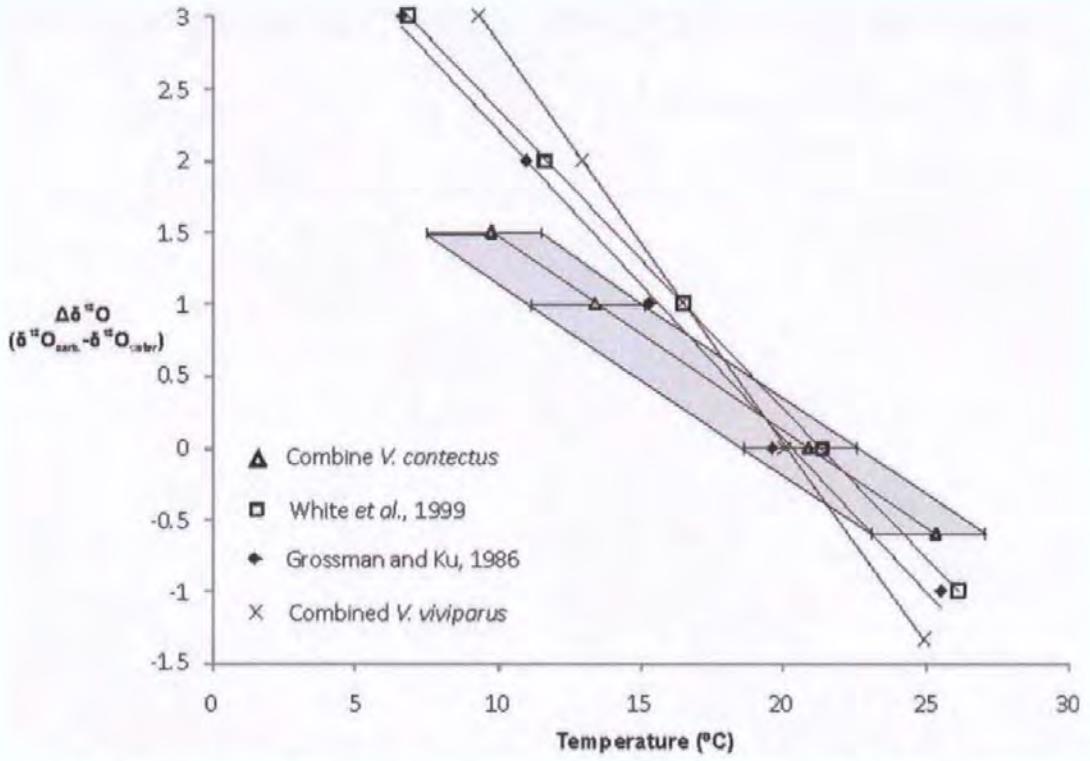

Figure 3.6 Graph showing the *V. viviparus* combined equation in comparison with the *V. contectus* combined equation; White *et al.* (1999) *Lymnaea* equation and Grossman and Ku (1986) general aragonite equation. The solid lines represent the temperature range used in the determination of the linear regression.

3.5 Summary

Experimental measurements of the $^{18}O/^{16}O$ isotope fractionation between the biogenic aragonite of *V. viviparus* (Gastropoda) and its host freshwater was undertaken to generate a species specific thermometry equation. The temperature dependence of the fractionation factor and the relationship between $\Delta\delta^{18}O$ ($\delta^{18}O_{carb.} - \delta^{18}O_{water}$) and temperature, were calculated from specimens maintained under laboratory and field conditions. The field specimens were grown, (Devon, UK) between August 2007 and August 2008, with water samples and temperature measurements taken monthly. Specimens grown in the laboratory experiment were maintained under constant temperatures (15°C, 20°C and 25°C) with water samples collected weekly. Application of a linear regression to the datasets indicated that the gradients of the two experiments were within experimental error of each other (±two time's standard error). Therefore, a combined (laboratory and field data) correlation

could be applied. The relationship between $\Delta\delta^{18}O$ ($\delta^{18}O_{carb.} - \delta^{18}O_{water}$) and temperature (T) for this combined dataset is given by:

$$T= -20.25(+7.22, -25.16)*\Delta\delta^{18}O +25.25(\pm 8.33)$$

(T is in °C, $\delta^{18}O_{carb.}$ is with respect to Vienna Pee Dee Belemnite (VPDB) and $\delta^{18}O_{water}$ is with respect to Vienna Standard Mean Ocean Water (VSMOW). Quoted errors are 2 times standard error).

The results indicate that this species from this location was not suitable for producing a robust linear regression due to the poor linear regression outputs calculated for the relationship between $\Delta\delta^{18}O$ and temperature for both the laboratory culturing experiments ($r^2 = 0.42$) and the field collection experiments ($r^2 = 0.29$). However, further investigation is required to eliminate the possibility that not all species of *Viviparus* fractionate according to expectation. The chemical corrosion of the *V. viviparus* shells was a concern in regards to the preservation of their shells isotopic composition and therefore experiments on this species should be carried out on specimens from a more suitable location in order to generate a *V. viviparus* thermometry equation. As the source of the chemical corrosion can not be determined (natural or man-made) this may have implication for those *Viviparus* specimens used in the fossil study.

CHAPTER 4 CARBONATE CLUMPED ISOTOPE THERMOMETRY: A TEST STUDY USING *VIVIPARUS CONTECTUS*

4.1 Introduction

Classic carbonate palaeothermometry equations rely on knowing the $\delta^{18}O$ of water as well as knowing the $\delta^{18}O$ of the carbonate in order to calculate absolute temperatures accurately. Material analysed from the geological record relies on either estimated values or sparsely calculated values via Mg/ Ca (e.g. Lear *et al.*, 2004, 2008; Katz *et al.*, 2008), tooth phosphate (e.g. Grimes *et al.*, 2003; 2005) and $\delta^{18}O_{carb.}$ for the $\delta^{18}O$ isotopic composition of the host water in which the carbonate mineral was formed. These assumptions are not required when analysing carbonate material using the newly developed 'clumped isotope method', as all the information required to reconstruct the equilibrium constant for that reaction is preserved within the carbonate mineral itself (Pioneered by Eiler *et al.*, 2007; Ghosh *et al.*, 2006, 2007; Huntington *et al.*, 2009).

Application of this relatively new technique to carbonate minerals is particularly useful when formulating a carbonate palaeothermometer, based on the formation of carbonate ion groups containing both $\delta^{18}O$ and $\delta^{13}C$. From the analysis of a carbonate mineral for its relative abundance of reactant and product isotopologues you can directly constrain the carbonate growth temperature (Eiler, 2007). Isotopologues are two or more variants of a molecule that differ in the isotopic identity of one or more of their constituent atoms (Elier, 2007). A carbonate mineral contains 20 different isotopologues or isotopic variants of the carbonate ion group (see Table 1 of Ghosh *et al.*, 2006). Four of these isotopologues make up 99.99% of the carbonate ions in a natural carbonate mineral:

$^{12}C^{16}O_3^{2-}$ (~98.2%) contains no rare isotopes.

$^{12}C^{16}O_3^{2-}$ (~1.1%)

$^{12}C^{18}O^{16}O_2^{2-}$ (~0.6%)

$^{12}C^{17}O^{16}O_2^{2-}$ (0.11%)

} Singly substituted (contains 1 rare isotope).

The remaining ~100ppm consists of 16 isotopologues that have double, triple or quadruple substituted carbonate ions and are produced by 'clumping' two rare isotopes together. Each of these has unique vibrational properties and therefore differs from one another in their thermodynamic stability (Ghosh *et al.*, 2006). There is a thermodynamic driving force that often promotes 'clumping' of heavy isotopes into multiply-substituted isotopologues at the expense of singly-substituted isotopologues (Elier *et al.*, 2007). In a carbonate crystal a thermodynamic equilibrium in the relative abundance of the various carbonate ion isotopologues must conform to equilibrium constraints for reactions such as:

$$^{13}C^{16}O_3^{2-} + {}^{12}C^{18}O^{16}O_2^{2-} \rightarrow {}^{13}C^{18}O^{16}O_2^{2-} + {}^{12}C^{16}O_3^{2-} \qquad \text{(Reaction 1)}$$

This reaction involves the most abundant doubly substituted isotopologue ($^{13}C^{18}O^{16}O_2^{2-}$) in a carbonate mineral. Urey (1947), Bigeleisen and Mayer (1947), and Wang *et al.* (2004) have shown that the equilibrium constant for such a reaction is temperature dependent and generally promote 'clumping' of heavy isotopes into bonds with each other (increasing the proportion of multiply substituted isotopologues) as temperature decreases. Combining the mass-spectrometric methods of Eiler and Schauble (2004) and Affek and Eiler (2006) with the phosphoric acid digestion method for carbonates (e.g. McCrea, 1950) modified by Swart *et al.* (1991) the equilibrium constant for Reaction 1 and therefore growth temperature can be constrained (Ghosh *et al.*, 2006).

This methodology has been successfully applied and calibrated through experimental analysis using laboratory culturing techniques and in the natural environment for synthetic

inorganic calcite (Ghosh *et al.*, 2006); carbonate minerals (Schauble *et al.*, 2006); palaeosols carbonates (Eiler *et al.*, 2006; Ghosh *et al.*, 2006); aragonitic corals (Ghosh *et al.*, 2006); aragonitic otoliths (Ghosh *et al.*, 2007) and aragonitic molluscs and calcitic brachiopods (Came *et al.*, 2007). Research to date indicates that the uniformity of the results (see figure 9 from Eiler *et al.*, 2007) implies that 'vital effects' are relatively unimportant, potentially allowing a generalised clump isotope thermometry equation to be used. However, the technique is certainly in its infancy and further calibration of a variety of organisms is required to confirm this.

The temperature determined by the 'carbonate clumped isotope thermometry equation' can be combined with the $\delta^{18}O$ composition of the carbonate mineral and the known temperature-dependent fractionation of oxygen isotopes between carbonate and water (calculated by McCrea, 1950; Epstein *et al.*, 1953 and Kim and O'Neil, 1997) to calculate the host waters $\delta^{18}O$ isotopic composition (Eiler, 2007). As with conventional oxygen isotope analysis the carbonate mineral must not have suffered post depositional diagenetic alteration e.g. recrystalisation (Ghosh *et al.*, 2006).

The strategy used in the formulation of the *Viviparus contectus* (*V. contectus*) thermometry equation has the potential to be used to generate a *V. contectus* clumped isotope thermometry equation. From the results given in Chapter 2, the field cage experiment would provide a tight constraint on temperature and shell growth, with regular water samples taken for oxygen and carbon isotopic analysis. This would allow the *V. contectus* specimens to remain within their natural environment throughout the experiment whilst closely monitoring the parameters controlling carbonate secretion. The results obtained from such an analysis would allow comparisons with previous calibrations and determine whether freshwater taxa show a lack of vital effects when compared to the already established clump isotope thermometry equations.

4.1.1 Aims and Objectives

The field cage experiment in the experimental determination of a *Viviparus contectus* thermometry equation (Chapter 2) yielded several specimens that had secreted enough carbonate to be considered for analysis using the clumped isotope method. These samples provided the opportunity to carry out a preliminary test study to determine whether *V. contectus* is capable of producing a species specific *V. contectus* clumped isotope thermometry equation.

The main aim of this study is to test whether *V. contectus* show any vital effects on the clumped isotope composition. To achieve this aim the following objective was to be met:

- Perform clumped isotope analysis on three samples from two *V. contectus* specimens obtained from the field cage experiment described in Chapter 2.

4.2 Methods

The cage experiment successfully incorporated a natural culturing environment whilst the important parameters (temperature, pH, salinity and $\delta^{18}O$ of the local water) that affect carbonate secretion could be regularly monitored. For more detailed information on the field cage experiment see Chapter 2 Section 2.4.1.2.

Upon return to the laboratory the *V. contectus* samples were ethically euthanized by cryogenesis. Their bodies were removed from the shells, sexed (males have a deformed fattened left tentacle forming the penis) and when eggs / juveniles occurred these were counted. A small hole (~0.3 mm in diameter) was drilled into the shell marking the position of the white paint lines (Chapter 2, Fig 2.7B/C), as during the removal of the residual organic material by NaOCl, the white paint was also removed. The shells were soaked overnight in dilute (2%) NaOCl to remove organic material including the

periostracum. The shells were then rinsed in ultra pure water and oven dried at 25°C. The length of time the specimen remained within the cage (e.g. greater than one month) determined whether the shell required infilling with resin for stabilisation purposes. A drill line was used to break away the shell section precipitated during a specific time period from the remainder of the shell. Each shell section was then crushed to a fine powder using an agate pestle and mortar.

As shown in Chapter 2 the *V. contectus* shell structure consists of carbonate crystals (in this case aragonite) surrounded by an organic protein secretion which binds the crystals and crystal layers together. It has been suggested that organic contaminants are potentially problematic for measurements of Δ_{47} (Ghosh *et al.*, 2006), so the carbonate powders have to be pre-treated before analysis. To remove the organic content the carbonate powder was placed into a centrifuge tube, to which 13ml of 6% NaOCl was added, making sure that the powder was suspended in the solution. If the powder remained as a solid lump in the bottom of the centrifuge tube a sonicator was used to suspend the powder in the NaOCl. The powdered samples were then left in the NaOCl for approximately 24 hours. To remove the powdered carbonate sample from suspension a centrifuge was used at approximately 2000 revolutions per minute for 2 minutes. The NaOCl was then pipetted off from the sample and replaced with 13 ml of ultra pure water making sure the powder was re-suspended. The sample was then centrifuged to remove the powder from suspension and the ultra pure water was pipetted off. This was repeated two more times to ensure that all of the NaOCl was removed from the sample. On the last rinse the ultra pure water was removed leaving the carbonate sample in the centrifuge tube. The sample was then oven dried at 30°C for approximately 24 hours or until dry. Each sample was then homogenised and placed into glass vials as 8mg sub-samples. If the carbonate sample was greater than

8mg repeat samples were also weighed out. All of the remaining carbonate material not used for analysis was retained.

The samples were then sent to Caltech laboratories, Caltech University (USA) for clumped isotope analysis courtesy of Dr M. Daëron and Prof. J. Eiler. The analytical procedure was carried out by Dr M Daëron and analytical staff at Caltech laboratories.

4.2.1 Analytical procedure

The carbonate samples (approximately 8mg) were digested in anhydrous phosphoric acid following the methods of McCrea (1950), as modified by Swart *et al.* (1991). The CO_2 produced was recovered in a vacuum apparatus, purified and analyzed for its isotopic composition (including abundances of mass-47 isotopologues) using methods described by Ghosh *et al.* (2006). A Finnigan MAT 253 gas source isotope ratio mass spectrometer, configured to simultaneously collect ion beams corresponding to M/Z = 44, 45 and 46 (read through 3 - 10^8 to 1 . 10^{11} Ω resistors), as well as 47, 48 and 49 (read through 10^{12} Ω resistors) was used to analyse the isotopic composition (Ghosh *et al.*, 2007). As defined in Eiler and Schauble (2004), Wang *et al.* (2004) and Ghosh *et al.* (2006) the abundance of mass-47 isotopologues of CO_2 are reported using Δ_{47} values. The Δ_{47} value is defined as the difference in per mil between the measured 47/44 ratio ('R_{47}') of the sample and 47/44 ratio expected for that sample if its stable carbon and oxygen isotopes were randomly distributed among all isotopologues (Ghosh *et al.*, 2007).

4.3 Results

Table 4.1 summaries the results of isotopic analyses of the three *V. contectus* samples investigated in this preliminary study. A generalised clumped isotope thermometry equation was constructed, using the existing published raw datasets of Ghosh *et al.* (2006)

and Ghosh *et al.* (2007) (Table 4.2), where T is in Kelvin, and the relationship between Δ_{47} and T^{-2} is given by (Eq. 1):

$$\Delta_{47} = 0.056\ (\pm 0.003) \times (10^6/T^2)\ 0.011\ (\pm 0.038) \qquad (r^2 = 0.96) \qquad (1)$$

When the *V. contectus* results obtained from this preliminary study are combined with the clumped isotope thermometry equation, where T is in Kelvin, and the relationship between Δ_{47} and T^{-2} is given by (Eq. 2):

$$\Delta_{47} = 0.055(\pm 0.004) \times (10^6/T^2)\ 0.023(\pm 0.050) \qquad (r^2 = 0.92) \qquad (2)$$

The relationship between Δ_{47} and temperature shows a good statistical regression for both datasets (generalised clumped isotope regression ($r^2 = 0.96$) and the generalised clumped isotope regression including the *V. contectus* results ($r^2 = 0.92$)). When the generalised clumped isotope results are combined with the *V. contectus* results, the resultant regression define a strong positive correlation ($r^2 = 0.92$) between Δ_{47} and T^{-2}. However, if the *V. contectus* results are viewed alone they show an inverse relationship, which may reflect the uncertainties surrounding growth temperatures. This inverse relationship may also be responsible for the decrease in r^2 values when the *V. contectus* data are included in the generalised clumped isotope thermometry equation.

When the recorded water temperature and Δ_{47} values are plotted relative to the existing datasets of Ghosh *et al.* (2006, 2007), the *V. contectus* data point VC9-APR-JUN-1 appears to fit within the scatter defined by that dataset (Fig. 4.1). The two samples analysed from VC9 and VC2, for the period between February and April 2008, plot away from the other data points.

Temp. (Kelvin)	Temp. (°C)	Temp (°C) (stdev)	Date from	Date to	Total no. days in cage	Sample	Clump isotope analysis Delta 47
282.85	9.7	3.3	29/02/2008	03/04/2008	34	VC9-FEB-APR-1	0.6542 +/- 0.0124 permil (1s)
282.85	9.7	3.3	29/02/2008	03/04/2008	34	VC2-FEB-APR-1	0.6793 +/- 0.0116 permil (1s)
288.2	15.05	1.9	25/04/2008	06/06/2008	42	VC9-APR-JUN-1	0.6743 +/- 0.0102 permil (1s)

Table 4.1 The Δ^{47} results for the three *V. contectus* samples analysed using the clumped isotope methods are detailed above with information on the average water temperatures for the period in which the gastropod grew.

Author	Proxy	Sample details	Growth temp. (°C)	° kelvin	$10^6/T2$	Δ_{47}
Gosh *et al*., 2006	calcite (synthetic)	CalciteHA12, HA4	50.0	323.3	9.6	0.6
		Calcite HA3	1.0	274.3	13.3	0.8
		Calcite HA9	33.0	306.3	10.7	0.6
		Calcite HA1, HA2, HA7	23.0	296.3	11.4	0.7
	Coral (aragonite)	Deep sea corals	5.5	278.8	12.9	0.7
		Deep sea corals	8.0	281.3	12.6	0.7
		Surface coral	29.3	302.6	10.9	0.6
Gosh *et al*., 2007	Otoliths (aragonite)	bio 3	2.0	275.2	13.2	0.8
		bio8	3.0	276.2	13.1	0.7
		lacm 01	5.0	278.2	12.9	0.7
		bio5 (Av.)	7.0	280.2	12.7	0.7
		bio6	15.0	288.2	12.0	0.7
		bio4	20.0	293.2	11.6	0.6
		lacm 02	25.0	298.2	11.2	0.6
		bio7 (Av.)	25.0	298.2	11.2	0.6
This study	*Viviparus* (aragonite)	VC9-FEB-APR-1	15.1	288.2	12.0	0.7
		VC9-APR-JUN-1	9.7	282.9	12.5	0.7
		VC2-FEB-APR-1	9.7	282.9	12.5	0.7

Table 4.2 Data are shown for inorganic calcite grown under controlled conditions in the laboratory (Ghosh *et al.*, 2006); otoliths and aragonite coral which were collected from their natural habitat and have known or estimated growth temperatures (Ghosh *et al.*, 2006, 2007) and the results from the analysis of *V. contectus* specimens.

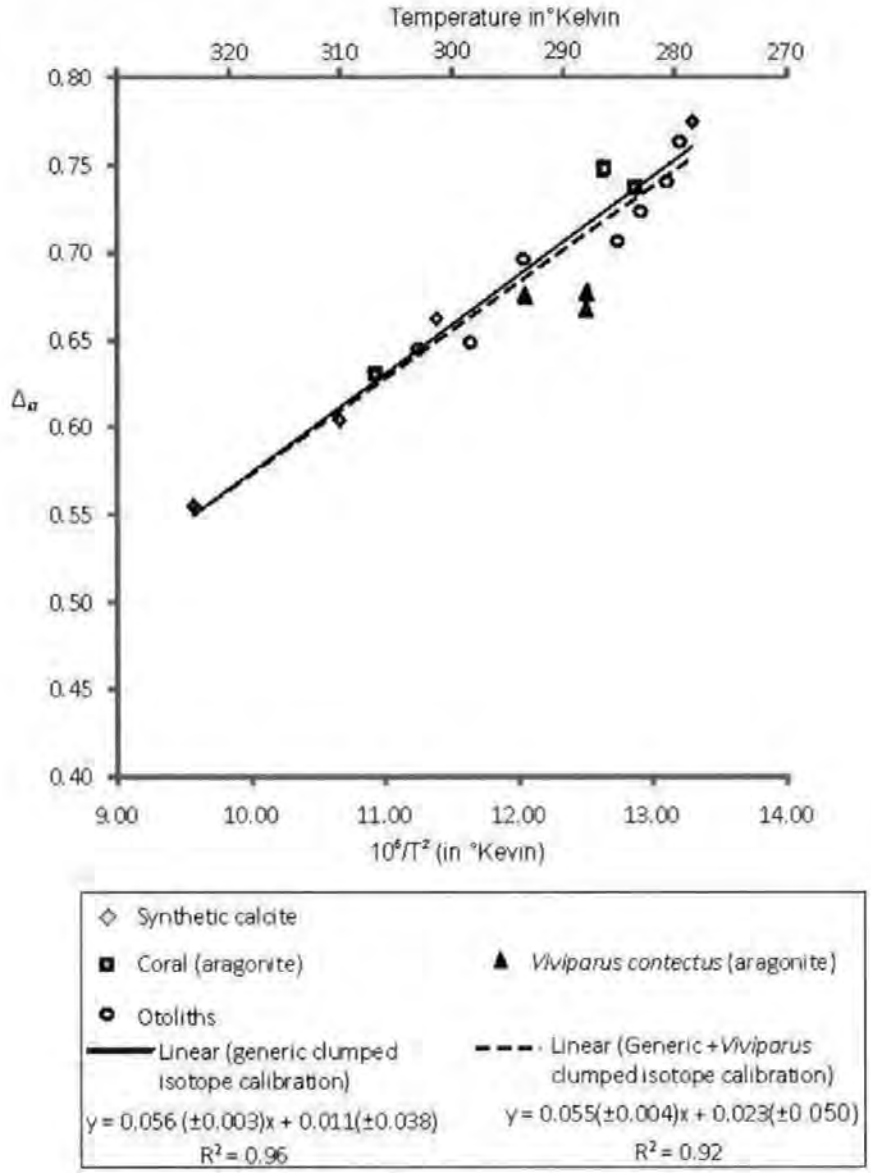

Figure 4.1 Results from the analysis of *V. contectus* are plotted against the raw data for inorganic calcite grown under controlled conditions in the laboratory (Ghosh *et al.*, 2006), and otoliths and corals collected in nature and having known or estimated growth temperatures (Ghosh *et al.*, 2006, 2007). A generalised linear regression calculated by the author is shown for the generalised clumped isotope thermometry calibration using existing published datasets of Ghosh *et al.* (2006) and Ghosh *et al.* (2007) (solid line) and a generalised plus *V. contectus* clumped isotope thermometry calibration.

4.4 Discussion

Results obtained from VC9 for the period between April and June would appear to suggest that *V. contectus* do not exhibit vital effects on the Δ_{47} composition of its shell carbonate. However, the two samples analysed from VC9 and VC2 for the period between February and April 2008, produce much higher clump temperatures (17.8°C (291.0 Kelvin) and

23.17°C (296.3 Kelvin)), calculated using the Ghosh *et al.* (2006) equation, and compared with the average recorded water temperature of 9.7°C ± 3.3.

Inexperience at collecting and sampling may have been an issue at this point in the experiment. The cage experiments were set up in February 2008 and therefore the growth from February to April (2008) was the first growth collected from the cage experiments. During each sampling visit the aperture or growing edge was marked with white paint so that any subsequent growth could be identified. Prior to cleaning, a drill hole (~0.4 mm in diameter) was used to identify the location of the white line as, during the cleaning process, the white line is removed. If the white line was thick and the drill hole was placed at the centre of the white line then it is possible that preceding autumn growth, secreted at slightly warmer temperatures, could have been incorporated into the sample. Assuming that winter growth is minimal the warm temperatures produced by the clumped isotopic analysis may indicate a late autumn temperature component (which tends to be the warmest water temperatures in the UK). The temperature records from both South Drain Canal (Chapter 2) and Exeter Canal (Chapter 3) indicate that water temperatures of 23°C could potentially be recorded by shell material secreted during early autumn (September 2007).

The clumped isotopes temperatures calculated for February to April 2008 are much higher than those measured during this time period. As previously mentioned these temperatures are closer to those measured in September 2007 (Chapter 2 Table 2.6). If the corresponding $\delta^{18}O_{carb}$ data is removed from the field cage calibration the r^2 values decreases from 0.67 to 0.40, suggesting that the removal of this data makes the calibration less robust. Another way of approaching the problem could be to use the $\delta^{18}O_{carb}$ values along with the $\delta^{18}O_{water}$ values measured from September 2007, rather than those from February to April

2008. If the $\delta^{18}O_{carb.}$ values and the clumped isotope temperatures are put into the rearranged thermometry equation:

$$\delta^{18}O_{water} = ((\text{clumped temp.} -22.89)+(-7.43* \delta^{18}O_{carb.}))/-7.43$$

The calculate $\delta^{18}O_{water}$ values produce an average value of –3.38‰, this is similar to the $\delta^{18}O_{water}$ value recorded for September 2007 (Table 4.3).

$\delta^{18}O_{carb.}$ (‰ VPDB)	clump temp	$\delta^{18}O_{water}$ (‰ VPDB)
-3.54	23.17	-3.58
-3.36	23.17	-3.40
-3.34	23.17	-3.38
-3.30	23.17	-3.34
-3.43	23.17	-3.46
-3.28	23.17	-3.31
-3.40	23.17	-3.44
-3.23	23.17	-3.27
-3.23	23.17	-3.27
	average=	-3.38

Table 4.3 The calculated $\delta^{18}O_{water}$ Values using the clumped isotope temperatures.

This appears to also decrease the r^2 value from (0.67 to 0.28) in the field cage calibration and produces a less robust equation. The large scatter at 15°C is most likely to be caused by temperatures fluctuating around this temperature. More detailed and precise measuring of water temperatures is required along with shorter periods of growth from which the shell material is sampled. Ideally laboratory condition would suit as the specimens could be cultured over a longer time period with water temperature and $\delta^{18}O_{water}$ tightly constrained. Once proven under these conditions the experimentation could move forward and incorporated specimens grown in cages within their natural environment with frequent monitoring of temperature and $\delta^{18}O_{water}$.

Many of the gastropods exhibited a cessation mark on their shells, which is associated with the cessation of growth brought about by cooler temperatures or disturbance. When looking at the shells in cross section the cessation marks show that new growth initiates behind the old shell, therefore an overlap occurs (Fig. 2.17). If this part of the shell was sampled this would incorporate shell growth secreted prior to the period secreted within the cage.

Kinetic effects may also play a part in the difference in carbonate secretion between specimens. For *V. contectus* specimens to be growing during February to April it would require them to be at least 1 year old. For the two specimens analysed:

VC2	H = 2.4 mm	W = 1.9mm	indicating ~ 2 yr old specimen.
VC9	H = 3 mm	W = 2.4 mm	indicating ~ 3 yr old specimen.

It is possible that older specimens grow their shell carbonate slower and this fractionates their shells isotopic composition differently from example, a year old sample. However, this has been suggested by the result in Chapter 2 as not affecting the isotopic composition of the shell carbonate. As discussed in Chapter 2, *Viviparus* become reproductively active at ~2 yrs old, after which there is an energy trade off between growth and reproduction. This made lead to selective growth with shell secretion during periods of minimal reproductive activity. It should be noted that kinetic effects also play an important part in clumped isotope analysis of speleotherms (Affek *et al.*, 2008); however these are authogenic not biogenic in origin. In order to understand whether this affects the clumped isotope analysis, further investigation would be needed.

4.5 Future work

The limited results reported here show that *V. contectus* can potentially be used in clumped isotope thermometry. However, further work and some modification of the field cage experiment technique is required. An accurate high resolution temperature record is vital to the success of future experiments; therefore an I-button data logger set to record temperature every two hours needs to be placed within the cage experiment. To overcome unpredictable technological error several I-buttons should be used. It is advised that temperature records should be downloaded on every sampling trip, firstly to check if the I-buttons are working correctly and secondly so that an up to date record can be kept. Ideally, the experiment should commence in early spring when the juveniles of *V. contectus* are released. Juveniles have been observed by the author to produce the greatest amount of shell secretion in the shortest space of time as they put all their energy into shell secretion, whereas those that have reached sexual maturity reserve their energy for reproduction.

Sample collections should also be carried out after periods of relatively sustained temperatures (approximately 2 to 3 weeks apart) where variation around a mean is minimal. This allows the shell growth to be constrained to the smallest temperature range. From the cage experiment in Chapter 2 evidence of growth rates suggests that 2-3 weeks is a minimum amount of time needed for a sufficient amount of shell material (~5mm) to be secreted for clumped isotope analysis. During the laboratory procedure care should also be taken to make sure that only the growth acquired during the specific time period is incorporated into the sample for analysis.

A disadvantage of the clumped isotope analysis method is the sample mass required. Currently, for a reliable result, 8mg of carbonate powder is required after treatment with NaOCl; this is a much larger amount of carbonate material than is required for establishing

the $\delta^{18}O$ ratio. Long counting times are often required, only allowing 1 to 2 samples to be run per day. Therefore, this method is also time consuming. Undoubtedly these issues will be rectified and the analytical process simplified and fully automated in the future.

4.6 Summary

From the limited results obtained so far the Δ_{47} - T° relationship determined by *V. contectus* is positive instead of negative, this evidence would suggest that there is a very large error on the temperature estimates. This evidence suggests that the samples analysed from Feb to April 2008 are not representative of the temperatures measured during this time period. Removal of these data points from the *V. contectus* field cage calibration did not improve the calibration, even when the $\delta^{18}O_{water}$ values were altered to those similar to September 2007.

The methods by which the samples were grown needs modification as suggested in Section 4.5. Further analyses on specifically cultured samples are needed to fully establish whether *V. contectus* exhibits vital effects on the Δ_{47} of its shell carbonates or whether a generalised clumped isotope equation would be adequate. Investigation into kinetic effects associated with the age of the specimen, sex and whether they are reproductively active would be beneficial in determining whether the clumped isotope equation produced can be successfully applied to the fossil record.

CHAPTER 5 APPLICATION OF THE PALAEOTHERMOMETRY EQUATIONS TO THE FOSSIL RECORD

In Chapter 2, the temperature dependence of the fractionation factor and the relationship between $\Delta\delta^{18}O$ ($\delta^{18}O_{carb.} - \delta^{18}O_{water}$) and temperature, were calculated from *V. contectus* specimens maintained under laboratory and field (collection and cage) conditions. The field specimens were grown (Somerset, UK) between August 2007 and August 2008, with water samples and temperature measurements taken monthly. Specimens grown in the laboratory experiment were maintained under constant temperatures (15°C, 20°C and 25°C) with water samples collected weekly. Application of a linear regression to the datasets indicated that the gradients of all three experiments were within experimental error of each other (±two times standard error) therefore, a combined (laboratory and field data) equation could be applied. The relationship between $\Delta\delta^{18}O$ ($\delta^{18}O_{carb.} - \delta^{18}O_{water}$) and temperature (T) for this combined dataset (laboratory and field data) is given by:

$$T = -7.43(+0.87, -1.13)*\Delta\delta^{18}O + 22.89(\pm 2.09)$$

(T is in °C, $\delta^{18}O_{carb.}$ is with respect to Vienna Pee Dee Belemnite (VPDB) and $\delta^{18}O_{water}$ is with respect to Vienna Standard Mean Ocean Water (VSMOW). Quoted errors are 2 times standard error).

In Chapter 3, the relationship between $\Delta\delta^{18}O$ ($\delta^{18}O_{carb.} - \delta^{18}O_{water}$) and temperature was also calculated from *V. viviparus* specimens maintained under laboratory and field (collection and cage) conditions. However, it was considered that *V. viviparus* from this location was not suitable for producing a robust linear regression due to the poor linear regression outputs calculated for the relationship between $\Delta\delta^{18}O$ and temperature for both the laboratory culturing experiments and the field collection experiments. The condition of the *V. viviparus* shells was a concern in regard to the preservation of their shells isotopic

composition and therefore experiments on this species should be carried out on specimens from a more suitable location in order to generate a *V. viviparus* thermometry equation.

Although *V. contectus* has been shown to be an accurate recorder of the combined isotopic signal produced by temperature variation and changes in $\delta^{18}O$ of the host water, the use of its isotopic composition to infer palaeotemperatures requires significant assumptions to be made, mainly due to the complexity of factors influencing the isotopic signal. Therefore, absolute temperatures are presently unattainable and relative temperature variation has its limitations. Currently, the most significant assumption involves the $\delta^{18}O$ isotopic composition of the host water from which the carbonate was secreted. This particularly influences the temperature estimates across events such as the Oi-1 glaciation, when it is known that the isotopic composition of the marine water and freshwater was influenced by increasing ice volumes (altering the $\delta^{18}O$ of seawater and in turn $\delta^{18}O$ of precipitation) as well as temperature fluctuations. In turn, both temperature and ice volume change will induce feedbacks in the system causing small, but possibly significant, alteration to the isotopic composition of the host water. Separating the signals of temperature and ice volume change (or change in $\delta^{18}O$ of precipitation) is problematic, although some success has been achieved using Mg/Ca ratios, sea-level changes (Lear *et al.*, 2000; 2004; 2008; Katz *et al.*, 2008) and TEX 86 (Liu *et al.*, 2009) in the marine realm. In both marine and freshwater environments Mg/Ca ratios of aragonitic mollusc shells cannot be used owing to the strong mineralogical control on Mg in the shell-forming extrapallial fluid which would mask any environmental signature (Anadón *et al.*, 2006). This is also complicated by the fact that a certain fraction of Mg is not bound to the crystal lattice, and, therefore, maybe preferentially leached during early digenesis (Rosenthal and Katz, 1989).

At present there are a limited number of methods for determining the $\delta^{18}O$ of water in ancient continental environments. Many of these involve indirect calculation of the $\delta^{18}O$ of

water from other proxies within the same sedimentary deposits. The $\delta^{18}O$ isotopic analysis of fossil wood cellulose by Richter *et al.* (2008) was used to try and determine the $\delta^{18}O$ isotopic composition of palaeoprecipitation over the past 45 Ma. Their findings indicated that the $\delta^{18}O$ isotopic composition of rainwater over the last 45Ma was similar to today and has not altered significantly. These results rely on the assumption that the composition of the cellulose has not been diagenetically altered during burial. Grimes *et al.* (2005) calculated $\delta^{18}O$ local water values from Eocene / Oligocene deposits on the Isle of Wight (UK), utilising fossil rodent tooth enamel from mammal bearing horizons. Rodents are considered to have small home ranges and lack migratory behaviour; therefore they are thought to drink from the same water body throughout their life time and in whose sediments they may be incorporated after death. Studies have shown that a mammal's body water $\delta^{18}O_{bw}$ and the local water $\delta^{18}O_{water}$ have a linear relationship and that their biogenic apatite is precipitated in equilibrium with the $\delta^{18}O_{bw}$ (Grimes *et al.*, 2004). Consequently, the $\delta^{18}O$ of the mammal tooth enamel phosphate can be used to calculate the $\delta^{18}O$ composition of the local water. This can be used in combination with the $\delta^{18}O$ of freshwater carbonate proxies from the same deposits to calculate palaeotemperatures. This method makes a number of assumptions. For example, in some environments evaporation can lead to isotopic stratification of the water source, therefore proxies located at depth maybe subjected to very different oxygen isotopic values in water to that experienced by mammals drinking from the surface waters. The association of the rodent specimens with *Lymnaea* species would indicate shallow ponds that are more susceptible to isotopic fractionation than deeper water bodies in which *Viviparus* lives. In the shallower ponded environments both temperature and isotopic stratification could potentially occur due to enhanced residence times associated with these environments. However, *Viviparus* tends to prefer water bodies that have a component of flow preventing such long water residence times.

The establishment of new analytical techniques to determine temperature changes from aragonitic proxies directly is a likely way forward. As shown in Chapter 4 the relatively new analytical procedure, the 'carbonate clumped isotope thermometry equation', maybe key to solving these problems and reducing some of the inaccuracies associated with other methods. Although clumped isotope analysis is not itself perfect, *V. contectus* specimens grown within the field cage experiment (Chapter 2) provided the opportunity to carry out an investigation into clumped isotope analysis (Chapter 4). From the limited results obtained so far there is the potential for *V. contectus* to be used in clumped isotope thermometry. However, further analyses on samples cultured under controlled conditions are needed to fully establish whether *V. contectus* exhibits vital effects on the Δ_{47} of its shell carbonates or whether a generalised clumped isotope equation would be adequate. Investigation into kinetic effects associated with the age of the specimen, sex and whether they are reproductively active would be beneficial in determining whether the clumped isotope equation produced can be successfully applied to the fossil record. This analytical method would provide the opportunity for temperatures to be directly calculated from fossil *Viviparus* carbonate material. However, this does not mean that the $\delta^{18}O_{carb.}$ record would become redundant. As explained in Chapter 4, a high resolution $\delta^{18}O_{carb.}$ record can be used in combination with the clumped isotope temperature calculations to produce an invaluable high resolution record of $\delta^{18}O_{water.}$ This information will aid in the interpretation of climatic events such as the Oi-1 glaciation.

Until experimentation can be undertaken comparison between already established thermometry equations (e.g. White *et al.*, 1999; Grossman and Ku, 1986) and the *V. contectus* thermometry equation will be carried out on the fossil material in Chapter 6.

Shell preservation is important when attempting to produce an isotopic record. As discussed in Chapter 3, evidence is provided for chemical corrosion and mechanical

breakage of the *V. viviparus* shells while the specimens were still alive. It is most likely that this chemical corrosion is a product of water chemistry and not the re-adsorption of the shell carbonate. As the source of the chemical corrosion cannot be determined (natural or man-made) this may have implication for those *Viviparus* specimens used in the fossil study. Therefore, carefully observations of the fossil shells are required before undertaking analysis.

As shown in Chapter 2 the *V. contectus* shell structure consists of carbonate crystals (in this case aragonite) surrounded by an organic protein secretion which binds the crystals and crystal layers together. It has been suggested that organic contaminants are potentially problematic for measurements of Δ_{47} (Ghosh *et al.*, 2006), so the carbonate powders have to be pre-treated before analysis. Therefore, a way to successfully remove this organic content needs to be investigated in more detail in order to produce a reliable clumped isotope calibration.

Cessation marks are particularly important in understanding the seasonal isotopic records obtained from high resolution analysis of *Viviparus* specimens. These cessation marks are often associated with winter hibernation and relatively positive $\delta^{18}O$ values (Schmitz and Andreasson, 2001). Therefore, they have been used to determine the age of individual specimens and seasonal changes in the isotopic record. However, as seen from modern specimens these cessation marks can be triggered by other stimuli (e.g. high temperatures, disturbance and lack of food).

PART 2: FOSSIL STUDY

CHAPTER 6 A *VIVIPARUS LENTUS* ISOTOPIC RECORD

6.1 Introduction

The introduction to this Chapter gives only a brief introduction to the E/O transition and Oi-1 glaciation, focusing on those studies pertinent to this investigation. Further discussion on broader issues associated with these events can be found in Chapter 1. Through isotopic analysis the $\delta^{18}O$ and $\delta^{13}C$ composition of continental freshwater will be investigated across this time period. Using known palaeotemperatures and the thermometry equation produced in Chapter 2 temperature will be calculate using the $\delta^{18}O$ record produced. The results obtained will be compared to local and regional faunal and floral turnover events and potential mechanisms for the climatic shifts discussed.

The E/O transition and Oi-1 glacial maximum defines a fundamental turning point in the Earth's climatic history. For the first time in the Cenozoic Era conditions existed that allowed the formation of permanent continental scale ice caps on Antarctica. Long term cooling commenced after the Early Eocene Climatic Optimum (52 to 50 Ma), as recorded by high resolution $\delta^{18}O$ records from the marine realm (for example Zachos *et al.*, 1996; 2001). This long-term cooling trend culminated in the build up of glacial ice on Antarctica, with an abrupt stepwise $\delta^{18}O$ shift at ~33.7 Ma (e.g. Zachos *et al.*, 2001; Coxall *et al.*, 2005; Lear *et al.*, 2008; Katz *et al.*, 2008)(Fig. 6.1). Causes of this long term cooling and abrupt glaciation have been widely debated. Suggested key mechanisms include decreasing pCO_2 (Deconto and Pollard, 2003; Deconto *et al.*, 2008; Pearson *et al.*, 2009), alteration of oceanic gateways changing ocean and atmospheric circulation (Kennet and Shackleton, 1976; Kennet, 1977; Berggren and Holister, 1977), orbital forcing (Deconto and Polard, 2003; Coxall *et al.*, 2005; Pälike *et al.*, 2006), biogeochemical processes for example

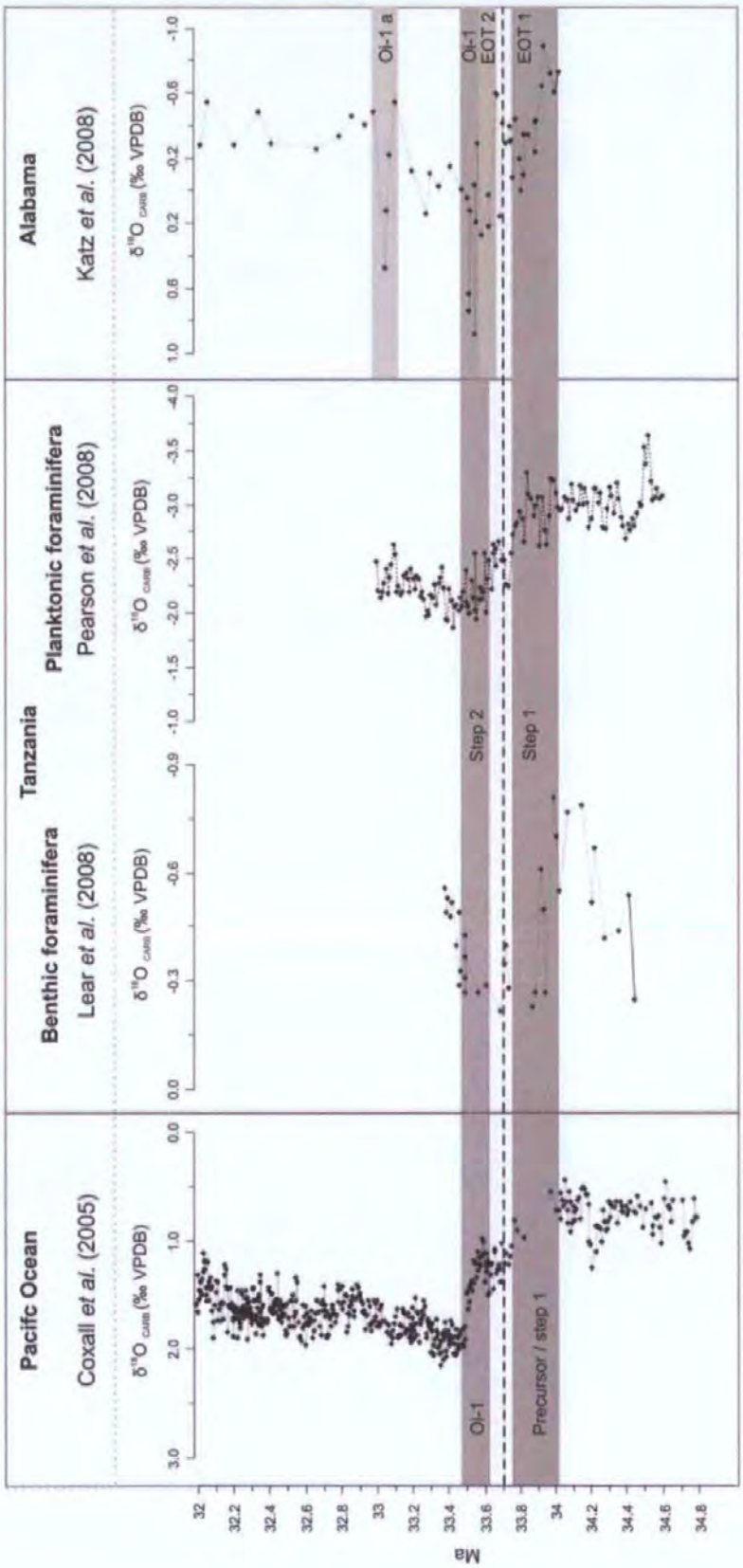

Figure 6.1 Four of the key high resolution $\delta^{18}O$ records obtained from marine sediments crossing the Eocene / Oligocene boundary and Oi-1 glaciation are presented. The isotopic excursions indicated (by these records and which are important to this investigation are highlighted. Dashed line represents the E/O boundary. Times scales used for Pearson *et al.*, (2008) and Katz *et al.*, (2008) is Berggren *et al.* (1995) and for Coxall *et al.* (2005) and Lear *et al.* (2008) is Cande and Kent (1995). EOT = Eocene / Oligocene transition.

change in pCO_2 (Pagani *et al.*, 2005; Deconto and Pollard, 2003; Huber and Norf, 2006; Deconto *et al.*, 2008; Pearson *et al.*, 2009) and Pacific arc volcanism (Jicha *et al.*, 2009).

A large proportion of the published high resolution isotopic records relating to the E/O transition and Oi-1 glaciation have been obtained from the marine realm. These $\delta^{18}O$ records have recently begun to provide information on temperature fluctuations and changes in the $\delta^{18}O_{water}$ relating to this event. As discussed in Part 1, there have been problems in distinguishing the amount of temperature change represented in the stepwise $\delta^{18}O$ isotopic shifts associated with the E/O transition and Oi-glacial maximum. This has led to the use of additional proxy information, for example temperatures that have been independently calculated using Mg/Ca ratios from foraminifera preserved above the calcium compensation depth (CCD) and TEX_{86} (Liu *et al.*, 2009). TEX_{86} is based on the relative distribution of glycerol dialkyl glycerol tetraether membrane lipids of marine non-thermophilic crenarchaetoa. The relative distribution of the lipids present in such organisms is known to vary with growth temperatures (Shouten *et al.*, 2002). Mg/Ca ratios showed that 0.5 ‰ of the first (~0.7‰) in the stepwise $\delta^{18}O$ shifts indicates a ~2.5 °C decrease in temperature, with the remaining 0.2‰ related to changes in ice volume (Lear *et al.*, 2008). According to Lear *et al.* (2008) the second $\delta^{18}O$ shift, into the Oi-1 glacial maximum itself, has no associated temperature change and therefore is solely ice volume related (Lear *et al.*, 2008). Katz *et al.* (2008) agree with the 2.5 °C temperature decrease associated with the first $\delta^{18}O$ shift in Lear *et al.*'s (2008) record. However, their data suggest a previously unidentified event between the two isotopic steps seen in Lear *et al.* (2008) $\delta^{18}O$ record, which they termed EOT 2. According to Katz *et al.* (2008). Mg/Ca temperature records across the Oi-1 glacial maximum, a temperature decrease of 2 °C is recorded . This is in stark contrast to the interpretation of no significant temperature

change by Lear *et al.* (2008) (See Fig. 6.1). However, Katz *et al.* (2008) also used sea level change, in particular sea level falls indicative of ice build-up, to determine the proportion of the $\delta^{18}O$ shift related to ice volume change, this may be responsible for the discrepancies between the two data sets. The section used by Katz *et al.* (2008) has variable preservation and the occurrence of glauconite would appear to indicate an agitated high energy environment. This change in lithology occurs during EOT2 (Fig. 6.1) and may have influenced the $\delta^{18}O$ record.

The terrestrial isotopic records across the Oi-1 are often inconsistent, fragmented and rarely produce consistent results crossing the E/O transition and Oi-1 glaciation. Currently the most detailed $\delta^{18}O$ terrestrial record extending across the E/O transition and Oi-1 glaciation uses a combination of fossil tooth enamel and fossil bone, to derive a high resolution continental temperature record for North America (Zanazzi *et al.*, 2007). Temperatures calculated from this isotopic study indicate a 8.2 ± 3.1 °C drop in mean annual temperature over a 400,000 year E/O transition, with no change in the $\delta^{18}O$ of local water. Another isotopic and temperature record independent of ice volume has been produced through the isotopic analysis of freshwater biotic carbonates and phosphates from the Isle of Wight (Grimes *et al.*, 2005) (for further detail see Section 6.3). These results, according to Hooker *et al.* (2009), indicate four periods of change (temperatures taken from Grimes *et al.*, 2005):

(1) Cooling (~4.7°C) in the Osborne Member;

(2) A warming (~7.5°C) in the Bembridge Limestone Formation;

(3) Cooling (~3.8°C) in the lower Hamstead Member that just precedes the Oi-1 glacial maximum and Grande Coupure; and

(4) Cool temperatures continuing into the upper Hamstead Member (post–Grande Coupure).

These shifts in temperature indicate a stepwise cooling during the E/O transition. Other terrestrial isotopic and temperature records from European sequences are low in resolution for the time period in question (e.g. Uhl *et al.*, 2007; Betchtel *et al.*, 2008; Sheldon *et al.*, 2009) and are therefore are not capable of recording these stepwise shifts. Sheldon and Retallack (2004), Zanazzi *et al.* (2007) and Sheldon *et al.* (2009) all suggest that the E/O transition in North America is part of a long-term (36 – 26 Ma), cooling event with no stepwise transition. Contradictory evidence, presented by Kohn *et al.* (2004) from a study of mammal teeth from high-latitude southern Argentina, in combination with palaeofloral observations and geographic considerations, suggest that climate was essentially constant across the Oi-1 glacial maximum.

A recent investigation using terrestrially derived spore and pollen assemblages preserved in marine sediments from the Norwegian- Greenland Sea indicates a cooling of 5 °C in cold-month (winter) mean temperatures to 0–2 °C, and a concomitant increased seasonality before the Oi-1 glaciation event (Eldrett *et al.*, 2009). Seasonality across the E/O transition and Oi-1glaciation will be discussed in greater detail in Chapter 7. This cooling is shown to commence at ~38Ma, with a shift in temperatures to cooler conditions occurring at ~36 Ma and stabilising after the E/O boundary (IOPD/ODP site 643, Eldrett *et al.*, 2009). However, it must be noted that this shift coincides with a change in the core site. Data from site 643 is the only dataset that covers the time period in question (~38 to 33 Ma), if a line were to be drawn between the single data point at ~ 37.6 Ma and the cluster of data at ~34 Ma no significant change in temperature is observed.

Evidence in the form of ice-rafted debris found in sediments from the Greenland Sea (Moran *et al.*, 2006; Eldrett *et al.*, 2007; Tripati *et al.*, 2008) and the Arctic Ocean (St John, 2008) suggest the possibility of bipolar glaciation around the E/O transition. According to Moran *et al.* (2006) the oxygen isotope record (Coxall *et al.*, 2005) and synchronous

calcium carbonate compensation depths (Tripati *et al.*, 2005) are supporting evidence for a synchronised glaciation. The amount of ice involved remains controversial as the source may be small isolated ice caps and high elevation alpine outlet glaciers, therefore not related to full scale continental glaciations (Eldrett *et al.*, 2007). Browning *et al.* (1996) suggested that a small to medium sized ice sheets in the Northern hemisphere existed in the middle to late Eocene. Winter temperatures calculated by Eldrett *et al.* (2009) suggest the presence of extensive Arctic Ocean winter sea-ice; it is thought that this may have increased deep convection and been responsible for the apparent initiation of Northern Component Water formation prior to the Oi-1 glacial maximum (Via and Thomas, 2006).

Both marine and continental records appear to show distinct regional and continental differences in response to climate change across this event. It would appear that a large part of these $\delta^{18}O$ shifts, associated with the Oi-1 glacial maximum in the marine records, is related to ice volume changes rather than large shifts in temperature. However, the terrestrial records appear to indicate large variations in the temperature estimates obtained from different proxies from very different regimes (e.g. Grimes *et al.*, 2005; Zanazzi *et al.*, 2007).

6.2 Aims and Objectives

Continental based $\delta^{18}O$ records have not achieved spatial or temporal resolution comparable to those of the marine realm. Data are particularly lacking from north western Europe, both in continental and marine records. The Isle of Wight (Hampshire Basin, UK) has a sedimentary sequence that encompasses Upper Eocene to Lower Oligocene strata, containing several well preserved freshwater species that cross the E/O transition and Oi-1 glacial maximum. One such species, the freshwater gastropod *Viviparus lentus* (Solander) (*V. lentus*), provided the opportunity to carry out a high resolution isotopic analysis

throughout the long succession of continental freshwater deposits exposed on the Island. The use of a single species or genus allows direct comparison of $\delta^{18}O$ results without concerns over species specific variation in vital effects. *V. lentus* also meets the strict isotopic criteria required to establish a high-resolution $\delta^{18}O$ isotopic record across the E/O transition of Europe. The criterion followed requires that the specimens used must not have been diagenetically altered; the specimens must be identifiable and abundant throughout the sedimentary sequence and within individual horizons. The high resolution $\delta^{18}O$ record produced has the potential to be used to calculate continental freshwater temperature variation across the E/O transition and Oi-1 glacial maximum.

This investigation will therefore, focus on producing a high resolution $\delta^{18}O$ record from a sedimentary sequence in North Western Europe. To achieve this, the following objectives were set:

- Production of a high resolution $\delta^{18}O$ and $\delta^{13}C$ profile across the E/O transition and Oi-1 glaciation;
- Using this high resolution $\delta^{18}O$ record to calculate changes in predominantly spring / summer freshwater temperatures (due to the process of shell secretion by *Viviparus* (see Chapter 2 for more information));
- Compare the temperature results to known extinction events, to establish whether palaeoenvironmental changes are synchronous with the turnover of the mammalian fauna and diversity fall during the Oi-1 glaciation; and
- Compare the results of this work with other continental and marine records from the same time period.

6.3 Isle of Wight

The Isle of Wight (IOW), located in the Hampshire Basin (UK), provides a suitable sequence of deposits encompassing Cretaceous to Oligocene strata, clearly exposed in coastal sections (Daley and Edwards, 1971). The Paleogene sediments are particularly thick due to tectonic downwarping during deposition (Daley and Edwards, 1971). Post-deposition, the area was subjected to tectonic activity relating to the Alpine Orogeny in the late Oligocene to early Miocene creating two en echelon asymmetrical anticlines (Brightstone Anticline and Sandown Anticline) (Daley and Insole, 1984), ensuring good exposure of the sedimentary sequence. The oldest Cenozoic sediments exposed on the island are the Reading Formation, associated with deposition in fluvial swamps (Daley and Insole 1984). The following collection of sediments; the Thames Group; Bracklesham Group; Barton Clay and Becton Sand Formations represent a number of transgressive and regressive phases during the Paleogene (Plint, 1988; Amorosi and Centineo, 1997). The youngest strata (late Eocene to early Oligocene in age) are represented by the Solent Group, deposited in mainly non-marine conditions, although some short lived transgressions from the east brought more brackish / estuarine conditions and one fully marine interval in the east.

The historical evolution of the IOW stratigraphy is summarised in Table 6.1. Forbes (1853; 1856) was the first to carry out a comprehensive stratigraphical account of what is now the Solent Group, with minor alterations by Bristow *et al.* (1889). Stinton (1975) brought the classification more in line with modern stratigraphic concepts by revising the British Eocene stratigraphy adding the terms Formation and Member, but without providing formal definitions. This was extended into the Early Oligocene by Cooper (1976) and Curry *et al.* (1978). The formal classification of the lithostratigraphy by Insole and Daley (1985) is the most complete and appropriate classification of this part of the succession commonly used in the current literature.

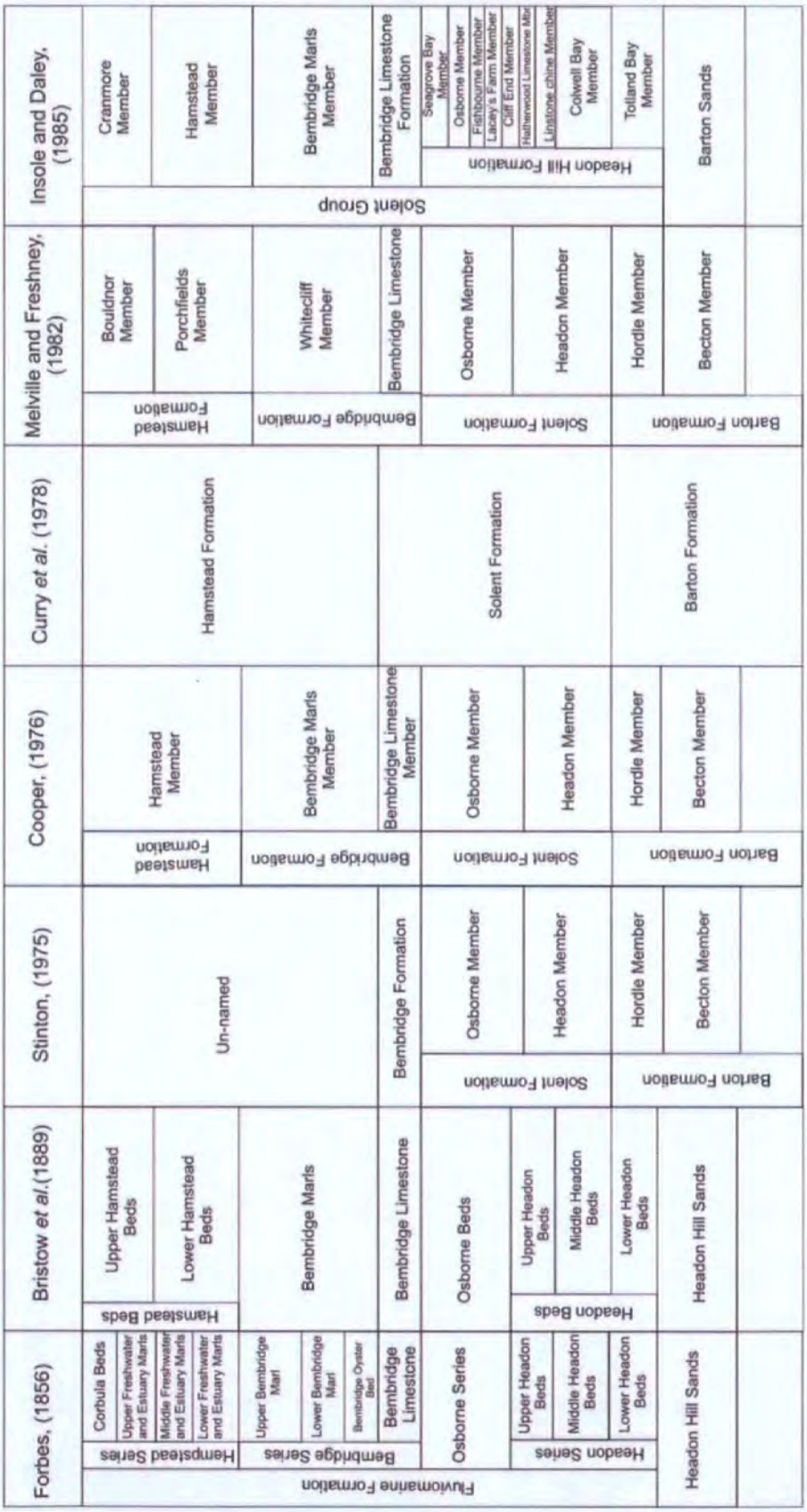

Table 6.1 Summary of the historical evolution of the Isle of Wight stratigraphy over time (Re-drawn from Insole and Daley (1985).

Owing to the lateral variation and discontinuous nature of terrestrial sediments, correlation of the IOW Solent Group to the global stratigraphic time scale has not been without controversy. The Solent Group contains few fully marine time-diagnostic intervals (Hooker *et al.*, 2009), making a direct comparison to fully marine sections problematic. Correlation of continental and marine sediments poses problems, particularly when specific boundaries are based on the extinction of a marine species e.g. the E/O boundary. As the sediments of the Solent Group are dominantly non-marine, correlation to the Global Stratotype Section and Point (GSSP) in Massignano (Italy) is difficult. Added complications in the terrestrial realm include large hiatuses and lateral variation across short distances. Until recently, publications have been unsuccessful in correlating these and other European continental deposits with the marine realm. One of the more recent examples comes from Gale *et al.* (2006), who produced a robust magnetostratigraphy for the Solent Group. They attempted to correlate this information along with, clay mineralogy, cyclostratigraphy and sequence stratigraphy. Their correlation placed the E/O boundary at the base of the Bembridge Limestone, with the onset of the Oi-1 glaciation at the base of the Seagrove Member.

The sea-level fall (~15m) that is identified high in the Seagrove Member beneath the Bembridge Limestone is interpreted to be a response to the Early Oligocene eustatic event, about 150– 160 ka before Chron C13n and thus probably coincident with the very commencement of Oi-1 (Gale *et al.*, 2006). However, this amount of sea level fall is much smaller than those quoted from the marine realm for example; 70m (Pekar *et al.*, 2002); 65m (Miller *et al.*, 2008); and 67m (Katz *et al.*, 2008). Gale *et al.* (2006) suggest that the suppression of incision by a rapid subsidence rate (Davies and Gibling, 2003) explains the sea level short falls.

Recently, Hooker *et al.*(2009), who used the lithostratigraphic scheme of Insole and Daley (1985), produced a refined correlation of the late Eocene to early Oligocene Solent Group. Hooker *et al.* (2009) achieved a good correlation with other continental deposits in Europe (e.g. Ebro Basin Spain, and the Aquitaine Basin, in France, Belgium, and Italy) using mammals and charophytes (Riveline, 1984; Hooker, 1987; 1992; Hooker *et al.*, 1995, 2004; Sille *et al.*, 2004) along with a recorrelation of the magnetostratigraphy of Gale *et al.* (2006) (Fig. 6.2). These European continental deposits (e.g. Belgian succession with first and last occurrences of dinoflagellates and calcareous nannoplankton zones) intercalate with fully marine sediments which have been directly correlated to the well constrained marine record at Massignano.

Hooker *et al.* (2004) used a chain of biostratigraphical markers and sea level changes in the Paris and Belgian Basins to correlate a major mammalian faunal turnover, 'the Grande Coupure' to the Oligocene isotopic event, the Oi-1. Their evidence disagrees with Gale *et al.*'s (2006) interpretation of the magnetostratigraphy, placing the sedimentary sequence which includes the E/O boundary and Oi-1 glaciation much later than Gale *et al.* (2006). According to Hooker *et al.* (2009) the Grande Coupure (G.C.) can be correlated with the Oi-1 glacial event in Belgium as the early post-G.C. Hoogbustel Mammal Bed containing a number of pre-G.C. endemics as well as newcomers from Asia immediately succeeds strata with the well dated last occurrence of the dinoflagellae *Areosphaeridium diktoplokum*. The boundary between the two corresponds to the Oi-1 isotopic shift recorded in the more marine facies in Belgium (De Man *et al.*, 2004). In the Hampshire Basin the G.C. occurs within the Hamstead Member at the base of the *Nematura* Bed (marking the boundary between the lower and upper parts of the Hamstead Member) (Hooker *et al.*, 2004). The hiatus (~400,000 years) at the base of the *Nematura* bed is interpreted to have resulted from erosion initiated by sea level fall associated with the Oi-1 glaciation. Hooker *et al.*

(2004) placed the highest G.C. fauna (MP20) immediately below the *Nematura* bed and the lowest post-G.C. fauna occur 5m higher in the upper Hamstead Member.

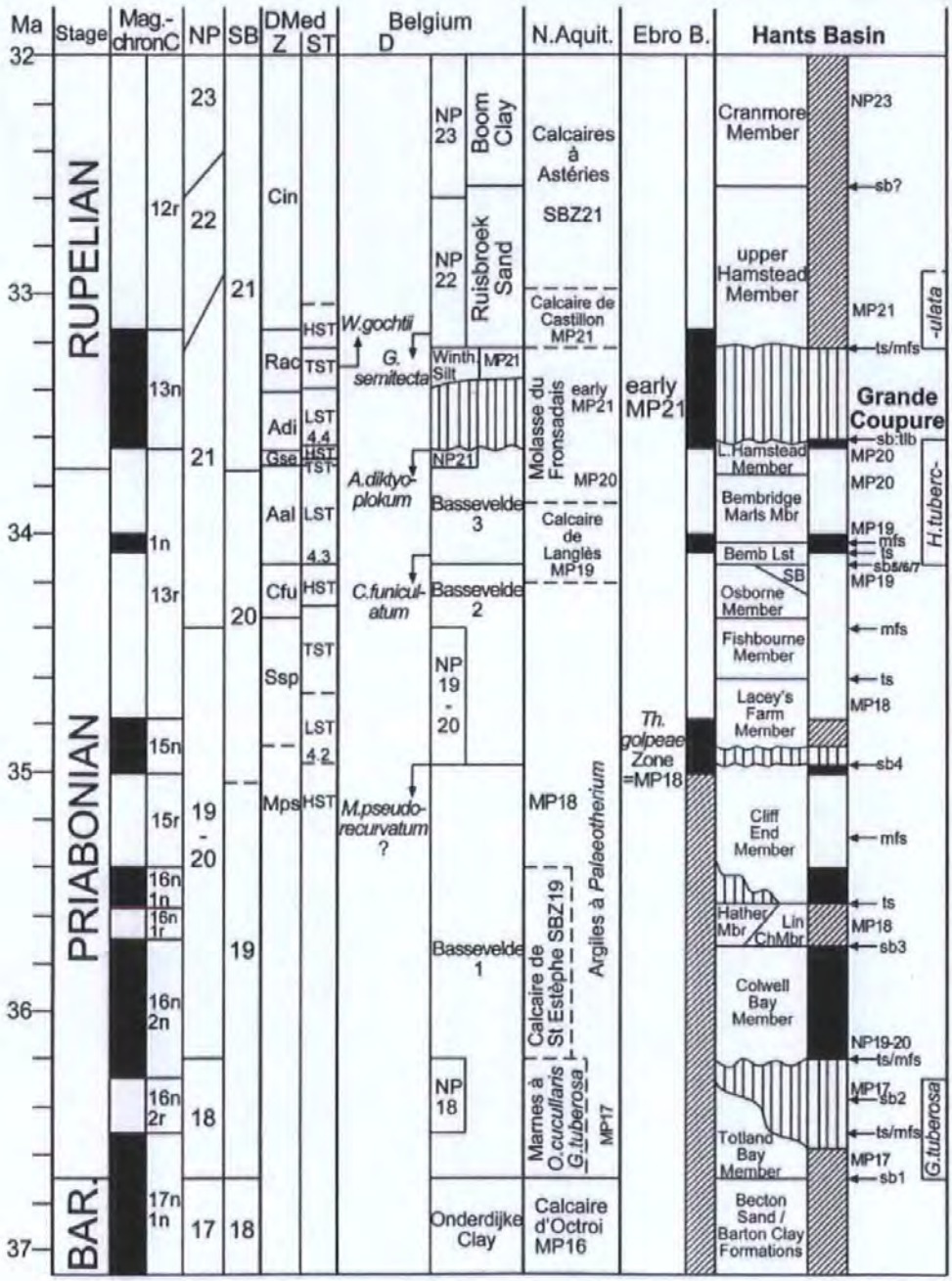

Figure 6.2 The correlation of the Hampshire Basin Solent Group with the geomagnetic polarity time scale via biostratigraphy, magnetostratigraphy, and sequence stratigraphy in the Ebro Basin, Spain, the Aquitaine Basin, France, Belgium, and Italy (taken from Hooker *et al.*, 2009). Additional abbreviations: BAR—Bartonian; BNPZ—Bembridge normal polarity zone; Hather—Hatherwood; HHNPZ—Headon Hill normal polarity zone; L—lower; Lin Ch—Linstone Chine; Lst—Limestone; Mbr Member; mfs—maximum flooding surface; SB—Seagrove Bay Member; sb—sequence boundary; *Nem—Nematura* Bed; tlb—top log bed; Winth—Wintham.

Hooker *et al.* (2009) indicate that Gales *et al.*'s (2006) normal polarity sample, 8m above the base of the Hamstead Member, is likely to represent the beginning of chron C13n, most of which could be missing in the hiatus at the base of the *Nematura* Bed (Hooker *et al.*, 2004). Hooker *et al.* (2009) placed the E/O boundary high in the Bembridge Marls or low in the lower Hamstead Member and the Oi-1 isotopic event below the *Nematura* Bed at the boundary between the lower and upper Hamstead Members (Fig. 6.2).

6.3.1 Isotopic and temperature records of the Solent Group strata

The terrestrial sedimentary record from the Hampshire Basin (UK) has so far provided limited isotopic data owing to restricted taxonomic distribution and potential isotopic fractionation (Grimes *et al.*, 2003). To overcome these issues Grimes *et al.* (2003; 2005) analysed various genera throughout the Solent Group including rodent cheek tooth enamel, gastropod shells (*Lymnaea longiscata* (Brongniart, 1810)), charophyte gyrogonites, fish otoliths, and fish scale ganoine. The $\delta^{18}O$ of the mammal tooth enamel phosphate can be used to calculate the $\delta^{18}O$ composition of the local water. The calculated $\delta^{18}O$ composition of the local water can be used in combination with the $\delta^{18}O$ of freshwater carbonate specimens (such as those stated above) from the same sedimentary deposits to calculate palaeotemperatures. Their analysis produced isotopic snap shots from four Eocene horizons, a data point within Oligocene deposits prior to Oi-1 glacial maximum and a single (charophyte) data point above Hooker *et al.*'s (2004, 2009) placement of the Oi-1 glacial maximum. All of the proxies used by Grimes *et al.* (2005) show a positive shift in the $\delta^{18}O$ record from the beginning of the Osborne Member to the lower Hamstead Member. Palaeotemperatures calculated using these isotopic data indicate a temperature change prior to the E/O transition and Oi-1 glacial maximum (within the Osborne Member decrease of ~4.7°C) (Grimes *et al.*, 2005). However, their results indicate no significant temperature change across the Oi-1 glacial maximum itself.

6.4 Freshwater Gastropods: Why *Viviparus?*

Freshwater gastropod genera (for example *Lymnaea*, *Australorbis* and *Viviparus*) can be located in multiple freshwater horizons throughout the Solent Group. Daley (1969; 1972a) used the fossil gastropod assemblages along with palaeoecological and sedimentological information to determine the depositional setting within the Bembridge Marls Member. He used this information to illustrate a hypothetical reconstruction of lake to brackish water environments (Fig. 6.3), all of which are considered representative of the depositional settings within the Bembridge Marls Member. These hypothetical reconstructions divide the Member into three broad facies: lake, brackish lagoon and brackish bay. The freshwater genera of interest to this study are located within the lake deposits, where *Viviparus* is accompanied by *Lymnaea* and *Australorbis* ('*Planorbina*') in the littoral zone. According to Daley (1969, 1972a) this combination of genera indicates a purely freshwater environment that has a minimal flow component. However, an assemblage of this type is rare in the Solent Group. *Viviparus* is more frequently found in horizons where it is the dominant genus and on occasions intermixed with brackish tolerant species such as *Melanoides* and *Potamaclis*. Less common are lagoonal deposits with seasonally varying salinity, producing assemblages where the high salinity loving serpulids are found in association with *Viviparus* and *Melanoides*. These brackish deposits may contain *Viviparus* shells that have washed in with flood debris from freshwater environments.

According to Daley's (1969; 1972a) hypothetical model there are several species of freshwater gastropod from the Solent Group deposits that are available for isotopic analysis including:

- *Lymnaea* (often referred to as *Galba* within the literature);
- *Australorbis* (often referred to as *Planorbina* in the literature – see Paul (1989));

- *Potamaclis;*
- *Viviparus;* and
- *Melanopsis.*

These species are often found associated with littoral to open lake conditions (Fig. 6.3). *Potamaclis* and *Melanopsis* were not considered suitable for isotopic analysis as they are not restricted to a freshwater environment and were an impractical size for high resolution sampling. The prosobranch species *Viviparus lentus* (Solander) was chosen over the pulmonate species *Lymnaea longiscata* (Brongniart, 1810), *Planorbidea obtusus* (Muller, 1774) and *Planorbidea euomphalus* (Rafinesque, 1815) (Fig. 6.4) based on Warrington's (1990) investigation into isotopic fractionation in a number of different groups of freshwater and terrestrial gastropods. He found that, whilst purely sub-aquatic, gill-bearing (prosobranch) species formed shells close to isotopic equilibrium with the local water, the air breathing pulmonate species had very variable isotope compositions that could only reflect very local changes in microenvironments. Shanahan *et al.* (2005) conducted a year-long, intensive monitoring program of live aquatic gastropods (*Helisomaduryi, Melanoides tuberculata, Physa virgata, Pyrgulopsis* sp., and *Tyronia* sp.) and their host springs in the Ash Meadows National Wildlife Refuge of southern Nevada. Their results confirm that the observed differences in the shell isotopic composition of lung and gill breathing freshwater gastropods are related to the combination of behaviour and physiological factors. This result suggests that different organisms growing in identical or nearly identical environmental conditions may not produce shells with equilibrium isotopic compositions and that these offsets from equilibrium may differ by small, but statistically significant amounts (Shanahan *et al.*, 2005).

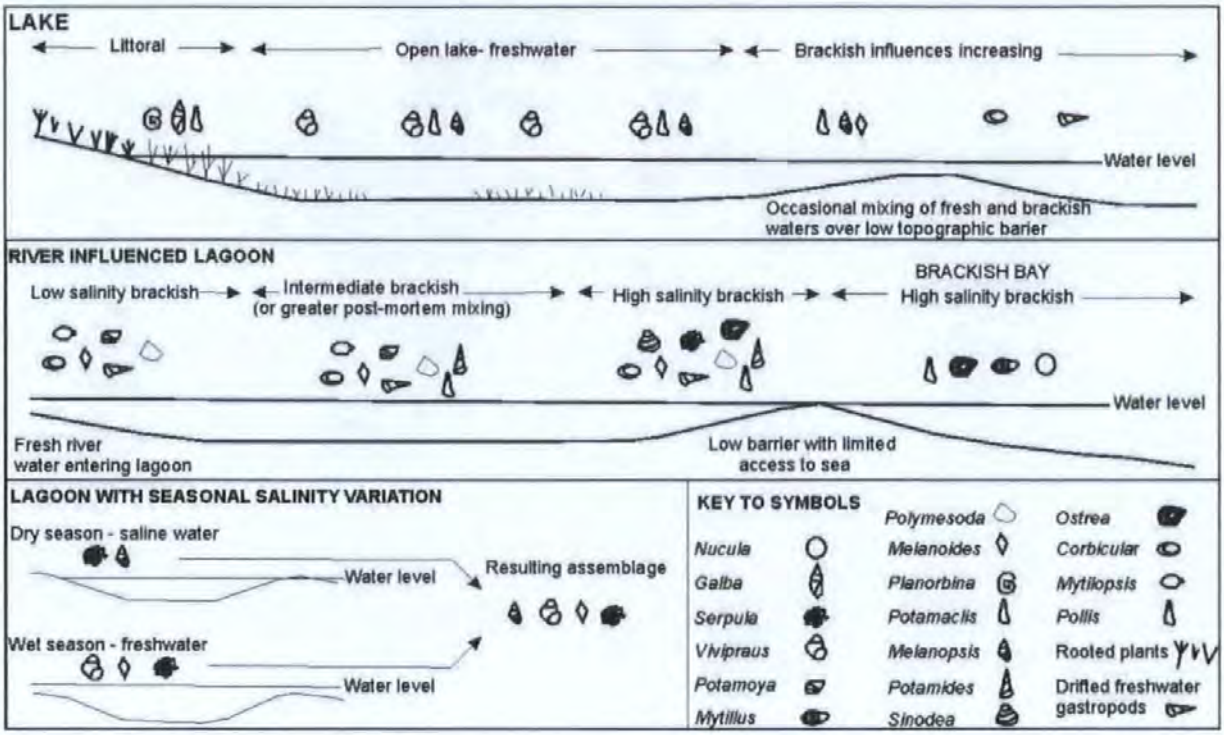

Figure 6.3 Macrofossil distribution illustrated in a hypothetical section encompassing lake to brackish bay environments (taken from Daley, 1969; 1972a).

According to Russell-Hunter and Eversole (1976), pulmonate species experience little or no growth during the winter months and may experience tissue re-adsorption, whereas *Viviparus* are known to grow throughout the year. However, winter growth is less vigorous than spring / summer; therefore the isotopic signal produced is predominantly a record of spring and summer values. This continuous growth has been attributed to a difference in feeding habits. *Viviparus* predominantly filter feed on detritus which is available throughout the year. Also prosobranch species remain within slow flowing water therefore are likely to reflect slightly buffered temperatures and not record rapid changes in daily temperature. As a consequence a more averaged seasonal temperature profile is likely to be obtained when samples are drilled at high resolution. Finally, *Viviparus* tends to be well preserved as whole specimens within the fossil record whereas the slightly thinner shelled pulmonate species are often found crushed.

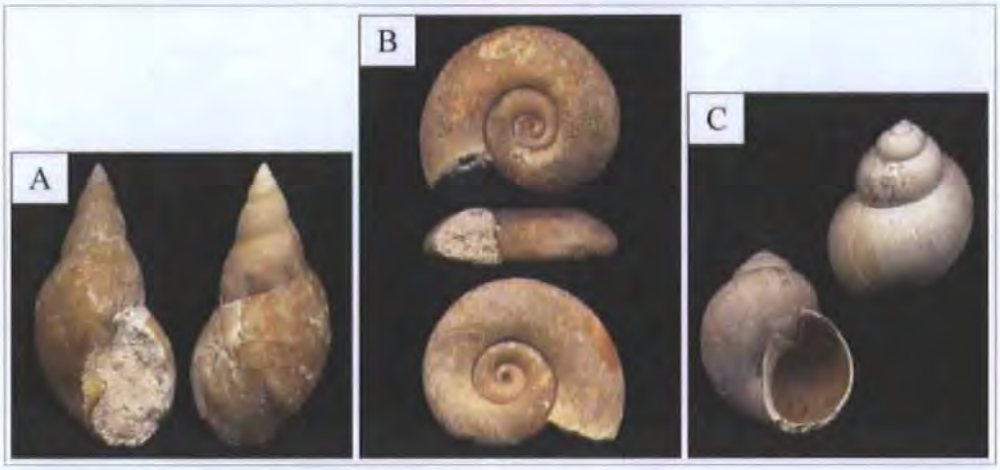

Figure 6.4 Examples of the freshwater gastropod species present in the Solent Group (A. *Lymnaea longiscata*; B. *Australorbis discus*; C. *Viviparus lentus*. (Taken from: A Collection of Eocene and Oligocene Fossils compiled by Alan Morton http://www.dmap.co.uk/fossils/hamstead/gast/hamgast.htm).

6.4.1 *Viviparus lentus* (Solander)

The fossil species *V. lentus* (Solander) is found in abundance through much of the Solent Group, although in fewer horizons in the Headon Hill Formation than in the Bembridge Limestone or Bouldnor Formation. It is mainly concentrated in large numbers within freshwater marls or clay sediments. This species is typically found in clastic deposits of large lakes or slow moving rivers, commonly associated with laminated sands and shelly beds (Paul, 1989). Within certain deposits the apices of the shells are thickened by internal deposition. This shell adaptation is thought to increase the weight of the shells, assisting in stabilizing the gastropod within moving water currents (Russell-Hunter, 1978). Evidence of this nature suggests that *V. lentus* lived in open or flowing water systems, giving us an indication of the type of environment which the gastropod inhabited. This is important for interpreting the $\delta^{18}O$ data, as larger or flowing water bodies are less susceptible to isotopic fractionation by evaporation (White *et al.*, 1999). *V. lentus* is absent from horizons in the Solent Group, which are brackish to marine in nature. For example, the rare occurrence of *Viviparus* from the Colwell Bay Member is attributed to a transgressive event producing brackish to marine environments. The Brockenhurst Bed at the base of the Colwell Bay

Member represents the only fully marine horizon with global marine indicators (Hooker *et al.*, 2009) including nannoplankton zone NP19–20 (Aubry, 1985, 1986).

Reference to *V. lentus* in the literature generally does not provide information on preservation; therefore not all levels described in the literature are of suitable preservation for isotopic analysis. These locations are often where *V. lentus* or *V. angulosa* are present in low abundance and are often associated in limestone facies. In clastic deposits *V. lentus* is often found on its own in large accumulations which are likely to represent death assemblages, produced either (i) by post mortem concentration via current transport; (ii) the rapid drying out of lakes during summer when the species congregates in large numbers; (iii) the (apparently natural) mortality that follows reproduction (yielding spectacular accumulations of dead shells (Dillon, 2007)) (iv) or seasonal variations in salinity. Layers containing both *Viviparus* sp. and brackish tolerant gastropod species can be used in this study, as the *Viviparus* shells are likely to have been washed into the brackish environment via high energy freshwater flows e.g. storm events. This is because, even though the specimens were found within sediments of a brackish nature, *Viviparus* can only tolerate low salinities, generally lower than 0.3 ‰ to 0.7 ‰ (Glöer and Meier-Brook, 1998). Therefore, this species must have originally lived and grown in a freshwater environment.

6.4.2 The evolution of Viviparidae

According to Prashad (1928) the origin of the Family Viviparidae occurred in western Europe, with the oldest fossils found in southern England. Dispersal of this family to the east and southeast along rivers, streams or an extensive network of freshwater basins within Europe has been confirmed by the similarities between German Eocene species (*V. hammeri* (DeFrance) and *V. splendidus* (Ludwig)) and the English species *V. lentus* (Solander).

Prashad (1928) concluded that the family had a polyphyletic origin and that it was possible to distinguish at least four main zones in which the members of this family evolved by moving from a marine to a freshwater environment:

1. Western Europe;
2. North America;
3. Peninsular India; and
4. Australia.

When part of the Mediterranean (Tethys) Sea was enclosed by land the trapped water gradually freshened through freshwater inputs, allowing the Viviparidae to flourish (Prashad, 1928).

Sollas (1905), building upon the earlier work of Bouvier (1887), derives the Viviparidae family from the trochids and the turbinids. These two families are both geologically old (occur in Silurian and in some cases Cambrian beds), their anatomical characteristics including the ctenidia, nervous system and relationship of the heart and the rectum, suggesting a close relationship. It is likely that the Viviparidae arose from the less highly modified common stem of these families in the Early Jurassic (Prashad, 1928).

From the Cretaceous onwards, members of the family became separated from the ancestral marine and estuarine forms, adapting to a freshwater life (Prashad, 1928). The overall direction of morphological evolution of Viviparidae is from a trochoidal shell to the paludinal form, with the compression of the upper two spiral ribs and then the peripheral carina (Starobogatov, 1985).

Freshwater environments are transient in time and exhibit a high degree of small scale short term isolation (Hubendick, 1952, 1954, 1960; Russell-Hunter, 1952, 1957, 1961,

1964, 1970). Isolation of populations can result in rates and modes of evolutionary change which are markedly different from terrestrial or marine gastropods (Russell-Hunter, 1978). The adaptive plasticity of freshwater gastropods allowed them to undertake the primary physiological adaptation for life in freshwater, namely the capacity for osmoregulation and the ability to adapt to more varying environmental conditions e.g. physical, chemical and trophic-biotic (Russell-Hunter, 1978). Late Jurassic and Cretaceous species, found in the Purbeckian and Wealden strata of England and Germany are thought to represent the first extensive occurrences of Viviparidae. Three species form the main constituents of the Purbeck deposits:

- *V. fluviorum* (Montfort);
- *V. elongatus* (Sowerby);
- *V. inflatus* (Sandberger).

Deposition of the Purbeck strata occurred within the Purbeck lagoons, which were formed in the land-locked portion of the Portlandian Sea (Radley, 2006). It is thought that viviparids dispersed from local estuarine areas into these freshwater environments.

Eocene / Oligocene species of Viviparidae of England, France and Germany, which represent closely related species, are apparently descendents of the Cretaceous forms which had become established in suitable areas (Prashad, 1928). During the Cenozoic changes undergone by the river systems of Europe caused the Thames, Seine, Rhine, Rhone, and Danube to become more closely connected than they are today. This is thought to have played a significant role in the distribution of Viviparidae in Europe from the West to the East. The Danube is the most important river system as it connected the whole of Central and Eastern Europe, while the Rhine and its connections with rivers of the Western region determined the distribution in those areas (Prashad, 1928).

Newton (1891) produced a comprehensive list of Eocene and Oligocene species; however many of the *Viviparus* species were first described by Sowerby (1817):

- *Viviparus angulosus* and *V. orbicularis* – from the Bembridge Limestone were originally referred to as the genus *Phasianella.*
- *V. lentus* (*Solander*) – from the Eocene and Oligocene of what is now the Solent Group includes specimens referred to as *V. vestitus* (*Edwards Mss*) Newton also referred to this species by this name.

The Eocene and Oligocene *Viviparus* show a very close relationship between those found in England and those found in the Paris beds. All of these fossil Viviparidae are smooth shelled forms, not at all specialized and seem to have undergone little change from the earliest known species to the recent forms found in the UK. The less specialized smooth-shelled species persisted and spread over Europe, where they are represented today by *V. Viviparus* (Linnaeus) and *V. fasciatus* (Müller) and in North America by *V. georgianus.*

6.4.3 Freshwater gastropods as recorders of palaeotemperature / palaeoenvironments

Gastropods, both marine and freshwater, have been widely used to reconstruct past environmental conditions (Andreasson and Schmitz, 1996; Schmitz and Andreasson, 2001; Accour *et al.*, 2003; Latal *et al.*, 2004; Anadon *et al.*, 2006). Their robust shell contains a detailed geochemical archive of past environmental changes, making molluscs particularly appealing for isotopic analysis. The $\delta^{18}O$ composition of their shell carbonate (both aragonite and calcite) is considered to have been precipitated in near isotopic equilibrium with the surrounding host water (Fritz and Poplawski, 1974, Grossman and Ku, 1986, Leng *et al.*, 1999). The process by which $\delta^{18}O$ is incorporated into the shell is, in the majority of cases, temperature dependent. Any increase in temperature will cause isotopic fractionation between the host water and the carbonate mineral to decrease (Leng and Marshall, 2004).

Therefore, the shell $\delta^{18}O$ composition is a combined signal of temperature and changes in the $\delta^{18}O$ of the host water. Interpretation of the $\delta^{18}O$ record obtained from the analysis of gastropod shells requires an understanding of the environment in which the gastropod grew. The impact of environmental factors (e.g. evaporation (resulting from heat, humidity and /or wind), water retention times (open or closed system), and precipitation (intensity, frequency and source) on the fractionation of isotopes), in particular the O^{18}:O^{16} ratio. In order to calculate reliable palaeotemperatures the $\delta^{18}O$ of the water must be known.

6.4.4 *Viviparus* as a climate proxy

Schmitz and Andreasson (2001) have successfully used the freshwater gastropod genus *Viviparus* to produce seasonal palaeoenvironmental reconstructions for the Early Eocene of the Paris Basin. They compared the fossil *Viviparus* specimens to modern *Viviparus* specimens collected from a variety of locations from middle to low latitude climatic zones. The range of $\delta^{18}O$ and $\delta^{13}C$ values obtained from the analysis of these modern and fossil specimens can be seen in Figure 6.5. From these data it can be seen that the climatic zones have differing $\delta^{18}O$ and $\delta^{13}C$ values, although the subtropical and dry tropical have overlapping values. This may allow the identification of particular climatic zones from $\delta^{18}O$ and $\delta^{13}C$ values obtained from fossil specimens. Schmitz and Andreasson (2001) compared the $\delta^{18}O$ and $\delta^{13}C$ values obtained from the fossil specimens of *Viviparus lentus* and *Viviparus suessoniensis* collected from the Paris Basin. Their results indicate that these specimens were living in a subtropical to dry tropical climatic zone during the earliest Eocene. From this and other sedimentological and palaeontological information, Schmitz and Andreasson (2001) suggested that the climate of northern France during the Early Eocene was subtropical with pronounced seasonal droughts.

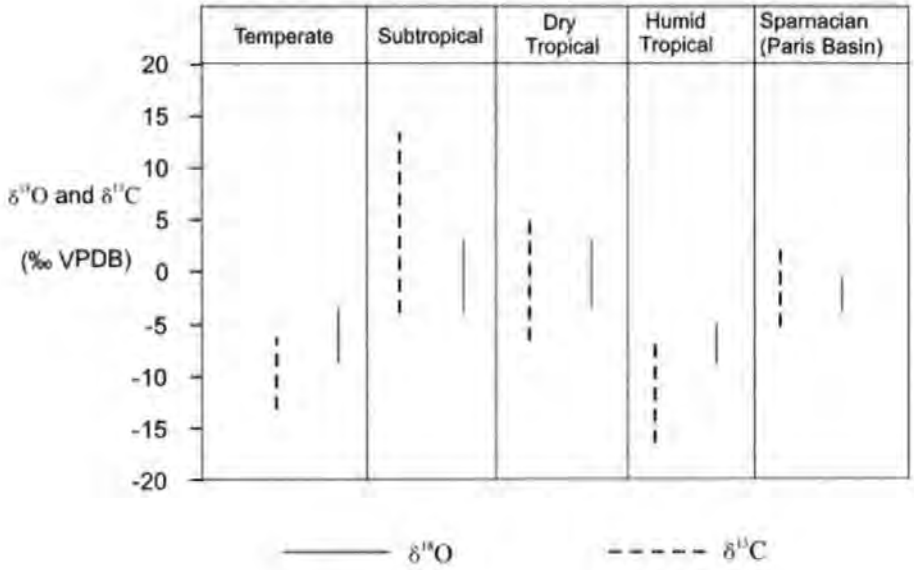

Figure 6.5 Results from the analysis of recent *Viviparus* shells showing the range of $\delta^{18}O$ and $\delta^{13}C$ values obtained from different climatic zones, compared with fossil specimens from the Paris Basin (Schmitz and Andreasson (2001).

Confirmation that the genus *Viviparus* is capable of recording a geochemical record of past and present climates has also been provided in Part 1, Chapter 2 and by Bugler *et al.* (2009) through the experimental calibration of the $^{18}O/^{16}O$ isotope fractionation between the biogenic aragonite of *Viviparus* and its host freshwater. As Shown in Chapter 2 this genus is capable of recording the combined signal of temperature and the $\delta^{18}O$ composition of the host water. Bugler *et al.* (2009) also suggest that during shell secretion the $\delta^{18}O$ composition of the shell carbonate is unlikely to be influenced by size, sex or whether females contained eggs or juveniles. This is important when applying the *Viviparus* thermometry equation to the fossil record as it is not possible to determine sex from the remaining hard part anatomy (Bugler *et al.*, 2009).

To understand the meaning behind the isotopic records obtained from *Viviparus* an investigation into the biology of *Viviparus* and its effect on it shell composition was reported in Chapter 2. From this investigation it has been shown that if a whole shell was crushed and analysed the resultant $\delta^{18}O$ values / temperatures were biased towards spring

and summer values. This is due to *Viviparus* secreting larger amounts of calcium carbonate (aragonite) during periods of warmer temperatures and greater food supply. Migration of *Viviparus* to deeper waters in the late summer, where they remain until spring, will also have an effect upon the carbonate secretion. However, so long as the water temperatures do not fall below the growth temperature threshold, shell growth continues throughout winter but, at a reduced rate. It was observed that during experimentation with modern specimens of *Viviparus* that growth rates significantly reduced below a water temperature of ~5°C. However, the actual growth cessation temperature threshold has not been determined.

For further information on *Viviparus* biology and how this affects its shell secretion, see Chapters 2 Section 2.6, Chapters 3 and 4.

6.5 Methodology

To achieve the objectives outlined in Section 6.2, the IOW in the Hampshire Basin was chosen, as it contains the most complete section encompassing Eocene / Oligocene strata in N.W Europe. This sedimentary sequence also contains a carbonate proxy (*V. lentus*) capable of producing a high resolution $\delta^{18}O$ and $\delta^{13}C$ record across this time period.

6.5.1 Fieldwork

The samples used in this study were collected on three different occasions during 2007 and 2008. The selection of sampling sites relied on the work of previous authors, namely Insole and Daley (1985) Daley (1969), Jerry Hooker (pers. comm. and works cited) and Margaret Collinson (pers. comm). The sampling strategy was to concentrate on the collection of both whole, well preserved gastropods and bulk sediment samples from beds rich in freshwater gastropods, particularly *V. lentus*. During the initial field season (2007) the collection of samples from horizons rich in freshwater gastropods concentrated around

E/O boundary and Oi-1 glacial maximum as positioned by Hooker *et al.* (2004; 2009) (Fig. 6.6). During the 2008 field season horizons containing *V. lentus* from the remaining members of the Solent Group, not sampled during the 2007 field season, were collected. Bulk sediment samples approximately 2-3 kg in weight were collected from beds which were rich in *V. lentus* shells or fragments. Any well preserved specimens (complete and unfragmented) were placed into plastic tubs and cushioned with tissue.

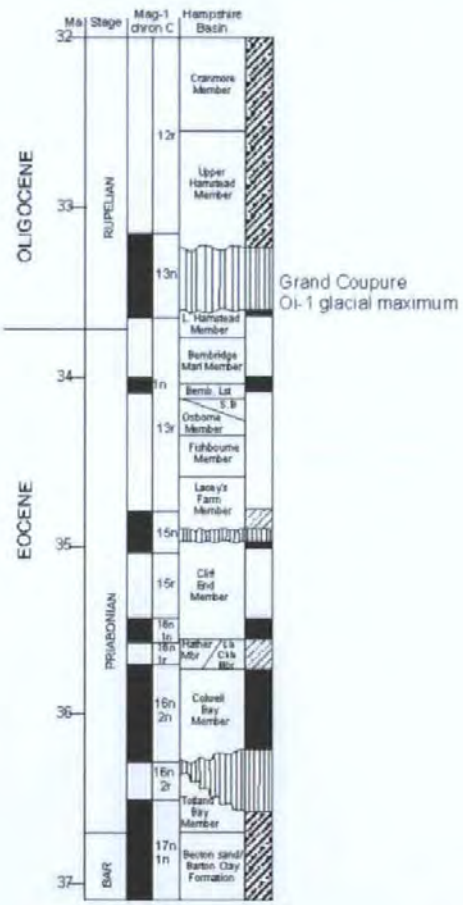

Figure 6.6 Hooker *et al.* (2009) placement of the E/O boundary and approximate location of the Oi-1 glacial maximum within the Hamstead Member hiatus.

6.5.2 Laboratory work

The laboratory work for this project was carried out by the author, from preparation to running of the analysis, at the University of Plymouth. The only exception to this was

some XRD analyses of gastropod shell fragments which were carried out at Royal Holloway University of London by Dr Dave Alderton.

6.5.2.1 Preparation of *V. lentus* fragments

After the 2007 and 2008 field collections the bulk sediment samples were returned to the laboratory where they were air dried and placed in warm water to disaggregate the clay particles. Each sample was then wet sieved using sieve mesh sizes of 2 mm, 1 mm, and 250 μm. Each size fraction was oven dried at 25 °C. For horizons where shell specimens were fragile, and it was thought that material would be lost during the sieving process, the samples were removed by hand and individually cleaned. Ten randomly selected *V. lentus* fragments (ranging from the aperture to the apex) were picked from the >2 mm size fraction, cleaned in an ultra sonic bath and photographed. The individual fragments were then crushed using an agate pestle and mortar. A small amount of the powder (between 0.30 mg to 0.50 mg) was placed into vials for isotope analysis. The remainder was retained for repeat analysis and X-Ray Diffraction (XRD) in order to check for any alteration of the original aragonite mineralogy (Section 6.5.2.2 for the method). For the isotopes analysis procedure for $\delta^{18}O$ and $\delta^{13}C$ see Section 6.5.2.3.

6.5.2.2 X-Ray Diffraction analysis

To determine preservation of shells from individual horizons, the remaining powder from 3 to 5 *V. lentus* fragments from each horizon was analysed. The samples were analysed at the University of Plymouth and Royal Holloway University of London (RHUL).

At Plymouth University the samples were analysed by the author, using a Phillips PW1792 X-ray diffractometer (XRD) with High-Score Plus identification software. The *V. lentus*

powder was aligned along a metal plate, which was then placed into a sealed chamber within the XRD. A Cu anode source was used with generator settings of 30kV and 40 nA. Each sample was exposed to x-rays of a known wavelength for 15 minutes, measuring the intensity of the diffracted radiation as a function of beam and sample orientation. From this exposure an intensity verses angle chromatograph was formulated. Expert High Score was used to analyse the x-ray chromatography produced. The computer package used search-match algorithms combining peak and net profile data to identify the best mineralogical match. At RHUL samples were analyzed courtesy of Dr Dave Alderton using a Philips Analytical XRD PW3710 machine with PC-APD diffraction software. Samples were scanned between 20° to 50° (2θ) using a copper tube anode.

6.5.2.3 Isotopic analysis of *V. lentus* fragments

The carbonate powders were reacted with 100 % phosphoric acid at 90 °C for approximately 1hour. The CO_2 produced was analysed on a GV Instruments Isoprime Mass Spectrometer with a Gilson Multiflow carbonate auto-sampler. Any isotopic results below 1.2 nA peak heights were removed from the dataset and rerun if material was available. The results were calibrated against Vienna Peedee Belemnite (VPDB) using the international standards NBS-19 (National Bureau of Standards 19; $\delta^{13}C$ = 1.95 ‰ $\delta^{18}O$= –2.20 ‰), IAEA -CO-8 (International Atomic Energy Agency -CO-8 published values; $\delta^{13}C$ –5.75‰ $\delta^{18}O$= –22.67‰), and IAEA-CO-9 (International Atomic Energy Agency -CO-9 published values; $\delta^{13}C$ = –45.12‰ $\delta^{18}O$= –15.28‰). Five NBS-19 standards were also evenly distributed throughout the individual isotope runs to correct for daily drift. An aragonite fractionation factor (1.01034 taken from Friedman and O'Neil, 1977), was

applied to convert the measured isotope compositions of CO_2 generated by the reaction of aragonite with ortho-phosphoric acid to the isotope compositions of aragonite.

6.5.2.4 Clumped isotopes

The opportunity arose for a single fossil *V. lentus* fragment to be analysed using the relatively new technique known as clumped isotope thermometry. Further discussion on the status of this new analytical technique can be found in Chapter 4. As shown in Chapter 2 the *V. contectus* shell structure consists of carbonate crystals (in this case aragonite) surrounded by an organic protein secretion which binds the crystal layers together. It has been suggested that organic contaminants are potentially problematic for measurements of Δ_{47} (Gosh *et al.*, 2006); therefore, the carbonate powders have to be pre-treated before clumped isotope analysis. Although the majority of organic matter will have been degraded during burial and fossilisation of the *V. lentus* specimens it is thought that the organic protein binding the crystal layers together may still remain. Therefore, the fossil samples were subjected to the same pre-treatment as the modern specimens (Chapter 4 Section 4.2). To remove the organic content the carbonate powder was placed into a centrifuge tube, to which 13ml of 6% NaOCl was added. The powdered sample was then left in the NaOCl for approximately 24 hours. Multiple washing of the carbonate powder with ultra pure water was carried out to ensure that all of the NaOCl was removed from the sample. On the last rinse the ultra pure water was removed leaving the carbonate sample in the centrifuge tube. The sample was then oven dried at 30°C for approximately 24 hours or until dry. Once dry it was homogenised and placed into glass vials as 8mg sub-samples. The sample was then sent to Caltech laboratories, Caltech University (USA) for clumped isotope

analysis courtesy of Dr M. Daeron and Prof. J. Eiler. The carbonate powder was subjected to the same analytical procedure as that outlined in Chapter 4 Section 4.2.1.

6.6 Results

6.6.1 Field work: Locations and composite section

In total seven locations identified in Figure 6.7 were sampled for horizons containing the freshwater gastropods *V. lentus*. The locations visited during the 2007 and 2008 field seasons were as follows:

1. Headon Hill (50° 40.364'N 1° 33.962'W) (Fig. 6.7 / 6.8; Appendix 3, Fig. 1);
2. Colwell Bay/Cliff End (50° 41.370'N 1° 32.327'W) (Fig. 6.7 / 6.8; Appendix 3, Fig.2);
3. Sconce (50° 42.372'N 1° 31.411'W) (Fig. 6.7 / 6.8; Appendix 3, Fig. 2);
4. Whitecliff Bay (50° 40.128'N 1° 5.829'W) (Fig. 6.7 / 6.9; Appendix 3, Fig. 3);
5. Hamstead Ledge (50° 43.482'N 1° 25.960'W) (Fig. 6.7 / 6.9; Appendix 3, Fig. 4);
6. Top of Bouldnor Cliff (50° 42.920'N 1° 26.908'W) (Fig. 6.7 / 6.10; Appendix 3, Fig. 5); and
7. Bouldnor Foreshore (50° 42.699'N 1° 27.904'W) (Fig. 6.7 / 6.10; Appendix 3, Fig. 5).

Other locations visited that did not yield *V. lentus* specimens:

8. Gurnard Ledge (50° 44.484'N 1° 20.983'W) (Appendix 3, Fig. 6); and
9. NE Headon Hill (50° 40.364'N 1° 33.962'W) (Appendix 3, Fig. 1).

Maps showing the individual locations can be found in Appendix 3 (Figs. 1- 6), along with a description of each sample collected including grid reference, location, code, Formation /

Member, from which it was collected (Appendix 3, Table 1). Each sample was given a letter code unique to the location of collection and a sample number e.g. S1, S2, S3. From locations 1 to 6 a total of 52 horizons were sampled. Samples from another two horizons were provided by J.J, Hooker; HOR S1 from the Mammal Bed, Hordle (mainland, UK) and HOW S1 from the How Ledge Limestone at Headon Hill, both Totland Bay Member. Each sample was plotted onto a stratigraphic section which was logged using standard sedimentary methods

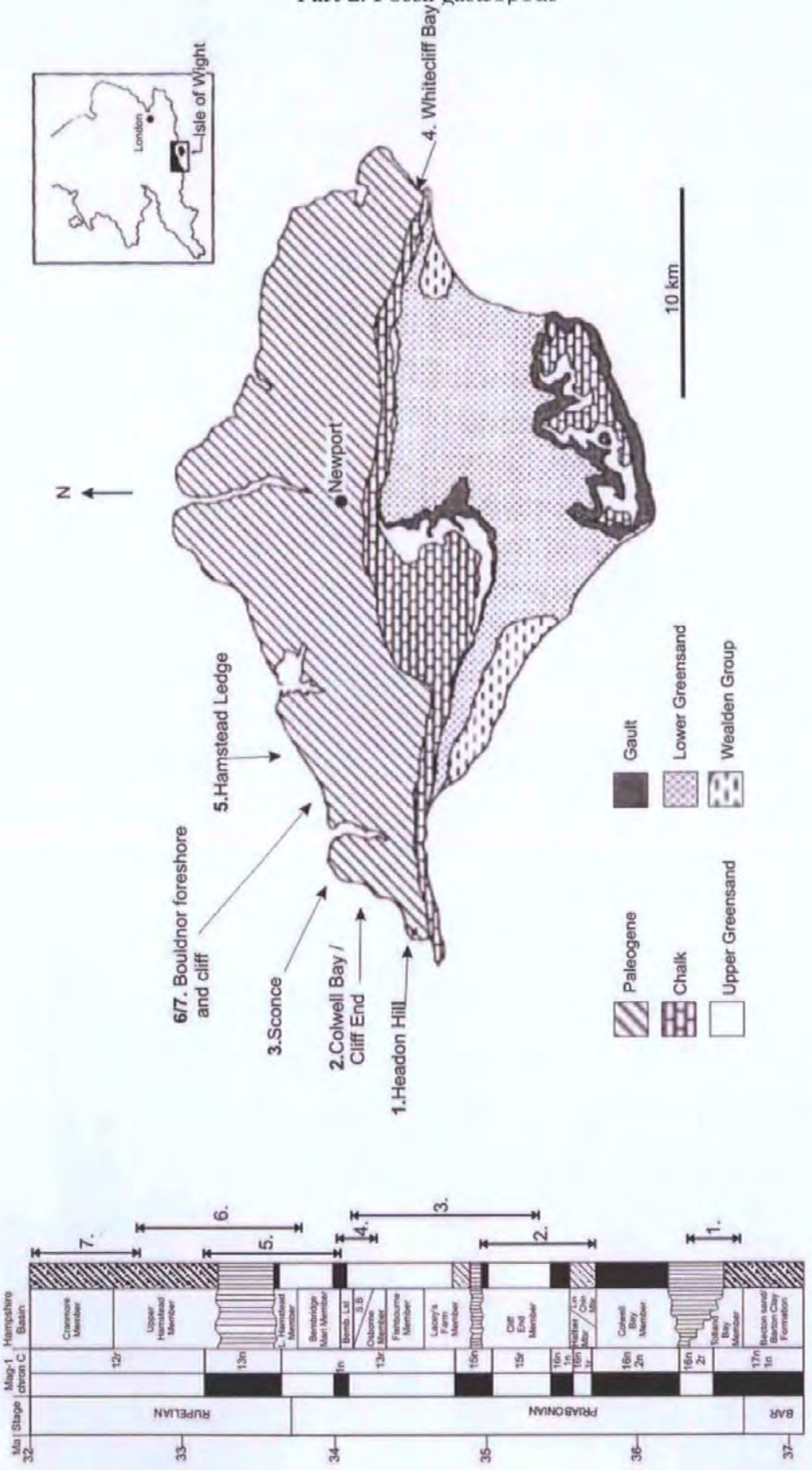

Figure 6.7 Location of the Isle of Wight in relation to the U.K. The main stratigraphical units are marked onto the map with key sample location indicated and numbered (Map modified from Daley, (1999)). The relative stratigraphic position of the sampling sites (1-7) shown against the stratigraphic column of Hooker *et al.* (2009).

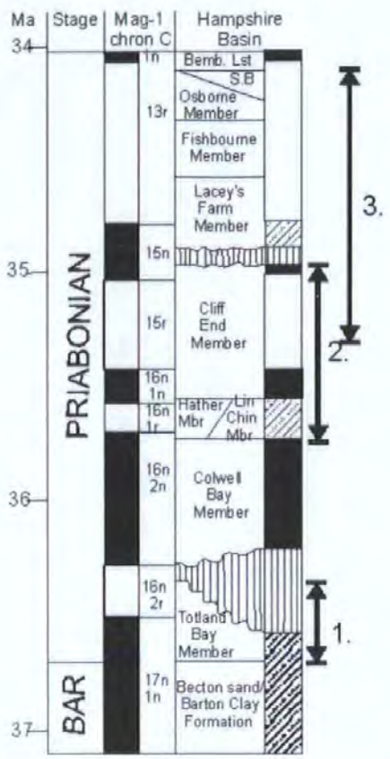

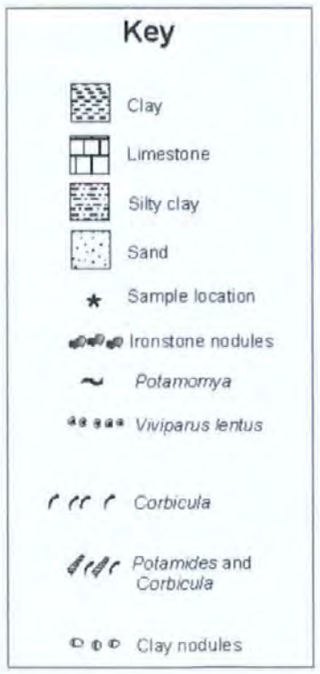

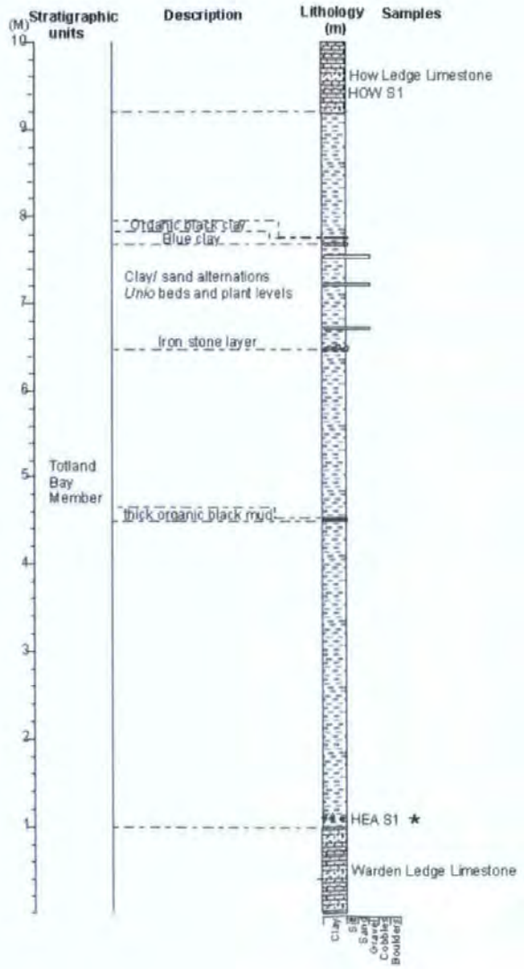

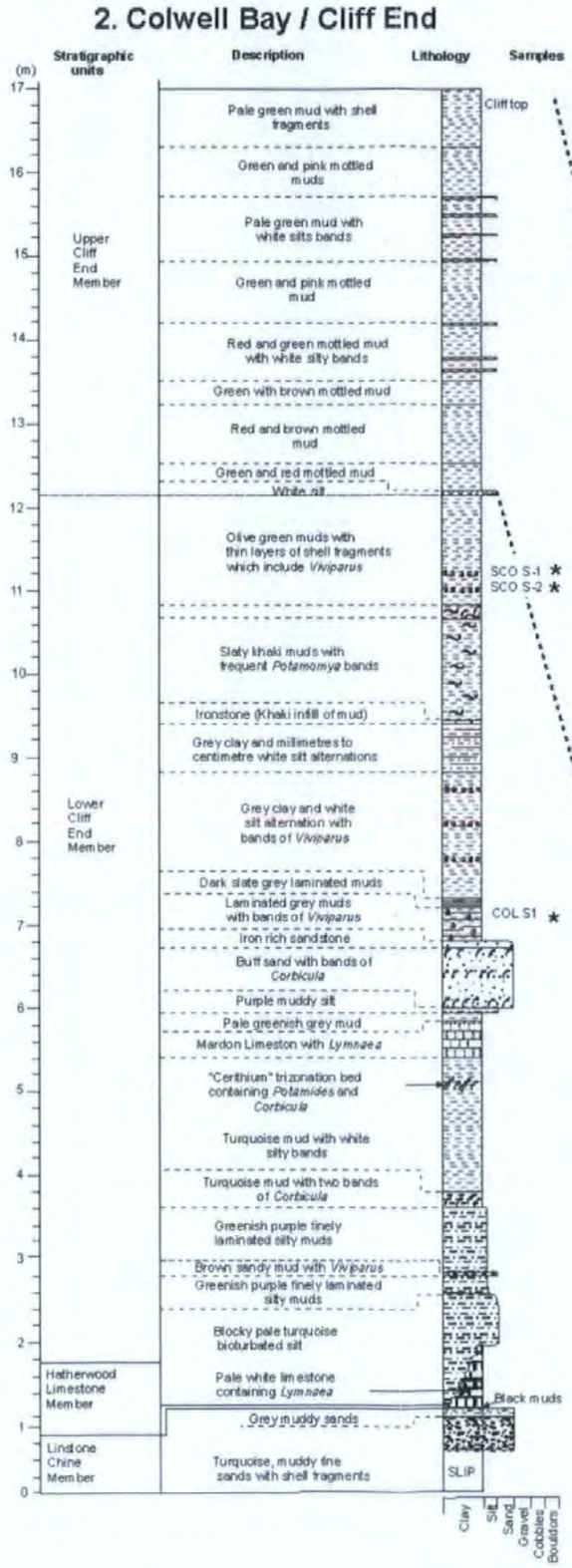

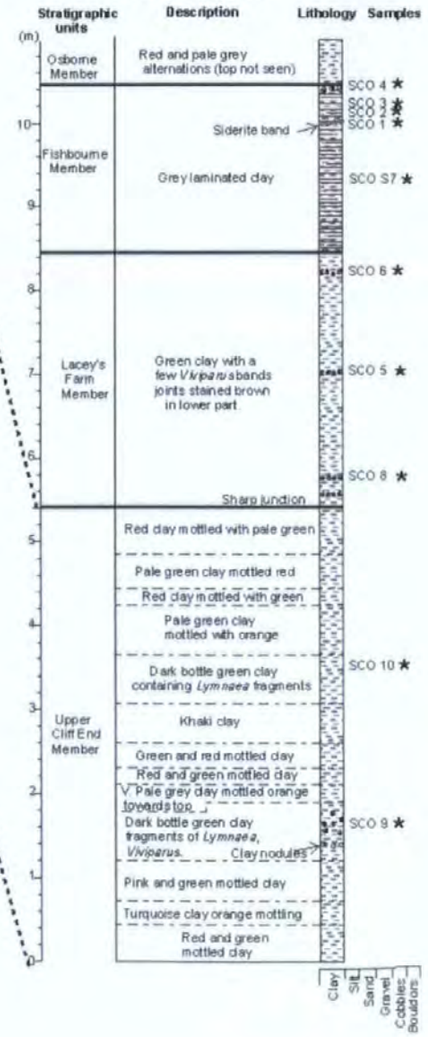

Figure 6.8 Lower part of the sequence (from the Totland Bay Member to the Bembridge Limestone Formation) showing the stratigraphical relationship between the sampling sites and any overlaps that occur (for example the overlap between sites 2 & 3 and 3 & 4). The Colwell Bay, Cliff End and Sconce logs are taken from Hooker (pers. Comm.).

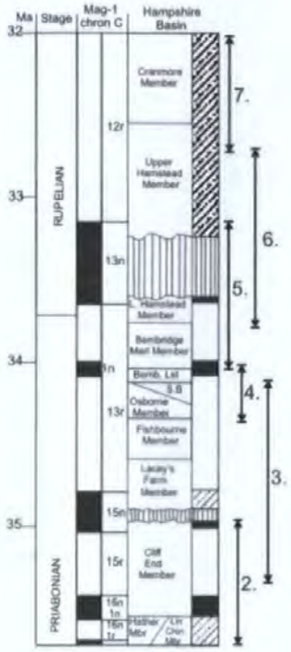

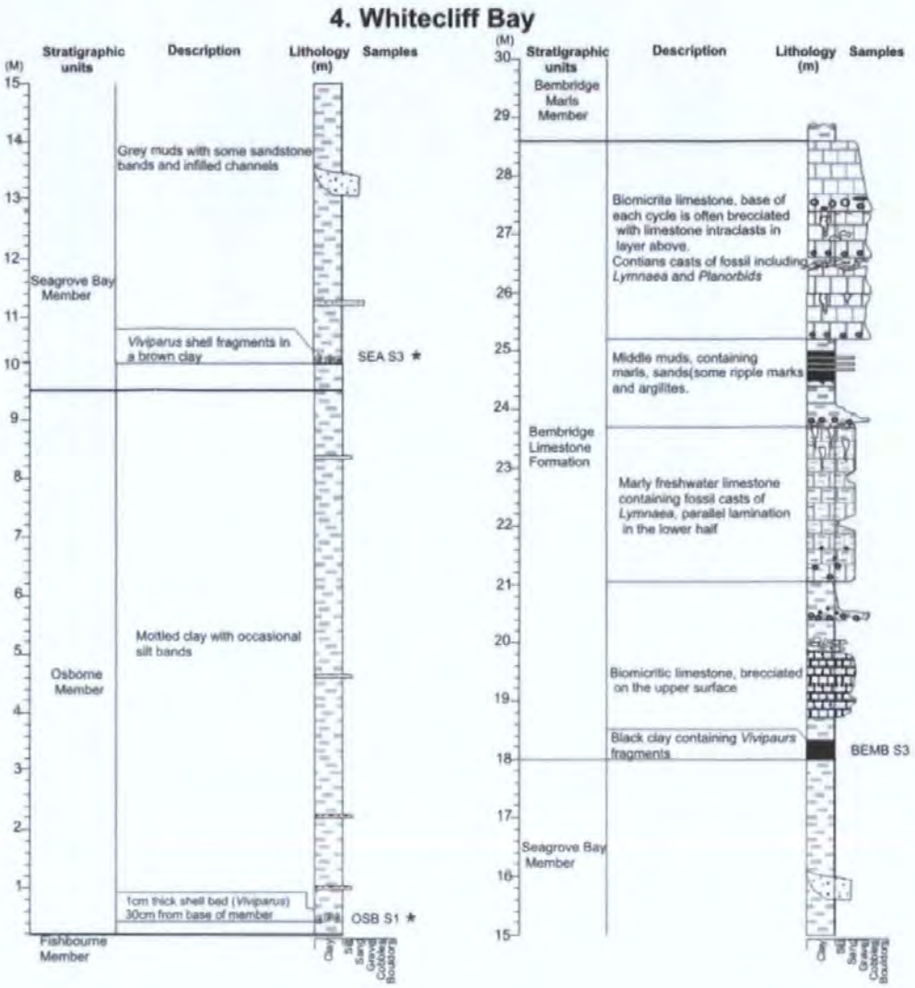

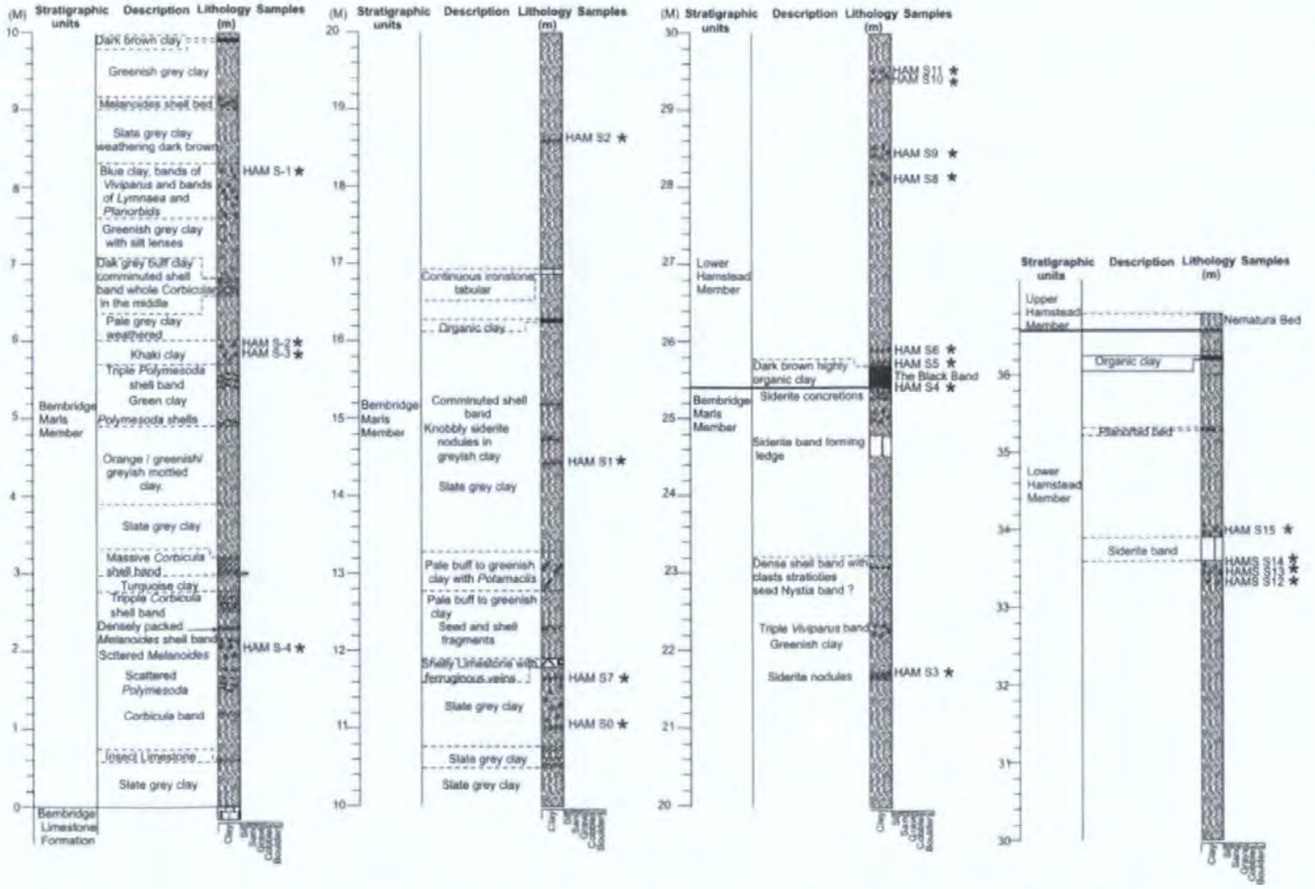

Figure 6.9 Middle to Upper part of the stratigraphy (from the top of the base of the Linestone Chine Member to the Cranmore Member) showing the stratigraphical relationship between the sample locations from which the samples were collected and where any overlaps occur. The Hamstead Ledge log has been taken from Hooker (pers. comm.) and the Whitecliff Bay log was taken from Armenteros *et al.* (1997).

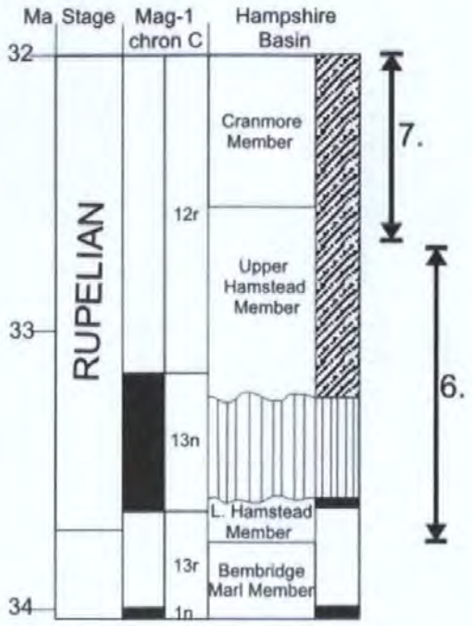

7. Top of Bouldnor Cliff

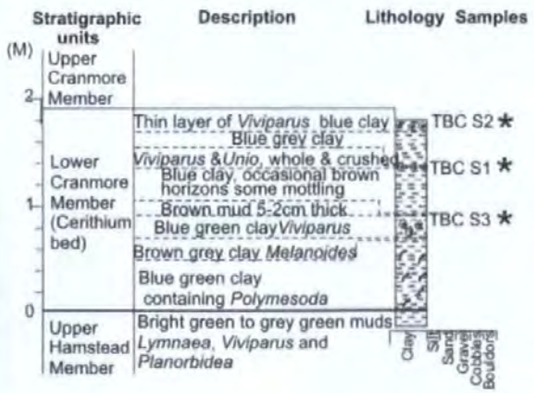

Key

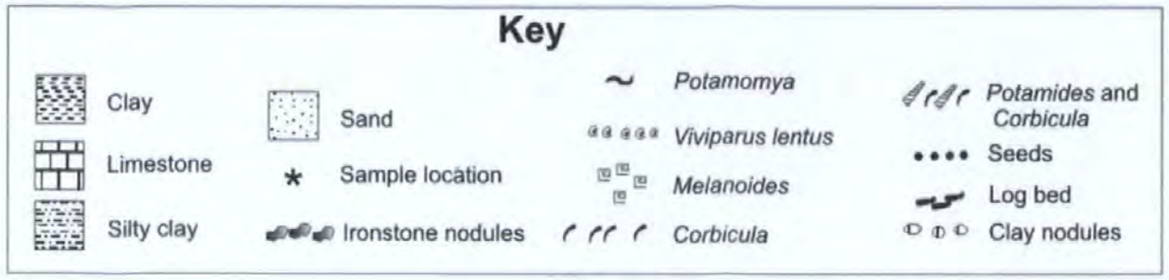

6. Bouldnor Foreshore

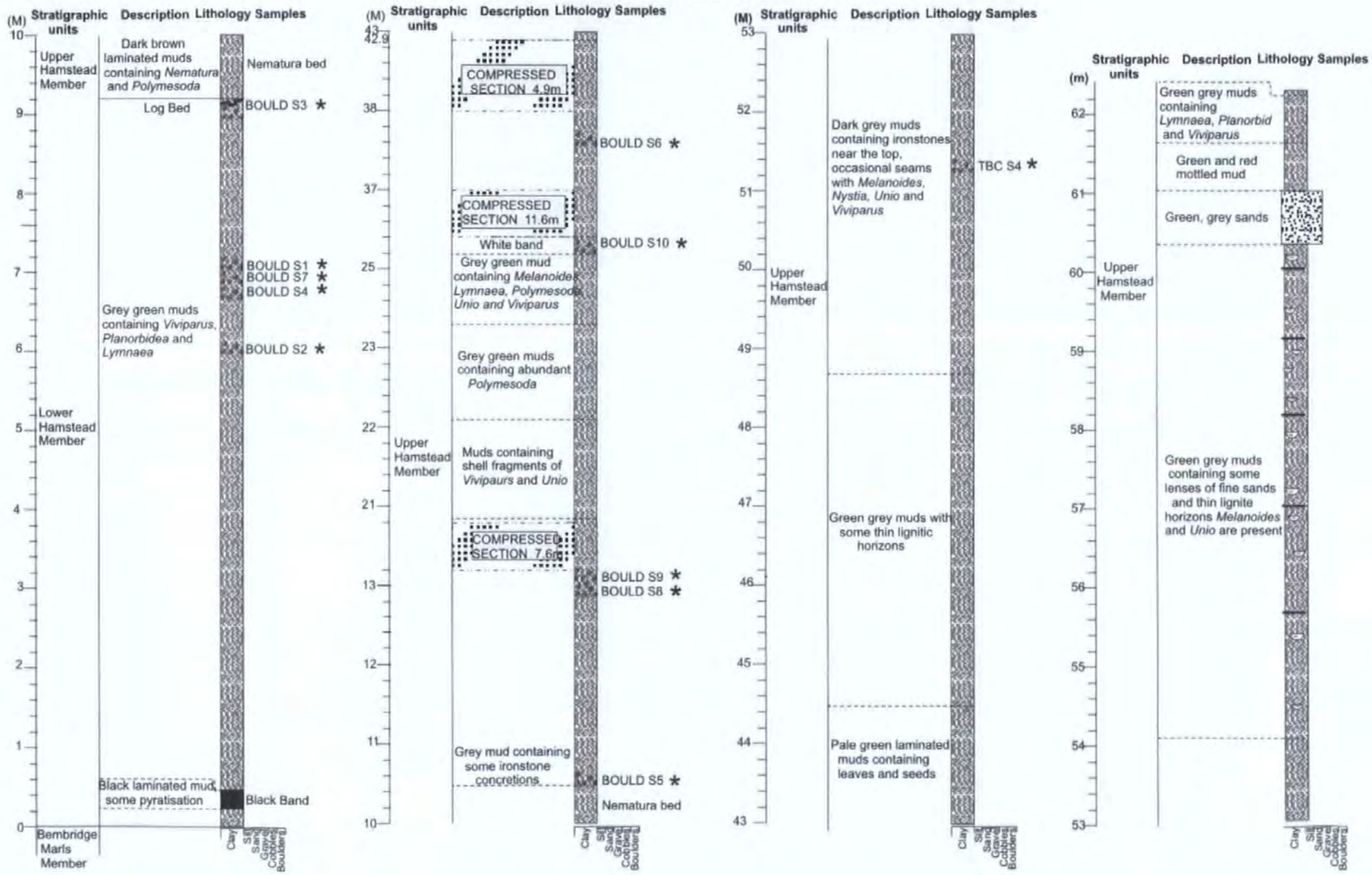

ure 6.10 Upper part of the stratigraphy (from the top of the Bembridge Limestone Formation to the Cranmore Member) showing the stratigraphical relationship between the sample locations from which the samples were collected and where any overlaps occur (for example the overlap between location 5 & 6). The Top of Bouldnor Cliff and Bouldnor Foreshore logs are taken from Hooker (pers. comm.).

6.6.2 Laboratory results

6.6.2.1 Preservation

The results from the XRD analyses can be found in Appendix 3 (Table 2). In summary, all of the shell carbonate from the *V. lentus* fragments analysed using the XRD method have an aragonitic composition.

6.6.2.2 Isotopic results $\delta^{18}O$ and $\delta^{13}C$

Out of the 52 horizons sampled 44 were successfully analysed (Table 6.2). The isotopic data obtained from the analysis of *V. lentus* fragments from the 44 individual stratigraphic horizons in the Solent Group are presented in Figure 6.11 and Table 6.2. Each stratigraphic level was assigned an age based on age tie points for the upper and lower constraints of each member by J.J Hooker (Appendix 2, Table 3). Between these points sedimentation rates were assumed to be constant. Using these ages, the $\delta^{18}O$ and $\delta^{13}C$ ratios were plotted against time and displayed against Hooker *et al.* (2009) redefined correlation of the Solent Group strata. Each data point is a mean of at least 7 analyses and the associated error bars are the standard deviation (1 sigma) from the mean. The raw data used to calculate the average values for each horizon can be found in Appendix 2 (Tables 4 to 12).

6.6.2.3 *$\delta^{18}O$ record from the analysis of V. lentus fragments*

The $\delta^{18}O$ profile produced by the analysis of *V. lentus* fragments shows a number of isotopic shifts (Fig. 6.11). Overall, the trend shows $\delta^{18}O$ values becoming more positive from the base of the Solent Group (Totland Bay Member) to the upper Hamstead Member. The most negative values (-2.5 ‰) are found in the Cliff End Member and the most positive values above the hiatus, in the upper Hamstead Member (0.2 ‰). Therefore, the

maximum range in $\delta^{18}O$ for the Solent Group is 2.7‰. This change in $\delta^{18}O$ composition from the Eocene to Oligocene takes place in a distinct number of shifts. The first of these shifts takes place between the top of the Lacey's Farm Member and the top of the Osborne Member (1.5 ‰); the second in the Bembridge Marls Member (1.0 ‰) and the third in the lower Hamstead Member (1.2 ‰) (see Fig. 6.11). The largest isotopic shift occurs between the Osborne Member and the Bembridge Limestone Formation (first isotopic shift), totalling a 2.1 ‰ shift towards more positive values, followed by a rapid return to more negative values (-1.7 ‰) after the Bembridge Limestone Formation. After the hiatus (located between the lower and upper Hamstead Member) $\delta^{18}O$ gradually decreases to more negative isotopic values but does not return to the most negative values observed prior to the Hamstead Member hiatus.

6.6.2.4 $\delta^{13}C$ *record from the analysis of V. lentus fragments*

The $\delta^{13}C$ record (Fig. 6.11) exhibits a smoother profile than the $\delta^{18}O$ record and can be roughly divided into two distinct periods of change. From the Cliff End Member to the Osborne Member values gradually become more positive, exhibiting a +7.0 ‰ shift. A short excursion (3.7 ‰ shift) to more negative values occurs within the Fishbourne Member. A sharp return to more negative values in the Osborne Member represents the most positive values (1.3‰) within the dataset before returning to more negative values in the Bembridge Marls Member and lower Hamstead Members. One exception is the distinct shift to –7.5‰ shown by the sample from the Black Band, forming the junction between the Bembridge Marls Member and the lower Hamstead Member. Above the hiatus (between the lower and upper Hamstead Members) values shift more positive (–1.1‰), after which, a gradual decrease to negative values is followed by a return to values within the range of those samples nearer the base of the Solent Group.

Date (Ma)	Horizon	Average $\delta^{13}C_{Carb.}$ (‰/PDB)	Stdev $\delta^{13}C_{Carb.}$ (‰/PDB)	Average $\delta^{18}O_{Carb.}$ (‰/PDB)	Stdev $\delta^{18}O_{Carb.}$ (‰/PDB)	No. of fragments analysed	Interpolated $\delta^{18}O_{water}$ (‰/PDB)	Average Palaeotemp. (°c) *V. contectus* EQ.	Stdev palaeotemp. (°C) *V. contectus* EQ.	Average Palaeotemp. (°c) Grosman and Ku, 1986	Stdev palaeotemp. (°C)Grossman and Ku, 1986.
32.41	TBC S2	-4.9	1.0	-1.6	0.6	9	0.9	41.4	3.6	31.81	2.12
32.48	TBC S1	-5.3	1.4	-0.6	0.6	10	0.9	33.2	5.9	26.98	3.47
32.53	TBC S3	-2.4	1.1	-0.5	0.8	11	0.9	32.6	6.2	26.66	3.60
32.73	TBC S4	-2.6	1.2	-0.8	0.9	11	0.9	34.9	6.0	28.01	3.52
32.90	BOULD S6	-3.3	1.5	0.1	0.5	10	0.9	27.8	3.9	23.87	2.26
33.00	BOULD S10	-3.1	2.2	-0.8	0.6	10	0.9	32.4	4.8	26.53	2.80
33.05	BOULD S8	-2.1	1.4	-0.1	0.9	9	1.1	29.9	4.2	25.09	2.46
33.20	BOULD S5	-1.1	0.9	0.1	0.7	10	1.4	31.8	5.2	26.19	3.03
							HIATUS				
33.63	BOULD S1	-4.0	1.5	-1.7	0.7	10	1.7	49.1	3.7	36.30	2.14
33.64	BOULD S2	-3.0	1.1	-1.1	0.6	10	2.0	44.1	4.1	33.37	2.41
33.64	BOULD S4	-5.9	1.5	-1.1	0.7	10	2.2	46.8	5.4	34.94	3.18
33.64	HAM S15	-3.9	1.4	-0.6	0.6	15	2.2	43.3	4.4	32.92	2.57
33.65	HAM S14	-3.9	1.3	-1.2	0.7	15	2.1	47.4	4.9	35.30	2.99
33.66	HAM S13	-3.3	1.3	-0.9	0.6	14	2.1	43.5	5.1	33.00	2.99
33.68	HAM S11	-3.7	0.6	-1.5	0.5	10	2.1	48.1	4.2	35.73	2.46
33.69	HAM S10	-3.6	0.8	-1.9	0.9	10	2.1	52.2	6.4	38.09	3.74
33.69	HAM S9	-3.4	0.6	-1.7	0.6	10	2.1	50.5	3.6	37.10	2.12
33.70	HAM S8	-3.4	0.5	-1.4	0.7	10	2.1	47.1	4.8	35.13	2.83
33.73	HAM S6	-3.3	1.4	-1.7	0.7	12	2.1	49.8	5.3	36.68	3.12
33.74	HAM S5	-3.4	0.9	-2.2	0.5	10	2.0	53.9	3.3	39.10	1.94
33.74	HAM S4	-7.5	1.3	-1.8	0.6	10	2.0	50.6	4.1	37.14	2.41
33.79	HAM S3	-3.2	0.7	-1.4	0.5	12	2.0	48.4	4.3	35.86	2.54
33.82	HAM S2	-2.8	0.7	-1.5	0.5	12	2.0	48.3	3.9	35.83	2.26
33.85	HAM S1	-3.3	1.1	-1.4	0.8	10	2.0	46.8	4.5	34.94	2.62
33.86	HAM S0	-4.0	0.9	-1.4	0.7	10	2.0	49.2	5.8	36.37	3.36
33.89	HAM S7	-3.7	0.9	-0.8	0.4	10	2.0	43.2	2.2	32.85	1.31
33.97	HAM S-2	-2.4	0.4	-2.2	0.6	9	1.9	49.8	9.2	36.69	5.37
33.97	HAM S-3	-2.3	0.6	-1.6	0.5	10	1.9	49.0	3.8	36.21	2.23
34.03	HAM S-4	-2.1	0.8	-1.5	1.1	9	1.9	50.0	4.2	36.81	2.46
34.13	BEMB S3	-3.7	1.2	-0.6	0.7	10	1.2	33.9	6.1	27.44	3.55
34.20	SEA S1	-0.8	1.5	-0.7	0.6	10	0.5	31.5	4.6	25.99	2.68
34.30	OSB S2	1.3	0.9	-1.5	0.7	9	-0.2	30.6	4.1	25.47	2.37
34.36	SCO S4	-3.7	0.6	-2.4	0.9	9	0.1	41.7	6.8	31.99	3.99
34.46	SCO S3	-2.9	0.7	-1.5	0.7	10	0.4	35.9	4.6	28.57	2.69
34.51	SCO S2	-3.5	0.5	-2.2	0.5	10	0.7	43.6	3.8	33.09	2.21
34.52	SCO S1	-1.7	1.1	-2.1	0.7	7	1.0	45.9	5.5	34.43	3.19
34.62	SCO S7	-2.0	0.9	-1.7	0.5	10	1.3	46.0	2.0	34.48	1.20
34.68	SCO S6	0.3	0.6	-0.7	0.3	14	1.6	39.6	1.8	30.74	1.04
34.83	SCO S8	-2.1	0.8	-1.1	0.4	15	1.2	39.6	2.8	30.75	1.62
35.23	SCO S -1	-2.3	0.6	-2.5	0.5	13	0.8	39.6	1.8	34.81	2.49
35.28	SCO S-2	-3.3	0.9	-2.6	0.7	10	0.4	45.0	5.5	33.88	3.19
35.50	COL 1	-3.9	1.1	-2.2	0.6	14	0.0	39.4	4.4	30.61	2.58
36.40	HOW S1	-5.3	1.3	-0.9	0.7	10	-0.4	25.8	5.3	22.70	3.10
36.50	HEA S1	-5.3	1.7	-1.3	1.1	14	-0.4	29.2	8.1	24.67	4.76
36.67	HOR S1	-5.7	0.9	-2.0	0.9	10	-0.4	35.8	4.6	28.51	2.68

Table 6.2 The average $\delta^{18}O$ and $\delta^{13}C$ values for each horizon produced from the analysis of *V. lentus* fragments are given along with the standard deviation. The number of fragments analysed per horizon is given along with its approximate date of deposition. The average temperatures, calculated using Bugler *et al.* (2009) and Grossman and Ku (1986) thermometry equations (±stdev) are given along with the interpolated $\delta^{18}O_{water}$ values from Grimes *et al.* (2005) used in the equation.

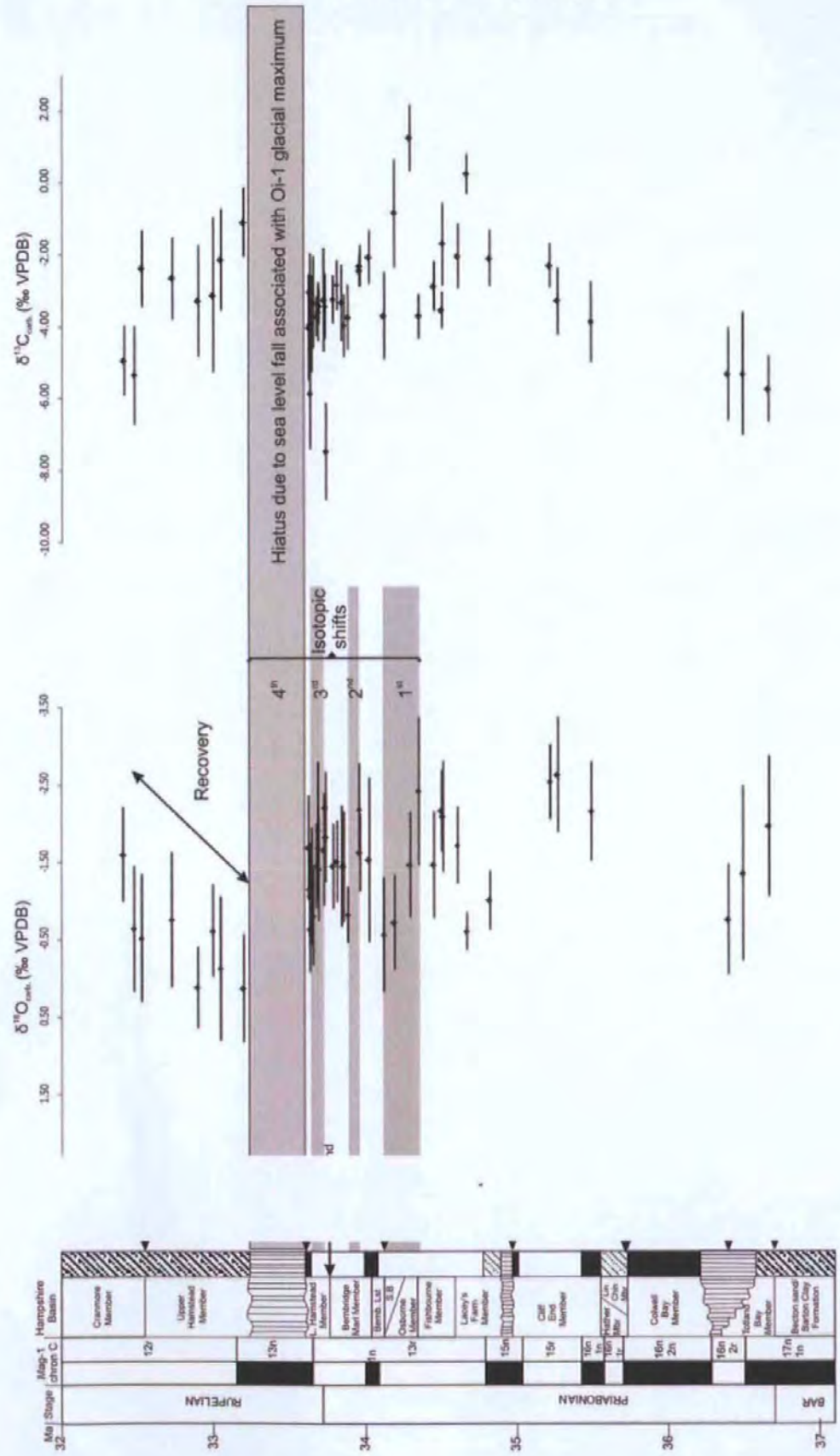

Figure 6.11 The bulk $\delta^{18}O$ and $\delta^{13}C$ isotopic profiles produced from the analysis of *V. lentus* shell fragments is plotted against the Solent Group Sequence from Hooker *et al.* (2009). Each stratigraphic level was attributed an age based on age tie points for the upper and lower constraints of each member (J. J Hooker *pers. comm.*) Each data point is a mean of at least 7 analyses and the associated error bars are the standard deviation (1 sigma) from the mean.

6.6.2.5 Palaeotemperature calculations

The high resolution $\delta^{18}O$ profile obtained from the analysis of *V. lentus* can be used to calculate palaeotemperatures across the E/O transition and Oi-1 glacial maximum. Bugler *et al.* (2009) produced a *Viviparus* genus specific thermometry equation through the experimental calibration of oxygen isotope fractionation (see Chapter 2 for further information). A requirement of this equation is that the $\delta^{18}O$ of the water in which the isotopic proxy (*V. lentus*) lived is known. Grimes *et al.* (2005) produced $\delta^{18}O_{water}$ values from 6 horizons in the Solent Group, using enamel of rodent teeth from mammal bearing horizons. These mammal bearing horizons are less common than those containing *V. lentus* and, therefore, provide $\delta^{18}O_{water}$ values at a much lower resolution than the *V. lentus* bearing beds. Interpolations between these six $\delta^{18}O_{water}$ horizons was necessary to calculate a temperature for each horizon in the *V. lentus* $\delta^{18}O$ record.

Using the Bugler *et al.* (2009) equation (Eq. 1) and Grossman and Ku (1986) equation in combination with the high resolution *V. lentus* $\delta^{18}O_{carb.}$ (Fig. 6.11) and the Grimes *et al.* (2005) interpolated $\delta^{18}O_{water}$ values (Table 6.2 and Fig. 6.12), a high resolution freshwater temperature record was produced (Fig. 6.12).

$$\text{Temperature (°C)} = -7.43(+0.87, -1.13)*\Delta\delta^{18}O + 22.89(\pm 2.09) \qquad \text{(Eq. 1)}$$

The temperatures produced by Bugler *et al.* (2009) equation range from 25.8°C to 52.9°C. As mentioned previously the freshwater temperatures produced from the analysis of *V. lentus* are considered to be dominantly spring to summer averages. Taking this into account the calculated freshwater temperatures produced by the Bugler *et al.* (2009) equation are extremely high when compared with modern water temperatures from subtropical to tropical climates. For example, water temperatures measured from the Florida Everglades, vary between 22°C to 33°C (Schaffranek and Jenter, 2001). These

temperatures are considered to be to high for biota to survive and are relatively high in comparison with other European datasets from this time period (e.g. Mosbrugger *et al.*, 2005; Uhl *et al.*, 2007). Whereas the temperatures calculated using Grossman and Ku (1986) thermometry equation range from 22.7°C to 39.1°C. In comparison with Bugler *et al.* (2009) equation the temperatures calculated using Grossman and Ku (1986) thermometry equation have lower maximum temperatures and a reduced range in temperature. These temperatures are within a more realistic range for biota to thrive.

However, as previous discussed in Chapter 5, the use of isotopic composition to infer palaeotemperatures requires significant assumptions. The most significant assumption involves the $\delta^{18}O$ isotopic composition of the host water from which the carbonate was secreted. There are several issues concerning the use of the Grimes *et al.* (2005) $\delta^{18}O_{water}$ values to calculate temperatures from the *V. lentus* $\delta^{18}O_{carb.}$ record. Only a single *V. lentus* $\delta^{18}O_{carb.}$ horizon corresponds with one of Grimes *et al.* (2005) data points located in the lower Hamstead Member at Bouldnor Foreshore. This is the lateral equivalent of the siderite band at Hamstead Ledge from which samples HAM S14 and S15 were collected. The remaining $\delta^{18}O_{water}$ values of Grimes *et al.* (2005) are produced from shallow ponded environments, whereas *V. lentus* inhabits slow flowing deeper water bodies. Therefore, as suggested by Grimes *et al.* (2005), the calculated $\delta^{18}O_{water}$ values may have experienced isotopic fractionation due to evaporation in contrast to the deeper water environments which *V. lentus* inhabits. As shown in Figure 6.12 temperatures calculated using these $\delta^{18}O_{water}$ values overestimate absolute temperatures. On this basis the temperatures calculated using the interpolated $\delta^{18}O_{water}$ values of Grimes *et al.* (2005) are unrealistic.

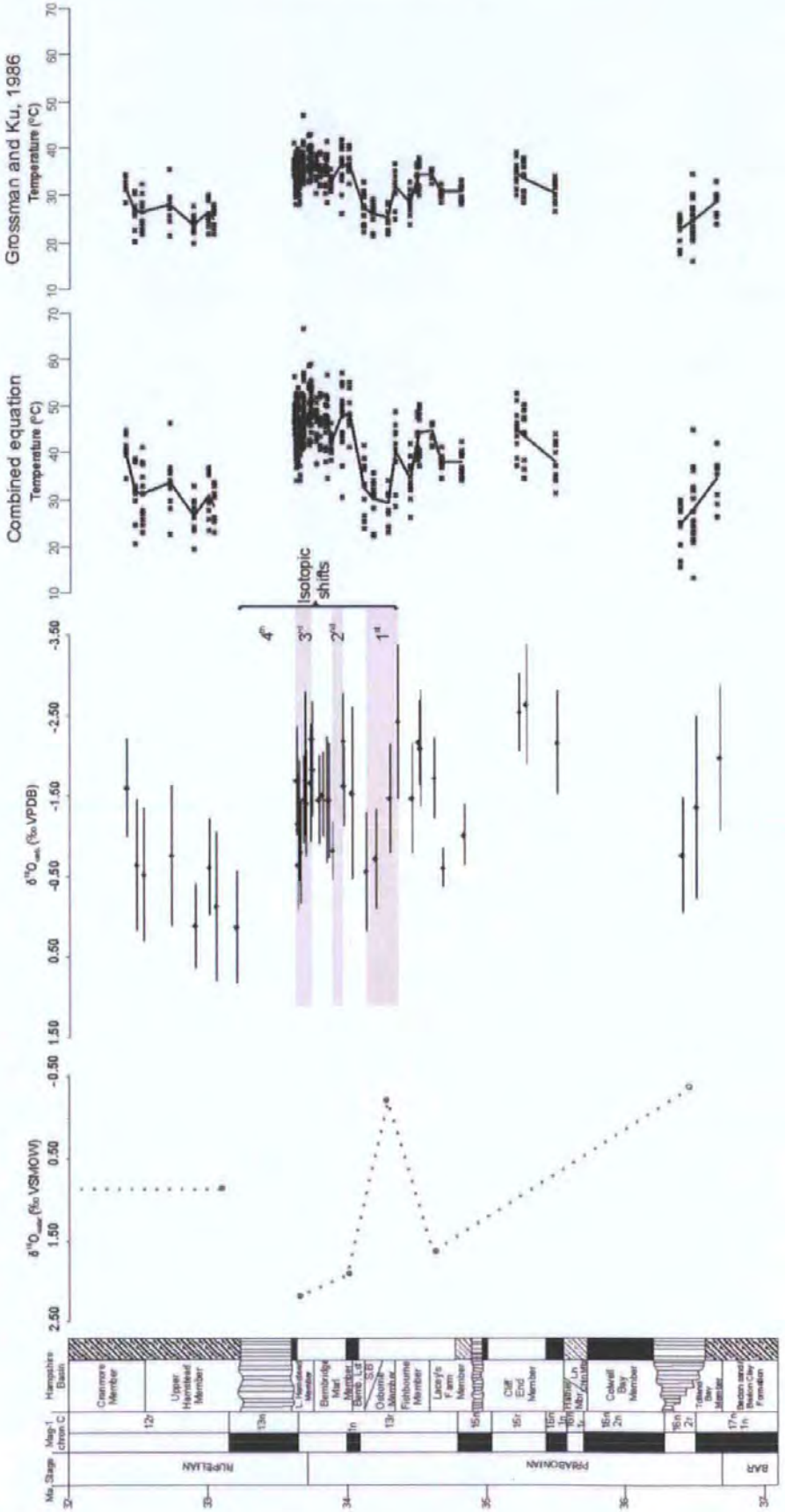

Figure 6.12 Grimes *et al.* (2005) $\delta^{18}O_{water}$ values and the high resolution $\delta^{18}O_{carb.}$ record from the analysis of *V. lentus* fragments. These two individual dataset were used in combination with the *V. contectus* thermometry equation and Grossman and Ku (186) thermometry equation to calculate palaeotemperatures. Oi-1 = Oligocene glaciation; EOT- 1/2 = Eocene / Oligocene transition event 1/2.

6.6.2.6 Clumped isotope temperature

In an attempt to produce realistic $\delta^{18}O_{water}$ values clumped isotope thermometry was investigated, to test whether temperature and $\delta^{18}O_{water}$ values could be produced from the same specimen. The sample HAM S1 8A (~33.8 Ma) produced a delta 47 value of 0.6646 +/- 0.0105 ‰ (1σ). Using the Ghosh *et al.* (2006) equation (Eq. 2) a temperature of 20.9 +/- 2.3 °C (1s) was calculated.

$$\Delta_{47} = 0.0592 * 10^6 * T^{-2} - 0.02 \qquad \text{(Eq. 2)}$$

The temperature equation produced by Bugler *et al.* (2009) was rearranged (Eq. 3) so that the $\delta^{18}O_{water}$ value could be calculated using the temperature calculated by the clumped isotopes analysis and $\delta^{18}O_{carb}$ for the sample HAM S1 8A (Table 6.4).

$$\delta^{18}O_{water} = (\text{clumped temp} - 22.89) / -7.43) - \delta^{18}O_{carb.}) * -1 \qquad \text{(Eq. 3)}$$

$\delta^{18}O_{carb.}$ (‰ VPDB)	Clump Temp (°C)	$\delta^{18}O_{water}$ (‰ VPDB)
-1.3	20.9	-1.5

Table 6.3 from the analysis of HAM S1 8A $\delta^{18}O_{carb.}$ and clump isotope temperature was produced from which the $\delta^{18}O_{water}$ was calculated.

The $\delta^{18}O_{water}$ value was calculated as –1.5‰ for HAM S1 8A (Table 6.4). In comparison with the Grimes *et al.* (2005) $\delta^{18}O_{water}$ values the calculated $\delta^{18}O_{water}$ value for HAM S1 8A (–1.5‰) is 1.2‰ more negative than their most negative value (2.2‰) (Fig. 6.13).

However, a clear comparison can not be made as the samples are from different horizons. As indicated in Chapter 5 (p. 145) the association of the rodent specimens with *Lymnaea* species would indicate shallow ponds that are more susceptible to isotopic fractionation than deeper water bodies in which *Viviparus* lives. In the shallower ponded environments both temperature and isotopic stratification could potentially occur due to enhanced residence times associated with these environments. However, *Viviparus* tends to prefer water bodies that have a component of flow preventing such long water residence times.

$\delta^{18}O_{water}$ values calculated using the $\delta^{18}O_{carb.}$ *V. lentus* record and Grimes *et al.* (2005) temperature produced $\delta^{18}O_{water}$ values that are more positive than Grimes *et al.* (2005) $\delta^{18}O_{water}$ values. However, the single $\delta^{18}O_{water}$ value calculated using the clumped isotope temperature produces the most negative isotopic values. Although this method requires further calibration, it is considered to be more reliable than the other data sets as both the temperature and $\delta^{18}O_{carb.}$ values were obtained from the same specimen. Discussion on the reliability of Grimes *et al.* (2005) $\delta^{18}O_{water}$ value can be found in Chapter 5.

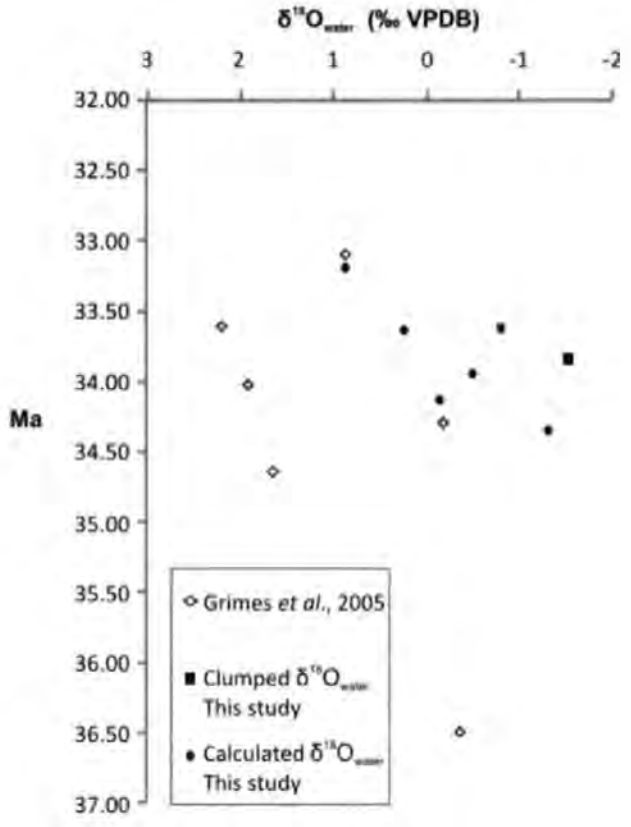

Figure 6.13 Comparison of the $\delta^{18}O_{water}$ values calculated by this study with those of Grimes *et al.* (2005) $\delta^{18}O_{water}$.

Using the $\delta^{18}O_{water}$ where calculated for HAM S1 8A (–1.5‰) in combination with the $\delta^{18}O_{carb.}$ and thermometry equation of Bugler *et al.* (2009), temperatures were calculated for the remaining *V. lentus* fragments obtained from horizon HAM S1. These results are compared with those calculated using the interpolated $\delta^{18}O_{water}$ values of Grimes *et al.* (2005) in Table 6.5.

The palaeotemperatures calculated using the clumped $\delta^{18}O_{water}$ values for *V. lentus* shell fragments from the horizon HAM S1 range between 13.7°C and 32.8°C and yield an average temperature of 22.3 (±5.8) °C. On the other hand, the temperatures calculated from the same shell fragments using the interpolated $\delta^{18}O_{water}$ values taken from Grimes *et al.* (2005) yield temperatures between 39.3°C and 53.6°C with an average of 46.8 (±4.5) °C.

Date (Ma)	Horizon / Sample name	$\delta^{18}O_{Carb}$ (‰VPDB)	Interpolated $\delta^{18}O$ water Grimes *et al.* (2005)	Temp. (°C)	Av. Temp. (°C)	STDEV Temp. (°C)	Clump $\delta^{18}O_{water}$ (‰ VPDB)	Temp. (°C)	Av. Temp. (°C)	STDEV Temp. (°C)
33.8	HAM S1 V2	-1.2	2.0	48.4	46.8	4.5	-1.5	20.2	22.3	5.8
	HAM S1 V3	-0.7	2.0	45.7			-1.5	17.1		
	HAM S1 V4	-2.2	2.0	42.6			-1.5	28.1		
	HAM S1 5	-2.0	2.0	53.6			-1.5	26.3		
	HAM S1 1	-0.3	2.0	51.8			-1.5	13.9		
	HAM S1 10	-1.7	2.0	39.3			-1.5	24.0		
	HAM S1 6	-1.5	2.0	49.5			-1.5	22.5		
	HAM S1 7	-1.4	2.0	48.0			-1.5	21.6		
	HAM S1 8	-0.6	2.0	47.1			-1.5	16.4		
	HAM S1 9	-2.9	2.0	41.8			-1.5	32.8		

Table 6.4 Temperatures calculated for each of the fragments analysed from HAM S1 using Bugler *et al.* (2009) thermometry equation. One temperature dataset was calculated using interpolated $\delta^{18}O_{water}$ values from Grimes *et al.* (2005) and the other using the clumped $\delta^{18}O_{water}$ value. For the two temperature datasets an average temperature was calculated.

6.7 Discussion

6.7.1 Association of *Viviparus* with brackish species

Within the Solent Group strata there are a few sampled horizons (e.g. SCO S-2; SCO S-1; COL 1 and HAM S-4 which was found just above a serpulid worm layer) which contain both *V. lentus* and brackish tolerant gastropod species. As *V. lentus* would have originally lived and grown in a freshwater environment, as indicated by modern species which are unable to tolerate salinities above 0.7 ‰ (Glöer and Meier-Brook, 1998) owing to their low blood salt concentrations (Potts and Parry, 1963), these specimens were still considered suitable for isotopic analysis. Evidence of seasonal or intermittent differences in salinity is inferred from several beds containing serpulid worm tubes overlain by *V. lentus* shells. Daley (1969) suggested that *V. lentus* would thrive during the wet season when heavy rainfall dilutes brackish waters or could have been brought in from freshwater areas by flooding rivers. The more frequent occurrence of serpulid worm tubes in the lower members, for example the Cliff End Member (author's pers. obs.), may be related to relatively low amounts of mean annual precipitation (Sheldon *et al.*, 2009). However, the

V. lentus specimens from SCO S-2 in particular show that growth continued over several years. Therefore, it is unlikely that these are seasonal changes in salinity, but rather flood deposits from freshwater sources. Not all of the horizons analysed produced a mixed assemblage with the serpulids and therefore may have been deposited once freshwater condition returned. However, it must be noted that palaeoecological interpretations based on direct taxonomic comparison do not necessarily indicate the conditions which existed at the site of burial (Daley, 1967).

6.7.2 Comparison of the isotopic shifts observed in the Solent Group strata to those in the marine realm.

A comparison of the $\delta^{18}O$ excursions seen in the Solent Group with key $\delta^{18}O$ events from the marine record can be seen in Figure 6.14. Within the confines of attainable correlation (independent of isotopic data), key isotopic events from recent high resolution marine isotopic records have been plotted against the Solent Group sequence. This comparison indicates that a number of positive $\delta^{18}O$ excursions in the Solent Group between 34 and 33 Ma similar to those in the marine realm with the likelihood that they correspond directly. For example:

- The first positive $\delta^{18}O$ shift from the top of the Fishbourne Member to the base of the Bembridge Limestone Formation (shift of ~1.50 ‰) coincides with the Late Eocene Event, as seen in several marine $\delta^{18}O$ profiles (for example Zachos *et al.*, 1996; Bohaty and Zachos, 2003; Coxall *et al.*, 2005;)
- The second positive $\delta^{18}O$ shift, which occurs within the Bembridge Marls Member (~33.8 Ma), coincides with Lear *et al.* (2008) Step 1 and Katz *et al.* (2008) EOT 1.

- The third positive $\delta^{18}O$ shift, which occurs in the lower Hamstead Member (~33.6 Ma), coincides with EOT 2 of Katz *et al.* (2008). However, this could alternatively be linked to the initial part of the isotopic excursion relating to the Oi-1 glacial maximum, if dating uncertainties are taken into consideration.
- As the Oi-1 glacial maximum (~33.6 Ma) is encompassed within the hiatus between the lower and upper Hamstead Members, the most positive $\delta^{18}O$ values associated with this event are not recorded. Therefore, the $\delta^{18}O$ record from *V. lentus* is unlikely to show the most positive isotopic values associated with this event.
- The most positive $\delta^{18}O_{carb.}$ values are recorded by the first horizon analysed after the Hamstead Member hiatus (~33.2 Ma). By the middle of the Cranmore Member the $\delta^{18}O_{carb.}$ values have returned to values similar to those recorded prior the hiatus in the lower Hamstead Member.

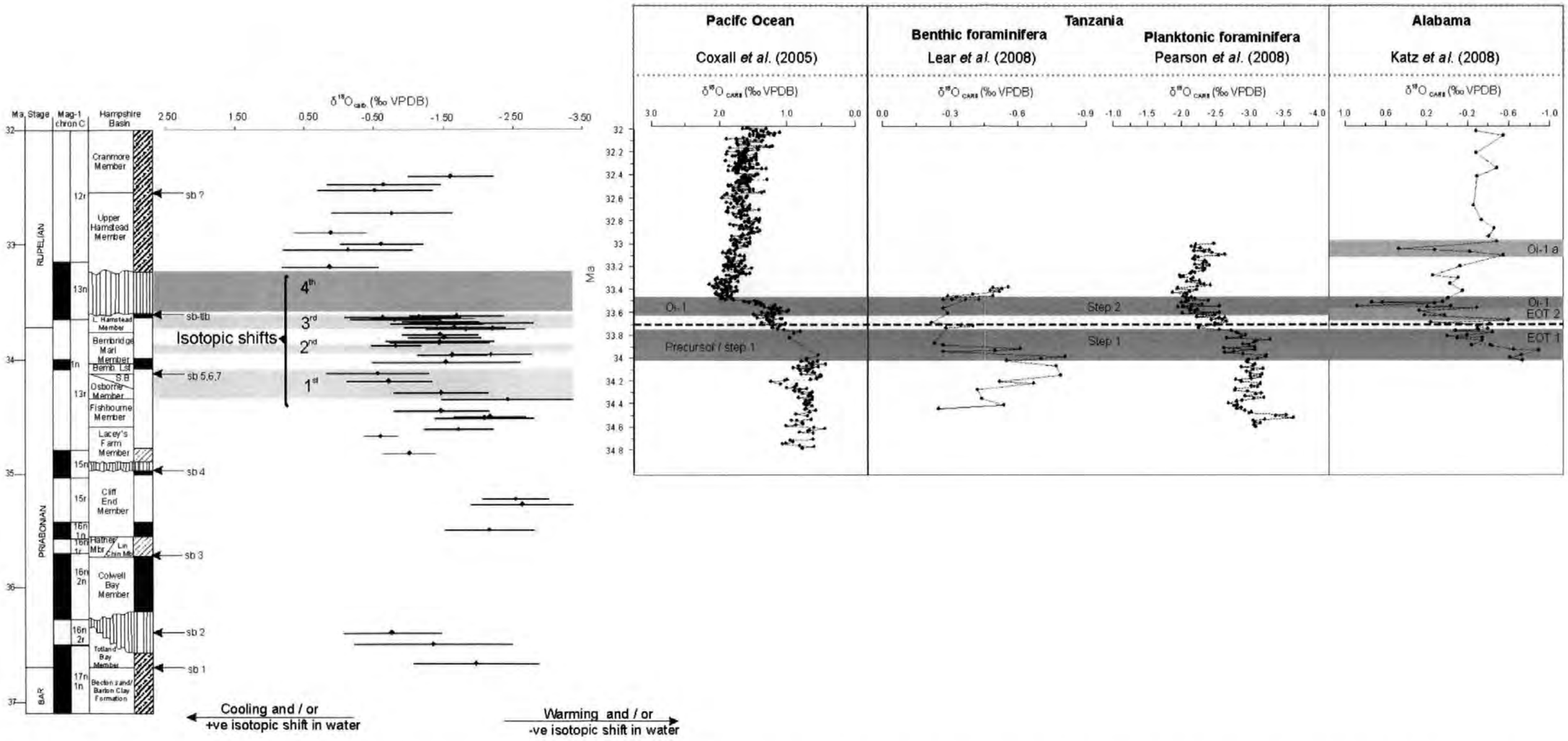

Figure 6.14 The high resolution *V. lentus* $\delta^{18}O$ profile (each of the data point represents a mean at least 7 analyses with a standard deviation around that mean) showing the position of the isotopic excursions. A comparison of the high resolution *V. lentus* $\delta^{18}O$ profile with key isotopic events from recent high resolution marine isotopic records which have been plotted as highlighted boxes representing the entire $\delta^{18}O$ shifts from Lear *et al.* (2008) and arrows representing the most positive value in the $\delta^{18}O$ shift of Katz *et al.* (2008). Abbreviations: SB = Seagrove Bay Member; sb = sequence boundaries; tlb = top log bed; mbr = Member.

The IOW $\delta^{18}O$ record follow a similar pattern to those seen in the marine realm. The similarity of the $\delta^{18}O$ records, in particular the shifts near the E/O transition and Oi-1 glacial maximum, suggests the possibility that there is a coupling of terrestrial and marine environments via atmosphere and ocean circulations. Evidence from Miocene shallow marine cores in the North Sea Basin provide temperatures calculated from fossil branched glycerol dialkyl glycerol tetraethers (terrestrial) and dinocysts (sea surface temperatures) (Donder *et al.*, 2009). Both this investigation and the study undertaken by Donder *et al.* (2009) appear to suggest that coastal terrestrial environments are more sensitive to changes in sea surface temperatures than continental interiors. Europe may also be more 'sensitive' to these changes as during a large part of the Eocene when Europe was an archipelago of large and small islands. It also suggests that this connection may alter through time due to changes in the palaeogeography of the oceans, in particular a regional effect from the isolation of the Tethys Ocean. The *V. lentus* record from the Eocene / Oligocene and those from the Miocene (temperatures calculated from fossil branched glycerol dialkyl glycerol tetraethers (terrestrial) and dinocysts (sea surface temperatures)) suggests that this terrestrial and marine coupling survived the Oi-1 glacial maximum and consequent shift into a new climatic regime.

Included on Figure 6.14 are the positions of sequence boundaries taken from Hooker *et al.* (2009). Sequence boundaries (SB) often mark significant erosional unconformities. These boundaries are the product of a fall in sea level that usually erodes the subaerially exposed sediment surface of the earlier sequence or sequences. The basal sediments of a sequence may be diachronous, capping the previous Highstand Systems Tract and eroding the surface of the downstepping sediments deposited during a forced regression associated with the sea level fall (Catuneanu, 2002). Therefore, a sequence boundary is where the sea level is at its lowest and maybe a result of polar ice build up (Westerhold *et al.*, 2005). Several of the $\delta^{18}O$ excursion in the *V. lentus* record coincide with the proposed sequence

boundaries of Hooker *et al.* (2009). The most positive part of the $\delta^{18}O$ excursions termed the 'Late Eocene Event' coincides with the sequence boundary 5, 6, and 7, located at the junction of the Seagrove Bay Member and the Bembridge Limestone Formation in Whitecliff Bay (Fig. 6.14). The next sequence boundary is located at the top of the lower Hamstead Member, representing the Oi-1 glacial maximum. However, owing to the sea level fall associated with this event, the most positive $\delta^{18}O$ values are thought to be missing. One other $\delta^{18}O$ excursion located in the How Ledge Limestone could have possible links with sequence boundaries. The $\delta^{18}O$ excursions reach positive values similar to those associated with the Late Eocene Event. However, deposits containing *V. lentus* are rare in these lower members; therefore, the resolution of the $\delta^{18}O$ record is not adequate to determine the significance of this excursion. Evidence for fluctuations in sea level during this time period is lacking from published data. Clumped isotope analysis may provide more detailed evidence on whether this isotopic excursion is related to temperature and / or change in the $\delta^{18}O_{water}$. Information on the latter will aid in determining whether ice volume changes are associated with the sequence boundaries.

The marine isotopic record from the North Sea Basin, which encompasses the E/O transition and Oi-1 glacial maximum, provides the opportunity for a regional comparison between marine and terrestrial isotopic records. The North Sea Basin $\delta^{18}O$ record (De Man, 2006) uses a multiproxy approach utilising benthic foraminifera (*Cibicidoides* spp., *Asterigerinoides guerichi),* nuculid bivalves (*Nuculana deshayesiana*) and otoliths (Gadidae, Ophidiidae, Congridae) from the middle Eocene (47 Ma) to late Oligocene (24 Ma) (Fig. 6.15). Correlation of these events requires additional investigation of the stratigraphy which was not achievable due to the scope of this project and time constraints.

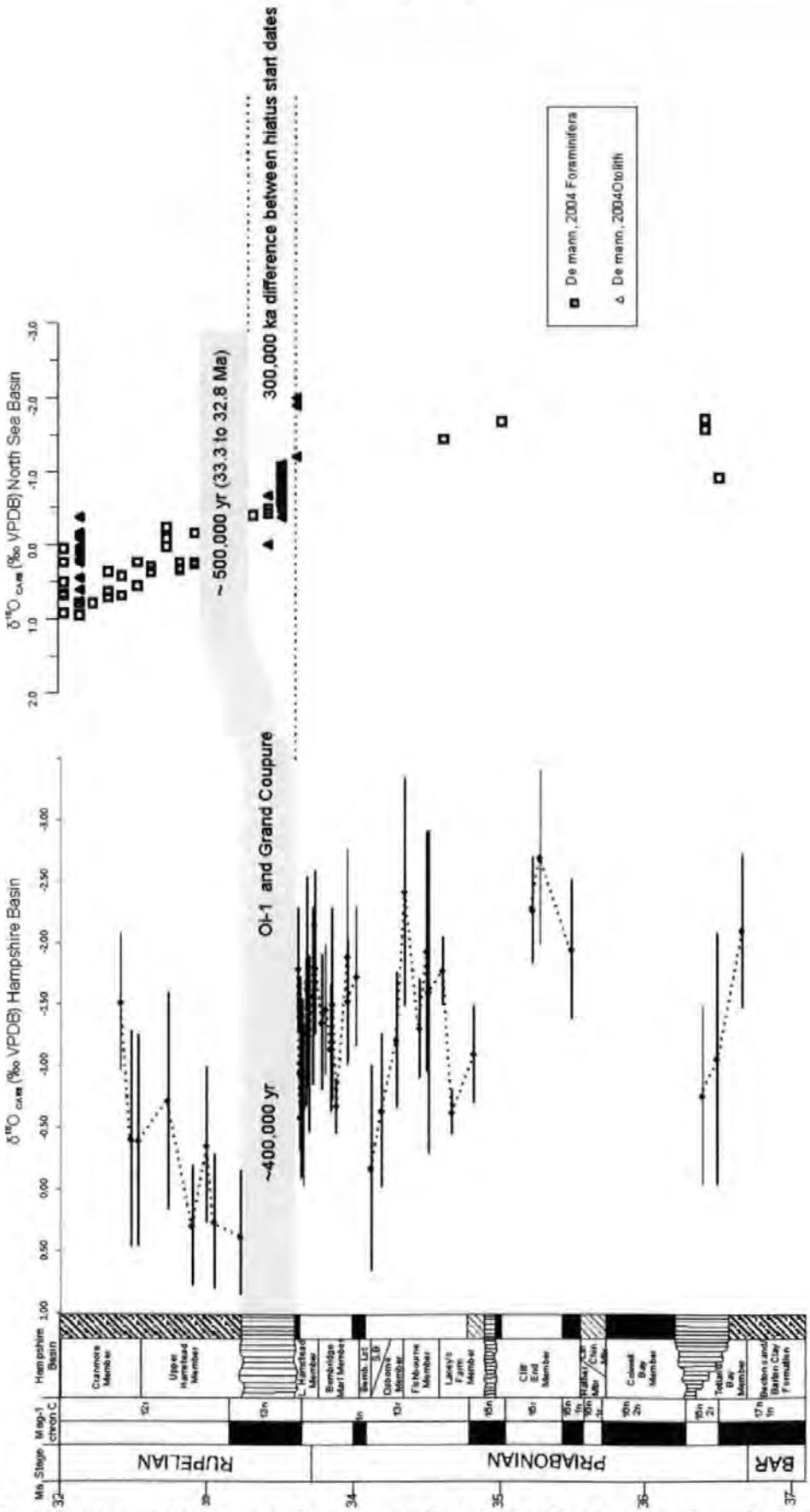

Figure 6.15 Stable oxygen isotope results from the middle Eocene to late Oligocene from the southern North Sea Basin in comparison with the isotopic results from the IOW. Samples from the Bartonian are from the Barton Clay and Becton Sand formations in the Hampshire Basin. Data taken from De Man (2006).

Sample resolution in the North Sea Basin record is significantly lower than that obtained from the analysis of *V. lentus* fragments from the Solent Group strata. In the *Cibicidoides* spp. $\delta^{18}O$ record for the E/O transition two positive steps occur which are similar to those seen in the *V. lentus* $\delta^{18}O$ record. However, the *Cibicidoides spp* $\delta^{18}O$ record requires additional data points to demonstrate that these excursions are real. De Man (2006) tentatively correlates a ~1.5 ‰ isotopic shift to the Oi-1glacial maximum. Unlike the *V. lentus* record the $\delta^{18}O$ values remain relatively positive after the isotopic shift. The resolution of De Man's (2006) data combined with the multiproxy approach may have masked any short term shifts.

6.7.3 Comparison of the palaeotemperature records obtained from the Solent Group strata

As discussed in Section 6.6.2.5 the temperatures calculated using the Bugler *et al.* (2009) palaeothermometry equation with Grimes *et al.*'s (2005) interpolated $\delta^{18}O_{water}$ values should not be used. Temperatures calculated using Grossman and Ku (1986) thermometry equation produced more realistic temperatures. However, due to uncertainties surrounding the use of Grimes *et al.*, (2005) interpolated $\delta^{18}O_{water}$ values, the temperatures calculated are unreliable. In order to calculate temperatures from the *V. lentus* $\delta^{18}O$ record a method by which the $\delta^{18}O_{water}$ can be directly determined is essential for calculating realistic temperatures. As shown in Fig. 6.13 the $\delta^{18}O_{water}$ calculated from the clumped isotope analysis is 1.2‰ more negative than Grimes *et al.* (2005), providing further support that Grimes *et al.* (2005) $\delta^{18}O_{water}$ values have been subject to evaporation.

A single clumped isotope temperature was calculated for horizon HAM S1 (lower Hamstead Member) and is compared with Grimes *et al.* (2005) and Sheldon *et al.* (2009) temperature records (Fig. 6.16). A clear difference can be seen between this temperature and that of Grimes *et al.* (2005) and Sheldon *et al.* (2009). This is partially due to Sheldon

et al. (2009) temperatures representing mean annual temperatures whereas Grimes *et al.* (2005) are summer dominated temperatures. Sheldon *et al.* (2009) calculated palaeotemperatures for the Solent Group using paleosols; their results indicate that mean annual temperature remained fairly consistent (~13°C) throughout the late Eocene to early Oligocene. Sheldon *et al.* (2009) imply that mean annual temperature changes may not be the dominant control on the climate at this time. Grimes *et al.* (2005) produced a temperature record of similar resolution which indicates several shifts in the summer dominated temperatures prior to the Oi-1 glacial maximum. Across the Oi-1 event itself both Sheldon *et al.* (2009) and Grimes *et al.* (2005) records are in agreement, indicating an insignificant temperature change.

A single clumped isotope temperature calculated from one *V. lentus* shell fragment from horizon HAM S1 (lower Hamstead Member) plots between the palaeosol and the three other datasets at 20.9°C. Although this spring / summer dominated temperature appears more realistic, this method is still in its trial stages, so a single analysis should be treated with caution. Further analyses are due to be carried out on 9 further samples (with additional repeats) through the Solent Group. Recent clumped isotope analysis on modern *Viviparus* specimens (see Chapter 4) suggests that this method of analysis is potentially applicable to fossil *Viviparus*. However, confirmation is required through extensive testing and calibration. Bearing all of this in mind, the clumped isotope temperature produced in this study does seem to correlate well with other temperature proxies from NW Europe, which produce mean annual temperatures between 15 °C and 30 °C for this time period (Mossbrugger *et al.*, 2005; Uhl *et al.*, 2007).

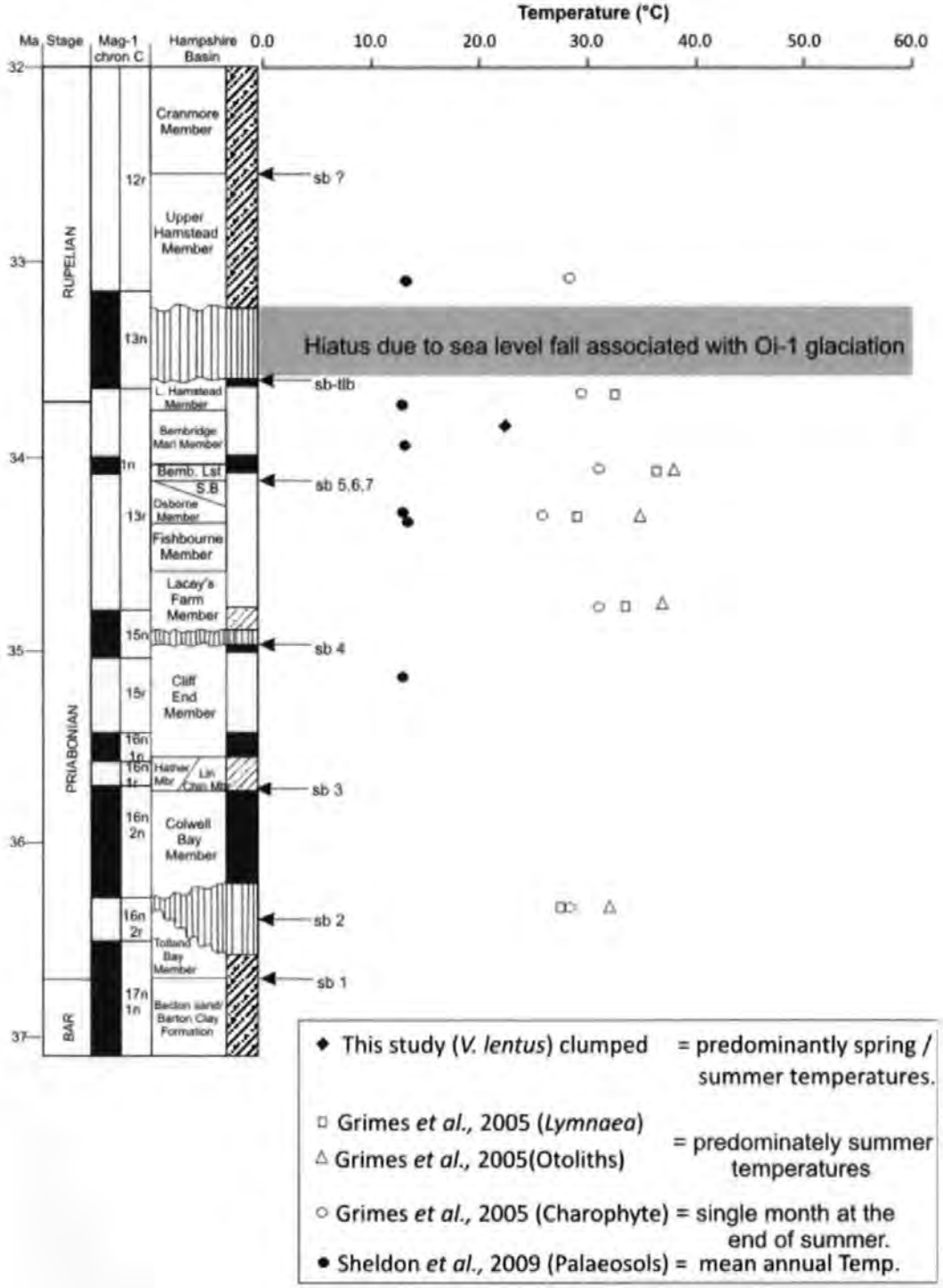

Figure 6.16 A single temperature for one horizon in the lower Hamstead Member was calculated using clumped isotope analyses and compared with the temperatures calculated by Grimes *et al.* (2005) and Sheldon *et al.* (2009).

6.7.4 Global significances of the key isotopic excursions in terms of palaeoclimatic / palaeoenvironmental events in the Solent Group strata

6.7.4.1 Late Eocene Event

Isotopic evidence from the analysis of *V. lentus* has revealed a significant and rapid shift in $\delta^{18}O_{carb.}$ between the Fishbourne Member and the base of the Bembridge Limestone Formation from –2.4 ‰ to –0.3 ‰ (a 2.1 ‰ shift). This isotopic shift coincides with the Late Eocene Event (34.2 Ma), which has been recorded in several marine records (Zachos *et al.*, 1996; Bohaty and Zachos, 2003; Coxall *et al.*, 2005). Although this excursion reaches relatively positive $\delta^{18}O_{carb}$ values the subsequent $\delta^{18}O_{carb.}$ values return rapidly to relatively negative values, similar to the shift seen in the marine record (Bohaty and Zachos, 2003; Coxall *et al.*, 2005; Katz *et al.*, 2008). Within the $\delta^{18}O_{carb.}$ records obtained from marine sediments the $\delta^{18}O_{carb.}$ values after the Oi-1 glacial maximum remain positive, gradually becoming more negative over a significantly long time period (Zachos *et al.*, 1996; Bohaty and Zachos, 2003; Coxall *et al.*, 2005). A small hiatus associated with Hooker *et al.* (2009) sequence boundaries 5, 6 and 7 occurs after the Late Eocene Event. According to Hooker *et al.* (2009) this hiatus is not significant enough to be consistent with the sea level fall associated with the Oi-1 glacial maximum.

Gale *et al.* (2006) provided sedimentological evidence (gravels and conglomerates underlying the Bembridge Limestone Formation) implying that a sequence boundary occurs within the Seagrove Bay Member and implied by the unconformity at the base of the Bembridge Limestone Formation where the Seagrove Bay Member was absent. They associate this sequence boundary (sb 5) with the largest sea level fall (minimum of 15 m) in the Solent Group succession and with magnetostratigraphical evidences that attributes this sea level fall to the Oi-1 glacial maximum specifically the Oi-1a of Zachos *et al.* (1996). Hooker *et al.* (2009) argued against this in their recalibration of the Solent Group sequence. Hooker *et al.* (2009) reinterpreted lowstand thickness in sequence 5, indicating that the extent of incision at the base of sequence 5 (Gale *et al.*, 2006) is small and does not

provide evidence for the degree of sea level fall associated with the Oi-1 glacial maximum as claimed by Gale *et al.* (2006). The *V. lentus* $\delta^{18}O$ record supports Hooker *et al.*'s (2009) interpretation that the Oi-1 glacial maximum does not occur between within the Seagrove Bay Member or at the base of the Bembridge Limestone Formation but, between the lower Hamstead Member and the upper Hamstead Member .

Comparison of the *V. lentus* high resolution $\delta^{18}O_{carb.}$ record with the lower resolution $\delta^{18}O_{carb.}$record from Grimes *et al.* (2005) confirms the existence of at least two cooling phases in the Solent Group strata. Palaeotemperatures calculated by (Grimes *et al.*, 2005) suggest that the $\delta^{18}O_{carb.}$ excursion in the Osborne Member is related to a cooling phase. The data indicate that this cooling begins in the upper part of the Fishbourne Member with the most positive $\delta^{18}O_{carb.}$ (coolest temperatures) in the organic mud between the Seagrove Bay Member and Bembridge Limestone in Whitecliff Bay (BEM S3) (Fig. 6.12 & 6.14). The $\delta^{18}O_{carb.}$ shift associated with this is more extensive than those seen in the Bembridge Marls Member and lower Hampstead Member. However, Hooker *et al.* (2004) indicated that part, if not all of the Oi-1 isotopic excursion is missing within the Hamstead Member hiatus, preventing the preservation of the most positive values (Hooker *et al.*, 2004).

Several independent freshwater proxies indicate cooling during the Osborne Member and lower and upper Hamstead Members suggesting that each proxy is recording a climatic signal. As indicated by Hooker *et al.* (2009) the warming peak in the Bembridge Limestone Formation coincides with the warming interval and shoaling of the CCD in site 1218 (Coxall *et al.*, 2005), around 34 Ma (Hooker *et al.*, 2009). Several pieces of independent evidence from Solent Group support the notion that part of the negative $\delta^{18}O$ excursion after the Late Eocene Event could be related to changes in temperature. Investigation into the evolution of the charophyte genus *Harrisichara* has revealed a sharp morphological shift between the Headon Hill Formation (Osborne Member) and the

Bembridge Limestone Formation (Sille *et al.*, 2004) (Fig. 6.17). This morphological evolution had the effect of doubling the volume of the gyrogonites. It was considered by Sille *et al.* (2004) that this change was related to a reproductive strategy concentrating more energy into fewer and larger gyrogonites. This increase in storage would be beneficial for both the establishment and persistence of the sporelings during unfavourable conditions, most likely linked to environmental stresses related to changes in temperature and seasonality (Sille *et al.*, 2004). This morphological evolution in charophytes also coincides with the first mammal faunal turnover in the Solent Group as documented by Hooker *et al.* (1995) (Fig. 6.17). A short term climatic fluctuation was thought to have brought the distinctive 'lower' and 'upper' mammalian faunas into superposition at Headon Hill (Hooker *et al.*, 1995). This first mammal faunal turnover event was much smaller than that of the second turnover known as the 'Grande Coupure', associated with the hiatus between the upper and lower Hamstead Members (Hooker *et al.*, 2004).

Mammal species richness in the Solent Group strata also appears to be a good indicator of temperature changes, as mammal diversity appears to track the temperature shifts recorded by Grimes *et al.* (2005) (Hooker *et al.*, 2009). The lowest mammal diversity is recorded in the Osborne Member (21 species) (Hooker *et al.*, 2009) and the highest within the Bembridge Limestone Formation (47 species) (Hooker *et al.*, 1995; 2004). These shifts in mammal diversity correspond well with the shift to cooler temperatures associated with the Late Eocene Event and the warm interval in the Bembridge Limestone Formation (Fig. 6.17).

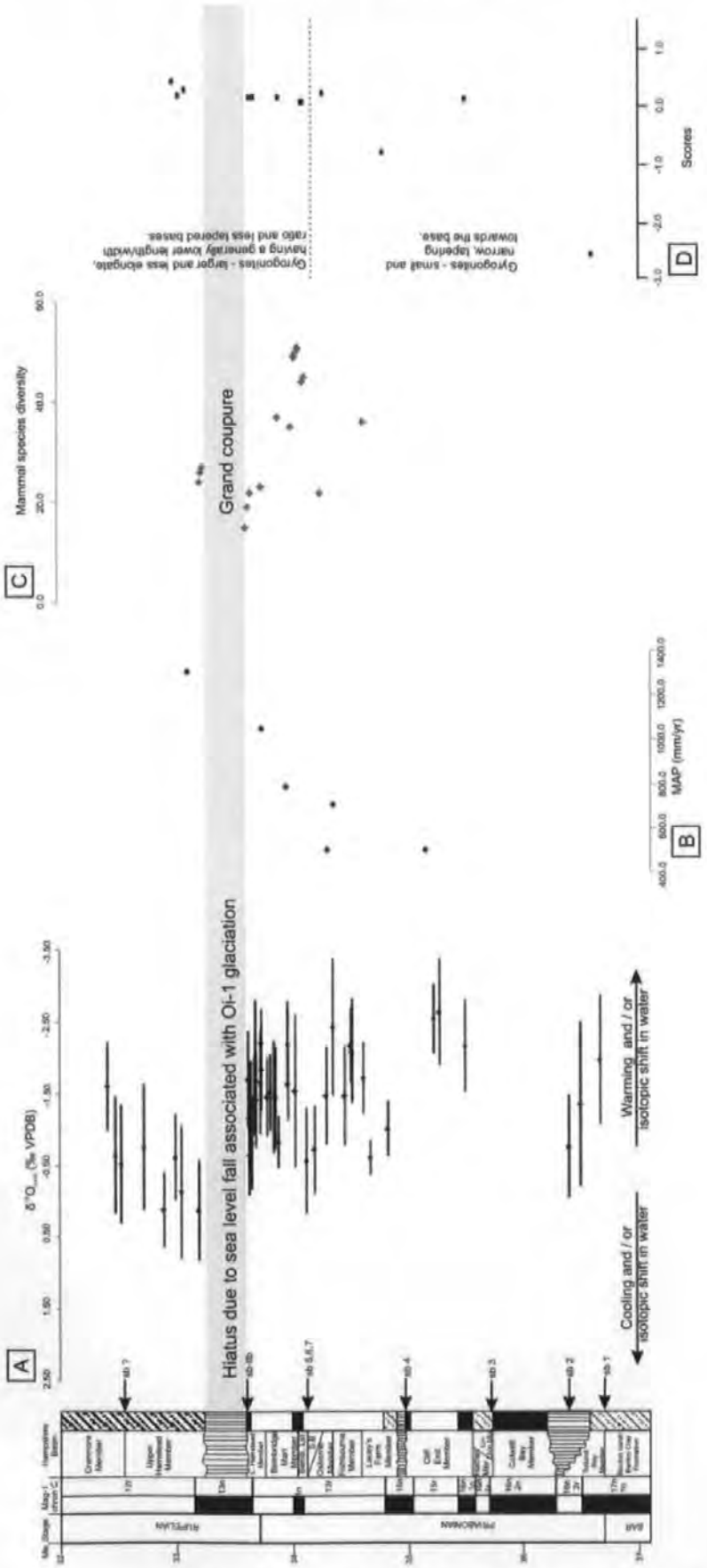

Figure 6.17 A. high resolution $\delta^{18}O$ record from the analysis of *V. lentus* fragments. B. Mean annual precipitation (MAP) in mm/year taken from Sheldon *et al.* (2009). C. Mammal species diversity taken from Hooker *et al.* (1995) and Hooker *et al.* (2004). D. Correspondence analysis of charophyte floras showing changes through time along the first correspondence axis from Sille *et al.* (2004).

After the Grande Coupure within the upper Hamstead Member, 29 species are recorded (Hooker *et al.*, 2004; 2009) (Fig. 6.17). Collinson *et al.* (1993) noted that the flora of the Bembridge Limestone Formation is a short lived distinctive flora possibly reflecting fluctuations in temperature prior to the E/O boundary. Overall, vegetation shifted from a diverse forest of tropical aspect in the middle Eocene, to an environment dominated by swamps and marshes with patches of woodland of a partly tropical aspect by the Late Eocene (Collinson, 1992). These vegetational changes occurred prior to the E/O transition and Oi-1 glaciation suggesting that climate change was already in progress. The *V. lentus* isotopic results provide further support that aquatic and terrestrial biotas were being affected by climate change in the form of temperature fluctuations prior to the E/O boundary and Oi-1 glaciation.

The Late Eocene Event has been recognised in several marine isotopic records, although few suggest its cause. Katz *et al.* (2008) suggest that the entire isotopic signal for the Late Eocene Event is solely related to changes in ice volume. Their hypothesis was based on the presence of a hiatus at Saint Stephen's Quarry, Alabama (Miller *et al.*, 2008) and the lack of significant change in the Mg/Ca temperatures calculated by Lear *et al.* (2004) from the ODP core 1218. However, these Mg/Ca records may have provided a misleading temperature record because of a deepening of the calcite compensation depth (Coxall *et al.*, 2005) which, may have caused changes in carbonate ion activity masking the cooling in Mg/Ca records (Lear *et al.*, 2004). High resolution pCO_2 records (Pearson *et al.*, 2009) suggest that levels did not decrease below the Antarctic threshold (~750 p.p.m.v. Deconto and Pollard, 2003; Deconto *et al.*, 2008) until the Oi-1 glaciation when continental scale glaciation took place (Fig. 6.18).

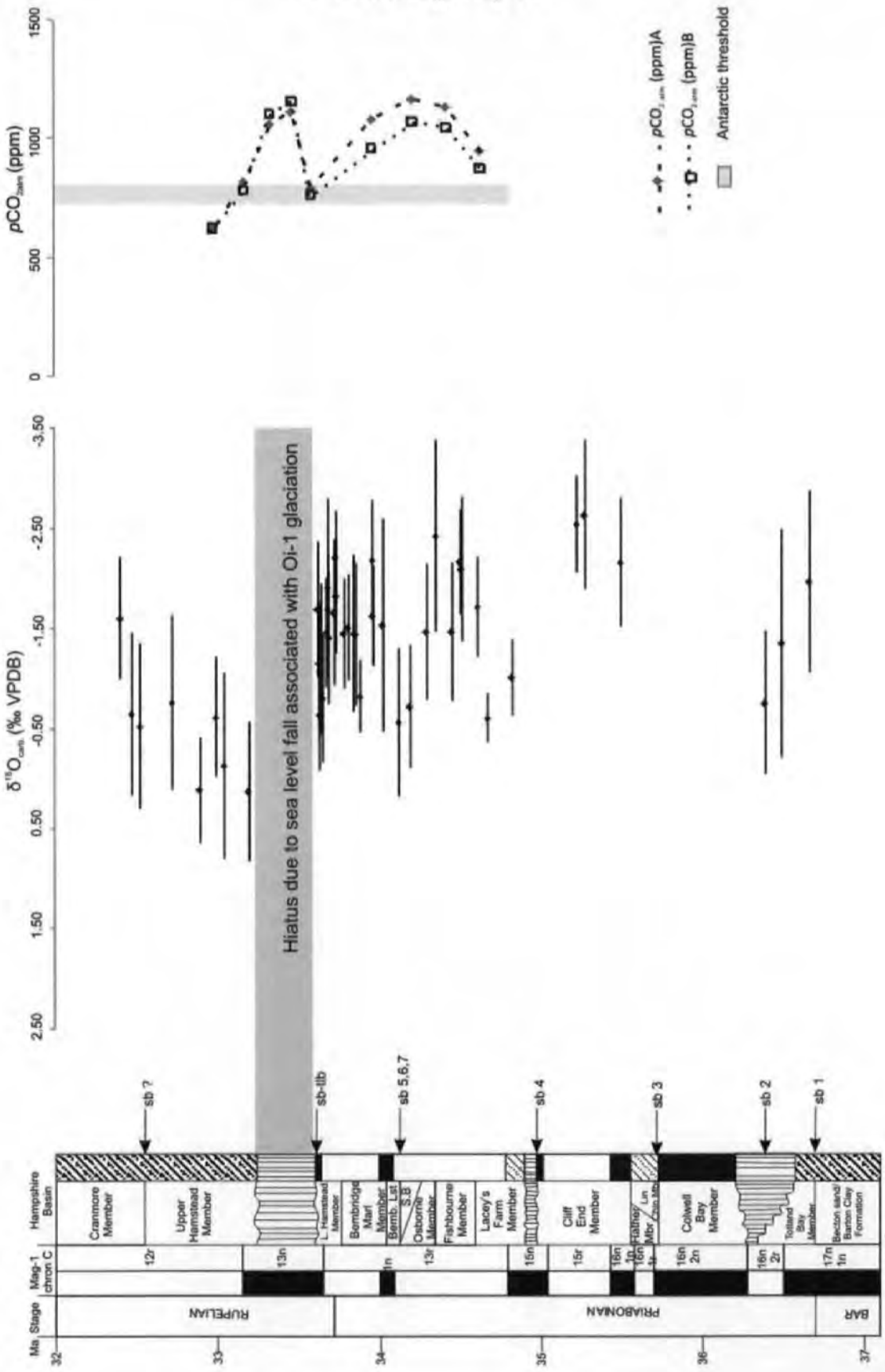

Figure 6.18 Pearson *et al.* (2009) high resolution pCO_2 record is compared with the *V. lentus* $\delta^{18}O$ record.

Changes in regional oceanic palaeogeography could be considered as a potential cause for the positive $\delta^{18}O_{water}$ shift and associated cooling that initiates at ~34.6 Ma in the Fishbourne Member. Allen and Armstrong (2008) suggest that the Arabia–Eurasia collision and the closure of the Tethys ocean gateway began in the late Eocene at ~35 Ma, up to 25 million years earlier than in many reconstructions. Boulton's (2009) research has also shown that the initial continental collision occurred after the Lutetian (40.4 Ma) and before the Aquitanian (23.03 Ma) supporting the hypothesis that the southern Neotethys Ocean may have closed during the late Eocene to Oligocene. However, she does not suggest a specific date. There is some debate on the actual timing of the closure (e.g. Allen, 2009; Bea *et al.*, 2009) with suggestions that a synchronous collision throughout all of south Asia cannot reasonably be expected (Bea *et al.*, 2009). As a consequence of this the implication for Cenozoic cooling has yet to be fully established.

If the suggestion by Allen and Armstrong (2008) that global cooling was forced by processes associated with the initial collision of Arabia–Eurasia (e.g. reduction in atmospheric CO_2) is correct, this could have significant consequences for the interpretation of the Late Eocene Event. One of the stated processes leading to this cooling, a shift towards modern patterns of ocean currents, may have had a significant effect on the $\delta^{18}O$ composition of local precipitation on the IOW and in turn on the $\delta^{18}O$ of *V. lentus* shell carbonate. Evidence which may support this theory is taken from Sheldon *et al.* (2009), their results suggesting that mean annual precipitation increased after the Bembridge Limestone Formation (Fig. 6.17). Figure 6.19 presents the palaeogeographic and oceanographic reconstruction taken from Allen and Armstrong (2008). They show that during the Eocene a westerly transport of warm Indian Ocean water enters the Atlantic via the Tethys Ocean. By the Early Oligocene the connection between the Indian and Atlantic Oceans is impeded by the Arabian – Eurasian collision zone causing this warm water transport to cease. This alteration in ocean circulation led to the initiation of North Atlantic

Deep Water formation which became a major influence on the climate of North Western Europe.

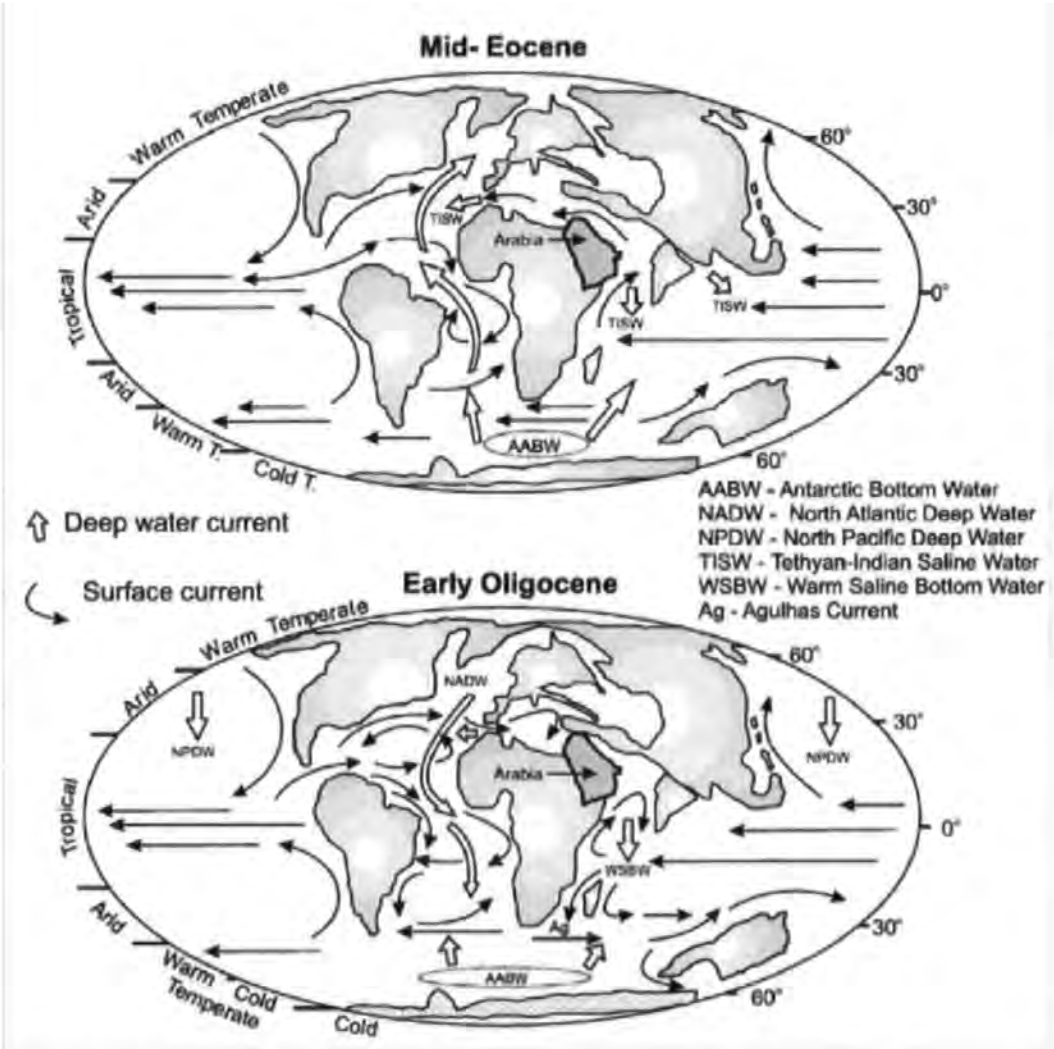

Figure 6.19 Palaeogeographic and oceanographic reconstructions before and after the demise of the Tethys Ocean gateway. (A) Eocene Epoch, with westerly transport of warm Indian Ocean water into the Atlantic via Tethys. (B) Oligocene, with connection between the Indian and Atlantic oceans impeded by the Arabia–Eurasia collision zone. Ocean currents derived from Bush (1997), Diekmann *et al.* (2004), Kennett and Barker (1990), Stille *et al.* (1996), Thomas *et al.* (2003), Via and Thomas (2006), von der Heydt and Dijkstra (2006). Figure taken from Allen and Armstrong (2008).

6.7.4.2 Eocene / Oligocene boundary

Placement of the E/O boundary is currently based on the local extinction of the tropical planktonic foraminiferal family Hantkeninidae. Van Mourik and Brinkhuis (2005) have challenged the use of Hantkeninidae as the E/O boundary marker, as the extinction of *Hantkenina* and its relatives is considered to be diachronous in nature, representing an

isolated event that may not be suitable for global correlation. Also the *Hantkenina* extinction event does not correlate with the most negative part of the $\delta^{18}O$ excursion associated with the Oi-1 glacial maximum (e.g. Brinkhuis and Visscher, 1995; Zachos *et al.*, 2001). Recently, Pearson *et al.* (2008) successfully correlated the *Hantkenina* extinction event with their Tanzanian $\delta^{18}O$ record, showing that the extinction takes place between the precursor event and the Oi-1 glacial maximum. If correct, the *V. lentus* isotopic record would place the E/O boundary within the Solent Group succession to ~33.74 Ma, coinciding with the distinctive Black Band marking the boundary between the Bembridge Marls Member and the lower Hamstead Member. The Black Band was deposited during a period when subsidence was slow, insignificant or when sea level rise was equal to subsidence, allowing a prolonged period of very slow sedimentation (Collinson, 1992) and build up of organic material.

6.7.4.3 E/O transition and Oi-1 glacial maximum

The *V. lentus* $\delta^{18}O_{carb.}$ profile indicates a two step shift(represented by the 2nd and 3rd isotopic shift in Fig 6.14) into the Oi-1 glacial maximum. However, as previously discussed these shifts are significantly smaller than the Late Eocene Event in the Osborne Member. As part of the $\delta^{18}O_{carb.}$ record is considered to be missing owing to the Hamstead Member hiatus, it is possible that the most positive values associated with the Oi-1 glacial maximum are also missing in a ~350 k.y hiatus relating to the sea level fall associated with continental scale ice formation on Antarctica. If we assume that the third $\delta^{18}O$ shift is related to the Oi-1 glacial maximum, which is partially missing, then the prior isotopic shift within the Bembridge Marls Member could be that of the precursor or Step 1 of Coxall *et al.* (2005); Pearson *et al.* (2008) and Lear *et al.* (2008). Nevertheless the *V. lentus*

$\delta^{18}O$ record confirms the placing of the Oi-1 glacial maximum within the Hamstead Member hiatus, as suggested by Hooker *et al.* (2004; 2009) and Grimes *et al.* (2005) and indicates a direct link to the Grande Coupure. The high resolution pCO_2 record recently produced by Pearson *et al.* (2009) confirms the central role that pCO_2 played in the development of the Antarctic ice sheet, with the lowest levels coinciding with the hiatus between the lower and upper Hamstead Members.

Evidence for climate change prior to the Oi-1 glacial maximum and associated hiatus can be seen in several biotic proxies. Both vegetation and mammal assemblages show a distinctive change, from the underlying Bembridge Limestone and Bembridge Marls Member to the overlying Black Band and lower Hamstead Member (Hooker *et al.*, 2004). The Black Band appears to be a distinctive boundary after which warm loving palms and ferns (*Acrostichum*) disappear (Collinson, 1983; 2001) with the introduction of conifer pollen (*Inaperturopollenites magnus*) (Collinson, 1983). From the Bembridge Marl Member / lower Hamstead Member boundary (Black Band) upwards most of the new forms of vegetation have northern temperate affinities (Pallot, 1961). This change could be related to a local shift in the nature of vegetation proximal to the depositional environment or reflect climate cooling, or both (Hooker *et al.*, 2004). Elsewhere, Chateauneuf (1980) showed a dramatic fall in diversity of pollen taxa but an increase in conifer pollen (especially Bisaccate Pinaceae) in the Paris Basin, and related this to the changes associated with climatic cooling. However, in southern England few warm loving plants remained in the Bembridge Limestone Formation and younger floras (Cleal *et al.*, 2001). This was due to changing vegetation throughout the Eocene in response to long-term climatic cooling. It has therefore been suggested that climate change might be poorly expressed by fossil floras, where most of the warm loving plant elements have already

been eliminated (Hooker *et al.*, 2004), for example during the Late Eocene Event. The *V. lentus* $\delta^{18}O_{carb.}$ record and Grimes *et al.* (2005) palaeotemperatures indicate a cooling phase during the Bembridge Marls Member, which may be responsible for the final elimination of warm loving plants. Drier conditions have also been considered as a possible explanation for the subtle differences between the Bembridge Marls Member and the Bembridge Limestone Formation floras (Collinson, 1983). However, palaeosol formation suggests a long-term shift to wetter conditions (sub-humid to humid) (Fig. 6.17) with no significant cooling (Sheldon *et al.*, 2009).

The precursor event within the Bembridge Marls Member, immediately preceding the Grande Coupure, has been associated with a smaller mammal turnover, involving European mammals only (Hooker *et al.* 2004), coinciding with the already discussed vegetation changes. Near the top of the lower Hamstead Member three out of the four rodents that appear have teeth that show extra or stronger cresting than those of nearest relatives in the Bembridge Marls Member (Stehlin and Schaub, 1951; Bosma and de Bruijn, 1979; Vianey-Liaud, 1994). Hooker *et al.* (2004) suggest that this represents a slightly coarser diet perhaps brought about by the seasonal scarcity of food or occupation of habitats with different vegetation. Mammalian ecological diversity of Europe in the Late Eocene is indicative of drier more open habitats in southern France than in southern England (Franzenj, 1968; Hooker, 1992). Northward dispersal of certain mammalian taxa suggests northward expansion of such habitats (Hooker *et al.*, 1995). Drier conditions prior to the Oi-1 glaciation and post the Late Eocene Event could be related to the closure of the Tethys ocean gateway, thus terminating water exchange between the Indian and Atlantic oceans. This closure may have influenced moisture transport across Western Europe. This decrease in warm moist air may be responsible for the appearance of sclerophyllous

vegetation in SW Europe (Collinson and Hooker, 2003). A few sclerophyllous (e.g. *Palibinia* (Bembridge Limestone Formation and the Bembridge Marls Member) and *Zizyphus zizyphoides (*Bembridge Marls Insect limestone flora) have been recorded in the Solent Group (Collinson and Hooker, 2003).

Sheldon *et al.* (2009) interpreted the Solent Group palaeosols deposited following the Oi-1 glacial maximum as forming in wetter conditions. This suggested that the distribution of water masses and their proximity to orographic impedances may play a key role in local palaeoclimatic response to global events. They also noted that during the E/O transition differences between Oregon (drying) and the IOW (wetting) indicated a substantial reorganisation of the global hydrological cycle (Robert and Kennet, 1977; Wolfe, 1995). The ocean currents in Figure 6.19, derived by Allen and Armstrong (2008), indicate a change in the direction of oceanic currents in the Atlantic Ocean during the E/O transition. During the Eocene, the Atlantic Ocean currents are predominantly flowing south to north, whereas in the early Oligocene they have switched to the present day circulation of north to south. It is likely that the widening of the North Atlantic initiated the formation of North Atlantic Deep Water at ~35 Ma (Wold, 1994; Zachos *et al.*, 2001; Via and Thomas, 2006). However, Eldrett *et al.* (2009) have suggested that a 5°C cooling in cold month (winter) mean temperature may have increased deep convection and been responsible for the apparent initiation of Northern Component Water formation initiating at ~38Ma, two million years earlier than other records suggest.

An important connection of the Tethys with the polar sea existed during the Eocene via the Turgai Strait, on the far side of the Ural Mountains. This seaway around Asia and the connection with the Polar Sea enabled warm water exchanges and potentially explains the sustained warm climate during the Late Eocene (Rögl, 1999). However, tectonic closure of the Tethys ocean gateway and major sea level fall associated with the Oi-1 glacial

maximum led to the closure of the Turgai Strait, isolating the Tethys Ocean to a single connection with the North Atlantic. This change could be responsible for the changes in $\delta^{18}O_{water}$ of precipitation, by shifting the source region from predominantly the Tethys to the Atlantic Ocean. To determine whether changes in precipitation sources are a key factor in the $\delta^{18}O_{carb.}$ shifts recorded by *V. lentus*, requires a method by which the temperature and $\delta^{18}O_{water}$ signal can be directly deconvoluted. This could potentially be achieved through clumped isotope analysis, as discussed in Chapter 4.

Daley (1972b) referring to Brooks (1949) and Lamb (1961) has previously suggested that changes in ocean and atmospheric circulations may be linked to the observed changes that are seen in the Solent Group succession. He suggested that this region would normally have been dry under Mediterranean climatic conditions; however the northerly extension of the trade winds carried moisture from the Tethys to Western Europe during the Eocene as indicated by Rögl (1999). This wind regime had a greater influence on summer conditions, as the wind belts moved north producing rain all year round and in combination with high temperatures a semitropical to tropical climate (Daley, 1992). Stable isotope analysis of planktonic foraminifera obtained from North Sea wells have been used to infer any paleohydrological and biogeographical changes through the Eocene to Oligocene (Boersma, 1987). These data suggest a warm and equable circulation pattern during the Early Eocene. By the Middle Eocene deep water cooling initiates with a reduced heat transport by the latest Middle Eocene. Bottom water cooling and a diminished latitudinal thermal gradient takes place across the E/O transition into the Early Oligocene. This adds weight to the argument that parts of the *Viviaprus* $\delta^{18}O$ in this study and temperature changes observed in Grimes *et al.* (2005) could be related to closure of oceanic gateways,

in turn influencing regional ocean and atmospheric circulations, particularly in terms of heat and moisture transportation.

6.7.4.4 Regional temperature comparison of terrestrial temperature changes across the E/O transition and Oi-1 glacial maximum.

Lower resolution terrestrial temperature records only allow a comparison with the overall temperature shift across the E/O transition and Oi-1 glaciation, rather than the detailed comparison achievable in the marine realm. The Grimes *et al.* (2005) temperature record obtained from the charophyte proxy indicates that there was no significant temperature change across the E/O transition. However, modern charophyte calcification of their gyrogonites happens on a timescale of weeks usually towards the end of the summer, therefore the isotopic data represents a snapshot of the environmental conditions at the time of calcification. Furthermore the timing of calcification may itself be variable depending on environment and temperature; it is a major unknown that currently hinders interpretation of isotopic data (Andrews *et al.* 2004). Sheldon *et al.* (2009) using temperatures calculated from palaeosols from the IOW, also indicated that temperatures remained constant across the E/O transition and Oi-1 glaciation, with mean annual temperature ranging from 12 to 14°C. However, this may be a consequence of the low resolution of their data (Fig. 6.16). Uhl *et al.* (2007) used leaf floras from central Europe to calculate palaeotemperatures through Leaf Margin Analysis (LMA) and climate leaf analysis multivariate program (CLAMP). Estimates of mean annual temperature produced from their study range from 18.7°C to 29.0°C in the late Eocene and 12.5°C to 18.0°C in the early Oligocene, indicating a ~8.6°C decrease in mean annual temperature. Mean annual temperatures produced through the compilation of palaeobotanical data are also presented in Betchtel *et al.* (2008, fig. 7). Temperatures calculated by Betchtel *et al.* (2008) show a decrease from 20 °C in the late Eocene to 15 °C in the early Oligocene. These

calculated palaeotemperatures indicate a maximum decrease of 8 °C across the E/O transition, which is similar to Zanazzi *et al.* (2007).

6.7.5.5 Biotic turnover / extinction events, Oi-1 glaciation and sea level fall

Stehlin (1910) observed a striking change in the European fauna when passing from Eocene to Oligocene strata. He termed this event the 'Grande Coupure', marking a sudden change from the endemic European faunas to ones with major components of Asian origin (e.g. Heissig, 1987; Remy *et al.*, 1987; Hooker, 1987, 1992). Opinions as to the causes of this faunal turnover tend to be polarized between climatic deterioration at the beginning of the Oligocene (e.g. Legendre, 1989) and competition following dispersal into Europe of taxa from Asia (e.g. Hooker, 1989). Within the Solent Group strata the Grande Coupure occurs within the hiatus between the lower and upper Hamstead Members (Fig. 6.18).

Current research suggests that two physical changes are responsible for this turnover event:

- Climate change; and
- Formation of land bridges.

Climate change is thought to be a key forcing mechanism for global biotic change. Long-term cooling and associated climate change led to the long-term decline of mammalian faunas in North America (Prothero and Heaton, 1996) and a rapid turnover of mammals on the Mongolian plateau (Meng and McKenna, 1998). The rapid change in mammal faunas in Europe known as the 'Grande Coupure' is thought to be related to climate fluctuations associated with the Oi-1 glacial maximum and formation of land bridges. The impact of this climatic event was more greatly felt on the European continent than on the North American and Asian continents (Prothero, 1994; Hooker, 2000). European terrestrial records show that a major eustatic sea level fall is related to the Oi-1 glacial maximum (Gély and Lorenz, 1991; Steubaut, 1992; Hooker *et al.*, 2004). For a large part of the

Eocene, Europe was an archipelago of larger and small islands (Auge and Smith, 2009). The absence of land bridges between landmasses prevented or inhibited geographical range extensions and caused widespread endemism (Auge and Smith, 2009). Dispersal of new mammal faunas from Asia was facilitated by this sea level fall through migration along the newly formed land bridges. Vianey-Liaud (1976) suggested that the closure of the Turgai Strait enabled the migration of Asian taxa into Europe, stimulating competition between endemic European faunas and incoming Asian faunas, leading to a faunal turnover event. However, Heissig (1979) showed that crossing the Turgai Strait would not have helped the mammals reach the main European island because their passage would have been blocked by the Polish seaway. They probably came up through the Balkan islands, which became linked to the main European island by sea level fall and Alpine tectonics (J.J Hooker, Pers. comm.). These new faunas included more advanced types of mammalian carnivores (Auge and Smith, 2009). Hiatus bridging faunas from elsewhere in Europe record mainly post-Grande Coupure taxa, suggesting that the turnover occurred early in the hiatus (Hooker *et al.*, 2004). From this, Hooker *et al.* (2009) determined that the most positive $\delta^{18}O$ values associated with the Oi-1 isotopic shift are most likely to be at the beginning of this hiatus. This is consistent with the $\delta^{18}O$ isotopic excursion at the top of the lower Hamstead Member and provides further indication that this event could potentially be the initial part of the $\delta^{18}O$ excursion relating to the Oi-1 glacial maximum. Steady climate conditions across the Oi-1 glaciation reconstructed by Grimes *et al.* (2005) and Sheldon *et al.* (2009) imply that climate had little impact. Joomun *et al.* (2008) have hypothesised that changing food availability is an important factor in mammalian extinctions across the E/O transition and are currently investigating this further. Seasonality may also be key to these climatic and temperature changes, invoking subtle vegetation changes. A potential decrease in summer temperatures reducing the temperature range (seasonality) and MAT are recorded across this event (See Chapter 7). The calculated $\delta^{18}O_{water}$ values and lack of other biotic

(vegetation, charophytes etc) evidence from the IOW deposits indicates that the majority of the $\delta^{18}O_{carb.}$ shift (1.9‰) across this event may be related to ice volume changes and / or isotopic shifts in precipitation. For example, the charophyte genus *Harrisichara* does not show any evolutionary changes across the 'Grande Coupure' / Oi-1 glacial maximum, but does over the Late Eocene Warming Event indicating that any temperature changes associated with the Oi-1 were potentially small in comparison to the earlier event. However, mammal species richness does show evidence of a temperature decrease across the Oi-1 glacial maximum (Hooker *et al.*, 2004) (Fig. 6.17).

6.8 Summary

The high resolution continental $\delta^{18}O$ record covering the E/O transition and Oi-1 glaciation provides the first opportunity for a detailed comparison with global marine records. This comparison shows that the $\delta^{18}O_{carb.}$ profile produced from the analysis of the freshwater gastropod *V. lentus* records similar isotopic shifts to those seen in both deep and shallow marine records. Overall, this investigation confirms that long-term cooling was punctuated by rapid climatic change (cooling and warming episodes) that culminates in the crossing of a threshold into a new climate regime. The similarity of the $\delta^{18}O$ records, in particular the shifts relating to the E/O transition and Oi-1 glacial maximum, suggest the possibility that there is a coupling of continental and marine environments via atmosphere and ocean circulations. Evidence from this investigation and Donder *et al.* (2009) appear to suggest that coastal continental environments are more sensitive to changes in sea surface temperatures than intercontinental areas. Europe may also be more 'sensitive' to these changes as during a large part of the Eocene Europe was an archipelago of large and small islands. The evidence also suggests that this connection may alter through time because of changes in palaeogeography of the oceans, particularly regional effects from the isolation

of the Tethys Ocean. The new record from the Eocene / Oligocene and those from the Miocene suggest that this terrestrial and marine coupling survived the Oi-1 glacial maximum and consequent shift into a new climatic regime.

The findings of this investigation also suggest that changes in continental climate are synchronous with the turnover of the mammalian fauna and diversity fall during the Oi-1 glaciation. Short lived climatic change prior to the E/O transition and Oi-1 glacial maximum may have preconditioned the biota prior to crossing of a threshold into a new climatic regime. The results provided further support that aquatic and terrestrial biota were being affected by climate change associated with the Late Eocene Event, the decrease in mammal species richness in the Osborne Member, which seems to be related to the Late Eocene Event, reaches its climax at the end of the Osborne / Seagrove Bay Members. This event is followed by brief warming in the Bembridge Limestone which was marked by a within-Europe mammal turnover involving dispersal from the south and an increase in species richness, concurrent with this is an increase in size of *Harrisichara* gyrogonites. The biotic events and negative isotopic shifts in the Bembridge Limestone Formation coincides with the shoaling of the CCD in ODP 1218 (Coxall *et al.*, 2005).

CHAPTER 7 SEASONAL ISOTOPIC VARIABILITY IN THE FOSSIL RECORD

7.1 Introduction

There is strong evidence that extremes in seasonality are responsible for abrupt changes in both modern and past climates (e.g. Wolfe, 1978, 1994; Ivany *et al.*, 2000; Kobashi *et al.*, 2001; Denton *et al.*, 2005; Mosbrugger *et al.*, 2005; Fluckiger *et al.*, 2008; Bernard *et al.*, 2009; Eldrett *et al.*, 2009; Pross *et al.*, 2009). Since the initial formation of permanent ice on Antarctica at the E/O transition and Oi-1 glaciation, seasonality has been a key factor in switching between interglacial to glacial conditions during the Quaternary (Denton *et al.*, 2005). Many of these glacial events have been attributed to cooling of cold monthly mean (winter) temperatures with warm monthly mean (summer) temperatures remaining relatively constant, leading to an overall increase in seasonality (for example see Pross *et al.*, 2009; Bernard *et al.*, 2009; Fluckiger *et al.*, 2008). Evidence provided by Denton *et al.* (2005) suggests that seasonality switches controlled by cooling in the cold monthly mean were responsible for abrupt climate changes in the North Atlantic region during the Pleistocene late glacial maximum. Winter climate crossed the extreme winter threshold repeatedly, with marked changes in seasonality that may well have amplified and propagated a signal of abrupt change throughout the northern hemisphere and into the tropics (Denton *et al.*, 2005). These cooler extremes in winter temperatures may have been assisted by an extended duration of the cold monthly mean period, leading to shorter summers and / or growing season (Vandergoes *et al.*, 2008). Fraile *et al.* (2009) have suggested that the timing of this 'growing season', or as in their study, the timing of planktonic foraminiferal production may have occurred at a different time of the year when compared with modern examples. The maximum shift in seasonality was modelled as up to

6 months, questioning the assumption of a 'stable' seasonality through time. It was suggested by Frail *et al.* (2009) that this may lead to bias in estimates of palaeotemperatures calculated across such glacial events.

For many species the primary impact of climate change and changes in seasonality may be mediated through effects on synchrony with that particular species' food and habitat resources (Parmesan, 2006). This can be seen when the coordination in timing between the life cycles of predators and their prey, herbivorous insects and their host plants, parasitoids and their host insects, and insect pollinators with flowering plants are disrupted (Harrington *et al.*, 1999; Visser & Both, 2005). These types of disruption may be responsible for the biotic turnover events, which coincide with significant climatic changes in the geological record.

7.2 Aims and objectives

In conjunction with the high resolution *Viviparus lentus* (*V. lentus*) $\delta^{18}O$ and $\delta^{13}C$ record produced from the analysis of *V. lentus* fragments across the E/O transition and Oi-1 glacial maximum (see Part 2, Chapter 6), an investigation into seasonal changes in $\delta^{18}O$ and $\delta^{13}C$ was carried out. The main aim of this investigation was to determine whether seasonality was a key factor influencing the observed climate changes associated with the E/O transition and Oi-1 glaciation; particularly whether seasonal changes in the temperature or $\delta^{18}O_{water}$ were responsible for the changes observed in the high resolution *V. lentus* $\delta^{18}O$ record in Chapter 6. To determine this, the following objectives were met:

- To produce high resolution $\delta^{18}O$ and $\delta^{13}C$ seasonality profiles from several horizons containing three or more whole, well preserved *V. lentus* specimens from key horizons through the Solent Group (within preservational constraints);

- From these profiles, the change in range between minimum and maximum $\delta^{18}O$ and $\delta^{13}C$ values were determined for each horizon analysed;
- To link any observed changes in seasonality with isotopic excursions in the *V. lentus* record in Chapter 6;
- The role of carbon across this time period and the ability of *V. lentus* as a record of these changes; and
- To relate any observed changes in seasonality with biotic extinctions or turnover events.

7.2.1 Seasonality, the E/O transition and Oi-1 glacial maximum

Numerous publications (e.g. Wolfe, 1978, 1994; Ivany *et al.*, 2000; Kobashi *et al.*, 2001; Mosbrugger *et al.*, 2005; Eldrett *et al.*, 2009) have attributed the observed decrease in mean annual temperature (MAT) occurring at the E/O transition to changes in seasonality. The majority of investigations suggest that the decline in MAT was brought about by a decrease in the cold monthly mean (CMM) temperature (e.g. Wolfe, 1978, 1994; Ivany *et al.*, 2000; Kobashi *et al.*, 2001; Mosbrugger *et al.*, 2005; Eldrett *et al.*, 2009) as seen in later glacial events (for example Denton *et al.*, 2005). Sedimentary cores from the Pacific Ocean were the first to show a distinctive stepwise pattern in their $\delta^{18}O$ record across the E/O transition and Oi-1 glacial maximum, with two shifts taking place in 40 kyr long steps (Coxall *et al.*, 2005). These step changes occurred after an interval of low eccentricity and low-amplitude change in obliquity which, is considered by Deconto and Pollard (2003) to favour dampened seasonality. This dampened seasonality is thought to have brought about a prolonged absence of warm summers, inhibiting summer snow melt, and not the occurrence of cooler winters favouring ice accumulation (Coxall *et al.*, 2005). Contradictory evidence from the Gulf Coast (Ivany *et al.*, 2000) and Mississippi

embayment (Kobashi *et al.*, 2001) indicate that winter temperatures became 4 to 5 °C cooler across this time period. Coxall *et al.* (2005) defended their interpretation by suggesting that the lack of otolith data from the transition interval of Ivany *et al.* (2000) reflects the effect of the Oi-1, where their data document its cause.

Seasonality trends in the North Sea Basin show that in the earliest Oligocene, before the hiatus associated with the Oi-1 glacial maximum, an 8 °C difference between summer and winter values indicates a high degree of seasonality (De Man, 2006). By the late Oligocene the seasonal range decreased significantly from 3.5 °C, prior to the Oi-1, to 1.5 °C, post the Oi-1 (De Man, 2006). This decrease in seasonality is attributed to changes in the climate regime associated with the Oi-1 glacial maximum. The seasonality data from the US Gulf Coastal Plain (Ivany *et al.*, 2000) and the North Sea Basin (De Man, 2006) differ significantly. Although the calculated winter temperatures are similar in both basins (11.8°C in De Man, (2006) versus 11-12°C in Kobashi *et al.* (2001) and Ivany *et al.* (2003)), summer temperatures stay much higher in the Gulf Coastal Plain than in the North Sea Basin (20.5 to 21.2°C versus15.4°C) (De Man, 2006). The differences between the two basins are thought to be related to the impact of the Gulf Stream. De Man (2006) refer to the Paleogene models produced by Huber *et al.* (2003), which demonstrate that sea water temperatures along the Gulf coast were determined by the interplay between the vigorous Gulf Stream, transporting warm salty water north and east and the subpolar gyre which transports cooler and fresher water southwards along the North East coast of the USA. Therefore, these regional differences are attributed to the positioning of oceanic currents.

Evidence obtained from terrestrial deposits confirms the cooling in CMM temperatures. Wolfe (1978; 1994) recorded a decline of 13°C over 1 Ma on the North American continent, brought about by a decrease in CMM temperatures, with minimal change in the

Warm Monthly Mean (WMM). This increased the MAT range from 5 to 25 °C (Wolfe, 1978). However, Zanazzi *et al.* (2007) suggested only a minor increase in seasonality from the isotopic analysis of fossil tooth enamel and bone from continental North America. Mosbrugger *et al.* (2005) showed that continental temperature records from central Europe indicate a decrease in CMM of 20 °C from the Eocene to the Pliocene. The divergence between the CMM and the WMM indicates an increase in seasonality. A recent investigation into high latitude terrestrial climatic change during the Eocene and Oligocene, using terrestrial spore and pollen assemblages preserved in marine sediments from the Norwegian–Greenland Sea, suggest a cooling in the CMM, with WMM temperature remaining stable, producing an increase in seasonality (Eldrett *et al.*, 2009). However, this change in seasonality occurs prior to the climatic changes observed at the E/O transition and Oi-1 glaciation. Overall, the majority of the evidence from terrestrial and marine records suggests a dampening in seasonality prior to the Oi-1 glacial maximum, after which seasonality increased.

7.2.2 Isotopic variability of carbon, the E/O transition and Oi-1 glacial maximum

A small, sharp, positive carbon isotopic excursion (~0.8‰) associated with the Oi-1 glaciation is shown by Zachos *et al.* (2001, see figure 2) to be one of three major perturbations in the global carbon cycle during the Cenozoic. These excursions had a widespread and lasting impact on the biosphere through biogeochemical feedbacks in the carbon cycle. The excursion associated with the Oi-1 glacial maximum was short lived, owing to other coupled biogeochemical processes gradually restoring the system to equilibrium (Zachos *et al.*, 2001). The cause of this isotopic excursion has been linked to shifts in the storage of carbon. Alteration in atmospheric CO_2 is thought to have played a

critical role in the history of climate change throughout the Cenozoic. It has been a long standing view that pCO_2 concentrations and associated thresholds are key in understanding the continental scale glaciations associated with the Oi-1 glaciation.

Estimates of atmospheric pCO_2 concentrations from continental deposits in Germany have been calculated from the analysis of stomatal parameters of fossil leaves (Roth-Nebelsick *et al.*, 2004). These parameters indicate that pCO_2 concentrations were higher in the late Eocene, decreasing during the early Oligocene, with a trend reversal to increased levels towards the late Oligocene. Retallack (2002) used stomatal data of *Ginkgo* from North America to suggest a decrease in pCO_2 levels at the E/O boundary. Retallack (2001) compiled a large dataset on stomatal indices producing an atmospheric CO_2 record for the past 300 Ma. This record indicates a long-term decline in CO_2 concentration from ~50 Ma to the present. It has been suggested that the spread of grasses and grazers during the E/O transition created more rapidly weathered soils of greater carbon storage capacity, sediments of higher carbon content and ecosystems with higher albedo and lower transpiration than pre-existing woodlands (Retallack, 2001).

Further indication that pCO_2 has influenced the build up of ice on Antarctica comes from the Deconto and Pollard (2003) and Deconto *et al.* (2008) models. They modelled the threshold response of long-term Cenozoic decline in atmospheric pCO_2 levels and idealised orbital forcing. In their model output the decline in atmospheric pCO_2 levels caused the initiation of ice-sheet height and mass balance feedbacks, causing the ice sheets to expand rapidly pulsating in size with orbital variations (particularly the 41 kyr obliquity and 110kyr and 405 kyr eccentricity cycles). Antarctic ice sheets grew rapidly once CO_2 reached critical threshold values of 2.8 to 2.6 times 'pre-industrial' atmospheric levels (750 p.p.m.v) (Deconto *et al.*, 2008), causing the coalescence of individual ice caps to form the continental scale Antarctic ice-sheets. The model output showed that two rapid jumps

in ice formation occurred as a response to height/mass balance and albedo feedbacks when snowline intersects high plateaus during orbital periods producing cold austral summers (Deconto and Pollard, 2003). These two jumps are comparable to the two steps seen in the foraminiferal $\delta^{18}O$ isotope records (Coxall *et al.*, 2005; Lear *et al.*, 2008). It is still however unknown exactly why pCO_2 levels initially declined. A recent high resolution investigation suggests that a reduction in pCO_2 occurred before the main phase of ice growth (Oi-1glacial maximum), followed by a sharp recovery to pre-transition values and then a more gradual decline into the early Oligocene (Pearson *et al.*, 2009) (see Fig. 1.6 in Chapter 1). This implies that declining pCO_2 had a central role in the development of the Antarctic ice sheet.

7.2.3 Carbon in the freshwater environment

Seasonal changes in the $\delta^{13}C$ obtained from carbonate freshwater proxies tend to co-vary with the equivalent $\delta^{18}O$ profiles (e.g. Leng *et al.*, 1999; Schmitz and Andreasson, 2001; Wurster and Patterson, 2001; Gajurel *et al.*, 2006). However, the $\delta^{13}C$ profiles are more complicated to interpret then the $\delta^{18}O$ profiles owing to the variety of influential source.

Exchanges between gaseous, liquid and solid carbon phases are accompanied by isotopic fractionation. A good understanding of these isotopic fractionations is needed when trying to make sound interpretations from the $\delta^{13}C$ values obtained from a proxy indicator (e.g. gastropod). The large variety of sources that affect surface water dissolved inorganic carbon (DIC), which is available for uptake by carbonate proxies, are as follows:

- Carbon bearing reactants (e.g. limestone);
- Solid carbonate phase;
- Exchange with the atmospheric CO_2;

- Soil biogenic CO_2 exchange, plant respiration and decay of terrestrial organic matter in soil waters and shallow ground water;
- Proportions of C3 to C4 plants may influence the carbon isotopic composition of the inflow;
- C4 plants (grasses) have values $\delta^{13}C$ of -17 ‰ to -9‰;
- C3 plants and terrestrial material derived from C3 organic matter have $\delta^{13}C$ values between -20‰ and -32‰ (average -27‰); and
- A change in the soil, e.g. long term alteration from forest to open grassland caused by a change in climate, can affect the $\delta^{13}C$ values entering surface waters.

A summary of the carbon isotope values from the major sources of carbon into lakes and examples of the range in resulting $\delta^{13}C_{TDIC}$, can be found in Figure 7.1. The three dominant factors controlling the DIC of lake and river waters are discussed further in the following sections:

- Gaseous exchange;
- Isotopic composition of inflowing water; and
- Photosynthesis and respiration of aquatic plants.

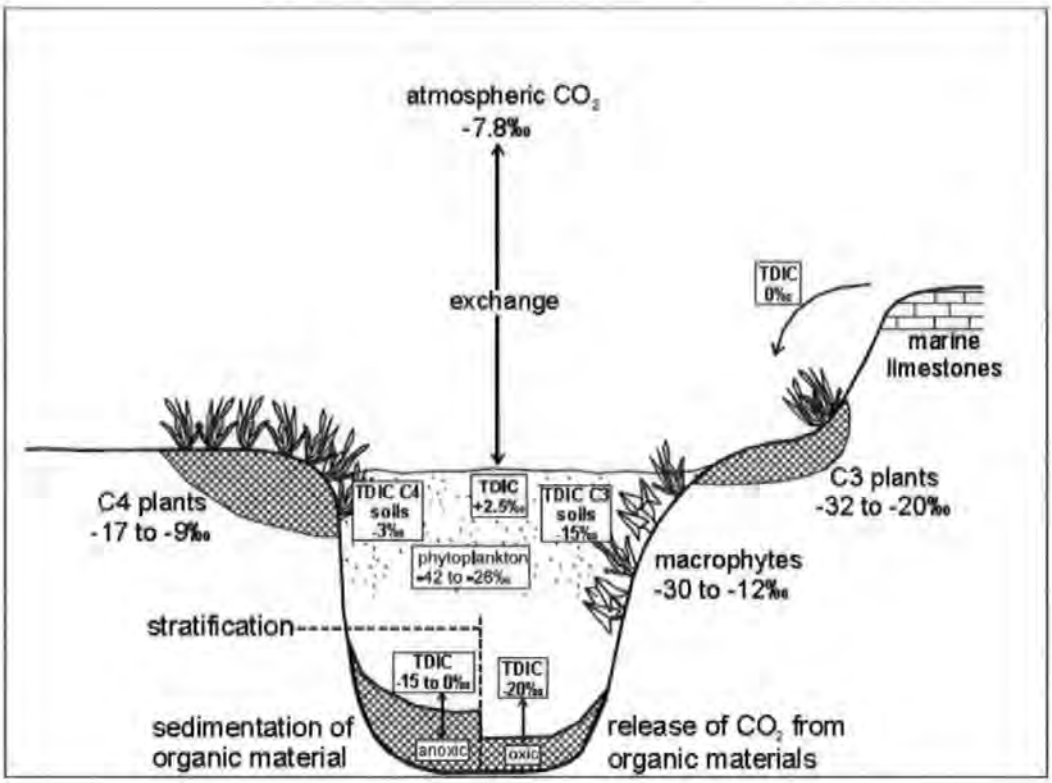

Figure 7.1 Carbon isotope values for the major sources of carbon into lakes and examples of the range of resulting $\delta^{13}C_{TDIC}$.Taken from Leng and Marshall (2004).

7.2.3.1 Gaseous exchange

The DIC composition of the host lake water is dominated by the composition of the non-aqueous reservoirs (solid or gaseous phases), due to aqueous CO_2 budgets being much lower than those in co-existing solid or gaseous phases (Darling *et al.*, 2006). These non-aqueous reserves are modified by fractionation between each other (Darling *et al.*, 2006). These fractionation effects can be influenced by kinetic processes which are more likely to occur with irreversible reactions (Darling *et al.*, 2006). For example, when isotopic fractionation occurs between CO_2 (gas) and CO_2 (aqueous) there is ~ –1‰ fractionation, e.g. if atmospheric CO_2 is –8‰ and if dissolved CO_2 is in equilibrium with the atmosphere then the $\delta^{13}C$ value of DIC would be –9‰.

When CO_2 exchange with the atmosphere is the dominant carbon input the water will become enriched in $\delta^{13}C$. In a closed lake system these $\delta^{13}C$ records could provide information on atmospheric CO_2 changes throughout geological history. During recent times global warming, enhanced by the increased anthropogenic input of greenhouse gases, has adjusted the $\delta^{13}C$ composition of atmospheric CO_2. A consequence of this change in atmospheric CO_2 has lead to the $\delta^{13}C$ of global lake waters to be modified. Keeling *et al.* (1979; 1980; 1995) have recorded the following $\delta^{13}C$ ratios:

- $\delta^{13}C$ -6.7 ‰ 1950
- $\delta^{13}C$ -7.2 ‰ 1979
- $\delta^{13}C$ -8.0 ‰ 1995

They indicate that the addition of isotopically lighter carbon by the burning of fossil fuels has lead to a negative trend in the isotopic composition of carbon in the atmosphere. This in turn would influence the isotopic composition of freshwater in a closed lake system. Evidence of this kind could potentially be recorded by lake sediments deposited during climatic events influenced by changes in atmospheric pCO_2 e.g. like that seen during the E/O transition and Oi-1 glaciation. In order to interpret any changes in lake $\delta^{13}C$ an understanding of the cause behind pCO_2 changes is needed.

7.2.3.2 Isotopic composition of inflowing water

In general, riverine water has widely ranging $\delta^{13}C$ values of between -28‰ to 1‰, where seawater has a more restricted range of 0‰ to 2‰ (Kroopnick, 1980). In Northern Europe groundwater and river waters have $\delta^{13}C_{TDIC}$ values that are typically low; with values for calcite precipitates between –10‰ and –15‰ being reported (Andrews *et al.*, 1993, 1997). A large proportion of the carbonate entering a fluvial system comes from plant respiration and production of CO_2 in nearby soils (Leng and Marshall, 2004). As shown in Figure 7.1

the C3 plants have $\delta^{13}C$ values between –30 to –12‰ and produce soils with $\delta^{13}C_{TDIC}$ of –15‰. Whereas, C4 plants have $\delta^{13}C$ values between –17 to –9‰ producing soils with $\delta^{13}C_{TDIC}$ of –3‰. The $\delta^{13}C_{TDIC}$ is leached from the soils and enters the water course via soil waters and shallow ground waters. However, C4 plants should not be an issue as they made up only a small proportion of the vegetation generally found in intercontinental areas (Retallack, 2001). Significant shifts in plant communities and in turn soil types can lead to significant shifts in this output, changing the $\delta^{13}C_{TDIC}$ of river and lake waters (Leng and Marshall, 2004). Development of ponds and marshes in the distal end of the catchment where water flows are of low energy have sources of carbon that are almost exclusively from the massive decay of $\delta^{13}C$ depleted organic matter (Bonadonna *et al.*, 1999).

The contribution of carbonate minerals to freshwater DIC can have a direct or indirect influence. The $\delta^{13}C$ content is determined by the origin and post depositional alteration of the source (Darling *et al.*, 2006). Surface waters flowing over marine derived bedrock would, on average, uptake $\delta^{13}C$ values of ~0‰ (range from -2‰ to 3‰) e.g. in karstic regions (Andrews *et al.*, 1997). This would be dependent on the age, depositional environment and pH of the water. These factors determine the $\delta^{13}C$ of freshwater carbonates relative to dissolved carbonate source water because of the pH-dependence of dissolved carbonate speciation and thus isotopic fractionation (Clark and Fritz, 1997).

7.2.3.3 Photosynthesis and respiration of aquatic plants.

Photosynthesis in aquatic plants preferentially uptakes ^{12}C, therefore, seasonal variation in the lake water TDIC will show a depletion of ^{12}C during summer and an augmentation in winter (Leng and Marshall, 2004). Respiration produces the reverse response, causing depletion in winter rather than summer. The balance between these two processes produces

a complicated signal in the fossil biogenic record. Lakes with a large biomass will show larger seasonal differences in the high latitudes (Leng *et al.*, 2005) due to seasonal loss of plant matter. Stratification of the water column during the summer months can also occur owing to photosynthesis and organic production in the surface waters. This stratification can be reflected in the fossil record if proxies that inhabit different depths in the water column are analysed. These individual proxies could potentially produce significantly different $\delta^{13}C$ and or $\delta^{18}O$ seasonal profiles (Leng and Marshall, 2004).

7.2.4 $\delta^{13}C$ in freshwater carbonate proxies

Variation in $\delta^{13}C$ values within the carbonate shell record of gastropods must be considered carefully owing to the unknown percentage of metabolic carbon from respiratory sources being incorporated into the shell lattice. The Tanaka *et al.* (1986) model indicates that on average 50 % of the $\delta^{13}C$ in mollusc shell carbonate is derived from metabolic carbon. However, these values alter depending on the season and biogenic productivity during that year (McConnaughey *et al.*, 1997). Fritz and Poplowski (1974) showed that aquatic snails reared under differing DIC conditions had $\delta^{13}C$ values that closely resembled the isotopic composition of the DIC rather than the food they ingested. Experiments carried out by Romenek *et al.* (1992) showed that skeletal incorporation of respired CO_2 typically reduce the shells $\delta^{13}C$ value by <2 ‰ and that the experimental determination of fractionation between inorganic aragonite and bicarbonate cannot be directly applied to reconstruct variation in the $\delta^{13}C_{TDIC}$ of the freshwater the proxy inhabited. They also indicate that the incorporation of $\delta^{13}C$ is weakly dependent on temperature and therefore can not be used as an indicator of temperature. When organisms obtain oxygen from their surrounding environment a proportion of the uptake includes CO_2 which is related to the environmental ratio of CO_2:O_2 (McConnaughey *et al.*, 1997). If the

environmental ratios are low, the proportion of CO_2 uptake will be low, increasing the proportion of metabolic carbon used in shell formation (McConnaughey *et al.*, 1997). As there is a higher ratio of CO_2:O_2 in water than in air, lung breathers will utilise more metabolic carbon in shell formation than gill breathers. This assumes however that CO_2 accompanies O_2 during exchange within the gills. As a larger proportion of CO_2 will be derived from the external environment the shell $\delta^{13}C$ precipitated should be similar to the DIC of the surrounding water at that time.

Seasonal variation in the DIC would suggest that metabolic effects are minimised during late autumn (prior to winter cessation) and early spring during the initiation of new growth (Veinott and Cornett, 1998). During this period in the annual cycle the percentage of metabolic carbon incorporated into the shell would equal 0%. Therefore, the shell $\delta^{13}C$ would be in equilibrium with the DIC. Investigations into modern *V. contectus* (see Chapter 2) indicate that metabolised carbon and the availability of carbon as a food source has had some influence on the $\delta^{13}C$ of the *V. contectus* shell carbonate.

7.3 Methods

7.3.1 Initial test study (2006) on the preparation of well preserved fossil specimens of *V. lentus*

Samples collected from a field excursion to the Isle of Wight (IOW) in 2006 (courtesy of Dr Grimes) were used to establish a repeatable method by which *Viviparus* shells could be cleaned and stabilised for high resolution isotopic sampling. The method comprised of an initial cleaning of the outer surface of the shell in ultra pure water. Once clean the shell

was photographed through a 360 ° rotation. Further cleaning of the inner shell took place while the shell was systematically dismantled into sections, if required. The main motivation for dismantling the shell was so that any contaminants within the shell (e.g. sediment) could be removed. Where possible, shells were kept intact (if preservation allowed) so long as they could be cleaned internally to a high standard. Each section was then photographed at several angles showing every part of the outer shell surface of each shell section. Stabilisation of the sections and whole shells involved embedding them in silicon with the outer shell surface placed down into the silicon; the inner surface of the shell was then in-filled with epoxy resin, which was dyed blue so that there was a clear difference between the shell and resin for drilling purposes (Fig. 7.2). It was found that larger sections or whole shells could be used when the shell was in-filled with resin in several stages. The sections or whole shells were then left for 24 hours or until the resin was dry.

Removal of each section was carried out by carefully peeling off the silicon. Each section was further cleaned in ultra pure water using an ultrasonic bath. Before the sections were drilled a photographic template was produced to show the location of each shell section on the 360° rotation of the whole gastropod (Fig. 7.3). A small dentist's drill (Dremel) was then used with a variable speed selector and the finest drill bit available (0.4 mm tungsten carbide spade drill bit) to drill each specimen at high resolution. Each drill line followed the growth banding parallel to the aperture, incorporating a minimal number of growth bands without compromising sample weight. From each drill line 0.30 to 0.50 mg of powder was produced, this was collected and stored in glass vials for isotopic analysis.

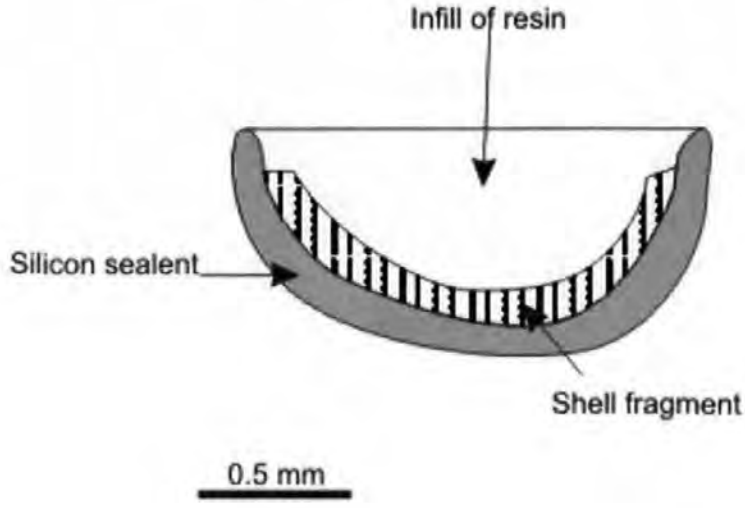

Figure 7.2 Diagrammatic representations showing a cross section of a shell fragment embedded in silicon and in-filled with resin.

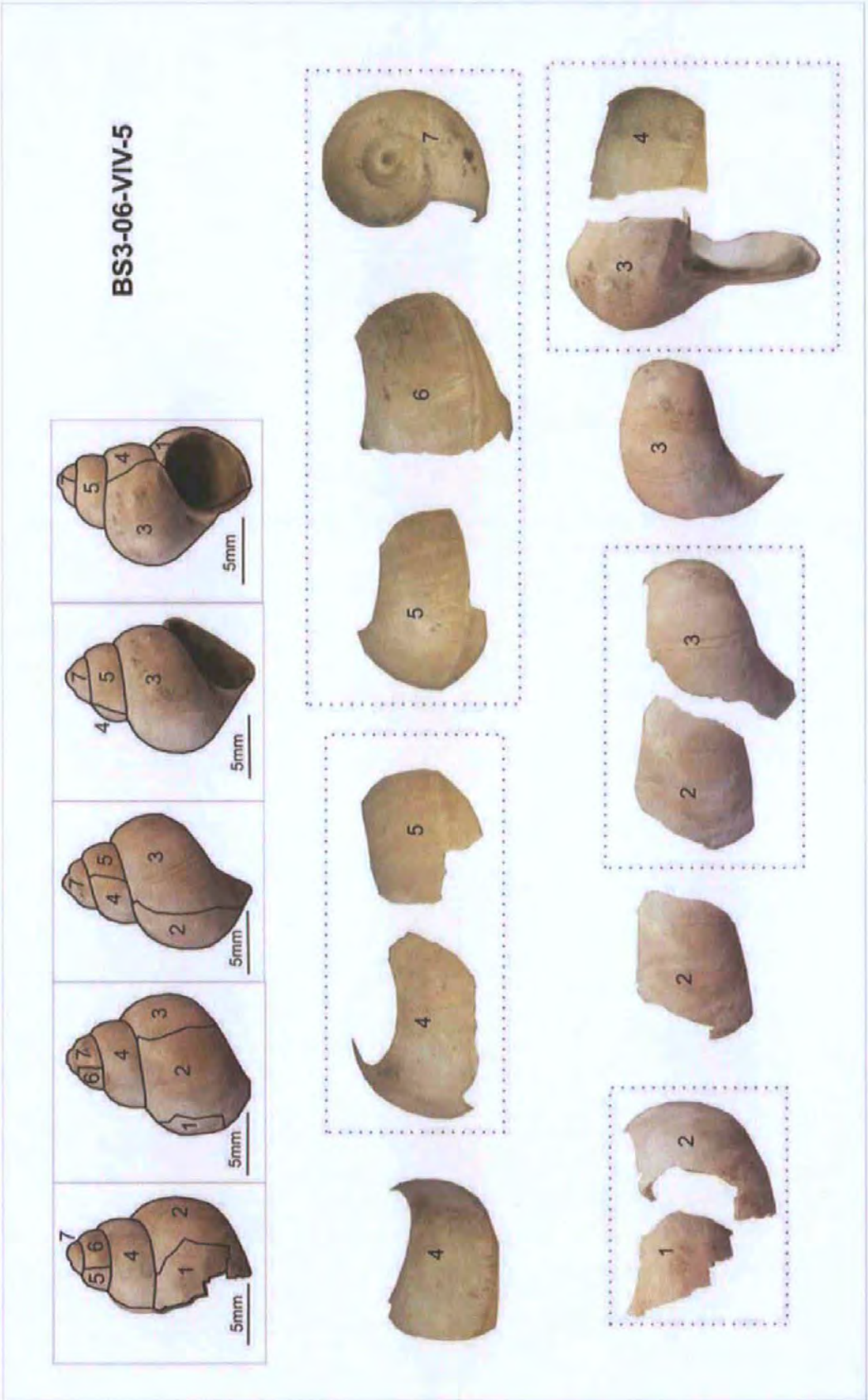

Figure 7.3 An example of a photographic template produced to show the position of the shell sections in relation to the whole gastropod (BS3-06-VIV-5).

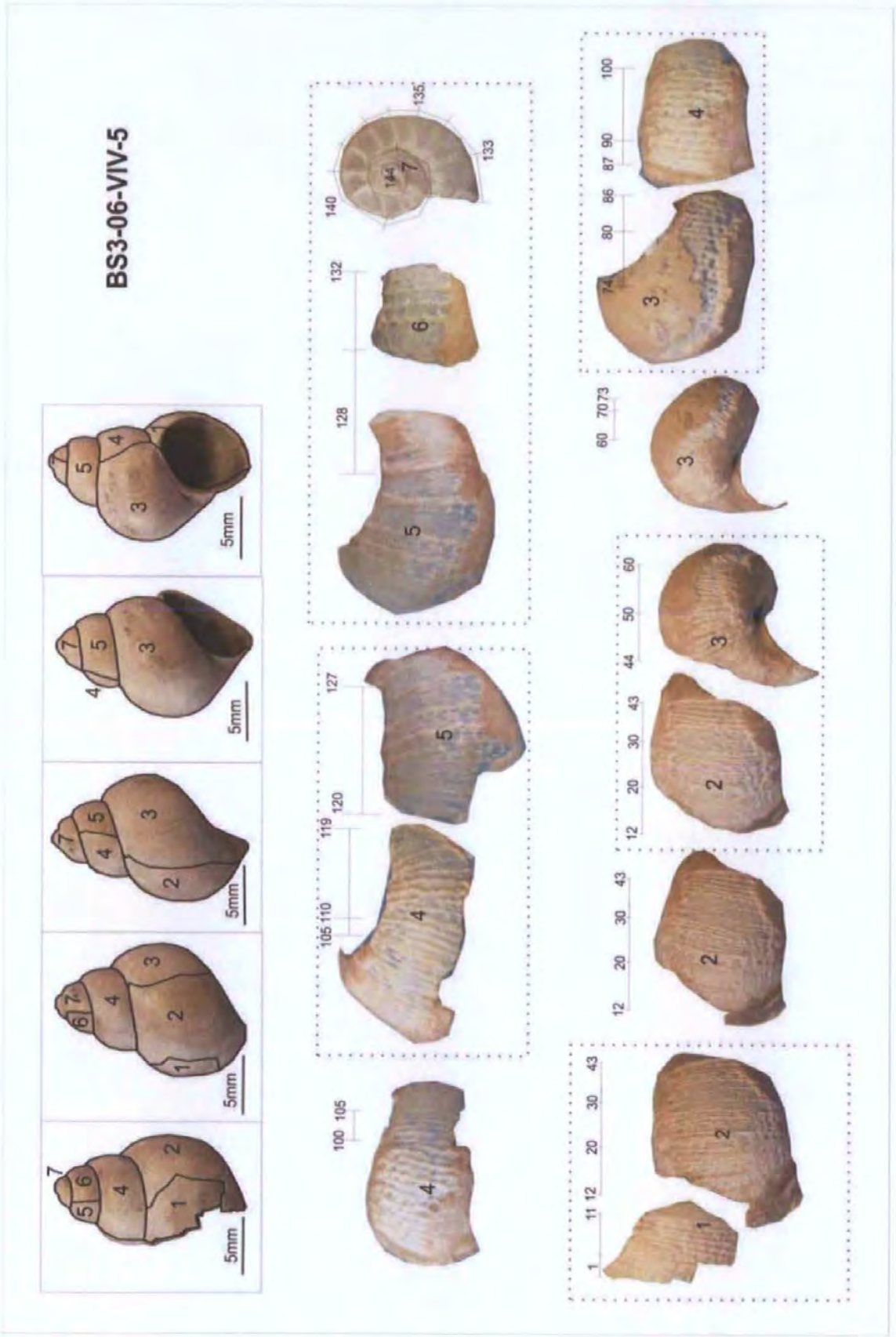

Figure 7.4 A photographic template showing the drilled section in relation to their position on the whole gastropod (BS3-06-VIV-5)

Once drilled each section was re-photographed and once again used to produce a final photographic template showing the drill-line positions on the shell (Fig. 7.4). A measurement of the distance between drill-lines was carried out using a travelling microscope. Figure 7.5 shows the measurement method used.

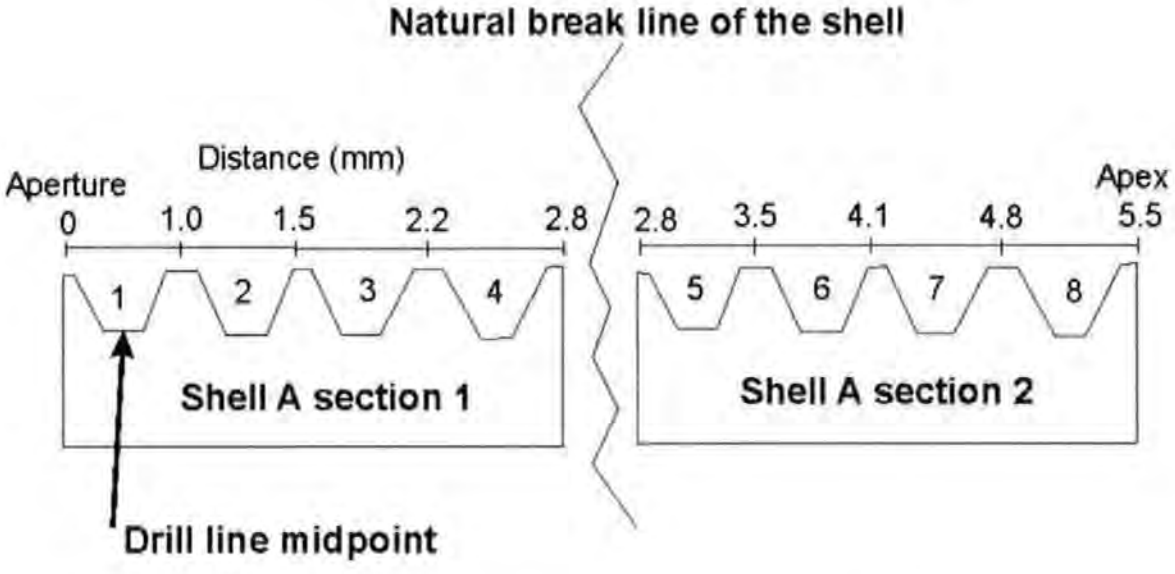

Figure 7.5 Cross section view of two individual gastropod shell sections showing the method of measuring the width of the drill line mid point and measurements between shell sections.

7.3.2 Preparation of samples from key horizons

Five horizons containing whole, well preserved *V. lentus* shells suitable for high resolution isotopic analysis were prepared following the methods described in Section 7.3.1:

- SCO S-2 (Cliff End Member);
- HAM S1 (Bembridge Marls Member);
- HAM S4 (base of the lower Hamstead Member);
- BS1/BS3 (equivalent of horizons BOULD S1 and BOULD S2 – upper part of the lower Hamstead Member); and
- BOULD S6 (upper Hamstead Member).

These five horizons were taken from key points through the Solent Group succession based upon the $\delta^{18}O$ record produced from the analysis of *V. lentus* shell fragment in Chapter 6. However, preservational issues were also influential in the ultimate choice of the horizon analysed. A minimum of three shells were drilled at high resolution from the shell aperture to the apex. The powders obtained from the high resolution drilling were analysed for $\delta^{18}O$ and $\delta^{13}C$. The midpoint of the drill line along with the isotopic results was used to construct a seasonal isotopic profile for each *V. lentus* analysed. The initial *V. lentus* specimen (BS3-06-VIV-5) used in the test study (Figs. 7.3, 7.4) was analysed for $\delta^{18}O$ and $\delta^{13}C$ every drill line. All subsequent gastropods were analysed every other drill line, as it was considered to be a sufficient number of analyses to produce a detailed high resolution isotopic profile and within the limitations of analysis time.

7.3.3 Isotopic analysis

Isotopic analyses were undertaken at the University of Plymouth during 2006 to 2008. The carbonate powders were reacted with 100 % phosphoric acid at 90 °C for approximately 1hour. The CO_2 produced was analysed on a GV Instrument Isoprime Mass Spectrometer with a Gilson Multiflow carbonate auto-sampler. Any isotopic results below 1.2 nA were removed from the dataset and rerun if material was available. The results were calibrated against Vienna Peedee Belemnite (VPDB) using the international standard NBS-19 (National Bureau of Standards 19; $\delta^{13}C$ = 1.95 ‰ $\delta^{18}O$= –2.20 ‰) IAEA-CO-8 (International Atomic Energy Agency -CO-8 published values; $\delta^{13}C$ –5.75‰ $\delta^{18}O$= –22.67‰), and IAEA-CO-9 (International Atomic Energy Agency-CO-9 published values; $\delta^{13}C$ = –45.12‰ $\delta^{18}O$= –15.28‰). Five NBS-19 standards were evenly distributed through the individual isotope runs. A comparison was made between the analysed NBS-19 values and published values for this standard. The difference between the two values was used to

correct for daily drift. An aragonite fractionation factor (1.01034 taken from Friedman and O'Neil, 1977), was applied to convert the measured isotope compositions of CO_2 generated by the reaction of aragonite with ortho-phosphoric acid to the isotope compositions of aragonite.

7.3.4 X-Ray Diffraction analysis

To determine preservation of individual horizons, the remaining powders from 3 to 5 *V. lentus* fragments from each horizon were analysed. These samples were analysed using X-Ray Diffraction at the University of Plymouth and Royal Holloway University of London (see Chapter 6 Section 6.5.2.2 for further details). XRD analysis was not possible on the individual *V. lentus* shells drilled at high resolution owing to the small volume of powder remaining after stable isotope analysis.

7.3.5 Shell structure

Understanding the shell formation process is vital for the removal of shell material and the correct interpretation of isotopic data. In the majority of cases it is assumed that shell secretion and in turn shell structure is similar to the closest living relatives of the species in question. To establish whether *V. lentus* had a shell structure that is equivalent to its closest living relative, a *V. lentus* specimen was selected for thin sectioning so that the shell structure could be viewed in greater detail.

The outer surface of a well preserved *V. lentus* shell was carefully cleaned and, where possible, sedimentary material infilling the aperture was removed. The whole shell was then submerged in resin and left to harden. The *V. lentus* shell encased in resin was then cut in half along the columella from the apex to the aperture (see Fig. 2.8 Chapter 2 for diagrammatical explanation). Any remaining sediment within the shell was removed, after which each shell half was in-filled with resin and left to harden. Each of the shell halves

were then dissected into smaller whorl sections so that the cut surface was parallel to the growth banding for each of the whorls. Each whorl section was numbered in order from the aperture to the apex. A thin section was made from each of the sections showing the cut surface parallel to the growth bands.

7.4 Results

7.4.1 Preservation

As mentioned in Section 7.3.4 individual powders could not be analysed by XRD however, individual shell fragments from the same horizon are aragonitic, suggesting good preservation. XRD analysis of the individual horizons showed that the samples analysed from each of the horizons were consistently aragonitic (See Appendix 3). Thin sectioning of a single *V. lentus* specimen (Fig. 7.14) has shown that the crystalline shell structure has been preserved suggesting that recrystalisation of the shell material had not taken place. Therefore, it is considered that the samples used in the seasonality investigation have retained their original isotopic composition.

7.4.2 Isotope results

The results from this investigation include:

- the photographic templates (before and after drilling) of each *V. lentus* specimen;
- data tables, including the isotopic results for each *V. lentus* specimen; and
- the individual isotopic profiles constructed from this data can be found in Appendix 3 (see Table 7.1 for details).
- Figures 7.6 to 7.10 combined all the isotopic profiles for each individual horizon so that they may be compared.

Horizon	*V. lentus* specimen	Appendix 3			Chapter 7
		Photographic template	Data Table	Isotopic profile	Combined Isotopic profile
SCO S-2 Cliff End Member	SCO S-2 08 VIV 2	Fig. 1	Table 1	Fig. 35	Fig. 7.6
	SCO S-2 08 VIV 3	Fig. 2	Table 1	Fig. 36	
	SCO S-2 08 VIV 4	Fig. 3	Table 1	Fig. 37	
HAM S1 Bembridge Marls Member	HAM S1 07 VIV 1	Fig. 4 and 5	Table 2	Fig. 38	Fig. 7.7
	HAM S1 07 VIV 1	Fig. 6 and 7	Table 2	Fig. 39	
	HAM S1 07 VIV 1	Fig. 8 and 9	Table 2	Fig. 40	
	HAM S1 07 VIV 1	Fig. 10 and 11	Table 2	Fig. 41	
	HAM S1 07 VIV 1	Fig. 12 and 13	Table 2	Fig. 42	
HAM S4 base of the lower Hamstead Member	HAM S4 07 VIV 1	Fig. 14	Table 3	Fig. 43	Fig. 7.8
	HAM S4 07 VIV 2	Fig. 15	Table 3	Fig. 44	
	HAM S4 07 VIV 3	Fig. 16	Table 3	Fig. 45	
	HAM S4 07 VIV 4	Fig. 17	Table 3	Fig. 46	
	HAM S4 07 VIV 5	Fig. 18	Table 3	Fig. 47	
BS1/BS3 upper part of the lower Hamstead Member	BS1 06 VIV 2	Fig. 19 and 20	Table 4	Fig. 48	Fig. 7.9
	BS1 06 VIV 3	Fig. 21 and 22	Table 4	Fig. 49	
	BS3 06 VIV 3	Fig. 23 and 24	Table 4	Fig. 50	
	BS3 06 VIV 5	Fig. 25 and 26	Table 4	Fig. 51	
BOULD S6 upper Hamstead Member	BOULD S6 07 VIV 1	Fig. 27 and 28	Table 5	Fig. 52	Fig. 7.10
	BOULD S6 07 VIV 2	Fig. 29 and 30	Table 5	Fig. 53	
	BOULD S6 07 VIV 3	Fig. 31 and 32	Table 5	Fig. 54	
	BOULD S6 07 VIV 4	Fig. 33 and 34	Table 5	Fig. 55	

Table 7.1 Information on the location of the *V. lentus* photographic templates, data table and isotopic profiles.

Horizon SCO S-2 from the Cliff End Member is the oldest horizon analysed for seasonality linked isotopic variability within the Solent Group strata. The isotopic profiles produced from the analysis of three *V. lentus* specimens (Fig. 7.6) have a small range in $\delta^{18}O$ implying low seasonal change throughout the lifetime of the specimens. This is further highlighted by the relatively small range of $\delta^{18}O$ values (3.2‰), when all of the $\delta^{18}O$ values for this horizon are combined (Figs. 7.6, 7.11). In general the transition between the most positive and negative $\delta^{18}O$ values in each of the *V. lentus* profiles (Fig. 7.6) is relatively sharp. This is particularly clear in the profile for SCO S-2 08 VIV 3. On average this horizon has the most negative values recorded for *V. lentus* (–3.4‰, see Fig. 7.11) in the Solent Group strata. The $\delta^{13}C$ profiles co-vary with the $\delta^{18}O$ profiles in each of the specimens analysed. The transition between positive and negative $\delta^{13}C$ values is also relatively sharp and consistent with those seen in the $\delta^{18}O$ profiles. In some cases these sharp transition are associated with growth cessations.

The horizon HAM S1, taken from the Bembridge Marls Member, was deposited approximately 1.43 My after the horizon SCO S-2. The isotopic profiles of the five *V. lentus* specimens analysed (Fig. 7.7) indicate seasonal changes in $\delta^{18}O$. The transition from positive to negative values appears to be more gradual in comparison with the specimens from SCO S-2. These gradual transitions are often accompanied by faint cessation marks which do not reach full growth cessation. For the specimens HAM S1 O7 VIV 1, 2 and 5 the $\delta^{18}O$ and $\delta^{13}C$ values appear to be more erratic, whereas HAM S1 O7 VIV 3 and 4 are less erratic producing smoother $\delta^{18}O$ and $\delta^{13}C$ profiles. The average obtained from combining all of the $\delta^{18}O$ data from the five specimens analysed indicates a shift to slightly more positive $\delta^{18}O$ values (–1.9‰) when compared with SCO S-2 (Fig. 7.11). This horizon also has the largest range of $\delta^{18}O$ values out of all the horizons analysed, ranging from –

5.0‰ to 0.1‰ (4.9‰). The $\delta^{13}C$ profiles appear to co-vary with the $\delta^{18}O$ profiles in each of the specimens analysed.

HAM S4 occurs during a shift to more negative $\delta^{18}O$ values between the two positive $\delta^{18}O$ shifts (in the Bembridge Marls Member and Lower Hamstead Member) in the isotopic profile from the analysis of *V. lentus* fragments (Fig. 6.15; Chapter 6). The individual profiles from HAM S4 (Fig. 7.8, 7.11) indicate a large range in $\delta^{18}O$ (4.8‰), encompassing values from −0.7‰ to −5.5‰. The clear seasonal isotopic trends show that the positive part of the $\delta^{18}O$ profiles covers a short period and often forms a narrow peak (e.g. HAM S4 07 VIV 5 between 25 to 40 mm), clearly different from the transitions observed in the previous horizons. Specimens HAM S4 07 VIV 2, 3 and 5 in particular show values initiating at approximately –3‰ after which they become more positive forming a narrow peak of positive values. This narrow peak is followed by a second negative trough covering a smaller section of shell than the initial negative trough. Covariance between $\delta^{18}O$ and $\delta^{13}C$ profiles occurs in portions of the isotopic profiles.

Four *V. lentus* specimens taken from horizons BS1 and BS3, just prior to the Hamstead Member hiatus, have $\delta^{18}O$ values ranging from –3.9 ‰ to –0.4‰ (3.5‰). The profile shape appears to change significantly in this horizon with an extended period of positive $\delta^{18}O$ values (Fig. 7.9) and contracted periods of negative $\delta^{18}O$ values (e.g. BS3 06 VIV 5). The average for this horizon when all of the $\delta^{18}O$ data from the four *V. lentus* specimens are combined (–1.9‰), is more positive than SCO S-2 and HAM S4 but is similar to HAM S1 (–1.9‰) (Fig. 7.11). The $\delta^{13}C$ for each of the *V. lentus* specimens analysed appears to co-vary with the $\delta^{18}O$ profiles.

Four *V. lentus* specimens taken from the horizon BOULD S6 were collected from sediments deposited after the Hamstead Member hiatus. The $\delta^{18}O$ profile shape for each of the *V. lentus* specimens shows an extended period of positive $\delta^{18}O$ values (Fig. 7.10) and contracted period of negative $\delta^{18}O$ values, to a greater extent than those specimens from horizon BS1/BS3. The range of $\delta^{18}O$ values (3.3‰) obtained from the specimens is much lower than the three preceding horizons (HAM S1, HAM S4 and BS1/BS3), but is not as low as SCO S-2. The average $\delta^{18}O$ calculated for the combined $\delta^{18}O$ data from four *V. lentus* specimens from horizon BOULD S6 is significantly more positive than the other four horizons analysed (Fig. 7.11). The $\delta^{13}C$ profiles indicate clear seasonal isotopic trends that appear to co-vary with the $\delta^{18}O$ profiles.

Evidence provided by the high resolution isotopic profiles shows that each individual *V. lentus* shell analysed produced clear $\delta^{18}O$ and $\delta^{13}C$ seasonal trends which, if the shell had been altered, would not have been preserved. This in combination with the XRD results from the *V. lentus* shell fragments taken from the equivalent horizons indicates that diagenetic alteration has not taken place.

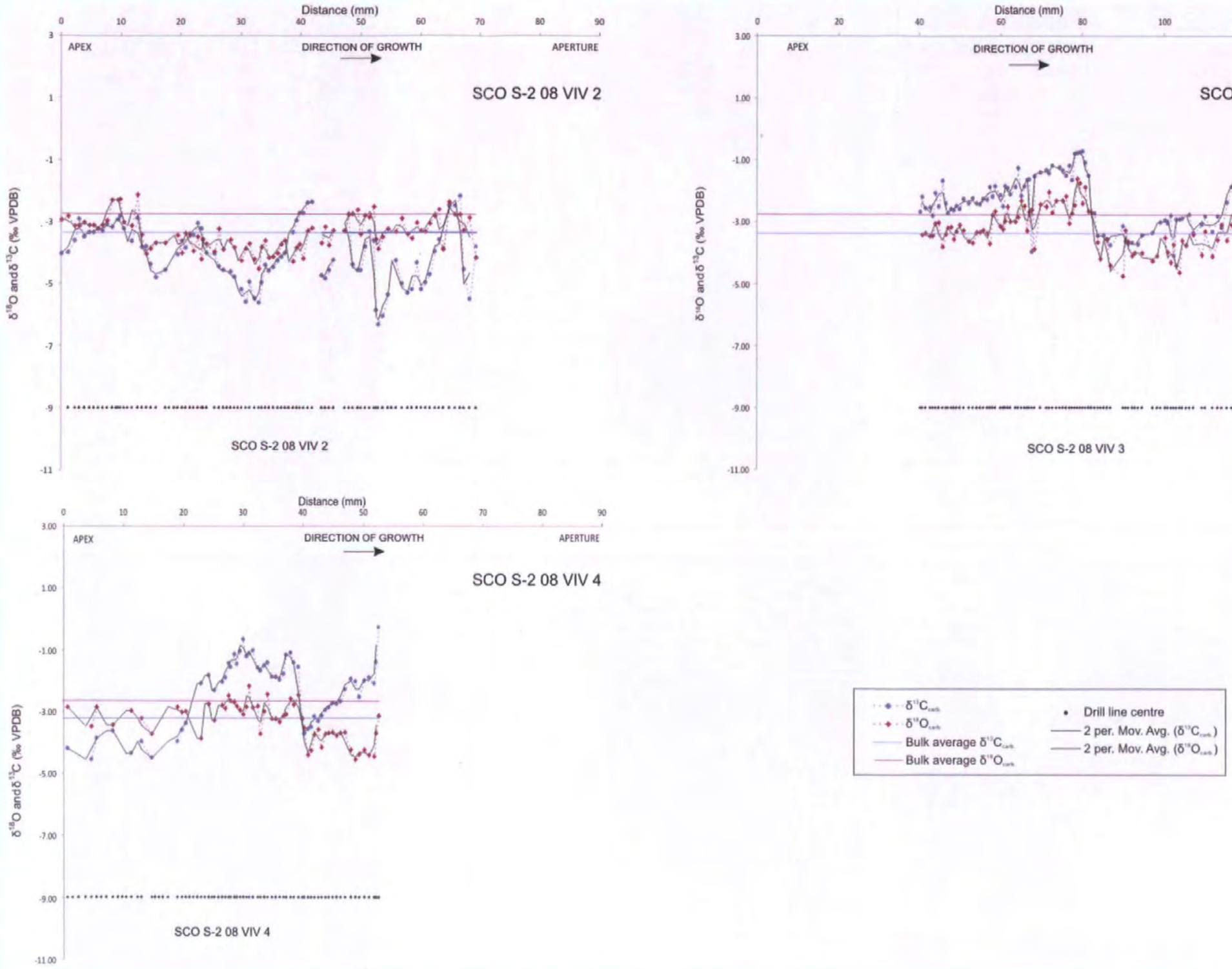

Figure 7.6 Isotopic profiles from three whole *V. lentus* specimens from horizon SCO S-2. The $\delta^{18}O$ and $\delta^{13}C$ data are plotted from the apex to the aperture (left to right), associated with the data is a 2 point moving average. The solid red line (oxygen) and blue line (carbon) is the average obtained from the analysis carried out on the *V .lentus* fragment for the same horizon (see Chapter 6). Preservation of the *V. lentus* shells allowed them to remain whole during sample collection.

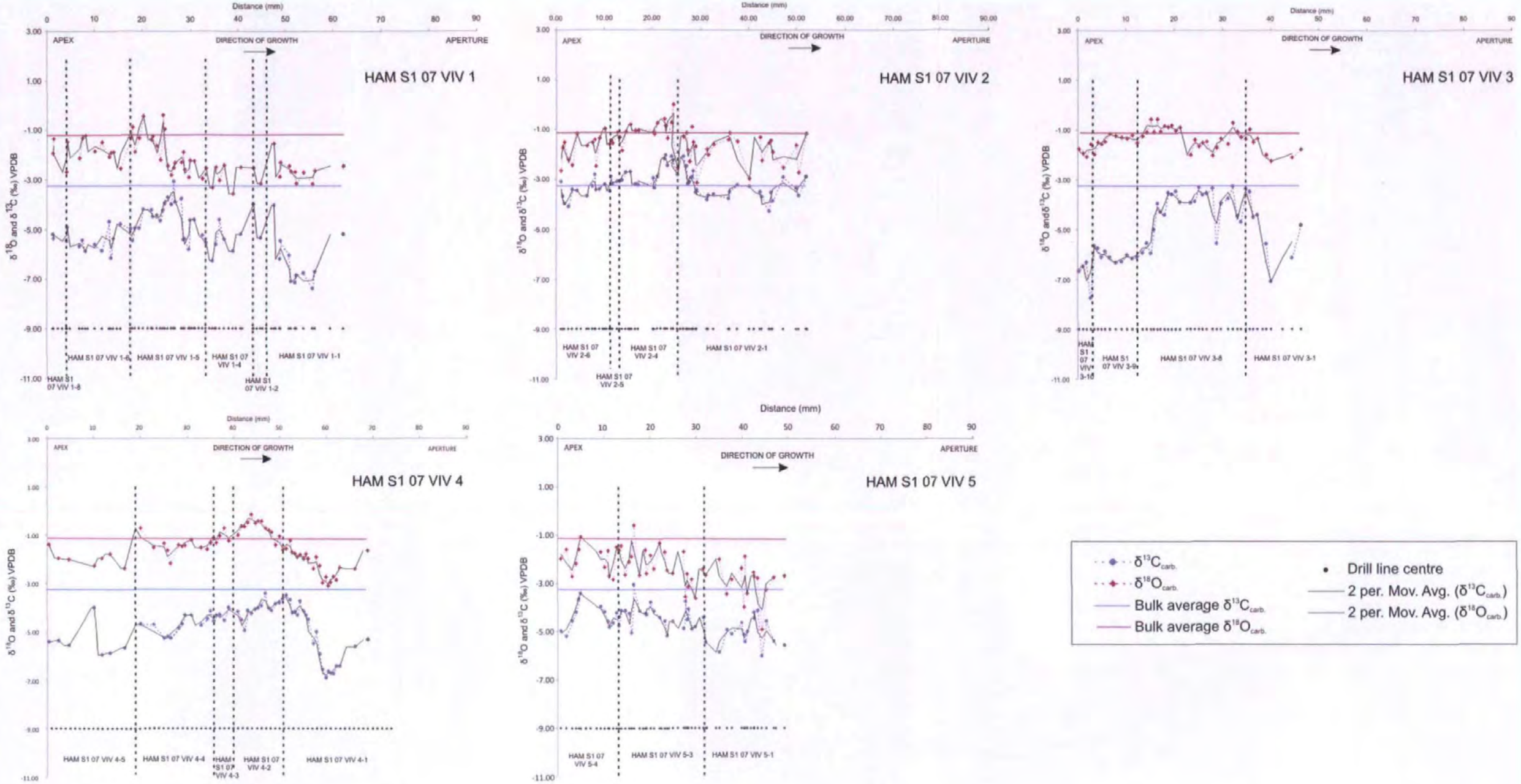

Figure 7.7 Isotopic profiles from five whole *V. lentus* specimens from horizon HAM S1. The $\delta^{18}O$ and $\delta^{13}C$ data are plotted from the apex to the aperture (left to right), associated with the data is a 2 point moving average. The solid red line (oxygen) and blue line (carbon) is the average obtained from the analysis carried out on the *V. lentus* fragment for the same horizon (see Chapter 6). Preservation of the *V. lentus* shells required them to be prepared as shell sections. Dashed vertical line is where one fragment ends and another begins.

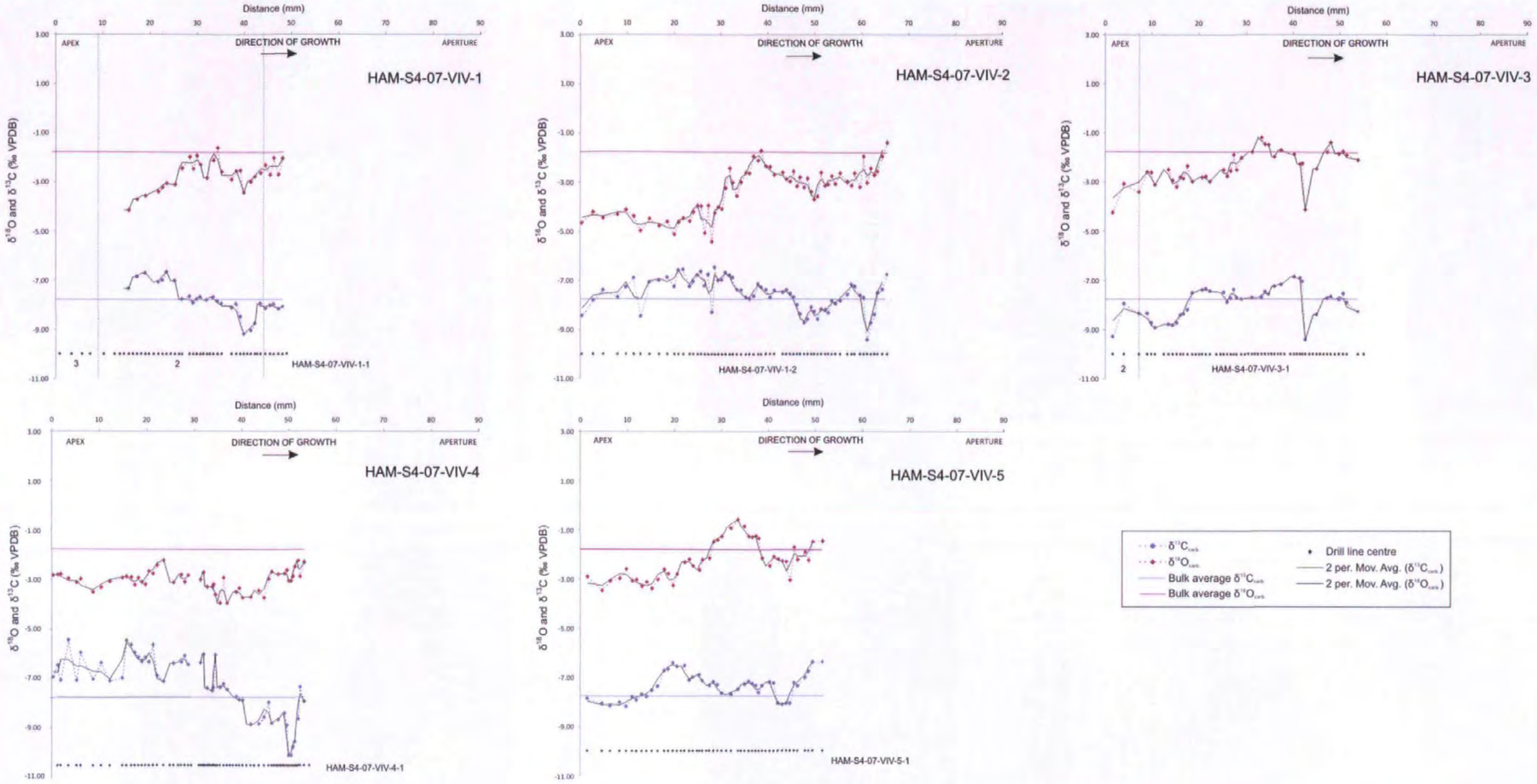

Figure 7.8 Isotopic profiles from five whole *V. lentus* specimens from horizon HAM S4. The $\delta^{18}O$ and $\delta^{13}C$ data are plotted from the apex to the aperture (left to right), associated with the data is a 2 point moving average. The solid red line (oxygen) and blue line (carbon) is the average obtained from the analysis carried out on the *V. lentus* fragment for the same horizon (see Chapter 6). Preservation of the *V. lentus* shells allowed them to remain whole during sample collection. Dashed vertical line is where one fragment ends and another begins.

Part 2: Fossil gastropods

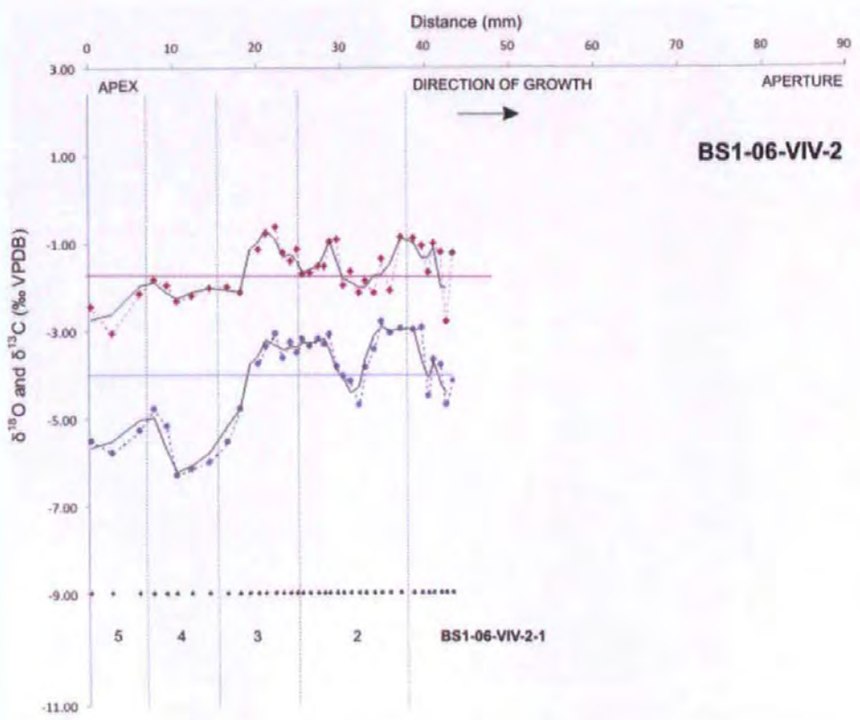

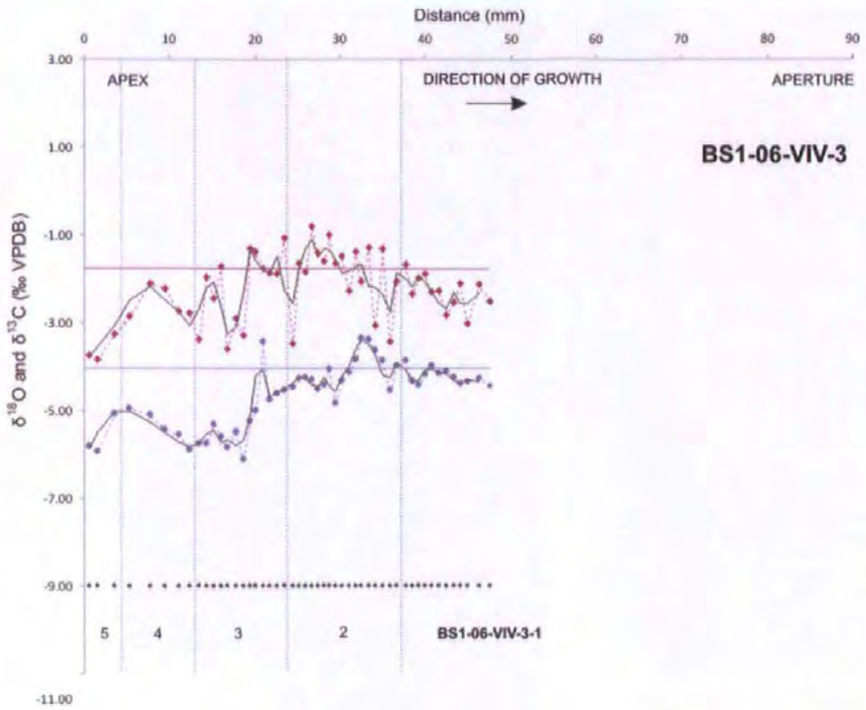

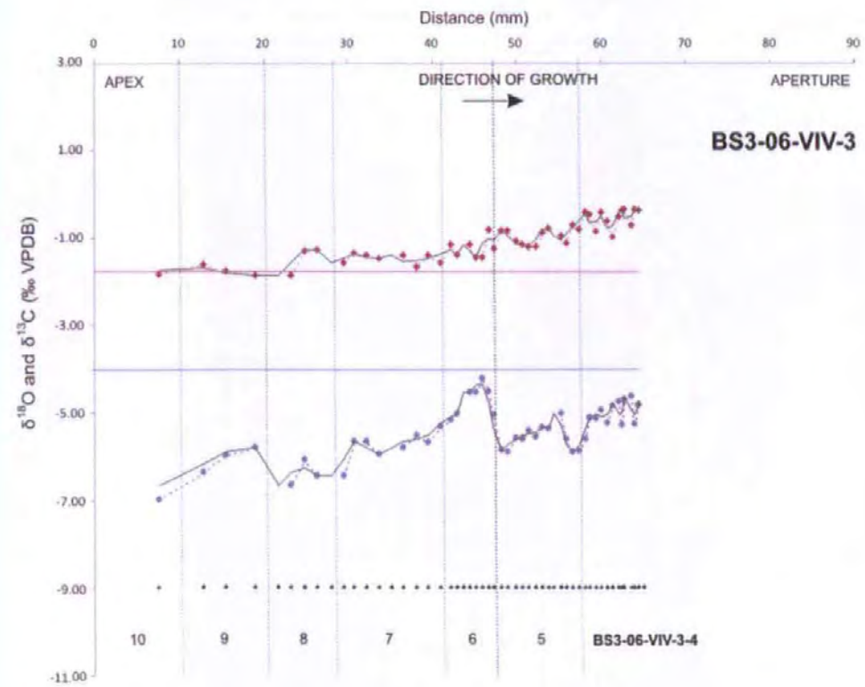

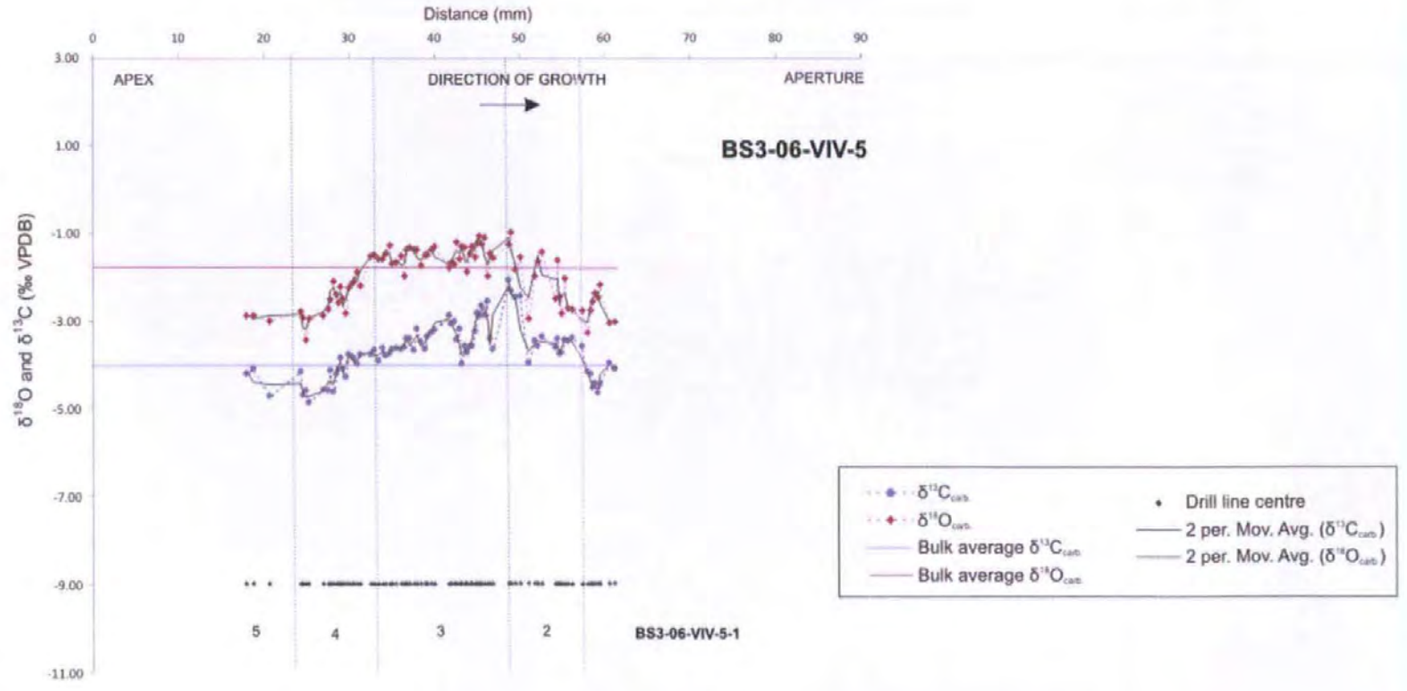

Figure 7.9 Isotopic profiles from four whole *V. lentus* specimens from horizon BS1/BS3. The $\delta^{18}O$ and $\delta^{13}C$ data are plotted from the apex to the aperture (left to right), associated with the data is a 2 point moving average. The solid red line (oxygen) and blue line (carbon) is the average obtained from the analysis carried out on the *V. lentus* fragment for the same horizon (see Chapter 6). Preservation of the *V. lentus* shells required them to be prepared as shell sections. Dashed vertical line is where one fragment ends and another begins.

Part 2: Fossil gastropods

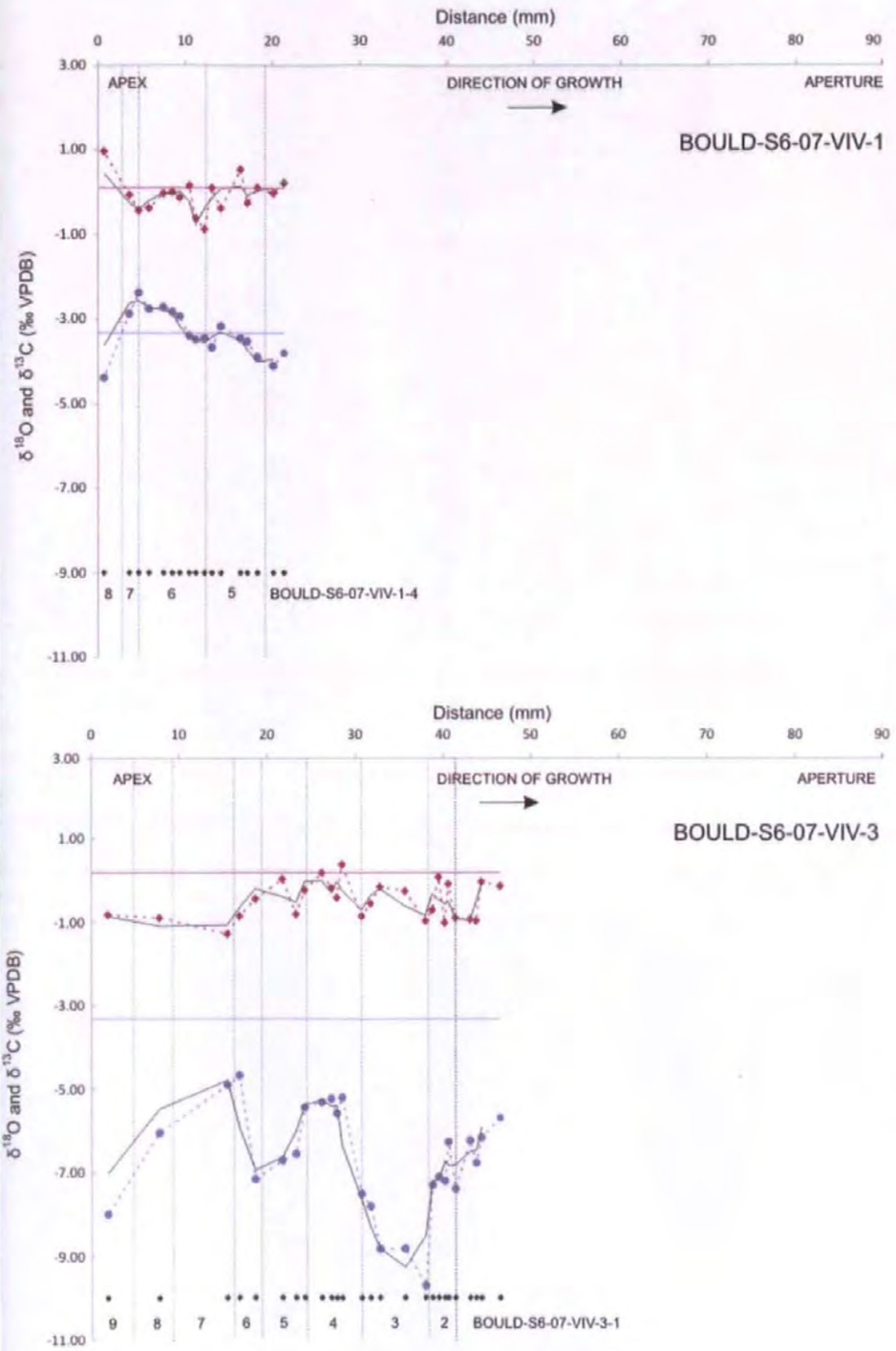

Figure 7.10 Isotopic profiles from four whole *V. lentus* specimens from horizon BOULD S6. The $\delta^{18}O$ and $\delta^{13}C$ data are plotted from the apex to the aperture (left to right), associated with the data is a 2 point moving average. The solid red line (oxygen) and blue line (carbon) is the average obtained from the analysis carried out on the *V. lentus* fragment for the same horizon (see Chapter 6). Preservation of the *V. lentus* shells required them to be prepared as shell sections. Dashed vertical line is where one fragment ends and another begins.

Part 2: Fossil gastropods

7.4.3 Isotopic variability of $\delta^{18}O$

A histogram for each horizon was constructed using the $\delta^{18}O$ values from the isotopic profiles of each *V. lentus* shell analysed. Each *V. lentus* specimen has been colour coded, see Fig. 7.11. Each histogram represents the frequency or number of times a $\delta^{18}O$ value appears in the seasonal profiles obtained from all of the *V. lentus* specimens analysed from that horizon. The $\delta^{18}O$ values are grouped into 0.3‰ bins between –6.0‰ to 1.2‰. The mean, standard deviation and range is given for the combined histogram using all of the $\delta^{18}O$ values from each individual *V. lentus* from that horizon.

The high resolution data indicates similar shifts to that seen in the $\delta^{18}O$ record obtained from the *V. lentus* fragments. Working from the base of the section the *V. lentus* specimens analysed at high resolution from horizon SCO S-2 indicate a normal distribution for each of the individual shells and combined histogram. The range of $\delta^{18}O$ values are similar for each of the three shells, ranging between –0.9‰ and –4.2‰.

The data obtained from horizon HAM S1indiates a shift to positive $\delta^{18}O$ values which, range between 0.6 ‰ and –3.3‰ (outlier at –4.2‰). Several of the specimens in this horizon show a normal distribution (e.g. HAM-S1-07-VIV-2 and 3) whereas several of the *V. lentus* show a double peaked histogram (e.g. HAM-S1-07-VIV-5).

Horizon HAM S4 has the largest range in $\delta^{18}O$ values from 0.0‰ to –4.8‰. The individual histograms in this horizon indicate that the trend identified in HAM S1 remains, with some the specimens showing a normal distribution where others indicate a double peaked histogram (e.g. HAM-S4-07-VIV 2 (red colour)).

The range of $\delta^{18}O$ values in BS1/BS3 is much narrower than in HAM S1 and HAM S4, ranging between –0.6‰ to –4.2‰. However, the mean of all the $\delta^{18}O$ values is overall more positive than HAM S4. There is some evidence of double peaked histogram for BS3-

06-VIV-5. Horizon BOULD S6 has the most positive mean when all of the $\delta^{18}O$ values from this horizon are considered as one. The $\delta^{18}O$ values range from 0. 9‰ to –2.1‰. However, the lack of data from the individual specimens makes it difficult to determine any trends.

There is a clear distinction between the histograms from SCO S-2 (Cliff End Member) and BOULD S6 (upper Hamstead Member) horizons. Firstly, the $\delta^{18}O$ values covered by these histograms are off-set, with SCO S-2 exhibiting $\delta^{18}O$ values between–0.9 ‰ and–4.9 ‰ and BOULD S6 having significantly more positive $\delta^{18}O$ values between 0.9‰ and –2.1 ‰. A small overlap occurs between the most positive $\delta^{18}O$ values in SCO S-2 and the most negative $\delta^{18}O$ values in BOULD S6. The shapes of the histogram are also different. SCO S-2 has a narrower range of $\delta^{18}O$ (3.2‰), with a higher density of values around the mean, producing a narrow and tall histogram with a normal distribution. Whereas, BOULD S6 has a larger spread of $\delta^{18}O$ values (3.3‰) and a lower density of $\delta^{18}O$ values around the mean. HAM S1 has the largest spread of $\delta^{18}O$ values (4.9‰). BS1/BS3 and HAM S1 have similar histogram shapes and spread of $\delta^{18}O$ values (BS1/BS3 = 3.5‰ and HAM S1= 5.5‰), although BS1/BS3 has a lower density around the mean. The most significant difference between the histograms in SCO S-2 (normal distribution) and the other horizons is that some of the individual specimen's histograms within HAM S4, HAM S1 and BS1/BS3 have a double peaked distribution rather than a normal distribution. These double peaks suggest that different years of growth had significantly different $\delta^{18}O$ value Comparison of the high resolution bulk $\delta^{18}O_{carb.}$with the average $\delta^{18}O_{carb}$ values obtained from the seasonality analysis are presented in Figure 7.12. The data show that the average $\delta^{18}O_{carb}$ values from the analysis of the *V. lentus* shell fragments plots towards more positive values than that of the average $\delta^{18}O_{carb}$ obtained from the shells analysed for seasonality. However there is some overlap with the standard deviation.

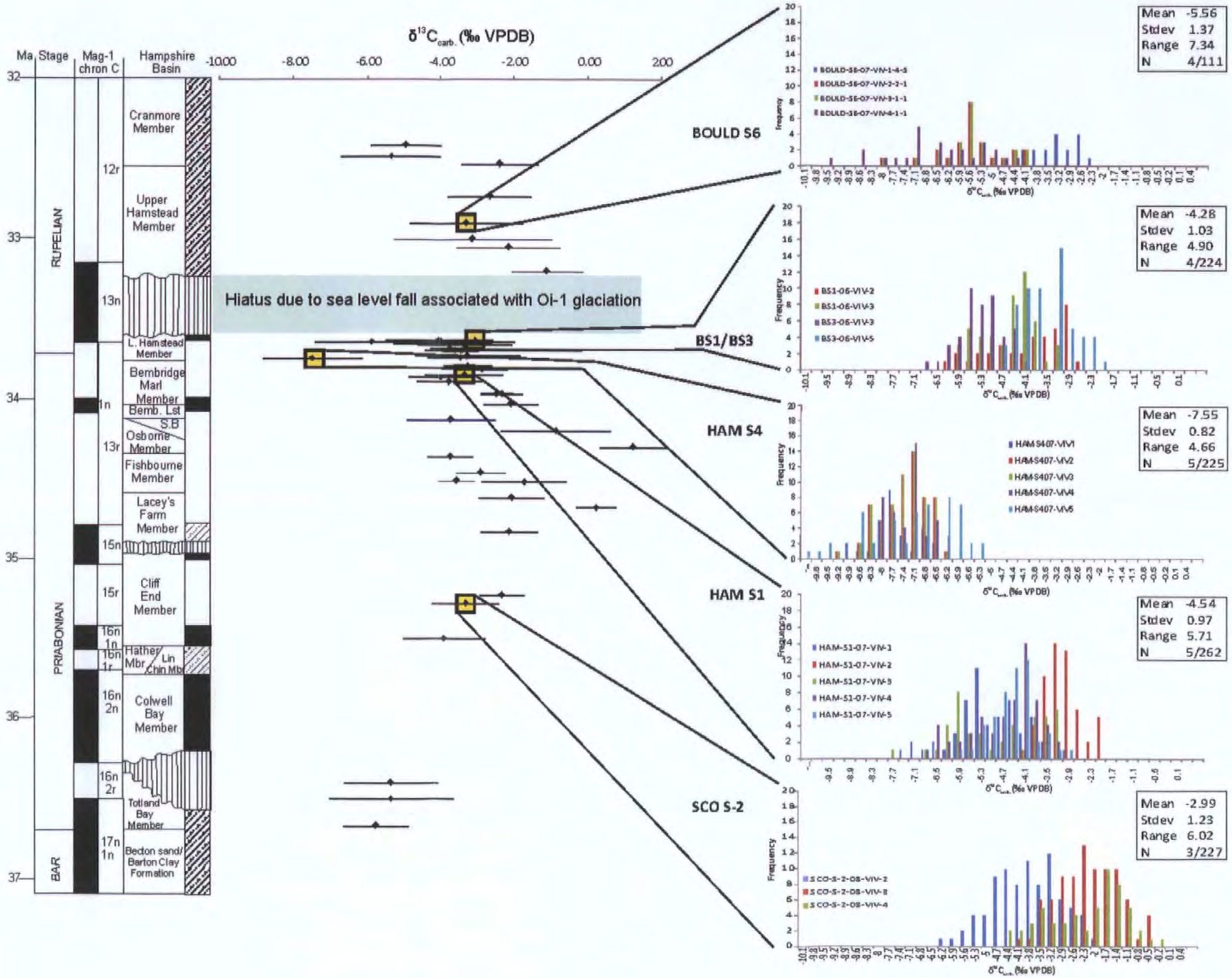

Figure 7.13 A histogram for five horizons in the Solent Group strata comprising of all the $\delta^{13}C$ data from each of the *V. lentus* specimens analysed from the horizon are compared with the $\delta^{13}C$ record produced from the analysis of *V. lentus* shell fragments (Chapter 6). Each histogram represents the frequency or number of times a $\delta^{13}C$ values appears in the seasonal profiles from all of the *V. lentus* specimens analysed from that horizon. The $\delta^{13}C$ values were grouped into 0.3‰ bins between –10.10‰ to 0.40‰. (N= number of gastropods per horizon/ number of analyses per horizon).

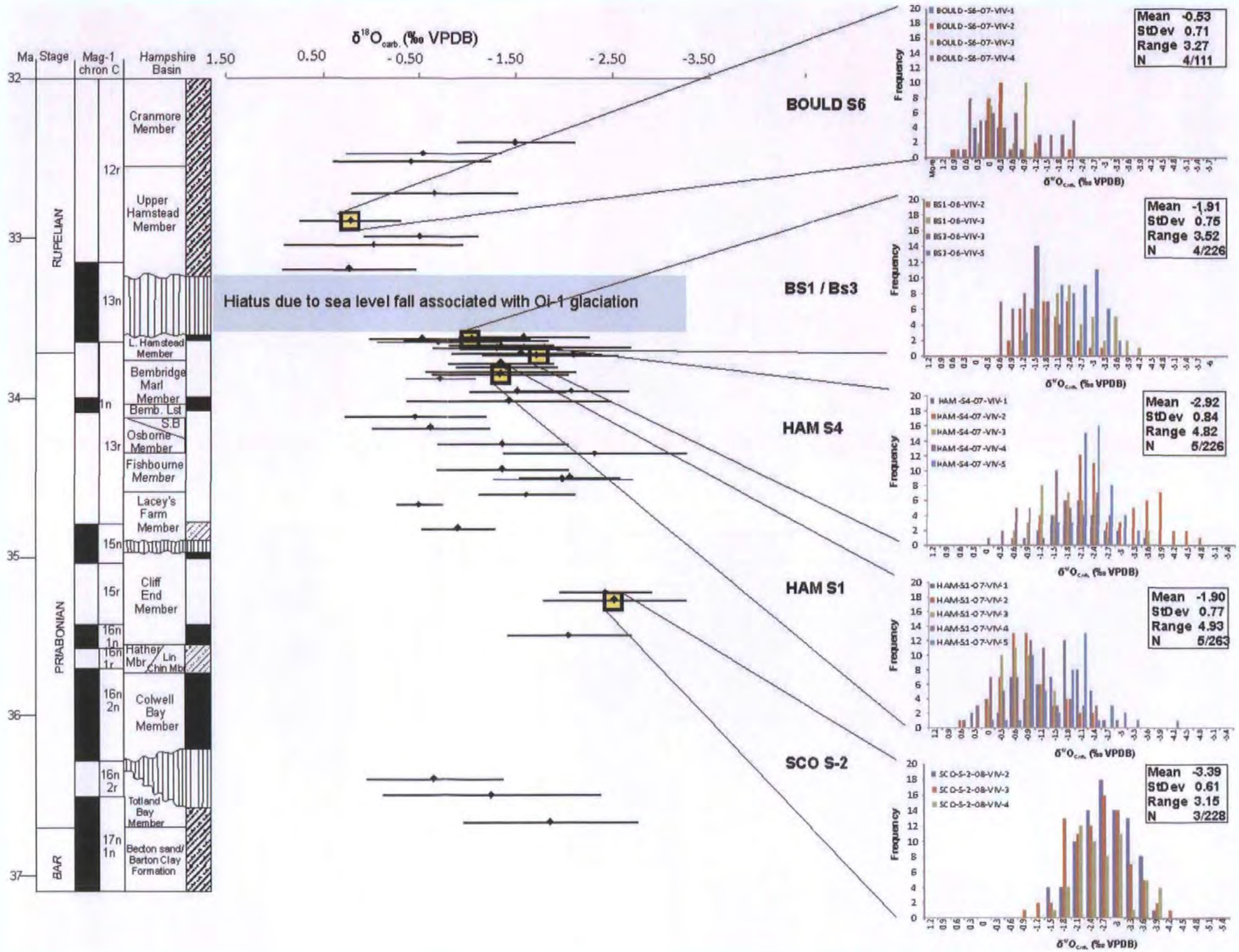

Figure 7.11 A histogram for five horizons in the Solent Group strata comprising all the $\delta^{18}O$ data from each of the *V. lentus* specimens analysed from the horizon are compared with the $\delta^{18}O$ record produced from the analysis of *V. lentus* shell fragments (Chapter 6). Each histogram represents the frequency or number of times a $\delta^{18}O$ value appears in the seasonal profiles from all of the *V. lentus* specimens analysed from that horizon. The $\delta^{18}O$ values were grouped into 0.3‰ bins between –6.00‰ to 1. (N= number of gastropods per horizon/ number of analyses per horizon).

The $\delta^{13}C$ values were grouped into 0.3‰ bins between −10.1‰ to 0.4‰. These histogram plots are presented in Figure 7.13. The mean, standard deviation and range is given for the combined histogram using all of the $\delta^{13}C$ values from the individual gastropods taken from that horizon.

Horizon SCO S-2 produces the most positive values, ranging between 6.3‰ to −0.3‰ with a mean of −3.0‰. HAM S1 has slightly more negative values with a mean of −4.5‰. HAM S4 has the most negative values over the smallest range (4.7‰), producing the most negative mean (−7.6‰) of all the horizons. This horizon also produces the most negative $\delta^{13}C$ values in the $\delta^{13}C$ record produced from the analysis of *V. lentus* shell fragments (Fig. 7.13). BS1/ BS3 produce similar values to HAM S1, with this horizon producing a mean of −4.3‰. BOULD S6 produces a very flat histogram with the largest range of $\delta^{13}C$ values. However, this large range is due to several $\delta^{13}C$ values of low frequency at the extreme ends of the histogram. Overall, the $\delta^{13}C$ values from the *V. lentus* specimens indicate little variation throughout the Solent Group Strata, bar one exception, HAM S4. Some of the individual specimen's histograms show double peaks (e.g. SCO-S-2-08-VIV-4 (green)). However, these do not coincide with the specimens showing doubles peaks in $\delta^{18}O$.

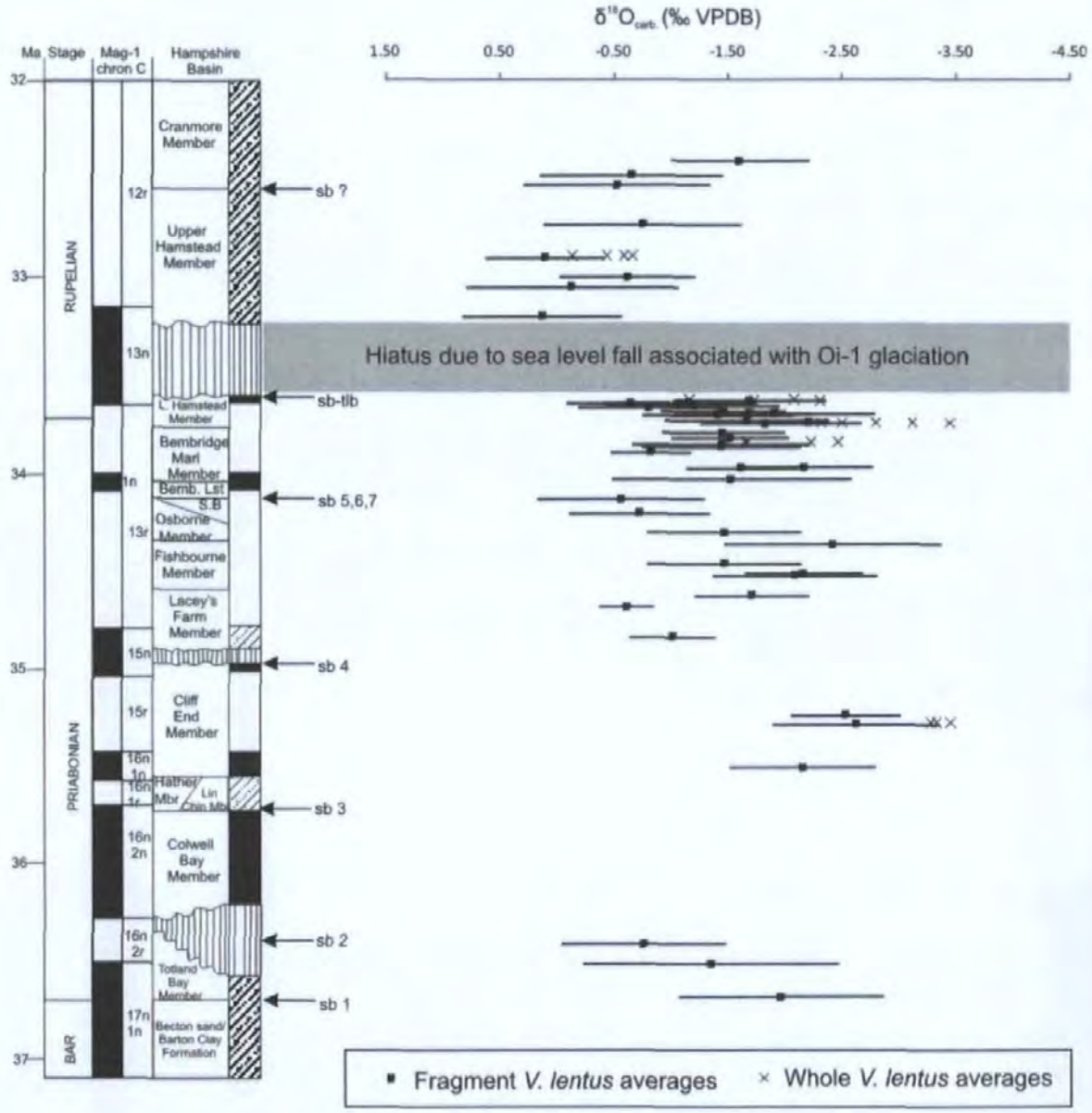

***Figure* 7.12 A comparison between the average $\delta^{18}O$ calculated from analysis *V. lentus* shell fragments and those calculated from the high resolution analysis of whole specimens.**

7.4.4 Isotopic variability of $\delta^{13}C$

A histogram for each horizon was constructed using the $\delta^{13}C$ values from the isotopic profiles of each *V. lentus* shell analysed. Each histogram represents the frequency or number of times a $\delta^{13}C$ value appears in the seasonal profiles from all of the *V. lentus* specimens analysed from that horizon. The individual specimens have been colour coded.

7.4.5 Shell structure

An example of a thin section of a *V. lentus* shell observed under crossed polarised light is shown in Figure 7.14. This figure clearly show that the fossil *V. lentus* has an outer layer which consists of alternating vertical crystals. The occurrence of a cessation in growth is represented by the new shell layer initiating underneath the older shell (Fig. 7.14 A). The older shell pinches out to a thin point prior to cessation.

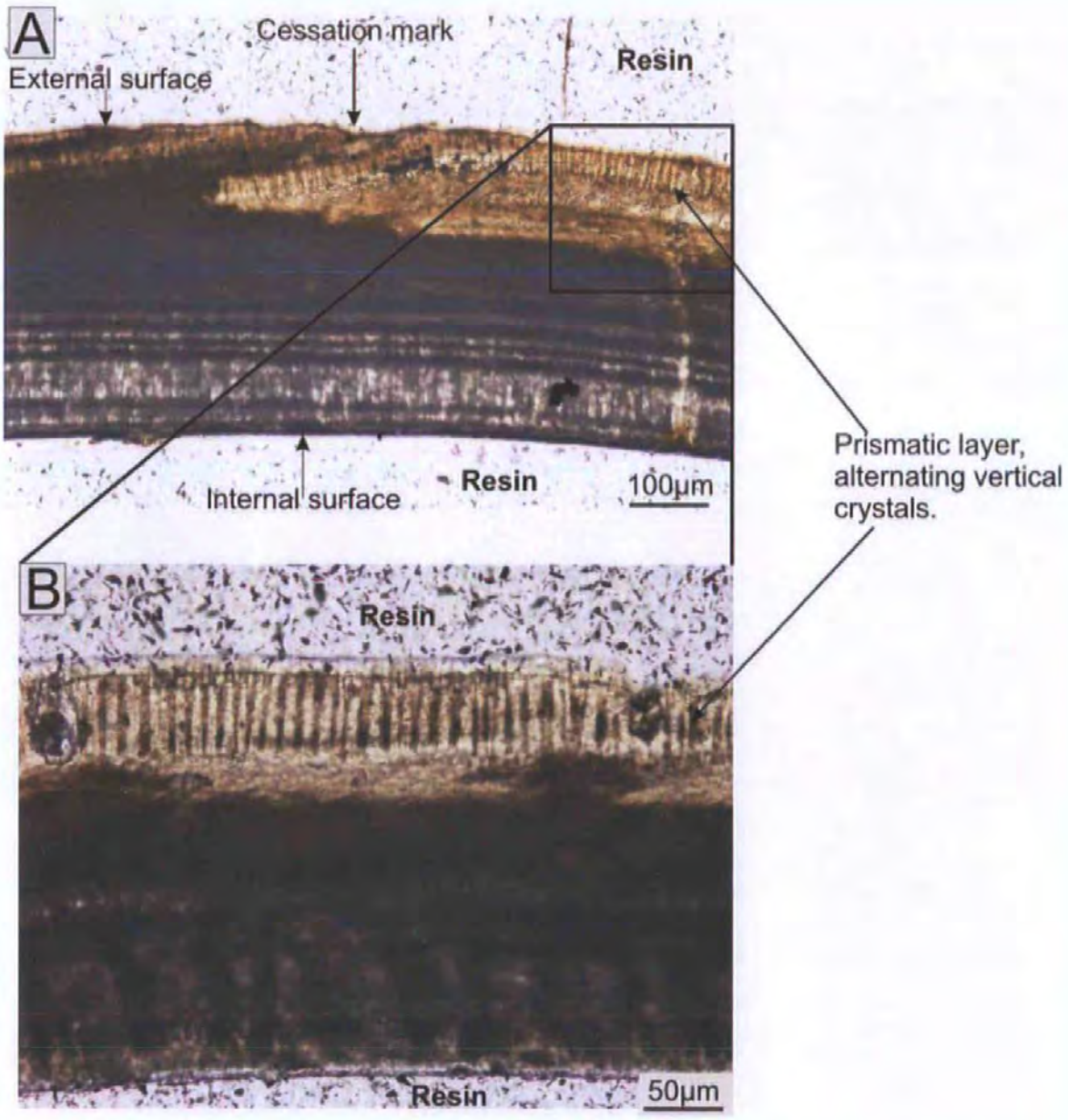

Figure 7.14 A thin section of a *V. lentus* shell observed under cross polarised light, showing the prismatic layer and an area of growth cessation.

7.5 Discussion

7.5.1 Preservation and shell structure

When comparisons are made between the shell structure of a fossil *V. lentus* specimen and that of a modern *Viviparus*, many similarities can be observed. On the outer edge of the shell the prismatic layer has the same crystal orientation and structure, with alternating ridges and troughs. This provides further evidence that post depositional alteration has not occurred on the sample in question. In Figure 7.14 A, the point of shell cessation forms the same structure as those seen in the modern *Viviparus* shells (Chapter 2, Fig. 2.15). Pinching out of the older shell prior to cessation indicates a slowing of shell secretion prior to cessation and deformation of the crystal structure in the prismatic layer. Initiation of the new growth occurs underneath the old shell preventing the formation of a weak area on the shell. The exact cause of cessation cannot be determined; therefore, it is not possible to equate this cessation to the crossing of a temperature threshold as disturbance, reproduction and predation are also possible causes.

All of the samples analysed using XRD analysis in Chapter 6 show that the composition of *V. lentus* shells were consistently aragonitic. The analysis of a modern *V. contectus* sample using XRD analysis showed that the shell carbonate of modern specimens is also aragonitic. The isotopic profiles produced from the high resolution drilling of whole *V. lentus* shells produces a cyclic isotopic pattern for both $\delta^{18}O$ and $\delta^{13}C$. If the isotopic composition had been diagenetically altered this signal would more than likely not have been preserved. Therefore, the fossil *V. lentus* specimens used in this investigation are considered to have retained their original isotopic composition.

7.5.2 Comparison of high and low resolution sampling

A comparison was made between the $\delta^{18}O_{carb.}$ isotope record produced in Chapter 6 with the average $\delta^{18}O_{carb.}$ values obtained from the high resolution analysis of individual specimens of *V. lentus* (Fig. 7.12). The data show that the average $\delta^{18}O_{carb.}$ values from the analysis of the individual specimens consistently plot towards more negative values.

A modern *Viviparus* specimen was subjected to both high resolution sampling and randomly selected fragments, both were analysed for $\delta^{18}O$ and $\delta^{13}C$. The data showed the same pattern that we see in the fossil material (Chapter 2; Fig. 2.18), where the average produced from the shell fragments plot towards more positive values than the average of the high resolution data. As suggested in Chapter 2 Section 2.6.11.1 the bulk fragments consist of the entire shell (all three shell layers) where during the micromilling procedure there is potential for part of the inner nacrecous layer to be missed during the drilling process. There is evidence that the nacrecous layer in bivalves may consist of re-deposited and / or isotopically heavy calcite (e.g. Cusack *et al.*, 2008). To test this several *Viviparus* shells (modern and fossil) could be sectioned into the individual shell layers, with each layer analysed for $\delta^{18}O$ and $\delta^{13}C$. This would potentially prove or disprove the theory of different shell layers having different isotopic compositions. This offset has implications for obtaining an isotopic seasonality profile and the calculation of palaeotemperatures (to be discussed in Section 7.5.5) from such data. In all instances the removal of the entire shell material was attempted however, it is possible that part of the inner nacrecous layer may have been missed during the sampling procedure. This must be kept in mind when making interpretations / conclusions from the data. Therefore, further investigations are required to understand the isotopic composition of the individual shell layers in *Viviparus*.

7.5.3 Seasonal Isotopic variability

A number of points need to be considered before an interpretation of the high resolution isotopic data can be made. Modern species of *Viviparus* on average live between 2 and 3 years (see Section 2.3.5, Chapter 2). Therefore, the isotopic values obtained from each individual gastropod specimen could represent between 2 and 3 years of growth. If we assume that each gastropod lived for at least 2 years (which their overall size would suggest) then for horizon SCO S-2, from which three *V. lentus* specimens were analysed, it can be estimated that the isotopic data obtained spans at least 6 years. This does assume that the specimens have not grown at the same time. It is not possible to determine whether these specimens grew at the same time as microenvironmental difference can subtly alter the isotopic signature preserved and minor reworking of the sediment may have mixed shells that lived at different times. However, freshwater gastropods are often found in large accumulations which are thought to represent death assemblages (Dillon, 2007) and therefore single events. The difference between a death event and a current sorted deposit are:

- Death event = range of sizes not too damaged
- Current sorted = broken, often unimodal size distribution.

It must also be noted that the amount of shell secreted once the specimen reaches sexual maturity (>2 years) reduces. The majority of the shell material analysed would therefore have been secreted within the specimens' first and second years. Although *Viviparus* are known to grow throughout the year, the largest proportion of the shell material will be secreted during spring and summer owing to food availability and life cycle (see Chapter 2 for more information). This would suggest that the specimens from each of the horizons would have recorded an isotopic history for a minimum of 6 years, but this isotopic record would have a predominantly spring / summer bias. In order for a climatic signal to be

produced a histogram combining all of the data from each horizon is required to draw out information on climate fluctuations. Each *V. lentus* specimen was drilled at the highest resolution achievable. However, analysis of the trial sample (BS3-06-VIV-5) showed that the isotopic analysis of every other drill line produced a sufficient record of the isotopic variability within that specimen. Owing to the constraints of time, instrument time and preservation of specimens, it was only possible to analyse a limited number of specimens per horizon. Although the 5 horizons analysed were chosen based on key isotopic excursions in the $\delta^{18}O$ record obtained from the analysis of *V. lentus* fragments (Chapter 6), several key events could not be analysed owing to preservational issues. This particularly applies to those horizons relating to the Late Eocene Event in the Osborne Member and up to the lower part of the Bembridge Marls Member.

How well the *V. lentus* specimens have recorded changes in seasonality depends on the crossing of thresholds and whether cessation of carbonate secretion has taken place. For example, if a reduction in growth rates occurs owing to the crossing of the winter temperature threshold, this would mean that the amount of material secreted would be significantly reduced during this time period (Fig. 7.15B). Therefore, the number of times the isotopic values are recorded for this time period is significantly less than those when the specimens are growing at a faster rate: e.g. during spring or summer. Growth cessation is also observed on the majority of *V. lentus* specimens analysed (see Table 7.2). The amount of time missing during these cessation periods is impossible to determine; therefore a part of the isotopic record is considered to be missing. The causes of cessation are variable ranging from: winter or annuli bands, formed during the winter when temperatures fall below the species cold temperature threshold; inhibition of growth at high temperatures; lack of food / starvation; physical disturbances (e.g. predation); reproduction

and fluctuations in salinity. The $\delta^{18}O$ profiles show that a large proportion of the cessation marks appear to coincide with relatively positive values (see Table 7.2). In some cases, for example specimen SCO S-2 08 VIV 2 line 55 (48.7 mm from the aperture), the cessation appears to mark a sharp shift from relatively positive to negative $\delta^{18}O$ values, suggesting that a significant time period is missing from the $\delta^{18}O$ profile. This sharp shift is mirrored by the $\delta^{13}C$ profile. Other specimens show several faint marks suggesting a slowing of growth but not complete cessation. In HAM S1 07 VIV4 section 2 has a large number of faint marks (42.4 to 50.7 mm from the apex). This would suggest that the specimen may have been under environmental stress at this time. This part of the shell has a prolonged period of positive $\delta^{18}O$ values and would suggest that temperature may have fluctuated around the lower growth temperature threshold inhibiting shell secretion. Life cycles may explain the small number of cessation marks coinciding with relatively negative $\delta^{18}O$ values, including reproduction which is known to take place during spring and summer. Males are known not to consume food during the reproductive period reserving all their energy for reproduction and this may also be responsible for growth cessation. It is impossible to determine the sex of a specimen from its hard part anatomy; therefore modern examples would need to confirm this theory.

Schmitz and Andreasson (2001) have shown that for all of the *Viviparus* shells they analysed from the temperate and subtropical zones the most positive $\delta^{18}O$ values coincide with a zone of thickened and irregular growth layers (cessation marks), reflecting decreased growth rates in connection with winter hibernation. Observation of modern *Viviparus contectus* and *Viviparus viviparus* (see Chapters 2 and 3) indicate that *Viviparus* translocates to the bottom muds during October / November depending on average water temperatures. The animals migrate back to the surface during April to release their young.

This life cycle has also been recorded for *V. ater* (Staub and Ribi, 1995) and *V. georgianus* (Jokinen *et al.*, 1982). How this migration affects the isotopic records obtained from this genus is an important consideration. If this migration were to affect the isotopic composition it would be most clearly seen from those specimens obtained from the horizon SCO S-2. Only one specimen indicates a significant shift in isotopic values which is though to be related to cessation of growth rather than migration. Owing to the relatively shallow nature of the water bodies in which *Viviparus* is found it is unlikely that the $\delta^{18}O_{water}$ values varied significantly with depth. However, a small temperature difference may be recorded depending on the depth of the water body. Collinson (1983) suggested that water depths in the plant bearing horizon of the Bembridge Marls Member reached depths of ~3 m. The biological requirement of *Viviparus* means that they would not be found in stratified water bodies (Harman, 1974; Jokinen, 1983; Strayer, 1990).

From this information it seems likely that the majority of growth cessations occur during the winter months owing to cooler temperatures. This confirms that the isotopic results obtained are likely to be biased to spring and summer values. Although some growth still occurs during the winter months as suggested by those shells that have faint marks indicating slower growth rates but not complete cessation, shell secretion is significantly reduced at this time of the year.

Horizon	Specimen	Drill line No.	Distance from apex (mm)	$\delta^{13}C$ (‰VPDB)	$\delta^{18}O$ (‰VPDB)	Average $\delta^{18}O$ (‰VPDB) for specimen
BOULD S6 (Upper Hamstead Member)	BOULD S6 07 VIV 1	No clear cessation marks				-0.2
	BOULD S6 07 VIV 2	No clear cessation marks				-0.4
	BOULD S6 07 VIV 3	3	44.0	-6.2	-0.1	-0.6
		13	35.2	-8.8	-0.3	
	BOULD S6 07 VIV 4	No clear cessation marks				-0.7
BS1/BS3 (Top Lower Hamstead Member)	BS1 06 VIV 2	13	38.6	-3.0	-1.0	-1.7
		51	22.1	-3.1	-0.7	
	BS1 06 VIV 3	29	35.0	-3.9	-1.4	-2.3
		45	28.8	-4.1	-1.1	
	BS3 06 VIV 3	No clear cessation marks				-1.2
	BS3 06 VIV 5	52	45.9	-2.9	-1.2	-2.1
		54	45.3	-2.9	-1.2	
HAM S4 (Base Lower Hamstead Member)	HAM S4 07 VIV 1	3	48.1	-8.1	-2.1	-2.2
		25	39.1	-8.5	-2.6	
		51	28.4	-7.7	-2.1	
	HAM S4 07 VIV 2	47	46.9	-8.4	-2.9	-1.7
		83	31.8	-6.8	-2.5	
	HAM S4 07 VIV 3	2	54.4	-	-	-1.5
		25	44.3	-	-	
		27	43.5	-	-	
		58	32.3	-	-	
	HAM S4 07 VIV 4	13	45.4	-7.3	-1.8	-1.7
		19	42.9	-8.1	-2.4	
		58	27.4	-7.3	-2.2	
	HAM S4 07 VIV 5					-2.5
HAM S1 (Bembridge Marls Member)	HAM S1 07 VIV 1	10	52.2	-7.1	-2.7	-2.8
		70	25.4	-3.7	-2.4	
	HAM S1 07 VIV 2	20	41.3	-	-	-3.5
	HAM S1 07 VIV 3	15	36.5	-4.5	-1.6	-2.5
		31	28.8	-5.5	-1.8	
		43	23.4	-3.9	-2.1	
		45	22.8	-	-	
	HAM S1 07 VIV 4	40	53.3	-4.2	-1.8	-2.3
		49	50.7	-3.6	-1.6	
		73	41.7	-4.5	-0.6	
		79	38.0	-4.5	-0.7	
	HAM S1 07 VIV 5	12	43.4	-4.1	-2.8	-3.1
		33	34.1	-	-	
		52	27.4	-4.9	-1.7	
SCO S-2 (Cliff End Member)	SCO S-2 08 VIV 2	3	68.3	-5.5	-2.9	-3.5
		41	53.0	-6.3	-3.9	
		53	48.7	-4.4	-2.8	
		55	48.0	-2.7	-2.8	
		109	29.6	-	-	
		154	14.2	-	-	
	SCO S-2 08 VIV 3	131	65.1	-2.2	-2.5	-3.3
	SCO S-2 08 VIV 4	41	39.2	-1.6	-2.5	-3.4
		135	9.1	-	-	

Table 7.2 Information on the position of cessation marks on each *V. lentus* specimen analysed including the isotopic values associated with them. The average $\delta^{18}O$ value for each specimen is also given so that a comparison can be made.

7.5.3.1 Isotopic profile shapes

Increased seasonal variability in both temperature and $\delta^{18}O_{water}$ along with periods of cessation can significantly affect the amplitude and frequency of the $\delta^{18}O$ profiles of individual shells. In an equable climate the $\delta^{18}O$ values obtained would show little variation because of the consistency of temperature (Fig. 7.15A). However, this assumes a humid environment where $\delta^{18}O_{water}$ values are not altered by significant evaporation. In a seasonal climate where temperature fluctuates in a cyclic pattern the amplitude is significantly increased (Fig. 7.15B). However, if cessation occurs this can alter the overall shape of the profiles by decreasing both amplitude and frequency producing a much sharper shaped profile (Fig. 7.15B). These profile shapes alter through the life cycle of the specimen, with the cyclic changes in isotopes composition becoming compressed towards the aperture where growth is compromised due to energy requirements for reproduction (Fig. 7.15C). This can be seen particularly well in specimens HAM S4 07 VIV 2; 3; 5 and HAM S1 07 VIV 4. The cyclic changes observed in these isotopic records suggest that these specimens lived for 2 to 3 years, confirming the hypothesis made previously regarding the amount of time recorded by an individual *V. lentus* specimens.

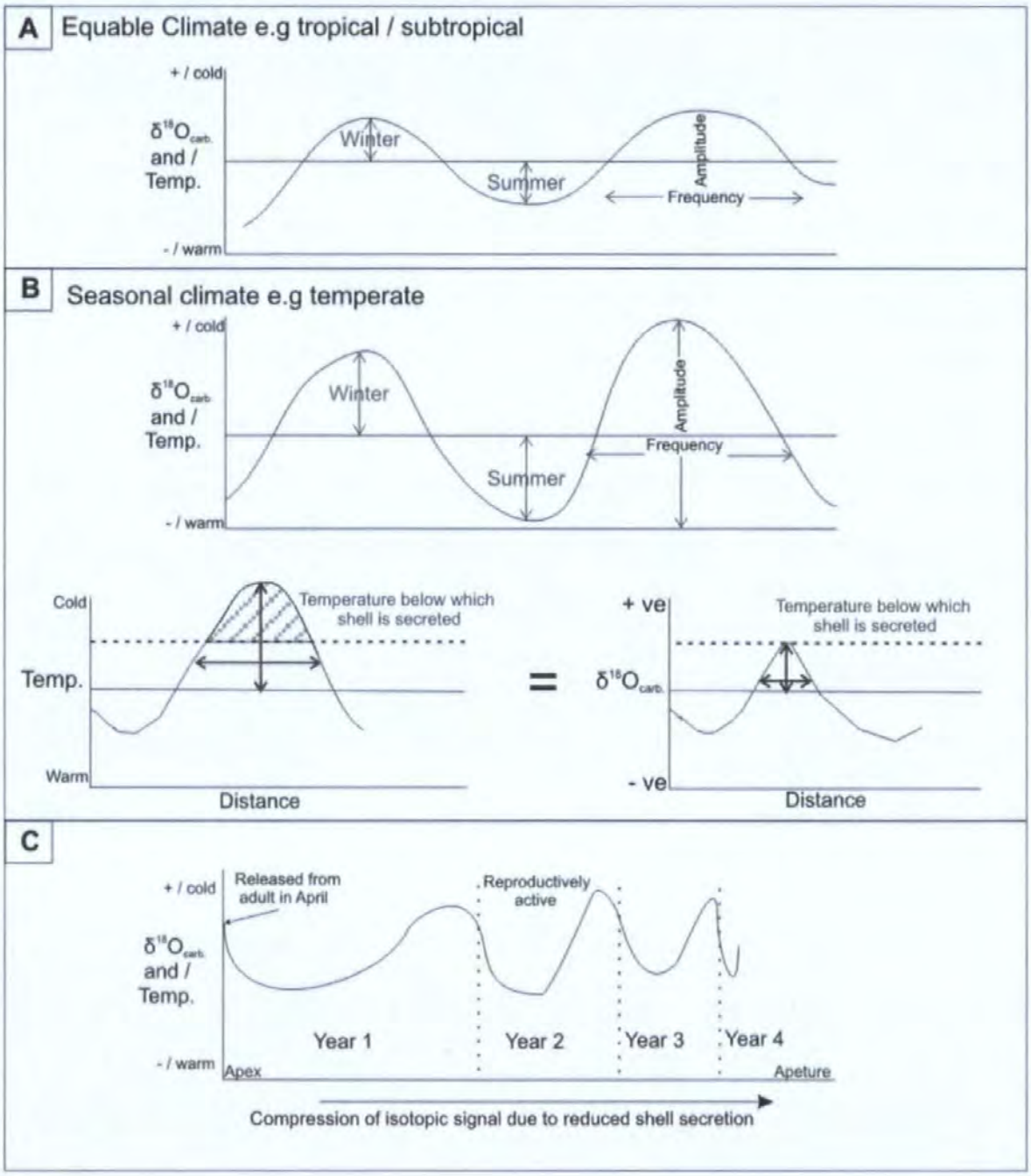

Figure 7.15 Two hypothetical examples of the $\delta^{18}O_{carb.}$ profiles from two climatic regimes. A. Shows the $\delta^{18}O_{carb.}$ profiles expected to be found from equable climates where both the $\delta^{18}O_{water}$ and temperature are relatively stable. B. Shows the likely $\delta^{18}O_{carb.}$ profiles obtained from a seasonal climate where temperature is the dominant control producing greater seasonal differences. An example is shown were the cold or winter temperature threshold is crossed after which shell secretion ceases. This halt in shell secretion produces a condensed $\delta^{18}O_{carb.}$ Profile. C. A hypothetical $\delta^{18}O_{carb}$ profile showing the compaction of the predicted isotopic record caused by the reduction in growth rates initiated by the specimen reaching sexual maturity after which energy is conserved for reproduction rather than for shell secretion.

7.5.3.2 Seasonality of $\delta^{18}O$

Determining seasonality from $\delta^{18}O$ in specimens of *V. lentus* firstly requires the acquisition of a high resolution $\delta^{18}O$ records from several specimens. Those specimens sampled from horizon BOULD S6 do not provide a sufficient amount of data to determine changes in the seasonality of $\delta^{18}O$. As indicated in Section 7.4.3 the most significant difference between the histograms in SCO S-2 and the other horizons is that some of the specimens individual histograms have a double peaked distribution rather than a normal distribution (as seen in those specimens in horizon SCO S-2). This is thought to be related to a significant difference in $\delta^{18}O$ values recorded from one year to the next. The specimen which shows this most clearly is HAM-S4-07-VIV-2, both in the isotopic profile (Fig. 7.8) and in the histogram in Fig.7.11. There are several theories that could be applied to this:

1. A seasonal difference in the $\delta^{18}O$ of the host water:
    a. Temperature related; and
    b. Changes in the hydrological system.
2. The *V. lentus* specimen had migrated to a different microenvironment; or
3. That the first year of the specimens life was spent in the bottom muds as a juvenile whereas during the second year, when the *Viviparus* become reproductively active, the specimen migrated to near surface waters.

As more than one specimen from more than one horizon has a double peaked distribution it would suggest that this is not an isolated event or specimen specific. This would suggest that seasonal differences are a plausible explanation. To define the source of this difference (e.g. temperature changes or changes in the meteorological cycle etc) clumped isotope thermometry may be key (see Chapter 4).

In summary a noticeable change in the histogram distribution between SCOS-2 and the remainder of the sections exists. To test whether this is significant several horizons between SCOS-2 and HAM S1 need to be analysed to confirm this shift from what could potentially be an equable to seasonal climate.

7.5.3.3 Seasonality of $\delta^{13}C$

The individual isotopic profiles suggest that in the majority of specimen's $\delta^{18}O$ and $\delta^{13}C$ profiles co-vary in a cyclic pattern. The majority of evidence from experimental analysis on molluscs suggests that the dominant control on the $\delta^{13}C$ composition of freshwater shell carbonate is total dissolved inorganic carbon (TDIC) of the host water (Fritz and Poplowski, 1974; Tanaka *et al.*, 1986; Romenek *et al.*, 1992; McConnaughey *et al.*, 1997). Controls on $\delta^{13}C_{TDIC}$ of the host water in lakes include changes in: lake residence time, catchment vegetation cover and lake productivity (Leng *et al.*, 2005). A seasonal increase in aquatic macrophyte coverage would have enriched the waters in ^{13}C, as photosynthesis preferentially uptakes ^{12}C, producing higher (positive) $\delta^{13}C_{TDIC}$. This can be clearly seen in the *V. lentus* profiles (Figs. 7.6 - 7.10). Such cyclic patterns would suggest that the environment which *V. lentus* inhabited had a seasonal aquatic biomass, where growth was occurring during the warmer months and died off in the cooler months. However, as discussed in Chapter 2 (Section 2.6.8) metabolised carbon and the availability of carbon as a food source has some influence on $\delta^{13}C$ of the *Viviparus* shell carbonate. The proportion of $\delta^{13}C_{TDIC}$ and metabolic $\delta^{13}C$ may change seasonally or be related to the species' life cycle, e.g. reproduction and associated migration. It is therefore difficult to determine the exact source of carbon influencing the *V. lentus* profiles.

When all the data from the individual specimens are combined for each horizon to construct a histogram, HAM S4 has significantly more negative $\delta^{13}C$ values than the other horizons. Development of ponds and marshes in the distal end of the catchment where water flows are of low energy, have sources of carbon that are almost exclusively from the massive decay of $\delta^{13}C$ depleted organic matter (Bonadonna *et al.*, 1999). This would produce relatively negative $\delta^{13}C$ values as the decomposition of organic matter involves respiration which would enrich the water with ^{12}C. HAM S4 was sampled from the basal part of the Black Band, a persistent organic layer forming the boundary between the Bembridge Marls and the Lower Hamstead Member. This type of environment could explain the shift to the relatively negative $\delta^{13}C$ values we see in this horizon.

7.5.4 Climatic zones

The horizons analysed have been divided into three different time periods:

1. Pre E/O transition (SCO S-2);
2. E/O transition (HAM S1; HAM S4; BS1/BS3); and
3. Post Oi-1 glacial maximum (BOULD S6).

The $\delta^{18}O$ values are plotted against the $\delta^{13}C$ values for each of the three time periods (Fig. 7.18). For comparison a single specimen of *V. contectus* (taken from Chapter 2) analysed at high resolution is also plotted to represent a modern northern temperate climatic zone. Added to the graph are three circles representing the subtropical, humid and temperate climatic zones. These zones were determined by the author from the isotopic results obtained by Schmitz and Andreasson (2001) who analysed a variety of modern *Viviparus* specimens from these different climatic zones.

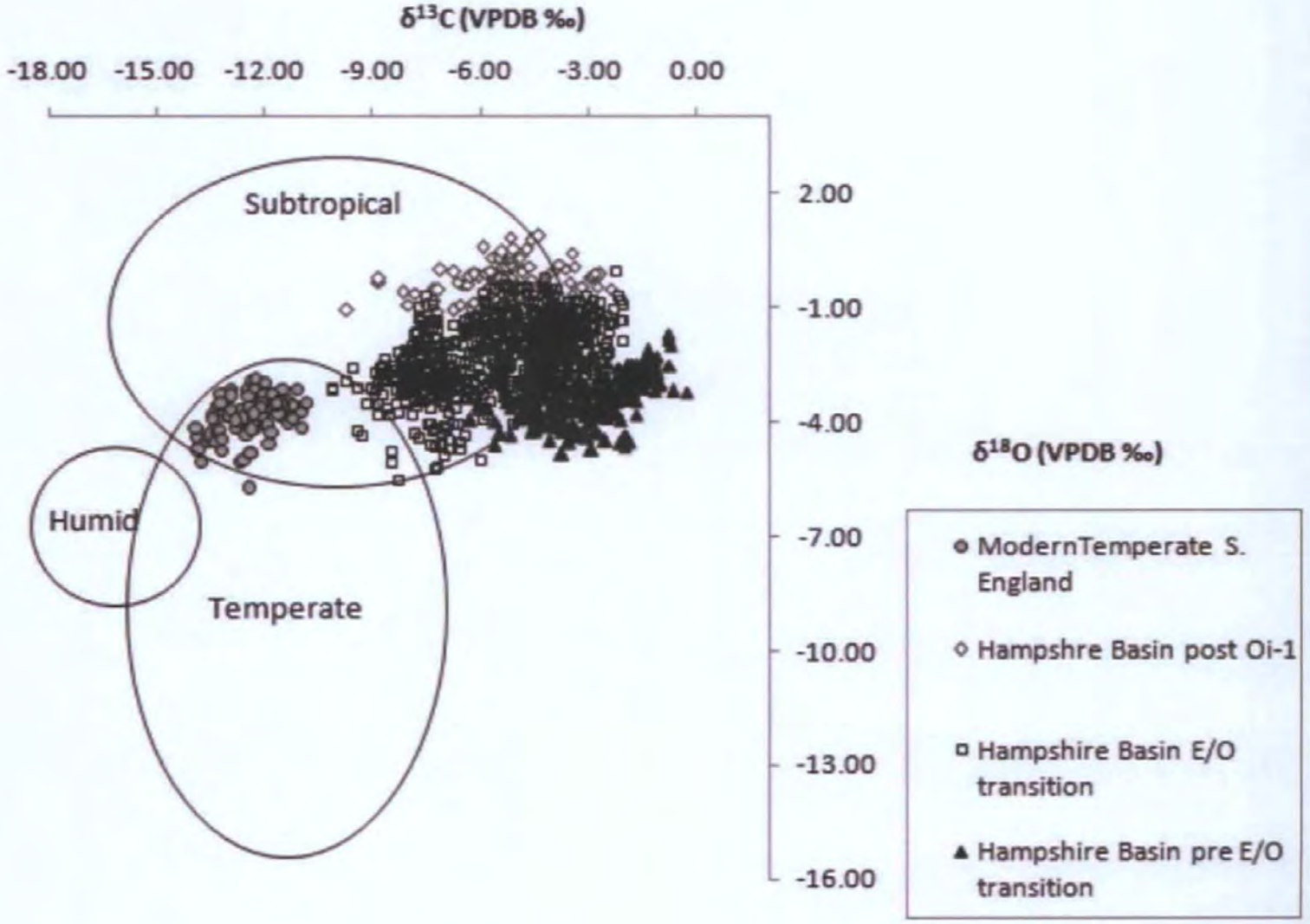
δ13C (VPDB ‰)
-18.00
-15.00
-12.00
-9.00
-6.00
-3.00
0.00
Subtropical
Humid
Temperate
2.00
-1.00
-4.00
-7.00
-10.00
-13.00
-16.00
δ18O (VPDB ‰)
ModernTemperate S. England
Hampshre Basin post Oi-1
Hampshire Basin E/O transition
Hampshire Basin pre E/O transition

Figure 7.16 Comparison of the isotopic composition of *Viviparus* spp. from modern climate zones indicated by the circles labelled subtropical, humid and temperate (taken from Schmitz and Andreasson, 2001). Plotted onto this are the isotopic fossil data obtained from the seasonality study from the Hampshire Basin (UK) and modern isotopic values obtained from the high resolution analysis of a *Viviparus contectus* specimen taken from South Drain Canal on the Somerset Levels (UK) (see Chapter 2).

All three time periods either fit within or are to the right of the area representing isotopic values obtained from the subtropical climatic zone. Although there are a few data points which cross into the subtropical / temperate overlap, but these may be related to the relatively negative $\delta^{13}C$ values associated with the deposition of the Black Band. Isotopic values obtained from a modern *V. contectus* specimen fit within the area defining the temperate climatic zone. A shift in the climatic zone would be expected, owing to the

northward displacement of Europe by plate tectonics over the last 45 million years. This would have produced an overall temperature decrease of 4 °C in the mean annual temperature when assuming that a decrease of 0.4°C per degree of MAT for the European latitudinal shift (Mosbrugger *et al.*, 2005). During the Paleogene Britain was ~10 degrees of latitude further south than it is today (Van der Voo and French, 1974; Hodgson *et al.*, 1990). This would place the Hampshire Basin at approximately the same latitude as present day Portugal. However, with a different global climate zone then today therefore not entirely comparable. Brooks (1949) considered climatic zones in the northern hemisphere during the Tertiary to lay 10 to 15° N off their present position. According to Collinson (2000) during the Eocene thermal maximum subtropical vegetation extended to palaeolatitudes of at least 55° North and South. This would put the Hampshire Basin in the tropical to subtropical climatic zone during the Eocene. However, Daley (1972b) implied that southern England had a western margin warm temperate or Mediterranean climate, with typically dry summers. Evidence from the present study does support his interpretation.

Reid and Chandler (1933) and Collinson (2000) both suggested the existence of a tropical climate in the Early to Early-Middle Eocene with periods of maximum warmth allowing *Nypa* to dominate coastal mangrove communities (Collinson, 1990). The presence of such plant communities suggests that the climate was frost free or remained above 5°C at this time. During the late Eocene, calcrete deposits within the sediments encompassing the Hatherwood Limestone Member to the Bembridge Limestone Formation provide evidence of relatively dry climatic conditions (Daley, 1999). Land snails found within these calcretes have living relatives which occupy shady forest habitats (Preece, 1980; Paul 1989). Edwards (1991) implied that these environments indicate dry conditions which occur during regressive and pedogenic phases; therefore, during these periods the climate may have alternated between humid and dry conditions.

The Bembridge Marls Member has received a large amount of attention over the years with various authors coming to varying climatic conclusions. Reid and Chandler (1926) concluded that the Bembridge flora indicated a humid subtropical climate. Chandler (1964) altered her interpretation after her re-investigation suggested that the flora was indicative of a tropical climate. Machin's (1971) palynological investigations led her to conclude that the Bembridge Marls Member was deposited in a subtropical climate. More recently, Jarzembowski's (1980) investigation into the insect assemblage of the Bembridge Marls Member, which included the presence of termites, indicated a climate close to the warm temperate (sub-tropical) to tropical boundary. In the present study isotopic values obtained from the upper part of the Bembridge Marls Member into the lower Hamstead Member suggest an increase in isotopic variability of $\delta^{18}O$. The floral transition at this time is gradual, with loss of paratropical elements and incoming of deciduous elements from the late middle Eocene (Collinson, 1992). In the late Eocene to early Oligocene Machin's (1971) palynofloral investigation implies a significant but not sudden change in palynoflora at the boundary of the Hamstead Member with the Bembridge Marls. Above the boundary most forms increasing or appearing for the first time are characteristically northern temperate forms with tropical forms disappearing (Machin, 1971). Collinson (1992) confirmed Machin's (1971) interpretation, suggesting that a warm and seasonal climate existed. The change to more temperate climates is also noted else-where in Europe during the late Eocene (e.g. Mosbrugger *et al.*, 2005). These changes in the palaeoflora indicate a climatic shift towards cooler conditions and confirm that the transition from tropical/ subtropical to subtropical / temperate occurred during the E/O transition. During this period mixed evergreen and deciduous forest replaced the evergreen subtropical forest of the late Eocene (Collinson, 1992). Grimes *et al.* (2005) suggest that the presence of numerous crocodilians, a variety of fruit-eating mammals, pollen of palm trees, and foliage (fertile and sterile) of the fern genus *Acrostichum* (Collinson, 1983; Collinson and Hooker,

1987, 1991; Markwick, 1994; Hooker *et al.*, 2004) indicate that coldest month mean temperature did not generally fall below freezing .

In summary the E/O transition, which takes place between the Bembridge Marls Member and the lower Hamstead Member represents the transitional period between Greenhouse and Icehouse climatic regimes. The climate instability at that time is indicated by the large range of $\delta^{18}O$ recorded from these horizons. Once climate had crossed the threshold into a new climatic regime and climate stability took hold the range of $\delta^{18}O$ values is reduced, as indicated by the horizon BOULD S6. The range for this horizon is similar to that of SCO S-2; however, the mean $\delta^{18}O$ is displaced by 2.9‰.

7.5.5 Temperature calculations

In order to fully understand the observed changes in the $\delta^{18}O$ and its relationship to seasonality, palaeotemperature calculations are necessary. Owing to the unknown seasonal variability of $\delta^{18}O_{water}$ it is currently impossible to calculate temperature from the $\delta^{18}O_{carb}$ profiles. It may be possible in the future for temperature and in turn the $\delta^{18}O_{water}$ to be calculated using clumped isotope analysis, as discussed in Chapter 4 and Chapter 6. However, the current sample mass required for analysis is far larger than the high resolution drilling process can provide from this study. However, seasonal temperature variation from otoliths has been achieved using clumped isotope analysis (Ghosh *et al.*, 2007). As discussed in Chapters 4 and 5, seasonal temperature variation may be achievable through clumped isotope analysis of *Viviparus* in the future.

7.5.6 Biotic turnovers and shifts in seasonality

An increase in seasonality isotopic variability has been shown to occur between the Cliff End Member (SCO S-2) and the Bembridge Marls Member (HAM S1). The $\delta^{18}O$ record from Chapter 6 has shown that a significant isotopic excursion took place (Late Eocene

Event) during the time period between these horizons. As discussed in Chapter 6, several pieces of independent evidence from the Solent Group support the notion that part of this $\delta^{18}O$ excursion could be related to changes in temperature. Although it was not possible to analyse any of the horizons across this time period for seasonality, the data prior to and post this excursion suggest a possible increase in seasonality.

If we assume that the environment *V. lentus* inhabited was part of an open hydrological system the uptake of $\delta^{18}O$ would be controlled by either changes in the $\delta^{18}O_{water}$ and / or temperature. Across the Oi-1 glacial maximum a significant shift in the $\delta^{18}O_{carb.}$ (1.3‰) can be seen. In the marine realm this shift is thought to be dominated by a shift in the $\delta^{18}O_{water}$ as a consequence of continental ice accumulation on Antarctica (e.g. Katz *et al.*, 2008). However, a small part of the shift has been attributed to the ongoing long-term cooling. From the limited number of horizons analysed it would appear that potential changes in seasonality may have had an impact on some of the IOW biota (e.g. charophytes and flora) before the Oi-1 glacial maximum. These changes may have impacted on the synchrony of particular species' food and habitat resources. Joomun *et al.* (2008) have hypothesised that changing food availability is an important factor in mammalian extinctions across the E/O transition and are currently investigating this further.

An increase in seasonal range, i.e., colder winters, could decrease the length of growing time and inhibit any growth during winter months. The shift from an equable to a seasonal climate, as seen in the E/O transition, would increase the amount of environmental stress inflicted on biota and may explain the biotic turnovers and morphological shifts seen in both terrestrial and aquatic biota.

7.5.7 Seasonality: A global perspective

Owing to a significant hiatus, it is impossible to determine seasonality changes associated with the Oi-1 glacial maximum itself. The horizon analysed after the Oi-1 glacial maximum suggests that seasonality had decreased which, is in contrast to other datasets (e.g. Ivany *et al.*, 2000). However, one horizon is not conclusive of the overall trend and further work is required. Further high resolution analyses are hindered by poor specimen preservation after the Hamstead Member hiatus. Nevertheless, this study has highlighted a potential climate change prior to the E/O transition, which at the present level of analysis is driven by an increase in seasonality into the E/O transition.

The majority of investigations suggest that the decline in MAT's across the Oi-1 glacial maximum was brought about by a decrease in the cold monthly mean (e.g. Wolfe, 1978, 1994; Ivany *et al.*, 2000; Kobashi *et al.*, 2001; Mosbrugger *et al.*, 2005; Eldrett *et al.*, 2009). From the $\delta^{18}O$ histograms it would appear that this may also be true for the freshwater temperatures of the Solent Group strata. Declining Pco_2 may have contributed to global cooling and preconditioned the system for explosive ice sheet growth during the Oi-1 glacial maximum (33.5 Myr ago) when orbital parameters were favourable (Pearson *et al.*, 2009).

7.6 Summary

The main conclusion from this investigation is that more research is required to fully understand the data presented. Several areas have been highlighted which require further investigation:

1. Sampling methodology:

It was highlighted by both the modern and fossil *Viviparus* studies that a difference between the $\delta^{18}O$ data from *Viviparus* shell fragments and high resolution samples exist. Work carried out on bivalves (Cusack *et al.*, 2008) has suggested a difference in the $\delta^{18}O$ composition of the prismatic and nacraceous exists. This needs further investigation on both modern and fossil specimens.

2. The high resolution $\delta^{18}O$ data suggests a possible shift from an equable to seasonal climate between the Cliff End Member and the Bembridge Marls Member. To determine whether this interpretation is correct:
    a. Increased number of gastropod specimens need to be analysed per horizon; and
    b. an increased number of horizons need to be sampled (particularly between the Cliff End Member and the Bembridge Marls Member).
3. An in depth investigation needs to be carried out into cessation marks, migration and life cycles of modern specimens and to a lesser extent fossil specimens of *Viviparus*.
4. An understanding of the process by which $\delta^{13}C$ is incorporated into the shell within modern specimens of *Viviparus* is needed so that it can be applied to the fossil specimens.
5. A study into the use of clumped isotope analysis is needed to define whether the perceived changes in seasonality and climate are related to temperature shifts or changes in the meteorological cycle.

CHAPTER 8 CONCLUSIONS

8.1 Modern study

To accomplish the overall aims of this study an investigation into modern specimens of *Viviparus* were required in order to make sound conclusions on the data obtained from the fossil record. The genus *Viviparus* was chosen based on its abundance and preservational quality within the Eocene / Oligocene sediments from Solent Group strata, Isle of Wight (IOW). An investigation into the biology of *Viviparus contectus* (*V. contectus*) and *Viviparus viviparus* (*V. viviparus*) and its affect on the isotopic composition of its shell carbonate was undertaken. Experimental measurements of the $^{18}O/^{16}O$ isotope fractionation between the biogenic aragonite of *V. contectus* and *V. viviparus* and its host freshwater were undertaken to generate species' specific thermometry equations. The condition of the *V. viviparus* shells and poor linear regression outputs calculated for the relationship between $\Delta\delta^{18}O$ ($\delta^{18}O_{carb.} - \delta^{18}O_{water}$) and temperature lead to the conclusion that the specimens of *V. viviparus* collected from Exeter Canal were not suitable for producing a robust thermometry equation. However, experimental analysis using specimens of *V. contectus* were successful in generating a thermometry equation. The temperature dependence of the fractionation factor and the relationship between $\Delta\delta^{18}O$ and temperature, were calculated from specimens of *V. contectus* maintained under laboratory and field (collection and cage) conditions. Application of a linear regression to the datasets indicated that the gradients of all three experiments were within experimental error of each other (±two times standard error) therefore, a combined (laboratory and field data) correlation could be applied. The relationship between $\Delta\delta^{18}O$ and temperature (T) for this combined dataset is given by:

$$T = -7.43(+0.87, -1.13)*\Delta\delta^{18}O + 22.89(\pm 2.09)$$

(T is in °C, $\delta^{18}O_{carb.}$ is with respect to Vienna Pee Dee Belemnite (VPDB) and $\delta^{18}O_{water}$ is with respect to Vienna Standard Mean Ocean Water (VSMOW). Quoted errors are 2 times standard error).

The results from this study indicate that *V. contectus* does not exhibit any significant species specific vital effects when secreting its shell carbonate. This species also appears to precipitate its shell in oxygen isotopic equilibrium with the host water, as the equation produced is within error of the previously published aragonitic equations (e.g. Grossman and Ku, 1986; White *et al.*, 1999). This confirms that this species is capable of recording the combined signal of temperature and the oxygen isotope composition of the host water. The isotopic signal of the secreted shell carbonate is dominated by temperature when the $\delta^{18}O$ of the host water remains relatively constant, as indicated by the laboratory experiment and cage specimens.

Although *Viviparus* has been shown to be an accurate recorder of the combined isotopic signal produced by temperature variations and changes in the $\delta^{18}O$ of the host water, the use of its isotopic composition to infer palaeotemperatures requires assumptions. Currently, the most significant assumption involves the $\delta^{18}O$ isotopic composition of the host water from which the carbonate was secreted. This particularly influences the temperature estimates across event such as the Oi-1 glaciation, when it is known that the isotopic composition of the marine water and freshwater was largely influenced by increasing ice volumes (altering the $\delta^{18}O$ of seawater and intern $\delta^{18}O$ of precipitation) and temperature fluctuations (e.g. Katz *et al.*, 2008; Lear *et al.*, 2008).

As shown in Chapter 4 the relatively new analytical procedure, the 'carbonate clumped isotope thermometry equation', maybe key to solving these problems and reducing some of

the inaccuracies associated with other methods. This analytical technique may be important in solving the current issues relating to the $\delta^{18}O$ isotopic composition of the host water. A temperature record can be calculated directly from the carbonate proxy via clumped isotope analysis, as all the information required to reconstruct the equilibrium constant for that reaction is preserved within the carbonate mineral itself (Eiler *et al.*, 2007). Temperatures determined by the carbonate clumped isotope thermometry equation can be combined with the $\delta^{18}O$ composition of the carbonate mineral and the known temperature-dependent fractionation of oxygen isotopes between carbonate and water (e.g. calculated by McCrea, 1950; Epstein *et al.* 1953; Kim and O'Neil, 1997; Bugler *et al.*, 2009) to calculate the host waters $\delta^{18}O$ isotopic composition (Elier, 2007).

From the limited results obtained from the analysis of modern specimens, there is the potential for *V. contectus* to the used in clumped isotope thermometry. However, the methods by which the samples were cultured requires modification. Further analyses on specifically cultured samples are needed to fully establish whether *V. contectus* exhibits vital effects on the Δ_{47} of its shell carbonate or whether a generalised clumped isotope equation would be adequate. Investigation into kinetic effects associated with the age of the specimen, sex and whether they are reproductively active would be beneficial in determining whether the clumped isotope equation produced can be successfully applied to the fossil record.

8.2 Fossil study

The overall aim of this investigation was to produce a high resolution terrestrial / freshwater isotopic and palaeotemperature record for NW Europe, in particular the Hampshire Basin (U.K). With the information gained through the study of modern species of *Viviparus* it was clear that the production of a high resolution temperature record

requires further investigation. To produce a reliable temperature record further clumped isotope calibration and analysis are essential. Due to the restrictions associated with analytical procedures further analysis is still pending. However, the production of a high resolution $\delta^{18}O$ record is essential for the interpretation of the $\delta^{18}O_{water}$ changes associated with the E/O transition and Oi-1 glacial maximum and therefore is a vital part of understanding this transitional period.

The high resolution terrestrial $\delta^{18}O$ record (produced in Chapter 6) encompassing the E/O transition and Oi-1 glaciation provides the first opportunity for a detailed comparison with global marine records. This comparison shows that the $\delta^{18}O_{carb.}$ profile produced from the analysis of the freshwater gastropod *V. lentus* records similar isotopic excursions to those seen in both deep and shallow marine records. These shifts include the Late Eocene Event; Step 1(Lear *et al.*, 2008) / EOT-1(Katz *et al.*, 2008) / precursor step (Coxall *et al.*, 2005); the initial part of the Oi-1 and a recovery period.

Isotopic evidence from the analysis of *V. lentus* has revealed a significant and rapid shift in $\delta^{18}O_{carb.}$ between the Fishbourne Member to the base of the Bembridge Limestone Formation (~23,000 years) from –2.4 ‰ to –0.3 ‰ (a 2.1 ‰ shift) which slightly pre-dates the Late Eocene Event (34.2 Ma).

The *V. lentus* $\delta^{18}O_{carb.}$ profile indicates a two step shift into the Oi-1 glacial maximum. As part of the $\delta^{18}O_{carb.}$ record is considered to be missing due to the hiatus between the lower and upper Hamstead Members it is assumed that the most positive values associated with the Oi-1 glacial maximum are also missing due to a ~350 k.y hiatus relating to the sea level fall associated with continental scale ice formation on Antarctica (Hooker *et al.*, 2009). The isotopic shift within the Bembridge Marl Member could be that of the precursor or Step 1 of Coxall *et al.* (2005); Pearson *et al.* (2008) and Lear *et al.* (2008). It may not be possible to confirm whether the excursion in the lower Hamstead Member is the initial part

of the $\delta^{18}O_{carb.}$ shift relating to the Oi-1 glacial maximum or to a precursor event, such as EOT 2 of Katz *et al.* (2008). Hooker *et al.* (2009) determined that the most positive $\delta^{18}O$ values associated with the Oi-1 isotopic shift are most likely to be at the beginning of this hiatus. This would fit with the $\delta^{18}O$ isotopic excursion at the top of the lower Hamstead Member and provided further information that this event could potentially be the initial part of the $\delta^{18}O$ excursion relating to the Oi-1 glacial maximum. The lack of biotic (e.g. vegetation, charophytes) evidence from the IOW deposits, with the exception of the Grande Coupure, indicates that the majority of the $\delta^{18}O$ shift (~1.9 ‰) across the hiatus between the lower and upper Hamstead Members may be related to ice volume changes and / or isotopic shifts in precipitation. This would indicate that any temperature changes associated with the Oi-1 were potentially small in comparison to earlier events, e.g. the Late Eocene Event. Overall, this investigation confirms that long-term cooling was punctuated by rapid climatic change (cooling and warming episodes) which, appears to culminate in the crossing of a threshold into a new climate regime.

Data from Poore (1984) and Pearson *et al.* (2008) indicate that the period between the two $\delta^{18}O$ isotopic steps has the potential to be used to identify the E/O boundary. If correct, the *V. lentus* isotopic record would place the E/O boundary within the Solent Group succession to ~33.74 Ma, coinciding with the distinctive Black Band marking the boundary between the Bembridge Marls Member and the lower Hamstead Member. The placement of the E/O boundary in this study is consistent with Hooker *et al.* (2009) placement, as they suggest that the boundary may lie high in the Bembridge Marls Member or low in the lower Hamstead Member.

8.2.1 Climatic change and biota

The isotopic shift associated with the Late Eocene Event indicates a cooling and / or change in $\delta^{18}O_{water}$ followed by a rapid shift to potentially warmer conditions in the Bembridge Limestone Formation. The results provided further support that aquatic and terrestrial biota was being affected by climate change associated with the Late Eocene Event. Changes in seasonality may also be influential with a notable increase in seasonal isotopic variability across this time period. However, a significant gap in the seasonality data needs to be filled in order to understand the role of seasonality during this time period.

The findings of this investigation also suggest that the continental climate related extinction events are synchronous with the turnover of the mammalian fauna and diversity fall during the Oi-1 glaciation. A mass extinction was avoided due to short lived climatic change prior to the E/O transition and Oi-1 glacial maximum, preconditioning the biota prior to the crossing of a threshold into a new climatic regime. Seasonality may also be key to these climatic and temperature changes, invoking subtle vegetation changes. A potential decrease in summer temperatures reducing the temperature range (seasonality) and spring / summer dominated temperatures are recorded across this event.

8.3 Future work

To support the main conclusions from this investigation it is important that more research be carried. Several areas have been highlighted which require further investigation:

1. Sampling methodology:
    a. It was highlighted by both the modern and fossil *Viviparus* studies that a difference between the $\delta^{18}O$ data from *Viviparus* shell fragments and high resolution samples exist. Work carried out on bivalves (Cusack *et al.*, 2008)

has suggested a difference in the $\delta^{18}O$ composition of the prismatic and nacraceous exists. This needs further investigation on both modern and fossil specimens.

2. The high resolution $\delta^{18}O$ data suggests a possible shift from an equable to seasonal climate between the Cliff End Member and the Bembridge Marls Member. To determine whether this interpretation is correct:
    a. An increased number of gastropod specimens need to be analysed per horizon; and
    b. an increased number of horizons need to be sampled (particularly between the Cliff End Member and the Bembridge Marls Member).
3. An in depth investigation needs to be carried out into cessation marks, migration and life cycles of modern specimens and to a lesser extent fossil specimens of *Viviparus*.
4. A better understanding of the process by which $\delta^{13}C$ is incorporated into the shell within modern specimens of *Viviparus* needs to be established and applied to fossil specimens.
5. It is also important to establish whether *V. contectus* exhibits vital effects on the Δ_{47} of its shell carbonates or whether a generalised clumped isotope equation would be adequate. Once this has been achieved a reliable high resolution temperature record produced from the analysis of *V. lentus* specimens can be achieved for the Solent Group strata. The resultant clumped isotope temperature record can be used in combination with the $\delta^{18}O_{carb.}$ record from this study to produce an invaluable high resolution record of $\delta^{18}O_{water.}$ This information can be used to determine changes in meteoric water, giving an insight into changes in atmospheric and oceanic circulation and also decouple ice and temperature changes from the $\delta^{18}O_{carb.}$ record.

6. There is also the potential for the production of a seasonal temperature record through clumped isotope analysis. At present the sample sizes required for analysis are extremely large (~8 mg) and it is unlikely that sampling resolution could equal that required for establishing the $\delta^{18}O$ ratio in the future. However, it may be possible to create a method by which individual shells can be section into 'clumped sized' sample masses to produce a low resolution record of seasonal temperature changes. This also has the potential to provide information of the seasonal variability of $\delta^{18}O_{water}$ providing information on residence times and evaporative effects

List of References

Abell, P. I., 1985. Oxygen isotope ratios in modern African gastropod shells - A database for palaeoclimatology. *Chemical Geology*, **58**: 183-193.

Abell, P. I., Amegashitsi, L. & Ochumba, P. B. O., 1995. The shells of *Etheria elliptica* as recorders of seasonality at Lake Victoria. *Palaeogeography, Palaeoclimatology, Palaeoecology*, **119**: 215 - 219.

Abell, P. I. & Williams, M. A. J., 1989. Oxygen and carbon isotope ratios in gastropods shells as indicators of paleoenvironments in the Afar Region of Ethiopia. *Palaeogeography, Palaeoclimatology, Palaeoecology*, **74**: 265-278.

Abelson, M., Agnon, A. & Almogi-Labin, A., 2008. Indications for control of the Iceland plume on the Eocene-Oligocene "greenhouse-icehouse" climate transition. *Earth and Planetary Science Letters*, **265**: 33-48.

Accour, A. M., Sheppard, M.F. & Savoye, R., 2003. $\delta^{13}C$ of fluvial mollusk shells (Rhône River): A proxy for dissolved inorganic carbon? *The American Society of Limnology and Oceanography*, **48**: 2186 - 2193.

Affek, H. P. & Eiler J. M., 2006. Abundance of mass 47 CO_2 in urban air, car exhaust, and human breath. *Geochimica et Cosmochimica Acta*, **70**:1–12.

Affek, H. P., Bar-Matthews, M., Ayalon, A., Matthews, A. & Eiler, J. M., 2008. Glacial / interglacial temperature variations in Soreq cave speleothems as recorded by 'clumped isotope' thermometry. *Geochimica et Cosmochimica Acta*, **72**:5351-5360.

Alakrinskaja, I.O., 1969. Morphological adaptations to viviparity in *Viviparus viviparus* (Gastropoda, Prosobranchia). *Zoology Zhurn.*, **48**, 11: 1608–1612 (in Russian, with English summary).

Allen, M. B., 2009. Discussion on the Eocene bimodal Piranshahr massif of the Sanadaj-Sirjan Zone, West Iran: a marker of the end of collision in the Zagros orogen. *Journal of the Geological Society, London*, **166**: 981-982.

Allen, M. B. & Armstrong, H. A., 2008. Arabia-Eurasia collision and the forcing of mid-Cenozoic global cooling. *Palaeogeography, Palaeoclimatology, Palaeoecology*, **265**: 52-58.

Alley, R. B., Marotzke, J., Nordhaus, W. D., Overpeck, J. T., Peteet, D. M., Pielke, R. A., Pierrehumbert, R. T., Rhines, P. B., Stocker, T. F., Talley, L. D. & Wallace, J. M., 2003. Abrupt climate change, *Science*, **299**: 2005-2010.

Amorosi, S. & Centineo, M.C., 1997. Glaucony from the Eocene of the Isle of Wight (southern UK): implications for basin analysis and sequence stratigraphic interpretation. *Journal of the Geological Society, London,* **154**:887-896.

Anadon, P., Moscariello, A., Rodriguez-Lazaro, J. & Filippi, M. L., 2006. Holocene environmental changes of lake geneva (Lac Leman) from stable isotopes (delta C-13, delta O-18) and trace element records of ostracod and gastropod carbonates. *Journal of Paleolimnology*, **35**: 593-616.

Andreasson, F.P. & Schmitz, B., 1996. Winter and Summer temperatures of the early middle Eocene of France from *Turritella* $\delta^{18}O$ profiles. *Geology*, **24**: 1067 - 1070.

Andrews, J. E., Riding, R. & Dennis, P. F., 1993. Stable isotopic composition of recent freshwater cyanobacterial carbonates from the British Isles - local and regional environmental controls. *Sedimentology*, **40**: 303-314.

Andrews, J. E., Riding, R. & Dennis, P. F., 1997. The stable isotope record of environmental and climatic signals in modern terrestrial microbial carbonates from Europe. *Palaeogeography, Palaeoclimatology, Palaeoecology*, **129**:171-189.

Armstrong, E., 1977. Transmission of *Nosema kingi* to offspring of *Drosophila willistoni* during copulation. *Zeitschrift filr Parasitcnkunde*, **53**: 311-315.

Aucour, A. M., Sheppard, S. M. F. & Savoye, R., 2003. Delta C-13 of fluvial mollusk shells (Rhone River): A proxy for dissolved inorganic carbon? *Limnology and Oceanography*, **48**: 2186-2193.

Aubry, M.P., 1985. North-western European Paleogene magnetostratigraphy, biostratigraphy, and paleogeography: calcareous nannofossil evidence. *Geology*, **13**: 198–202.

Aubry, M.P., 1986. Paleogene calcareous nannoplankton biostratigraphy of north-western Europe. *Palaeogeography, Palaeoclimatology, Palaeoecology*, **55**: 267–334.

Auge, M. & Smith, R., 2009. An assemblage of early Oligocene lizards (Squamata) from the locality of Boutersem (Belgium), with comments on the Eocene-Oligocene transition. *Zoological Journal of the Linnean Society*, **155**:148-170.

Barbera, X., Cabrera, L., Marzo, M., Pares, J. M. & Agusti, J., 2001. A complete terrestrial Oligocene magnetobiostratigraphy from the Ebro Basin, Spain. *Earth and Planetary Science Letters*, **187**: 1-16.

Barker, P. F. & Burrell, J., 1977. Opening of Drake Passage. *Marine Geology*, **25**: 15-34.

Barker, P.F., 2001. Scotia Sea regional tectonic evolution: Implications for mantle flow and palaeocirculation. *Earth-Science Reviews*, **55**: 1–39.

Bea, F., Scarrow, J. H., Mazhari, S. A., Molina, J. F., Montero, P., Amini, S. & Ghalamghash, J., 2009. Reply to discussion on the Eocene bimodal Piranshahr massif of the Sanadaj-Sirjan Zone, West Iran: a marker of the end of collision in the Zagros orogen. *Journal of the Geological Society*, London **166**: 983-984.

Bechtel, A., Gratzer, R., Sachsenhofer, R. F., Gusterhuber, J., Lucke, A. & Puttmann, W., 2008. Biomarker and carbon isotope variation in coal and fossil wood of Central Europe through the Cenozoic. *Palaeogeography, Palaeoclimatology, Palaeoecology*, **262**: 166-175.

Berger, W. H. & Winterer, E. L. 1974. Plate stratigraphy and the fluctuating carbonate line. *In: Pelagic Sediments on Land and in the Oceans*. Hsu, K. K. & Jenkyns, H. (eds). , Special. Publication of the International Association of Sedimentaloigists, **1**, Blackwell, Oxford. I l-48pp.

Berggren, W. A., Hilgen, F. J., Langereis, C. G., Kent, D. V., Obradovich, J. D., Raffi, I., Raymo, M. E. & Shackleton, N. J., 1995. Late Neogenne chronology - New perspectives in high resolution stratigraphy. *Geological Society of America Bulletin*, **107**: 1272-1287.

Berggren, W. A. & Hollister, C. D., 1977. Plate tectonics and paleo-circulation – commotion in ocean. *Tectonophysics*, **38**:11-48.

Bernard, A., Daux, V., Lecuyer, C., Brugal, J. P., Genty, D., Wainer, K., Gardien, V., Fourel, F. & Jaubert, J., 2009. Pleistocene seasonal temperature variations

recorded in the delta O-18 of Bison priscus teeth. *Earth and Planetary Science Letters*, **283**: 133-143.

Bigeleisen, J. & Mayer, M.G., 1947. Calculation of equilibrium constants for isotopic exchange reactions. *Journal of Chemistry and Physics*, **15**: 261–267.

Blair, 2007. Exeter Canal and quayside - a short history. www.exetermemories.co.uk [Accessed 20/7/2009].

Boersma, A., 1987. Atlantic Eocene planktonic foraminiferal paleohydrographic indicators and stable isotope paleoceanography. *Paleoceanography*, **2**: 297-331.

Boersma, A. & Premoli Silva, I., 1986. Terminal Eocene events – planktonic foraminifera and isotopic evidence. In: Pomerol, C., & Premoli Silva, I., (Eds). *Terminal Eocene Events*, Elsevier, 213–224.

Boggs, C.L. & Gilbert, L.E., 1979. Male contribution to egg production in butterflies: evidence for transfer of nutrients at mating. *Science,* **206:** 83-84.

Bohaty, S. M. & Zachos, J. C., 2003. Significant Southern Ocean warming event in the late middle Eocene. *Geology*, **31**:1017-1020.

Bohme, M., 2003.The Miocene Climatic Optimum: evidence from ectothermic vertebrates of Central Europe. *Palaeogeography, Palaeoclimatology, Palaeoecology*, **195**: 389-401.

Bonadonna, F. P., Leone, G. & Zanchetta, G., 1999. Stable isotope analyses on the last 30 ka molluscan fauna from Pampa grassland, Bonaerense region, Argentina. *Palaeogeography, Palaeoclimatology, Palaeoecology*, **153**: 289-308.

Bosma, A. A. & Bruijn, H. D., 1979. Eocene and Oligocene Gliridae (Rodentia, Mammalia) from the Isle of Wight, England .1. Gliravus-Priscus Gliravus-Fordi

Lineage. *Proceedings of the Koninklijke Nederlandse Akademie Van Wetenschappen Series B-Palaeontology Geology Physics Chemistry Anthropology*, **82**: 367-384.

Boss, K. J., 1978. On the evolution of gastropods in ancient lakes. In: Fretter, V., and Peake, J., (eds)., *Pulmonates: Sytematics, evolution and ecology,* Volume 2A, Acdemic press (INC London) LTD, p. 385-428.

Boulton, S. J., 2009. Record of Cenozoic sedimentation from the Amanos Mountains, Southern Turkey: Implications for the inception and evolution of the Arabia-Eurasia continental collision. *Sedimentary Geology*, **216**: 29-47.

Bouvier, E.L., 1887. Systeme nervcux, morphologiegenerate et classification des Gasteropodes Prosobranches: Annales des Sciences naturelles. *Zoologie*, **7**: 1-510.

Boycott, A. E., 1936. The habitats of fresh-water mollusca in Britain. *Journal of American Ecology*, **5**: 116-86.

Bowen, G. J., 2007. Palaeoclimate - When the world turned cold. *Nature*, **445**: 607-608.

Breza, J. & Wise, S.W., 1992. Lower Oligocene ice-rafted debris on the Kerguelen Plateau, evidence for East Antarctic continental glaciation. *Proceedings of the Ocean drilling program, Scientific Results,* **120**: 161-178.

Briers, R. A., 2003. Range size and environmental calcium requirements of British freshwater gastropods. *Journal of Global Ecology and Biogeography*. **12**: 47-51.

Brinkhuis, H.,Coccioni, R., 1995. *Is there a relation between dinocyst changes and iridium after all? Preliminary results from the Massignano section*. In: Montanari, A. & Coccioni, R. *The Effects of Impacts on the Atmosphere and Biosphere with*

Regard to Short- and Long-Term Changes: Abstracts and Field Trips: Ancona, Italy, European Science. 40 pp

Brinkhuis, H. & Visscher, H., 1995. The upper boundary of the Eocene series: a reappraisal based on dinoflagellate cysts biostratigraphy and sequencestratigraphy. *Society for Sedimentary Geology, Special Publication*, **54**: 295-304.

Bristow, H.W., Reid, C. & Strahan, A., 1889. *The Geology of the Isle of Wight* (2nd ed.): Memoirs Geological Survey, U.K., **xiv**: 349.

Broecker, W. S., 1994. Massive iceberg discharges as triggers for global climate change. *Nature*, **372**: 421-424.

Brooks, C.E.P., 1949. *Climate through the ages*. Ernest Benn, London.

Brown, D.S., 1980. *Freshwater snails of Africa and their medical importance*. Taylor & Francis, London.

Brown, K. M., Varza, D. & Richardson, T. D., 1989. Life histories and population dynamics of 2 subtropical snails (porsobranchia, Viviparidae). *Journal of the North American Benthological Society*, **8**: 222-228.

Brown, .K.M., 1991. Chapter 10: Mollusca: Gastropoda. In: Thorp, J.H., & Covich, A.P., *Ecology and classification of North American freshwater invertebrates*. Academic Press, London. Pp 285.

Browne, R. A., 1978. Growth, mortality, fecundity, biomass and productivity of 4 lake populations of prosobranch snail, *Viviparus georgianus. Ecology*, **59**: 742-750.

Browne, R.A. & Russell-Hunter, W.D., 1978. Reproductive effort in molluscs. *Oecologia* (Berl.) **37**: 23-27.

Browning, J. V., Miller, K. G. & Pak, D. K., 1996. Global implications of lower to middle Eocene sequence boundaries on the New Jersey coastal plain: The icehouse cometh. *Geology*, **24**: 639-642.

Buckley, D. E., 1986. Bioenergetics of age related versus size related reproductive tactics in female *Viviparus georgianus*. *Biological Journal of the Linnean Society*, **27**: 293-309.

Buffetaut, E., 1982. Les crocodiliens européens et la coupure Eocène-Oligocène. In: 9e réunion annuelle des sciences de la terre. Paris. *Société géologique de France Bulletin*, **101**: 1-15.

Bugler, M. J., Grimes, S. T., Leng, M. J., Rundle, S. D., Price, G. D., Hooker, J. J. & Collinson, M. E., 2009. Experimental determination of a *Viviparus contectus* thermometry equation. *Rapid Communications in Mass Spectrometry*, **23**: 2939-2951.

Bush, A. B. G., 1997. Numerical simulation of the Cretaceous Tethys circum global current. *Science*, **275**: 807-810.

Brongniart, A. de., 1810: Sur des terrains qui paraissent avoir form sous l'eau douce. *Annales du Museum d'Histoire naturelle*, vol. 15, p. 357–405, pls. 22–23.

Cande, S. C. & Kent D. V., 1995. Revised calibration of the geomagnetic polarity timescale for the Late Cretaceous and Cenozoic. *Journal of Geophysical Research*, **100**: 6093–6095.

Calow, P., 1978. The evolution of life-cycle strategies in fresh-water gastropods. *Malacologia*, **17**: 351-364.

Came, R. E., Eiler, J. M., Veizer, J., Azmy, K., Brand, U. & Weidman, C. R., 2007. Coupling of surface temperatures and atmospheric CO_2 concentrations during the Palaeozoic era. *Nature*, **449**:198-U193.

Catuneanu, O., 2002. Sequence stratigraphy of clastic systems: concepts, merits, and pitfalls. *Journal of African Earth Sciences*, **35**: 1-43.

Chacko, T. & Deines, P., 2008 Theoretical calculation of oxygen isotope fractionation factors in carbonate systems. *Geochimica et Cosmochimica Acta*, **72**: 3642-3660.

Charnov, E.L. & Bull, J., 1977. When is sex environmentally determined? *Nature* **266**:828-830.

Cheatum. E.P.,1934. New distributional record for the medusa *Craspedacusta*. *Science* **80**: 528

Cheng, K.M. & Burns, J.T., 1988. Dominance relationship and mating behaviour of domestic cocks. A model to study mate-guarding and sperm competition in birds. *Condor*, **90**: 697-704.

Clark, I. & Fritz, P., 1997. *Environmental isotopes in Hydrogeology*. Lewis Publishers. New York.

Cleal, C.J., Thomas, B.A., Batten, D.J. & Collinson, M.E., 2001. *Mesozoic and Tertiary Palaeobotany of Great Britain*. Geological Conservation Review Series, No. 22, Joint Nature Conservation Committee, Peterborough, 335 pages.

Collinson & M.E., 1983. Palaeofloristic assemblages and palaeoecology of the Lower Oligocene Bembridge Marls, Hamstead Ledge, Isle of Wight. *Botanical Journal of the Linnean Society*, **86**: 177 - 225.

Collinson, M.E. 1992. Vegetational and floristic changes around the Eocene / Oligocene boundary in western and central Europe. In: Prothero, D.R. & Berggren, W.A. (eds) *Eocene–Oligocene Climatic and Biotic Evolution*. Princeton University Press, Princeton, NJ, 437–450.

Collinson, M. E., 2000. Fruit and seed floras from the Palaeocene/Eocene transition and subsequent Eocene in southern England: Comparison and palaeoenvironmental implications. *Journal of the Geological Society of Sweden*, **122**: 36-37.

Collinson, M.E. & Hooker, J.J., 1987. Vegetational and mammalian faunal changes in the early Tertiary of southern England. In: Friis, E.M., Chaloner, W.G. & Crane, P.R., (eds). *The origins of angiosperms and their biological consequences*. Cambridge, Cambridge University Press, p. 259–304.

Collinson, M.E., & Hooker, J.J., 1991. Fossil evidence of interactions between plants and plant-eating mammals, *Philosophical Transactions of the Royal Society of London (B)*, **333**: 197–208.

Collinson, M.E. & Hooker, J.J., 2003. Paleogene vegetation of Eurasia: framework for mammalian faunas. *Deinsea*. **10**: 41-83.

Collinson, M.E., Singer, R.L. & Hooker, J.J., 1993. Vegetational change in the latest Eocene of southern England. In: Planderova, E., Konzalova, M., Kvacek, Z., Siter, V., Snopkova, P., Suballyova, D. (eds), *Paleofloristic and Paleoclimatic Changes during Cretaceous and Tertiary*. Geologicky Ustav Dionyza Stura, Bratislava, pp. 81–87.

Cook, P.M., 1949. A ciliary feeding mechanism in *Viviparus viviparus* (L.). *Proceedings of the Malacological Society of London*, **27**: 265 - 271.

Copper, J., 1976. British Tertiary Stratigrapical and rock terms, formal and informal, additional to Curry 1958, Lexique stratigraphique International. *Tertiary Research Special Paper*, **1**: 37.

Cox, L.R., 1964. *Gastropoda: General characteristics of gastropoda, in* Moore, R.C., Pitrat, C.W., (eds). *Treatise on invertebrate Paleontology*, Volume (I) Mollusca 1, Geological Society of America, Inc and University of Kansas Press.

Coxall, H. K., Wilson, P. A., Palike, H., Lear, C. H. & Backman, J., 2005. Rapid stepwise onset of Antarctic glaciation and deeper calcite compensation in the Pacific Ocean. *Nature*, **433**: 53-57.

Coxall, H. K., Wilson, P. A., Pearson, P. N. & Sexton, P. F., 2007. Iterative evolution of digitate planktonic foraminifera. *Paleobiology*, **33**: 495-516.

Coxall, H. R. & Pearson, P. N., 2006. *Taxonomy, biostratigraphy and phylogeny of Hantkeninidae (Clavigerinella, Hantkenina and Cribrohantkenina).* In: Pearson, P.N., Olsson, R.K., Hemleben, C., Huber, B.T., & Berggren, W.A., (eds). *Atlas of Eocene Planktonic Foraminifera*, Cushman Foundation of Foraminiferal Research, Special Publication No. 41, Lawrence, Kansas, Allen Press, 213–252.

Curtsinger, J.W., 1991. Sperm competition and the evolution of multiple mating. *American Naturalist,* **138:** 93-102.

Curry, D., Adams, C.G., Boulter, M.C., Dilley, F.C., Eames, F.E., Funnell, B.M. &Wells, M.K., 1978. A correlation of Tertiary rocks in the British Isles. *Geological Society of London Special Report*, **12**, 83pp.

Daley, B., 1969, *A palaeoenvironmental study of the Bembridge marls (Oligocene) of the Isle of Wight, Hampshire*, Unpublished PhD Thesis, University of Reading, 238pp.

Daley, B., 1972(a). Macroinvertebrate assemblages from the Bembridge marls (Oligocene) of the Isle of Wight, England, and their environmental significance. *Palaeogeography, Palaeoclimatology, Palaeoecology*, **11**:11-32.

Daley, B., 1972 (b). Some problems concerning the early Tertiary climate of Southern Britain: *Palaeogeography, Palaeoclimatology, Palaeoecology*, **11**:177 - 190.

Daley, B., 1973(a). Fluvio-lacustrine cyclothems form the Oligocene of Hampshire. *Geological Magazine*, **110**: 235 - 242.

Daley, B., 1973(b). The palaeoenvironments of the Bembridge marls (Oligocene) of the Isle of Wight, Hampshire. *Proceedings of the Geologists' Association*, **84**: 83 - 93.

Daley, B., 1999. Palaeogene sections in the Isle of Wight: A revision of their descriptions and significant in the light of research undertaken over recent decades. *Tertiary Research*, **19**: 1-60.

Daley, B. & Edwards, N., 1971. Palaeogene warping in the Isle of Wight. *Geological Magazine*, **108**: 399-405.

Daley, B. & Insole, A., 1984. *Geologists association guide: The Isle of Wight*, No.25, The Geologists' Association, 1-35 p.

Darling G.W., Bath, A.H., Gibson, J.J. & Rozanski, K., 2005. Isotopes in water. In: Leng, M.J. (ed), Isotopes in Palaeoenvironmental Research (Developments in Paleoenvironmental Research). Springer –Verlag (Heidelberg). p2-58

D'Asaro, C. N., 1988. Micromorphology of neogastropod egg capsules. *Nautilus*, **102**: 134–148.

Davies, R., Cartwright, J., Pike, J. & Line, C., 2001. Early Oligocene initiation of North Atlantic Deep Water formation. *Nature*, **410**: 917-920.

Davies, S. J. & Gibling, M. R., 2003. Architecture of coastal and alluvial deposits in an extensional basin: the Carboniferous Joggins Formation of eastern Canada. *Sedimentology*, **50**: 415-439.

De Bernardi R., Ravera K. W. & Oregioni B., 1976. Demographic structure and biometric characteristics of *Viviparus ater* Cristofori and Jan (Gastropoda: Prosobranchia) from Lake Alserio (Northern Italy). *Journal of Molluscan Studies*, **42**: 310–318.

Denton, G. H., Alley, R. B., Comer, G. C. & Broecker, W. S., 2005. The role of seasonality in abrupt climate change. *Quaternary Science Reviews*, **24**: 1159-1182.

De Man, E., Ivany, L. & Vandenberghe, N., 2004. Stable oxygen isotope record of the Eocene-Oligocene transition in the southern North Sea Basin: positioning the Oi-1 event. *Geologie En Mijnbouw*, **83**: 193-197.

DeConto, R. M. & Pollard, D., 2003. Rapid Cenozoic glaciation of Antarctica induced by declining atmospheric CO_2. *Nature*, **421**: 245-249.

Delaney, M. L. & Boyle, E. A., 1988. Tertiary paleoceanic chemical variability: unintended consequences of simple geochemical models. *Paleoceanography*, **3**: 137–156.

Dembski, W.J., 1968. Histochemische Untersuchungen über Funktion und Verbleib eu- und oligo-pyrener Spermien von *Viviparus contectus* (Millet, 1813). *Zeitschrift*

für Zellforschung und Mikroskopische Anatomie (Abteilung Histochemie), **89**: 151-179.

Dettman, D. L., Reische, A. K. & Lohmann, K. C., 1999. Controls on the stable isotope composition of seasonal growth bands in aragonitic fresh-water bivalves (unionidae). *Geochimica et Cosmochimica Acta*, **63**:1049-1057.

Diekmann, B., Kuhn, G., Gersonde, R. & Mackensen, A., 2004. Middle Eocene to early Miocene environmental changes in the sub-Antarctic Southern Ocean: evidence from biogenic and terrigenous depositional patterns at ODP Site 1090. *Global and Planetary Change*, **40**: 295-313.

Diester-Haass, L. & Zahn, R., 2001. Paleoproductivity increase at the Eocene-Oligocene climatic transition: ODP/DSDP sites 763 and 592. *Palaeogeography, Palaeoclimatology, Palaeoecology*, **172**:153-170.

Diester Haass, L. & Zahn, R., 1996. Eocene-Oligocene transition in the Southern Ocean: History of water mass circulation and biological productivity. *Geology*, **24**:163-166.

Dillon, J.R.T., 2000. *The Ecology of Freshwater Molluscs*, Cambridge University Press, Cambridge.

Dillon, R.T., 2007. *Freshwater gastropods of North America: Viviparus georgianus* (Lea 1834),Taken from : http://www.cofc.edu/~fwgna/species/viviparidae/v_georgianus.html . Accessed on the 16-8-2007.

Donders, T. H., Weijers, J. W. H., Munsterman, D. K., Hoeve, M., Buckles, L. K., Pancost, R. D., Schouten, S., Damste, J. S. S. & Brinkhuis, H., 2009. Strong climate

coupling of terrestrial and marine environments in the Miocene of northwest Europe. *Earth and Planetary Science Letters*, **281**: 215-225.

Drickamer, L.C., 1992. Oestrous female house mice discriminate dominant from subordinate males and sons of dominant from sons of subordinate males by odour cues. *Animal Behaviour*, **43**: 868-870.

Duch, T. M., 1976. Aspects of the feeding habits of *Viviparus georgianus*. *The Nautilus*, **90**:7-10.

Dunning, R., 2004. *A History of the County of Somerset: Volume 8: The Poldens and the Levels*. Victoria County History. pp. 1-7.Accessed: http://www.britishhistory.ac.uk/report.aspx?

Dupont-Nivet, G., Krijgsman, W., Langereis, C. G., Abels, H. A., Dai, S., & Fang, X. M., 2007. Tibetan plateau aridification linked to global cooling at the Eocene-Oligocene transition. *Nature*, **445**: 635-638.

Dussart, G. B. J., 1976. The ecology of freshwater molluscs in north west England in relation to water chemistry. *Journal of Molluscan Studies*, **42**: 181-198.

Edgar, K. M., Wilson, P. A., Sexton, P. F. & Suganuma, Y., 2007. No extreme bipolar glaciation during the main Eocene calcite compensation shift. *Nature*, **448**: 908-911.

Eiler, J. M., 2007. Clumped-isotope geochemistry - The study of naturally-occurring, multiply-substituted isotopologues. *Earth and Planetary Science Letters*, **262**: 309-327.

Eiler, J. M. & Schauble, E., 2004. (OCO)-O-18-C-13-O-16 in Earth's atmosphere. *Geochimica et Cosmochimica Acta*, **68**:4767-4777.

Elderfield, H., Rickaby, R. & Henderiks, J., 2006. How do marine carbonate Mg/Ca and Sr/Ca proxies constrain Cenozoic ocean history. *16th Annual V M Goldschmidt Conference*. Melbourne, Australia Aug-Sep. pp. A158-A158.

Eldrett, J. S., Greenwood, D. R., Harding, I. C. & Huber, M., 2009. Increased seasonality through the Eocene to Oligocene transition in northern high latitudes. *Nature*, **459**: 969-U991.

Eldrett, J. S., Harding, I. C., Wilson, P. A., Butler, E. & Roberts, A. P., 2007. Continental ice in Greenland during the Eocene and Oligocene. *Nature*, **446**: 176-179.

Eleutheriadis, N. and Lazaridou-Dimitriadou, M. 1995. Density and growth of fresh water snails (Bithynia graeca and Viviparus contectus) in relation to water chemistry in Serres, Northern Greece. *Journal of Molluscan Studies*, **61**:347-352.

Epstein, S., Buchsbaum, R., Lowenstam, H. A. & Urey, H. C., 1953. Revised carbonate water isotopic temperature scale. *Geological Society of America Bulletin*, **64**: 1315-1326.

Fluckiger, J., Knutti, R., White, J. W. C. & Renssen, H., 2008. Modeled seasonality of glacial abrupt climate events. *Climate Dynamics*, **31**: 633-645.

Forbes, E., 1853. On the fluvial-marine formation of the Isles of Wight. *Quarterly Journal of Geological Society, London*, **9**: 259 -270.

Forbes, E., 1856. *On the Tertiary fluvio-marine Formation of the Isles of Wight*. With appendix by H.W Bristow: Memoirs Geological Survey, U.K, **xvii**: 162.

Fraile, I., Mulitza, S. & Schulz, M., 2009. Modelling planktonic foraminiferal seasonality: Implications for sea-surface temperature reconstructions. *Marine Micropaleontology*, **72**: 1-9.

Franzenj, L., 1968. Revision der Gattung Palaeotherium Cuuier 1804 (Palaeotheriidae, Perissodactyla, Mammalia), **2**. Albert-Ludwigs- Universitat zu Freiburg i. Br., Freiburg.

Fretter, V. & Graham, A., 1994. *British prosobranch molluscs*. London: The Ray Society.

Fretter, V. & Graham, A., 1976 – 1986. The prospbranch molluscs of Britain and Denmark (Part 1-9). *Journal of Molluscan Studies*, **44**: 107-111.

Freidman I. & O'Neil J.B., 1977. Compilation of stable isotope fractionation factors of geochemical interest. In: Data of Geochemistry. 6th edn, Ed. M. Fleischer, Chapter KK. US Geol. Surv. Prof. Paper 440-KK

Fritz, P. & Poplawski, S., 1974. 18O and 13C in the shells of freshwater molluscs and their environments. *Earth and Planetary Science Letters*, **24**: 91–98.

Gajurel, A. P., France-Lanord, C., Huyghe, P., Guilmette, C. & Gurung, D., 2006. C and O isotope compositions of modem fresh-water mollusc shells and river waters from the Himalaya and Ganga plain. *Chemical Geology*, **233**: 156-183.

Gale, A. S., Huggett, J. M., Palike, H., Laurie, E., Hailwood, E. A. & Hardenbol, J., 2006. Correlation of Eocene-Oligocene marine and continental records: orbital cyclicity, magnetostratigraphy and sequence stratigraphy of the Solent Group, Isle of Wight, UK. *Journal of the Geological Society, London*, **163**: 401-415.

Gebhardt, M. & Ribi, G., 1987. Reproductive effort and growth in the prosobranch snail *Viviparus ater*. *Oecologia*, **74**: 209-214.

Gĕly, J. P. & Lorenz, C., 1991. Sequence analysis of the Eocene – Oligocene Paris Basin, France. *Revue de l' Institut Français du Pétrole*, **46**:713-747.

Ghosh, P., Adkins, J., Affek, H., Balta, B., Guo, W. F., Schauble, E. A., Schrag, D. & Eller, J. M., 2006. C-13-O-18 bonds in carbonate minerals: A new kind of paleothermometer. *Geochimica et Cosmochimica Acta*, **70**: 1439-1456.

Ghosh, P., Eiler, J., Campana, S. E. & Feeney, R. F., 2007. Calibration of the carbonate 'clumped isotope' paleothermometer for otoliths. *Geochimica et Cosmochimica Acta*, **71**: 2736-2744.

Glöer, P. & Meier-Brook, C., 1998. *Süsswassermollusken.* Hamburg, Deutscher Jugendbund für Naturbeobachtung, 136 pp.

Graham, S. A., Chamberlain, C. P., Yue, Y. J., Ritts, B. D., Hanson, A. D., Horton, T. W., Waldbauer, J. R., Poage, M. A. & Feng, X., 2005. Stable isotope records of Cenozoic climate and topography, Tibetan plateau and Tarim basin. *American Journal of Science*, **305**:101-118.

Grimes, S. T., Hooker, J. J., Collinson, M. E. & Mattey, D. P., 2005. Summer temperatures of late Eocene to early Oligocene freshwaters. *Geology*, **33**: 189-192.

Grimes, S. T., Collinson, M. E., Hooker, J. J., Mattey, D. P., Grassineau, N. V. & Lowry, D., 2004. Distinguishing the diets of coexisting fossil theridomyid and glirid rodents using carbon isotopes. *Palaeogeography, Palaeoclimatology, Palaeoecology*, **208**: 103-119.

Grimes, S. T., Mattey, D. P., Hooker, J. J. & Collinson, M. E., 2003. Paleogene paleoclimate reconstruction using oxygen isotopes from land and freshwater organisms: the use of multiple paleoproxies. *Geochimica et Cosmochimica Acta*, **67**: 4033-4047.

Grossman, E. L. & Ku, T. L., 1986. Oxygen and carbon isotope fractionation in biogenic aragonite - temperature effects. *Chemical Geology*, **59**: 59-74.

Hansen, T. A., Kelley, P. H. & Haasl, D. M., 2004. Paleoecological patterns in molluscan extinctions and recoveries: comparison of the Cretaceous-Paleogene and Eocene-Oligocene extinctions in North America', *Workshop on Mesozoic-Cenozoic Bioevents*. Berlin, Germany, 2002. pp. 233-242.

Haq, B. U., 1981. Paleogene paleoceanography - early Cenozoic oceans revisited. *Oceanology Acta*, **4**: 71-82.

Harman WN, (Ed.), 1974. Snails (Mollusca: Gastropoda). *Pollution Ecology of Freshwater Invertebrates*. Academic Press, New York.

Harrington, R., Woiwod, I. & Sparks, T., 1999. Climate change and trophic interactions. *Trends in Ecology & Evolution*, **14**: 146-150.

Harrison, A. D., Williams, N. V. & Greig G., 1970. Studies on the effects of calcium bicarbonate concentrations on the biology of biomphalaria pfeifferi (Krauss) (Gastropoda: Pulmonata). *Hydrobiologia*, **36**: 317.

Harzhauser, M., Latal, C. & Piller, W. E., 2007. The stable isotope archive of Lake Pannon as a mirror of Late Miocene climate change. *Palaeogeography, Palaeoclimatology, Palaeoecology*, **249**: 335-350.

Hay, W. W. & Soeding, E., 2000. The late Cenozoic uplift – climate change paradox. *International Journal of Earth Sciences*, **91**:746-774.

Hay, W.W., Flogel, S. & Soding, E., 2005. Is the initiation of glaciation on Antarctica related to a change in the structure of the oceans? *Global and Planetary change*, **45**: 23-33.

Heissig, K., 1987. Changes in the rodent and ungulate fauna in the Oligocene fissure fillings of Germany. *Münchner Geowissenschaftliche Abhandlungen*, (A), **10**: 101–108.

Heller, J. & Farsley, V., 1990. Sexual and parthenogenetic populations of the freshwater snail Melanoides Tuberculata in Israel. *Journal of Zoology*, **37**: 75–87.

Hickman, C. S. 2003. Evidence for Abrupt Eocene– Oligocene molluscan faunal change in the Pacific Northwest. In: Prothero, D.R., Ivany, L., & Nesbitt, E.A., (eds). *From Greenhouse to Icehouse*, New York, Columbia University Press, 71–87.

Hodgson, B., Dagley, P. & Mussett, A.E., 1990. Magnetostratigraphy of the Tertiary igneous rocks of Arran. *Scottish Journal of Geology*. **26**: 99–118.

Hooker, J.J., 1987. Mammalian faunal events in the English Hampshire Basin (late Eocene–early Oligocene) and their application to European biostratigraphy: *Münchner Geowissenschaftliche Abhandlungen, series A*, **10**: 109–116.

Hooker, J.J., 1992. *British mammalian paleocommunities across the Eocene-Oligocene transition and their environmental implications*. In: Prothero, D.R., & Berggren, W.A., (eds). Eocene-Oligocene Climatic and Biotic Evolution. Princeton, Princeton University Press, p. 494–515.

Hooker, J.J., Collinson, M.E., Van Bergen, P.F., Singer, R.L., De Leeuw, J.W. & Jones, T.P., 1995. Reconstruction of land and freshwater palaeoenvironments near the Eocene-Oligocene boundary, southern England. *Journal of the Geological Society, London*, **152**: 449 - 468.

Hooker, J. J., 2000. Paleogene mammals: crises and ecological change. In: Culver, S. J., Rawson, P. F., (eds). *Biotic response to global change*. Cambridge: Cambridge University Press, p. 333–349.

Hooker, J. J., Collinson, M. E. & Sille, N. P., 2004. 'Eocene-Oligocene mammalian faunal turnover in the Hampshire Basin, UK: calibration to the global time scale and the major cooling event. *Journal of the Geological Society, London*, **161**: 161-172.

Hooker, J., Collinson, M., Grimes, S., Sille, N., Mattey, D., Gale, A., Huggett, J. & Laurie, E., 2007. Discussion on the Eocene-Oligocene boundary in the UK . *Journal of the Geological Society, London,* **164:** 685-688.

Hooker, J.J., Grimes, S.T., Mattey, D.P., Collinson, M.E. & Sheldon, N.D., 2009. Chapter 12: Refined correlation of the UK Late Eocene–Early Oligocene Solent Group and timing of its climate history. In: Koeberland, C., & Montanari, A*.: The Late Eocene Earth—Hothouse, Icehouse, and Impacts.* The Geological Society of America, Special Paper, 452. 179-195pp.

Hubekdick, B., 1958. Factors conditioning the habitat of freshwater snails. *Bulletin of the World Health Organisation,* **18**: 1072-1080.

Huber, M., Brinkhuis, H., Stickley, C. E., Doos, K., Sluijs, A., Warnaar, J., Schellenberg, S. A. & Williams, G. L., 2004. Eocene circulation of the Southern Ocean: Was Antarctica kept warm by subtropical waters? *Paleoceanography*, **A4026**.

Huber, M. & Nof, D., 2006. The ocean circulation in the southern hemisphere and its climatic impacts in the Eocene. *Palaeogeography, Palaeoclimatology, Palaeoecology,* **231**: 9–28.

Hunt, R. M. & Stepleton, E., 2004. Geology and paleontology of the upper John Day beds, John Day River Valley, Oregon: Lithostratigraphic and biochronologic revision in the Haystack Valley and Kimberly areas (Kimberly and Mt. Misery Quadrangles). *Bulletin of the American Museum of Natural History*, **282**: 1-90.

Huntington, K. W., Eiler, J. M., Affek, H. P., Guo, W., Bonifacie, M., Yeung, L. Y., Thiagarajan, N., Passey, B., Tripati, A., Daeron, M. & Came, R., 2009. Methods and limitations of 'clumped' CO2 isotope (Delta (47)) analysis by gas-source isotope ratio mass spectrometry. *Journal of Mass Spectrometry*, **44**: 1318-1329.

Insole, A. & Daley, B., 1985. A revision of the lithostratigraphical nomenclature of the Late Eocene and Early Oligocene strata of the Hampshire Basin, Southern England. *Tertiary Research*, **7**: 67 - 100.

Ivanov, M., Rage, J.C., Szyndlar, Z. & Venczel, M., 2000. Histoire et Origine géographique des faunes de serpents en Europe. *Bulletin de la Société Herpétologique de France* **96**: 15–24.

Ivany, L. C., Lohmann, K. C., Hasiuk, F., Blake, D. B., Glass, A., Aronson, R. B. & Moody, R. M., 2008. Eocene climate record of a high southern latitude continental shelf: Seymour Island, Antarctica. *Geological Society of America Bulletin*, **120**: 659-678.

Ivany, L. C., Patterson, W. P. & Lohmann, K. C., 2000. Cooler winters as a possible cause of mass extinctions at the Eocene/Oligocene boundary. *Nature*, **407**: 887-890.

Jansen, E., Overpeck, J., Briffa, K. R., Duplessy, J.C., Joos, F., Masson-Delmotte, V., Olago, D. O.-B., B, Peltier, W. R., Rahmstorf, S., Ramesh, R., Raynaud, D., Rind, D., Solomina, O., R, V. & Zhang, D., 2007. *Palaeoclimate.* In: Solomon, S., Qin, D., Manning, M., Chen, Z., Marquis, M., Averyt, K.B., Tignor M. & Miller H.L.,

(eds) *Climate Change 2007: The PhysicalScience Basis. Contribution of Working Group I to the Fourth Assessment Report of the Intergovernmental Panel on Climate Change.* Cambridge University Press, Cambridge, United Kingdom and New York, NY, USA.

Jakubik, B., 2003.Year-to-year stability of aggregations of *Viviparus viviparus* (Linnaeus 1758) in littoral zone of lowland, rheophilic reservoir (Central Poland). *Polish Journal of Ecology*, **51**: 53-66.

Jakubik, B., 2006. Reproductive pattern of *Viviparus viviparus* (Linnaeus 1758) (Gastropoda, Viviparidae) from littoral aggregations in a through-flow reservoir (Central Poland). *Polish Journal of Ecology*, **54**: 39-55.

Jakubik, B., 2007. Egg number-female body weight relationship in freshwater snail (*Viviparus viviparus* L.) population in a reservoir. *Polish Journal of Ecology*, **55**: 325-336.

Jarzembowski, E. A., 1980. Fossil insects from the Bembridge Marls, Palaeogene of the Isle of Wight, southern England. *Bulletin of the British Museum* (Natural History) *Geology Series,* **33**: 237-293.

Jicha, B. R., Scholl, D. W. & Rea, D. K., 2009. Circum-Pacific arc flare-ups and global cooling near the Eocene-Oligocene boundary. *Geology*, **37**: 303-306.

John, K. S., 2008. Cenozoic ice-rafting history of the central Arctic Ocean: Terrigenous sands on the Lomonosov Ridge. *Paleoceanography*, **23**.

Jokinen, E. H., 1982. *Cipangopaludina chinensis* (Gastropoda, Viviparidae) in North America, review and update. *Nautilus*, **96**: 89-95.

Jokinen, E., 1983. The freshwater snail (Mollusca: Gastropoda) of New York State. *New York State Museum Bulletin*, **482**: 1-112.

Jones, M. D., Leng, M. J., Eastwood, W. J., Keen, D. H. & Turney, C. S. M., 2002. Interpreting stable-isotope records from freshwater snail-shell carbonate: a Holocene case study from Lake Golhisar, Turkey. *Holocene*, **12**: 629-634.

Joomun, S. C., Hooker, J. J. & Collinson, M. E., 2008. Dental wear variation and implications for diet: An example from Eocene perissodactyls (Mammalia). *Palaeogeography, Palaeoclimatology, Palaeoecology*, **263**: 92-106.

Katz, M. E., Miller, K. G., Wright, J. D., Wade, B. S., Browning, J. V., Cramer, B. S. & Rosenthal, Y., 2008. Stepwise transition from the Eocene greenhouse to the Oligocene icehouse. *Nature Geoscience*, **1**: 329-334.

Keeling, C. D., Bacastow, R. B. & Tans, P. P., 1980. Predicted shift in the C-13-C-12 ration of atmospheric carbon-dioxide. *Geophysical Research Letters*, **7**: 505-508.

Keeling, C. D., Mook, W. G. & Tans, P. P., 1979. Recent trends in the C-13-C-12 ratio of atmospheric carbon-dioxide. *Nature*, **277**:121-123.

Keeling, C. D., Whorf, T. P., Wahlen, M. & Vanderplicht, J., 1995. Interannual extremes in the rate of rise of atmospheric carbon-dioxide since 1980. *Nature*, **375**: 666-670.

Keller, G., Macleod, N. & Barrera, E. (1992) Eocene–Oligocene faunal turnover in planktonic foraminifera, and Antarctic glaciation. In: Prothero, D.R and Berggren, W.A., (eds) *Eocene and Oligocene Climatic and Biotic Evolution*. Princeton, Princeton University Press: 218–244.

Keller, G. & Ribi, G., 1993. Fish predation and offspring in the prosobranch snail *Viviparus alter*. *Oecologia*, **93**: 493-500.

Kennett, J. P., 1977. Cenozoic evolution of Antarctica glaciation, cirum Antarctic Ocean and their impact on global paleocenaography. *Journal of Geophysical Research-Oceans and Atmospheres*, **82**: 3843-3860.

Kennett, J. P. & Shackleton, N. J., 1976. Oxygen isotopic evidence for development of psychrosphere 38 Myr ago. *Nature*, **260**: 513-515.

Kim, S. T., Hillaire-Marcel, C. & Mucci, A., 2006. Mechanisms of equilibrium and kinetic oxygen isotope effects in synthetic aragonite at 25 degrees C. *Geochimica et Cosmochimica Acta*, **70**: 5790-5801.

Kim, S. T., O'Neil, J. R., Hillaire-Marcel, C. & Mucci, A., 2007. Oxygen isotope fractionation between synthetic aragonite and water: Influence of temperature and Mg2+ concentration. *Geochimica et Cosmochimica Acta*, **71**: 4704-4715.

Kim, S. T. & Oneil, J. R., 1997. Equilibrium and nonequilibrium oxygen isotope effects in synthetic carbonates. *Geochimica et Cosmochimica Acta*, **61**: 3461-3475.

Kobashi, T., Grossman, E. L., Yancey, T. E. & Dockery, D. T., 2001. Reevaluation of conflicting Eocene tropical temperature estimates: Molluskan oxygen isotope evidence for warm low latitudes. *Geology*, **29**: 983-986.

Kohn, M. J., Josef, J. A., Madden, R., Kay, R., Vucetich, G. & Carlini, A. A., 2004. Climate stability across the Eocene-Oligocene transition, southern Argentina. *Geology*, **32**: 621-624.

Kominz, M. A., Browning, J. V., Miller, K. G., Sugarman, P. J., Mizintseva, S. & Scotese, C. R., 2008. Late Cretaceous to Miocene sea-level estimates from the New Jersey

and Delaware coastal plain coreholes: an error analysis. *Basin Research*, **20**: 211-226.

Kominz, M. A. & Pekar, S. F., 2001. Oligocene eustasy from two-dimensional sequence stratigraphic backstripping. *Geological Society of America Bulletin*, **113**: 291-304.

Kramer, D. L., Lindsey, C. C., Moodie, G. E. E. & Stevens, E. D., 1978. Fishes and aquatic environment of central Amazon Basin, with particular reference to respiratory patterns. *Canadian Journal of Zoology-Revue Canadienne De Zoologie*, **56**: 717-729.

Kroopnick, P., 1980. The distribution of C-13 in the Atlantic Ocean. *Earth and Planetary Science Letters*, **49**: 469-484.

Kump, L. R. & Arthur, M. A. (1997) Global chemical erosion during the Cenozoic: Weatherability balances the budgets. In: Ruddiman, W. (Ed.) *Tectonics Uplift and Climate Change*. New York: Plenum Press. 399-426 pp.

Latal, C., Piller, W. E. & Harzhauser, M., 2004. Palaeoenvironmental reconstructions by stable isotopes of Middle Miocene gastropods of the Central Paratethys. *Palaeogeography, Palaeoclimatology, Palaeoecology*, **211**: 157-169.

Lawver, L. A. & Gahagan, L. M. (eds) (1998) *Opening of Drake Passage and its impact on Cenozoic ocean circulation. Conditions for Climate Reconstructions*. Oxford Monograph of Geology and Geophysics.

Lawver, L. A. & Gahagan L. M., (1998). *Opening of Drake Passage and its impact on Cenozoic ocean circulation.* In: T. J. Crowley and K. C. Burke (eds) *Tectonic Boundary Conditions for Climate Reconstructions*. Oxford University Press, New York.

Lawver, L. A. & Gahagan, L. M., 2003. Evolution of Cenozoic seaways in the circum-Antarctic region. Palaeogeography, Palaeoclimatology, Palaeoecology **198**: 11-37.

Legendre, S., 1989. Les communautĕs de mammife'res du Palĕogĕne (Eocĕne supĕrieur et Oligoce'ne) d'Europe occidentale: structures, milieux et ĕvolution. *Münchner Geowissenschaftliche Abhandlungen*, (A), **16**: 1–110.

Lear, C. H., Bailey, T. R., Pearson, P. N., Coxall, H. K. & Rosenthal, Y., 2008. Cooling and ice growth across the Eocene-Oligocene transition. *Geology*, **36**: 251-254.

Lear, C. H., Elderfield, H. & Wilson, P. A., 2000. Cenozoic deep-sea temperatures and global ice volumes from Mg/Ca in benthic foraminiferal calcite. *Science*, **287**: 269-272.

Leng, M. J., Lamb, A. L., Heaton, T. H. E., Marshall, J. D., Wolfe, B. B., Jones, M. D., Holmes, M. D., Holmes, J. A. & Arrowsmith, C. 2005. Isotopes in lake sediments. *In*: Leng, M.J. (Ed.) *Isotopes in Palaeoenvironmental Research*. Springer. Dordrecht.

Leng, M.J. & Marshall, J.D., 2004. Palaeoclimate interpretation of stable isotope data from lake sediment archives. *Quaternary Science Reviews*, **23**: 811-831.

Leng, M. J., Lamb, A. L., Lamb, H. F. & Telford, R. J., 1999. Palaeoclimatic implications of isotopic data from modern and early Holocene shells of the freshwater snail Melanoides tuberculata, from lakes in the Ethiopian Rift Valley. *Journal of Paleolimnology*, **21**: 97-106.

Lind, H., 1988. The behaviour of *Helix pomatia* L. (Pulmonata, Gastropoda) in a natural habitat. *Videnskabetige Meddelelser frå Dansk naturhistorisk Forening*, **147:** 67-92.

Liu, Z. H., Pagani, M., Zinniker, D., DeConto, R., Huber, M., Brinkhuis, H., Shah, S. R., Leckie, R. M. & Pearson, A., 2009. Global Cooling During the Eocene-Oligocene Climate Transition. *Science*, **323**: 1187-1190.

Livermore, R., Nankivell, A., Eagles, G. & Morris, P., 2005. Paleogene opening of Drake Passage. *Earth and Planetary Science Letters*, **236**: 459-470.

Lyle, M., Barron, J., Bralower, T. J., Huber, M., Lyle, A. O., Ravelo, A. C., Rea, D. K. & Wilson, P. A., 2008. Pacific Ocean and Cenozoic evolution of climate. *Reviews of Geophysics*, **46.**

Machin, J., 1971. Plant microfossils from the Tertiary deposits of the Isle of Wight. *New Phytologist*, **70**: 851–872.

Markwick, P. J., 1998. Fossil crocodilians as indicators of Late Cretaceous and Cenozoic climates: implications for using palaeontological data in reconstructing palaeoclimate. *Palaeogeography, Palaeoclimatology, Palaeoecology*, **137**: 205-271.

Markwick, P.J., 1994, ''Equability,'' continentality, and Tertiary ''climate'': The crocodilian perspective. *Geology*, **22**: 613–616.

McConnaughey, T.A., Burdett, J., Welhan, J.F. & Paul, C.K., 1997. Carbon isotopes in biological carbonates: Respiration and photosynthesis. *Geochimica et Cosmochimica Acta*, **61**: 611 - 622.

McConnaughey, T. A., 2003. Sub-equilibrium oxygen-18 and carbon-13 levels in biological carbonates: carbonate and kinetic models. *Coral Reefs*, **22**: 316-327.

McCrea, J. M., 1950. On the isotopic chemistry of carbonates and palaeo-temperatures scales. *Journal of Chemistry and Physics*, **18**: 849-857.

McFarlaine I.D., 1981. Trail following in the intertidal homing gastropod *Onchidium verruculatum* (Cuv.). The outward and homeward trails have a different information content. *Journal of Experimental Marine Biology and Ecology*, **51**: 207-218.

McMahon, R.F., 1983. Physiological ecology of freshwater pulmonates. In : Russell-Hunter W.D.,(Ed.). *The mollusca*. Academic Press, London. pp. 360–430

Melville, R.V. & Freshney, E.C., 1982. *British Regional Geology: The Hampshire Basin and Adjoining Areas*. Fourth Edition, Institute of Geological Sciences, London, Her Majesty's Stationery Office, 146pp.

Meng, J. & McKenna, M. C., 1998. Faunal turnovers of Palaeogene mammals from the Mongolian plateau. *Nature*, **394**: 364-367.

Merico, A., Tyrrell, T. & Wilson, P. A., 2008. Eocene/Oligocene ocean de-acidification linked to Antarctic glaciation by sea-level fall. *Nature*, **452**: 979-U976.

Mess, A., Mohr, B. & Martin, T., 2001. Evolutionary transformations of hystricognath Rodentia and the climatic change in the Eocene to Late Oligocene time interval. *Zoosystematic and Evolution*, **77**:193-206.

Meves, F., 1902. Über oligopyrene und apyrene Spermien und über ihre Entstehung, nach Beobachtungen an *Paludina* und *Pygaera*. *Archiv für Mikroskopische Anatomie*, **61**: 1-84.

Miao, Y., Fang, X., Song, Z., Wu, F., Han, W., Dai, S. & Song, C., 2008. Late Eocene pollen records and palaeoenvironmental changes in northern Tibetan Plateau. *Science in China series D: Earth Science*, **51**: 1089-1098.

Miller, K. G., Fairbanks, R. G. & Mountain, G. S., 1987. Tertiary oxygen isotope synthesis, sea level history and continental margin erosion. *Paleoceanography*, **2**: 1-19.

Miller, K. G., Wright, J. D. & Browning, J. V., 2005. Visions of ice sheets in a greenhouse world. *Marine Geology*, **217**: 215-231.

Miller, K. G., Wright, J. D. & Fairbanks, R. G., 1991. Unlocking the ice house – Oligocene / Miocene oxygen isotopes, eustasy and margin erosion. *Journal of Geophysical Research-Solid Earth and Planets*, **96**: 6829-6848.

Miller, K. G., Wright, J. D., Katz, M. E., Browning, J. V., Cramer. B. S., Wade, B. S. & Mizintseva, S. F., 2008. *A View of Antarctic Ice-Sheet Evolution from Sea-Level and Deep-Sea Isotope changes during the Late Cretaceous-Cenozoic*. In: Cooper, A. K., Barrett, P. J., Stagg, H., Storey, B., Stump, E., Wise, W., and the 10th ISAES editorial team (eds)., 2008. *Antarctica: A Keystone in a Changing World.* Proceedings of the 10th International Symposium on Antarctic Earth Sciences. Washington, DC: The National Academies Press.

Miloslavich, P., 1996. Biochemical composition of prosobranch egg capsules. *Journal of Molluscan Studies*, **62**: 133-135.

Moran, K., Backman, J., Brinkhuis, H., Clemens, S. C., Cronin, T., Dickens, G. R., Eynaud, F., Gattacceca, J., Jakobsson, M., Jordan, R. W., Kaminski, M., King, J., Koc, N., Krylov, A., Martinez, N., Matthiessen, J., McInroy, D., Moore, T. C., Onodera, J., O'Regan, M., Palike, H., Rea, B., Rio, D., Sakamoto, T., Smith, D. C., Stein, R., St John, K., Suto, I., Suzuki, N., Takahashi, K., Watanabe, M., Yamamoto, M., Farrell, J., Frank, M., Kubik, P., Jokat, W. & Kristoffersen, Y.,

2006. The Cenozoic palaeoenvironment of the Arctic Ocean. *Nature*, **441**: 601-605.

Morand, S., 1988. The developmental cycle of *Nemhelix bakeri* Morand and Petter (Nematoda, Cosmocercidae) parasite of the genital tract of *Helix aspersa* Mueller (Gastropoda, Helicidae). *Canadian Journal of Zoology*, **66**: 1796-1802.

Mosbrugger, V., Utescher, T. & Dilcher, D. L., 2005. Cenozoic continental climatic evolution of Central Europe. *Proceedings of the National Academy of Sciences of the United States of America*, **102**: 14964-14969.

Mutvei, H., 1978. Ultrastructual characteristics of the nacre of some gastropods: *Zoologica scripta*, **7**: 287-296.

Nesbitt, E.A., 2003. Changes in shallow marine faunas from the Northeastern Pacific margin across the Eocene–Oligocene boundary. In: Prothero, D.R., Ivany, L., & Nesbitt, E.A., (eds) *From Greenhouse to Icehouse*. New York, Columbia University Press, 57–70pp.

Newton, R.B., 1891. *Systematic lists of the Frederick E. Edwards collection of British Oligocene and Eocene Mollusca (London), British Natural History Museum*, **225**, 226 p.

Nocchi, M., Parisi, G., Monaco, P., Monechi, S. & Madile, M., 1988. Eocene and early Oligocene micropaleontology and paleoenvironments in SE Umbria, Italy. *Palaeogeography, Palaeoclimatology, Palaeoecology*, **67**: 181-244.

Oberhänsli, H., McKenzie, J., Toumarkine, M. and Weissert, H., 1984, A paleoclimatic and paleoceanographic record of the Paleogene in the central South Atlantic (Leg 73, Sites 522, 523, and 524, In: Hsu, K., LaBreque, J., et al., (eds), Initial

Reports of the Deep Sea Drilling Project, Volume **73**: Washington, D.C., U.S. Government Printing Office, p. 737 747.

Overpeck, J. & Trenberth, K. E., (2004). A Multi-Millennia Perspective on Drought and Implications for the Future. *Proceedings of a joint CLIVAR/PAGES/IPCC Workshop, 18-21 Nov. 2003, Tucson, AZ.* University Corporation for Atmospheric Research, Boulder CO, pp. 30.

Pallot, J.M. 1961. *Plant Macrofossils from the Oligocene of the Isle of Wight.* Unpublished PhD thesis, University of London, London, 206 pp

Pace, G. L. & Szuch, E. J., 1985. An exceptional stram population of the banded applesnail *Viviparus georgianus*, in Michigan. *Nautilus*, **99**: 48-53.

Pagani, M., Zachos, J. C., Freeman, K. H., Tipple, B. & Bohaty, S., 2005. Marked decline in atmospheric carbon dioxide concentrations during the Paleogene. *Science*, **309**: 600-603.

Palike, H., Norris, R. D., Herrle, J. O., Wilson, P. A., Coxall, H. K., Lear, C. H., Shackleton, N. J., Tripati, A. K. & Wade, B. S., 2006. The heartbeat of the Oligocene climate system. *Science*, **314**: 1894-1898.

Patterson. W.P., Smith. G. R. & Lohmann. K.C., 1993. Continental paleotheniiometry and seasonality using the isotopic composition of aragonitic otoliths of freshwater fishes. In: Swart, P.K., Lohmann, K.C., McKenzie, J., & Savin, S., (eds). Climate change in continental isotopic records. *American Geophysical Union Geophysical Monograph*, **78**: 191-202.

Parmesan, C., 2006. Ecological and evolutionary responses to recent climate change. *Annual Review of Ecology Evolution and Systematics*, **37**: 637-669.

Paul, C.R.C., 1989. The molluscan faunal succession in the Hatherwood Limestone Member (Upper Eocene), Isles of Wight, England. *Tertiary Research*, **10**: 147-162.

Pearson, P. N., Foster, G. L. & Wade, B. S., 2009. Atmospheric carbon dioxide through the Eocene-Oligocene climate transition', *Nature*, **461**: 1110-U1204.

Pearson, P. N., McMillan, I. K., Wade, B. S., Dunkley Jones, T., Coxall, H. K., Bown, P. R. & Lear, C. H., 2008. Extinction and environmental change across the Eocene-Oligocene boundary in Tanzania. *Geology*, **36**: 179-182.

Pearson, P. N. & Palmer, M. R., 2000. Atmospheric carbon dioxide concentrations over the past 60 million years. *Nature*, **406**: 695-699.

Pei, J. L., Sun, Z. M., Wang, X. S., Zhao, Y., Ge, X. H., Guo, X. Z., Li, H. B. & Si, J. L., 2009. Evidence for Tibetan Plateau Uplift in Qaidam Basin before Eocene-Oligocene Boundary and its climatic implications. *Journal of Earth Science*, **20**: 430-437.

Pekar, S. F., Christie-Blick, N., Kominz, M. A. & Miller, K. G., 2002. Calibration between eustatic estimates from backstripping and oxygen isotopic records for the Oligocene. *Geology*, **30**: 903-906.

Perera De Puoa, G. & Yono, M., 1984. The influence of some abiotic factors on the distribution freshwater molluscs on the isle of Youth (Isle of Pines) Cuba. Walkerana, *Transactions of the POETS Society*, **2**: 131-139.

Peters, R.S., 1964. Function of the cephalic tentacles in *Littorina planaxis* (Gastropoda: Prosobranchia) *Veliger* **7**: 143-148.

Peterson, L. C., Murray, D. W., Ehrmann, W. U. & Hempel, P., 1992 *Cenozoic carbonate accumulation and compensation depth changes in the Indian Ocean.* .In: Duncan, R. A., & Rea, D., (eds). *The Indian Ocean: A synthesis of Results from the Ocean Drilling Program.* Washington, D.C.: *Geophysical Monograph* **70**, American Geophysical Union. pp. 311-333.

Paul, C.R.C., 1989. The molluscan faunal succession in the Hatherwood Limestone Member (Upper Eocene), Isles of White, England: *Tertiary Research*, **10**: 147-162.

Piechocki, A., 1979. Mięczaki (Mollusca). Ślimaki (Gastropoda). Fauna Słodkowodna Polski 7, PWN, Warszawa–Poznań, 187 pp.

Plint, A.G., 1988. Global eustacy and the Eocene sequence in the Hampshire Basin, England. *Basin Research,* **1**:11-22;

Pointier, J. P., Delay, B., Toffart, J. L., Lefevre, M. & Romeroalvarez, R., 1992. Life history traits of 3 morphs of *Melanoides tuberculata* (Gastropoda, Thiaridae) an invading snail in the french West Indies. *Journal of Molluscan Studies*, **58**: 415-423.

Pollard, E., 1975. Aspects of the ecology of *Helix pomatia* L. *Journal of Animal Ecology,* **44**: 305- 329.

Poore, R. Z. & Matthews, R. K., 1984. Oxygen isotope ranking of Late Eocene and Oligocene plaktonic foraminifers - Implications for Oligocene sea surface temperature and global ice volume. *Marine Micropaleontology*, **9**: 111-134.

Potts, W. T. W. & Parry, G., 1963. *Osmotic and Ionic Regulation in Animals*. Pergamon, New York

Prashad, B., 1928. *Recent and fossil Viviparidae. A study in distribution, evolution and palaeogeography Memoirs of the Indian Museum.***VIII**: 153 - 249.

Preecer, C., 1976. 1980. The mollusca of the Creechbarrow Limestone Formation (Eocene) of Creechbarrow Hill Dorset. *Tertiary Research*, **2**: 169-184.

Premoli silva, I. & Jenkins, D. G., 1993. Decision on the Eocene–Oligocene boundary stratotype. *Episodes*, **16**: 379–381.

Pross, J., Kotthoff, U., Muller, U. C., Peyron, O., Dormoy, I., Schmiedl, G., Kalaitzidis, S. & Smith, A. M., 2009. Massive perturbation in terrestrial ecosystems of the Eastern Mediterranean region associated with the 8.2 kyr BP climatic event. *Geology*, **37**: 887-890.

Prothero, D.R., 1994. *The Eocene–Oligocene transition.* New York: Columbia University Press.

Prothero, D.R. & Heaton, T.H., 1996. Faunal stability during the Early Oligocene climatic crash. *Palaeogeography, Palaeoclimatology, Palaeoecology,* **127**: 257 - 283.

Rabosky, D. L. & Sorhannus, U., 2009. Diversity dynamics of marine planktonic diatoms across the Cenozoic. *Nature*, **457**:183-U173.

Radley, J.D., 2006. A Wealden guide I: the Weald Sub-basin. *Geology Today*, **22**: 109 - 118.

Rage, J.C.,& Augé, M., 1993. Squamates from the Cainozoic of the western part of Europe. A review. *Revue de Paléobiologie, Volume Special* **7**: 199–216.

Rahmstorf, S., 2001: *Abrupt climate change.* In: Steele, J., Thorpe, S., & Turekian, K., (eds). *Encyclopedia of Ocean Sciences*, **1**. Academic Press, London, pp. 1–6.

Rawlings T.A., 1999. Adaptations to physical stresses in the intertidal zone: the egg capsules of neogastropod molluscs. *American Zoology*, **39**: 230–243.

Rawlings T.A., 1994 .Encapsulation for eggs by marine gastropods: effect of variation in capsules form on the vulnerability of embryos to predation. *Evolution*, **48**: 1301–1313.

Raymo, M. E., Ruddiman, W. F. & Froelich, P. N., 1988. Influence of late Cenozoic mountain building on ocean geochemical cycles. *Geology*, **16**: 649-653.

Rea, D. K. & Lyle, M. W., 2005. Paleogene calcite compensation depth in the eastern subtropical Pacific: Answers and questions. *Paleoceanography*, **20**.

Reid, E.M. & Chandler, M.E.J., 1926. *Catalogue of Cainozoic plants in the Department of geology ,Volume 1. The Bembridge Flora. 206pp* British Museum (Natural History) London.

Reid, E.M. & Chandler, M.E.J., 1933. *The London clay flora.*Volume **7**, 54pp. British Museum (Natural History) London.

Remy, J. A., Crochet, J. Y., Sice, B., Sudre, J., Bonisl, D.E., Vianey-Liaud, M., Godinot, M,. Hartenbergje, .L.R., Lance-Badrbe, B. & Comte, B., 1987. Biochronologie des phosphorites du Quercy: Mise a jour des listes fauniques et nouveaux gisements de mammiferes fossiles. *Miinchner Geowissenschaftliche Abhandlungen*, **A10**: 169-188.

Retallack, G. J., 2001. A 300-million-year record of atmospheric carbon dioxide from fossil plant cuticles. *Nature*, **411**: 287-290.

Retallack, G. J., 2002. Carbon dioxide and climate over the past 300 Myr. *Philosophical Transactions of the Royal Society of London Series A, Mathematical Physical and Engineering Sciences*, **360**: 659-673.

Retallack, G. J., Orr, W. N., Prothero, D. R., Duncan, R. A., Kester, P. R. & Ambers, C. P., 2004. Eocene-Oligocene extinction and paleoclimatic change near Eugene, Oregon. *Geological Society of America Bulletin*, **116**: 817-839.

Ribi, G., 1986. Within lake dispersal of the prosobranch snails, *Viviparus ater* and *Potamopyrgus jenkinst*. *Oecologia (Berlin)*, **69**: 60-63.

Ribi G. & Gebhardt M., 1986. Age specific fecundity and size of offspring in the prosobranch snail, *Viviparus ater*. *Oecologia* (Berlin), **71**: 18–24.

Ribi, G. & Katoh, M., 1998. Weak preference for conspecific mates in the hybridizing snails *Viviparus ater* and *V-contectus* (Mollusca Prosobranchia). *Ethology Ecology & Evolution*, **10**: 383-392.

Richter, S. L., Johnson, A. H., Dranoff, M. M., LePage, B. A. & Williams, C. J., 2008. Oxygen isotope ratios in fossil wood cellulose: Isotopic composition of Eocene- to Holocene-aged cellulose. *Geochimica et Cosmochimica Acta*, **72**: 2744-2753.

Riveline, J., 1984. Les gisements à charophytes du Cénozoïque (Danien à Burdigalien) d'Europe occidentale. Lithostratigraphie, biostratigraphie, chronostratigraphie. *Bulletin d'Information des Géologues du Bassin de Paris (Mém. hors Série)*, **4**: 1–523.

Rögl, F., 1999. Mediterranean and Paratethys. Facts and hypotheses of an Oligocene to Miocene paleogeography (short overview). *Geologica Carpathica*, **50**: 339-349.

Romanek, C. S., Grossman, E. L. & Morse, J. W., 1992. Carbon isotopic fractionation in synthetic aragonite and calcite-Effects of temperature and precipitation rate. *Geochimica et Cosmochimica Acta*, **56**: 419 – 430.

Rosenthal, Y. & Katz, A., 1989. The applicability of trace elements in freshwater shells for paleogeochemical studies. *Chemical Geology*, **78**: 65-76.

Roth-Nebelsick, A., Utescher, T., Mosbrugger, V., Diester-Haass, L. & Walther, H., 2004. Changes in atmospheric CO2 concentrations and climate from the Late Eocene to Early Miocene: palaeobotanical reconstruction based on fossil floras from Saxony, Germany. *Palaeogeography, Palaeoclimatology, Palaeoecology*, **205**: 43-67.

Royer, D. L., 2006. CO_2 forced climate thresholds during the Phanerozoic. *Geochimica et Cosmochimica Acta*, **70** : 5665-5675.

Rundle, S. D., Spicer, J. I., Coleman, R. A., Vosper, J. & Soane, J., 2004. Environmental calcium modifies induced defences in snails. *Proceedings of the Royal Society of London Series B-Biological Sciences*, **271**: S67-S70.

Russell-Hunter, W., 1961. Life cycles of four freshwater snails in limited populations in Loch Lomond, with a discussion of infraspecific variation. *Proceedings of the Zoological Society of London,* **137**:135-171.

Russell-Hunter, W., 1964. Physiological aspects of ecology in nonmar-ine molluscs. In: Wilbur, K. M., & Yonge, C. M., (eds.). *Physiology of Mollusca*. Volume I. Academic Press, New York, New York, USA. pp. 83-126.

Russell-Hunter, W.D. & Eversole, A.G., 1976. Evidence for tissue degrowth in starved freshwater pulmonate snails *(Helisoma trivolvis)* from carbon: nitrogen analyses. *Comparative Biochemistry and Physiology A*, **54**: 447-453.

Russell-Hunter, W., 1978. Ecology of freshwater pulmonates. In: Fretter, V., & Peake, J., (eds.). *Pulmonates*. Volume **2A**. Academic Press, London, England. pp 335- 383.

Russell-Hunter W. D. & Buckley D. E., 1983. Actuarial bioenergetics of nonmarine molluscan productivity. In: Wilbur K. M. *Biology of the Mollusca,* Vol. **5**, New York, Academic Press, pp. 464–503.

Samovhwalenko, T. & Stanczykowska, A., 1972. Fertility differentiation of two species of Viviparidae (*Viviparus fascitus* Müll. and *Viviparus viviparus* L.) in some environments. *Polish Journal of Ecology (f. Ekologia Polska*), **20**: 479-492.

Schaffranek, R. W. & Jenter, H. L. 2001. Observations of Daily Temperature Patterns in the Southern Florida Everglades. In: Hays, D.F. (Ed.). *Proceedings of Wetlands Engineering and River Restoration Conference*. Reno, Nevada August 27-31 American Society of Civil Engineers, pp. 1-4.

Schauble, E. A., Ghosh, P. & Eiler, J. M., 2006. Preferential formation of C-13-O-18 bonds in carbonate minerals, estimated using first-principles lattice dynamics. *Geochimica et Cosmochimica Acta*, **70**: 2510-2529.

Scher, H. D. & Martin, E. E., 2004. Circulation in the Southern Ocean during the Paleogene inferred from neodymium isotopes. *Earth and Planetary Science Letters*, **228**: 391-405.

Scher, H. D. & Martin, E. E., 2006. Timing and climatic consequences of the opening of Drake Passage. *Science*, **312**: 428-430.

Schmitz, B. & Andreasson, F. P., 2001. Air humidity and lake delta O-18 during the latest Paleocene-earliest Eocene in France from recent and fossil fresh-water and marine gastropod delta O-18, delta C-13, and Sr-87/Sr-86. *Geological Society of America Bulletin*, **113**: 774-789.

Shanahan, T. M., Pigati, J. S., Dettman, D. L. & Quade, J., 2005. Isotopic variability in the aragonite shells of freshwater gastropods living in springs with nearly constant temperature and isotopic composition. *Geochimica et Cosmochimica Acta*, **69**: 3949-3966.

Shackleton, N.J. & Opdyke, N.D., 1973. Oxygen isotope and palaeomagnetic stratigraphy of equatorial Pacific core V28-238: oxygen isotope temperatures and ice volumes on a 10^5 and 10^6 year scale. *Quaternary Research* **3**, 39– 55.

Shackleton, N.J. & Kennett, J.P., 1975. Palaeotemperature history of the Cenozoic and the initiation of Antarctic glaciation, oxygen and carbon isotope analyses in DSDP Sites 277, 279 and 281. *Initial report; Deep Sea Drilling Programme*, **29**: 743-755.

Shackleton, N.J., and Kennett, J.P., 1975. Paleotemperature history of the Cenozoic and the initiation of Antarctic glaciation: oxygen and carbon isotope analyses in DSDP Sites 277, 279, and 281. *In* Kennett, J.P., Houtz, R.E., (eds) *Initial Reports of the Deep Sea Drilling Programme*, 29: Washington (U.S. Govt. Printing Office), 743-755.

Sheldon, N. D. & Retallack, G. J., 2004. Regional paleoprecipitation records from the late Eocene and Oligocene of North America. *Journal of Geology*, **112**: 487-494.

Sheldon, N. D. & Tabor, N. J., 2009. Quantitative paleoenvironmental and paleoclimatic reconstruction using paleosols. *Earth-Science Reviews*, **95**: 1-52.

Shipboard Scientific Party, 2002. Leg 199 summary. In: Lyle, M., Wilson, P.A., Janecek, T.R., et al., Proceeding of the Ocean Drilling Programme, Initial Reports, 199: College Station, TX (Ocean Drilling Program), pp. 1–87. doi:10.2973/odp.proc.ir.199.101.2002.

Shipboard Scientific Party, 2001. Leg 189 summary. In: Exon, N.F., Kennett, J.P., Malone, M.J., et al., Proceeding of the Ocean Drilling Programme, Initial Reports, 189: College Station, TX (Ocean Drilling Program), pp. 1–98. doi:10.2973/odp.proc.ir.189.101.2001

Schouten, S., Hopmans, E. C., Schefuss, E. & Damste, J. S. S., 2002. Distributional variations in marine crenarchaeotal membrane lipids: a new tool for reconstructing ancient sea water temperatures? *Earth and Planetary Science Letters*, **204**: 265-274.

Sille, N. P., Collinson, M. E., Kucera, M. & Hooker, J. J., 2006. Morphological evolution of Stratiotes through the paleogene in England: An example of microevolution in flowering plants. *Palaios*, **21**: 272-288.

Simmons, L.W., 1986. Female choice in the field cricket *Gryllus bimaculatus. Animal Behaviour*, **34**: 1463-1470.

Smith, J. R., Giegengack, R. & Schwarcz, H. P., 2004. Constraints on Pleistocene pluvial climates through stable-isotope analysis of fossil-spring tufas and associated gastropods, Kharga Oasis, Egypt. *Palaeogeography, Palaeoclimatology, Palaeoecology*, **206**: 157-175.

Sollas, W.J., 1905. *The age of the Earth and other Geologial Studies*. London, Fiser Unwin, London. 199 p.

Stanczykowska, A., Magnin, E. & Dumouche, A., 1971. Study on 3 population of *Viviaprus malleatus* (Reeve) (Gastropoda Prosobranchia) from Montreal. 1. Growth, fertility, biomass and yearly production. *Canadian Journal of Zoology*, **49**: 143-149.

Starobogatov, Y.I., 1985. Generic composition of the family Viviparidae (Gastropoda Pectinibranchia Viviparifonnes). *Transactions of the Zoological Institute, Academy of Sciences USSR*, **135**: 26-32

Staub, R. & Ribi, G., 1995. Size assortative mating in a natural population of *Viviparus alter* (Gastropoda Prosobranchia) in Lake Zurich, Switzerland. *Journal of Molluscan Studies*, **61**: 237-247.

Stehlin, H.G., 1910. Remarques sur les faunules de mammifères des couches éocènes et oligocènes du Bassin de Paris. *Bulletin de la Société Géologique de France*, **4**: 488–520.

Stehlin, H.G. & Schaub, S., 1951. Die Trigonodontie der simplicidentaten Nager. Abhandlungen Schweizerischen Paläontologischen. *Gesellschaft*, **67**: 1-15.

Steurbaut, E., 1992. Integrated stratigraphic analysis of lower Rupelian deposits (Oligocene) in the Belgiam Basin. *Annales de la Société Géologique de Belgique*, **115**: 287–306.

Stickley, C. E., Brinkhuis, H., Schellenberg, S. A., Sluijs, A., Rohl, U., Fuller, M., Grauert, M., Huber, M., Warnaar, J. & Williams, G. L., 2004. Timing and nature of the deepening of the Tasmanian Gateway. *Paleoceanography*, **19**: 25-37.

Stille, P., Steinmann, M. & Riggs, S. R., 1996. Nd isotope evidence for the evolution of the paleocurrents in the Atlantic and Tethys Oceans during the past 180 Ma. *Earth and Planetary Science Letters*, **144**: 9-19.

Stoll, H. M. & Schrag, D. P., 2000. High-resolution stable isotope records from the Upper Cretaceous rocks of Italy and Spain: Glacial episodes in a greenhouse planet? *Geological Society of America Bulletin*, **112**: 308-319.

Strayer D, 1990. *Freshwater Mollusca.* In: Peckarsky BL, Frassinet PR, Penton MA, Conklin DJ, (eds), *Freshwater Macroinvertebrates of Northeastern North America.* Cornell University Press, New York, pp. 335-372.

Studier, E. H. & Pace, G. L., 1978. Oxygen consumption in prosobranch snail *Viviparus contectoides* (Mollusca Gastropoda) 4. Effects of dissolved oxygen level, starvation, density, symbiotic algae, substrate composition and osmotic pressure. *Comparative Biochemistry and Physiology a-Physiology*, **59**: 199-203.

Swart, P. K., Burns, S. J. & Leder, J. J., 1991. Fractionation of the stable isotopes of oxygen and carbon in carbon dioxide during the reaction of calcite with phosphoric acid as a function of temperature and technique. *Chemical Geology*, **86**: 89-96.

Szyndlar, Z. & Rage, J. C., 2003. *Non-erycine Booidea from the Oligocene and Miocene of Europe.* Institute of Systematics and Evolution of Animals, Polish Academy of Sciences, Krakow.

Tanaka, N., Monaghan, M. C. & Rye, M. C., 1986. Contribution of metabolic carbon to mollusc and barnacle shell carbonate. *Nature*, **320**: 520– 523.

Tashiro J.S., 1982. Grazing in *Bithynia tentaculata*: age-specific bioenergetic patterns in reproductive partitioning of ingested carbon and nitrogen. *American Midland Naturalist*, **107**: 133–150.

Thomas, D. J., Bralower, T. J. & Jones, C. E., 2003. Neodymium isotopic reconstruction of late Paleocene-early Eocene thermohaline circulation. *Earth and Planetary Science Letters*, **209**: 309-322.

Tischler, W. 1973. Zur Biologie und Oekologie der Weinbergschnecke *{Helix pomatia). Faunistischdkologische Mitteilungen,* **4**: 283-298.

Tripati, A., Backman, J., Elderfield, H. & Ferretti, P., 2005. Eocene bipolar glaciation associated with global carbon cycle changes. *Nature*, **436**: 341-346.

Tripati, A. K., Eagle, R. A., Morton, A., Dowdeswell, J. A., Atkinson, K. L., Bahe, Y., Dawber, C. F., Khadun, E., Shaw, R. M. H., Shorttle, O. & Thanabalasundaram, L., 2008. Evidence for glaciation in the Northern Hemisphere back to 44 Ma from ice-rafted debris in the Greenland Sea. *Earth and Planetary Science Letters*, **265**:112-122.

Trivers, R. 1972. Parental investment and sexual selection. In: Campbell, B. (Ed.), *Sexual selection and the descent of man.* Heinemann, London. pp. 136-179.

Trott , T.J. & Dimock, R.V. Jr., 1978. Intraspecific trail following by the mud snail *Ilyanassa obsoleta. Marine Behaviour and Physiology,* **5**: 91-101.

Trub, H., 1990. ZUchtung von Hybriden zwischen *Viviparus ater* und *V. contectus* (Mollusca, Prosobranchia) im Zurichsee und dkologische Untersuchungen in einer gemischten Population tm Gardasee. Dissertation, Universit St Zurich.

Uhl, D., Klotz, S., Traiser, C., Thiel, C., Utescher, T., Kowalski, E. & Dilcher, D. L., 2007. Cenozoic paleotemperatures and leaf physiognomy - A European perspective. *Palaeogeography, Palaeoclimatology, Palaeoecology*, **248**: 24-31.

Urey, H.C., Lowenstam, H.A., Epstein, S. & McKinney, C.R., 1951. Measurement of palaeotemperatures and temperatures of the Upper Cretaceous of England, Denmark and Southeatern United Stated. *Geological Society of America Bulletin*, **62**: 399-416.

Van Andel, T. H. & Moore, Jr, T. C., 1974. Cenozoic calcium carbonate distribution and calcite compensation depth in the central equatorial Pacific Ocean. *Geology*, **2**: 87–92.

Vail, V. A., 1977. Observations on brood production in three viviparid gastropods. *Bulletin of the American Malacological Union*. 43:90.

Vandergoes, M. J., Dieffenbacher-Krall, A. C., Newnham, R. M., Denton, G. H. & Blaauw, M., 2008. Cooling and changing seasonality in the Southern Alps, New Zealand during the Antarctic Cold Reversal. *Quaternary Science Reviews*, **27**:589-601.

Van der Voo, R. & French, R. B., 1974. Apparent polar wandering for the Atlantic bordering continents: Late Carboniferous to Eocene. *Earth Science Reviews*, **10**: 99- 119.

Van Mourik, C. A. & Brinkhuis, H., 2005. The Massignano Eocene–Oligocene golden spike section revisited. *Stratigraphy*, **2**: 13–29.

Van Sickel, W. A., Kominz, M. A., Miller, K. G. & Browning, J. V., 2004. Late Cretaceous and Cenozoic sea-level estimates: backstripping analysis of borehole data, onshore New Jersey. *Basin Research*, **16**: 451-465.

Veinott, G. I. & Cornett, R. J., 1998.Carbon isotope disequilibrium in the shell of the freshwater mussel Elliptio complanata. *Applied Geochemistry*, **13**: 49– 57.

Via, R. K. & Thomas, D. J., 2006. Evolution of Atlantic thermohaline circulation: Early Oligocene onset of deep-water production in the North Atlantic. *Geology*, **34**: 441-444.

Vianey-Liaud, M., 1976. Les Issiodoromyinae (Rodentia, Theridomyidae) de l'Eocène supérieur à l'Oligocène supérieur en Europe occidentale. *Palaeovertebrata*, **7**: 1–115.

Villa, G., Fioroni, C., Pea, L., Bohaty, S. & Persico, D., 2008. Middle Eocene-late Oligocene climate variability: Calcareous nannofossil response at Kerguelen Plateau, Site 748. *Marine Micropaleontology*, **69**: 173-192.

Visser, M. E. & Both, C., 2005. Shifts in phenology due to global climate change: the need for a yardstick. *Proceedings of the Royal Society B-Biological Sciences*, **272**: 2561-2569.

Vonhof, H. B., Smit, J., Brinkhuis, H., Montanari, A. & Nederbragt, A. J., 2000. Global cooling accelerated by early late Eocene impacts? *Geology*, **28**: 687-690.

Wade, B. S. & Palike, H., 2004. Oligocene climate dynamics. *Paleoceanography*, **19**.

Warrington, A.G. 1990. *Stable isotopes of carbon and oxygen in the shells of terrestrial molluscs*, Unpublished PhD Thesis, University of Liverpool, 260pp.

Wang, D. N., Sun, X. Y. & Zhao, Y. N., 1990. Late Cretaceous to Tertiary palynofloras in Xinjiang and Qinghai, China. *Review of Palaeobotany and Palynology*, **65**: 95-104.

Wang, Z. G., Schauble, E. A. & Eiler, J. M., 2004. Equilibrium thermodynamics of multiply substituted isotopologues of molecular gases. *Geochimica et Cosmochimica Acta*, **68**: 4779-4797.

Ward, J. E., Cassell, H. K. & Macdonald, B. A., 1992. Chemoreception in the sea scallop *Placopecten magellanicus* (Gmelin). 1. Stimulatory effects of phytoplankton metabolites on clearance and ingestion rates. *Journal of Experimental Marine Biology and Ecology*, **163**: 235-250.

Westerhold, T., Bickert, T. & Rohl, U., 2005. Middle to late Miocene oxygen isotope stratigraphy of ODP site 1085 (SE Atlantic): new constrains on Miocene climate variability and sea-level fluctuations. *Palaeogeography, Palaeoclimatology, Palaeoecology*, **217**: 205-222.

White, R. M. P., Dennis, P. F. & Atkinson, T. C., 1999. Experimental calibration and field investigation of the oxygen isotopic fractionation between biogenic aragonite and water. *Rapid Communications in Mass Spectrometry*, **13**: 1242–1247.

Wilbur, K.M. & Saleuddin, A.S.M., 1983. *Physiology.* In: Wilbur, K.M., and Saleuddin, A.S.M., (eds)., *Shell Formation,* Volume Vol.**4**, Academic Press.

Wilbur, K.M. & Younge, C.M., 1964. *Physiology: Mollusc*. In: Wilbur, K.M., (Ed)., *Shell formation and regeneration*, Vol. **1**, Academic Press.

Williams, G.C., 1975. *Sex and evolution.* Princeton University Press: Princeton, New Jersey.

Wold, C. N., 1994. Cenozoic Sediment Accumulation on Drifts in the Northern North Atlantic. *Paleoceanography*, **9**: 917–941.

Wolfe, J. A., 1978. Paleobotanical interpretation of Tertiary climates in Northern Hemisphere. *American Scientist*, **66**: 694-703.

Wolfe, J.A., 1992. Climatic, floristic and vegetational changes near the Eocene / Oligocene boundary in North America. In: Prothero, D.R., & Berggren, W. A, (eds) *Eocene – Oligocene Climatic and Biotic Evolution*. Princeton University Press, Princeton, 421-436.

Wolfe, J. A., 1994. Tertiary climate changes at middle latitudes of Western North America. *Palaeogeography, Palaeoclimatology, Palaeoecology*, **108**: 195-205.

Wolfe, J. A., 1995. Paleoclimatic estimated from tertiary leaf assemblages. *Review of Earth and Planetary Sciences*, **23**: 119-142.

Wurster, C. M. & Patterson, W. P., 2001. Seasonal variation in stable oxygen and carbon isotope values recovered from modern lacustrine freshwater mollusks: Paleoclimatological implications for sub-weekly temperature records. *Journal of Paleolimnology*, **26**: 205-218.

Young, M.R., 1975. The life cycles of six species of freshwater molluscs in the Worchester-Birmingham Canal. *Proceedings of the Malacological Society of London*, **41**: 533 - 548.

Zachos, J., Pagani, M., Sloan, L., Thomas, E. & Billups, K., 2001. Trends, rhythms, and aberrations in global climate 65 Ma to present. *Science*, **292**: 686-693.

Zachos, J. C., Breza, J. R. & Wise, S. W., 1992. Early Oligocene ice sheet expansion on Antarctic - stable isotope and sedimentological evidence from Kerguelen Plateau, Southern Indian Ocean. *Geology*, **20**: 569-573.

Zachos, J. C., Quinn, T. M. & Salamy, K. A., 1996. High-resolution (10(4) years) deep-sea foraminiferal stable isotope records of the Eocene-Oligocene climate transition. *Paleoceanography*, **11**: 251-266.

Zachos, J. C. & Kump, L. R., 2005. Carbon cycle feedbacks and the initiation of Antarctic glaciation in the earliest Oligocene. *Global and Planetary Change*, **47**: 51-66.

Zachos, J. C., Rohl, U., Schellenberg, S. A., Sluijs, A., Hodell, D. A., Kelly, D. C., Thomas, E., Nicolo, M., Raffi, I., Lourens, L. J., McCarren, H. & Kroon, D., 2005. Rapid acidification of the ocean during the Paleocene-Eocene thermal maximum. *Science*, **308**: 1611-1615.

Zanazzi, A., Kohn, M. J., MacFadden, B. J. & Terry, D. O., 2007. Large temperature drop across the Eocene-Oligocene transition in central North America. *Nature*, **445**: 639-642.

Zeebe, R. E., 1999. An explanation of the effect of seawater carbonate concentration on foraminiferal oxygen isotopes. *Geochimica et Cosmochimica Acta*, **63**: 2001-2007.

Zhang, C. & Zhang, R. Q., 2006. Matrix proteins in the outer shells of molluscs. *Marine Biotechnology*, **8**: 572-586.

APPENDIX 1

(Part 1: Modern gastropods; Chapter 2 to 5)

APPENDIX 2

(Part 2: Chapter 6, A *Viviparus lentus* isotopic record)

APPENDIX 3

(Part 2: Chapter 7, Seasonality isotopic variability)

PUBLICATION

Bugler, M., Grimes, S.T., Leng, M.J., Rundle, S.D., Price, G.D., Hooker, J.J. & Collinson, M.E. 2009. Experimental determination of a *Viviparus contectus* thermometry equation Rapid Communication in Mass Spectrometry 23(18):2939-51.

RAPID COMMUNICATIONS IN MASS SPECTROMETRY
Rapid Commun. Mass Spectrom. 2009; **23**: 2939–2951
Published online in Wiley InterScience (www.interscience.wiley.com) DOI: 10.1002/rcm.4203

RCM

Experimental determination of a *Viviparus contectus* thermometry equation

Melanie J. Bugler[1]*, Stephen T. Grimes[1], Melanie J. Leng[2], Simon D. Rundle[3], Gregory D. Price[1], Jerry J. Hooker[4] and Margaret E. Collinson[5]

[1]School of Earth, Ocean & Environmental Sciences, University of Plymouth, Drake Circus, Plymouth PL4 8AA, UK
[2]NERC Isotope Geosciences Laboratory, British Geological Survey, Keyworth, Nottingham NG12 5GG, UK
[3]School of Biological Sciences, University of Plymouth, Drake Circus, Plymouth PL4 8AA, UK
[4]Department of Palaeontology, Natural History Museum, Cromwell Road, London SW7 5BD, UK
[5]Department of Earth Sciences, Royal Holloway University of London, Egham TW20 0EX, UK

Received 17 April 2009; Revised 10 July 2009; Accepted 11 July 2009

Experimental measurements of the $^{18}O/^{16}O$ isotope fractionation between the biogenic aragonite of *Viviparus contectus* (Gastropoda) and its host freshwater were undertaken to generate a species-specific thermometry equation. The temperature dependence of the fractionation factor and the relationship between $\Delta\delta^{18}O$ ($\delta^{18}O_{carb.} - \delta^{18}O_{water}$) and temperature were calculated from specimens maintained under laboratory and field (collection and cage) conditions. The field specimens were grown (Somerset, UK) between August 2007 and August 2008, with water samples and temperature measurements taken monthly. Specimens grown in the laboratory experiment were maintained under constant temperatures (15°C, 20°C and 25°C) with water samples collected weekly. Application of a linear regression to the datasets indicated that the gradients of all three experiments were within experimental error of each other (±2 times the standard error); therefore, a combined (laboratory and field data) correlation could be applied. The relationship between $\Delta\delta^{18}O$ ($\delta^{18}O_{carb.} - \delta^{18}O_{water}$) and temperature (T) for this combined dataset is given by:

$$T = -7.43(+0.87, -1.13) * \Delta\delta^{18}O + 22.89(\pm 2.09)$$

(T is in °C, $\delta^{18}O_{carb.}$ is with respect to Vienna Pee Dee Belemnite (VPDB) and $\delta^{18}O_{water}$ is with respect to Vienna Standard Mean Ocean Water (VSMOW). Quoted errors are 2 times standard error).

Comparisons made with existing aragonitic thermometry equations reveal that the linear regression for the combined *Viviparus contectus* equation is within 2 times the standard error of previously reported aragonitic thermometry equations. This suggests there are no species-specific vital effects for *Viviparus contectus*. Seasonal $\delta^{18}O_{carb.}$ profiles from specimens retrieved from the field cage experiment indicate that during shell secretion the $\delta^{18}O_{carb.}$ of the shell carbonate is not influenced by size, sex or whether females contained eggs or juveniles. Copyright © 2009 John Wiley & Sons, Ltd.

Fossil freshwater gastropods have been utilised as recorders of palaeoclimatic change[1–5] as their shell carbonate $\delta^{18}O$ value is generally thought to be derived from the carbonate having been precipitated in isotopic equilibrium with their host water.[6–9] In order to reconstruct past climates the relationship between the equilibrium $\delta^{18}O$ value of carbonate and the temperature of secretion must be well constrained.[10] The calculated fractionation factors differ significantly between different proposed relationships, such as those produced using experimental measurements (e.g.[11,12]); theoretical calculations (e.g.[13]); and biological specimens from natural settings (e.g.[7,9]). It is unclear from the literature which of these temperature–$\delta^{18}O$ relationships should be applied to a particular organism for a correct interpretation of the $\delta^{18}O$ data. However, this is further complicated by non-equilibrium isotopic effects which are generally attributed to either vital and/or non-vital kinetic effects.

These non-equilibrium vital effects are problematic when applying thermometry equations to the oxygen isotopic composition obtained from fossil shell carbonates. Taking such genus- or species-specific 'vital and/or non-vital kinetic effects' into account could be critical for the interpretation of temperature records calculated from proxy isotope data using current thermometry equations.[7,9] The influence of vital effects on oxygen isotope fractionation is directly

*Correspondence to: M. J. Bugler, School of Earth, Ocean & Environmental Sciences, University of Plymouth, Drake Circus, Plymouth PL4 8AA, UK.
E-mail: melanie.bugler@plymouth.ac.uk

related to the metabolic processes of a host organism or the differential composition of the internal fluids from which the mineral is precipitated.[11] The direction and magnitude of the fractionation vary from species to species as each organism has a unique calcification physiology.[11] External influences include changes in the microenvironment[14] which may also impact on the isotopic fractionation.

When the oxygen isotopic composition of the host water remains constant, temperature is the most important factor affecting the sign and magnitude of equilibrium isotope fractionations.[11] Zeebe[15] proposed a non-equilibrium effect on the oxygen isotope composition of biogenic carbonates. He suggested that the oxygen isotopic composition is also dependent on the relative abundance of the isotopically distinct carbonic acid species in solution or the pH at the time of precipitation. He hypothesises that calcium carbonate precipitated from a higher pH solution would have a lower $\delta^{18}O$ value because of a greater contribution from the isotopically lighter CO_3^{2-} ion among the carbonate acid species. Conversely, experimental analysis of synthetic aragonite indicates that statistically indistinguishable oxygen isotope fractionation factors were determined under distinctly different pH conditions.[11]

The effect of carbonate precipitation rate on the oxygen isotope composition is referred to as a non-vital kinetic effect. Experimental evidence concerning non-vital kinetic effects provides contradictory results. Kim *et al.*[11] suggest that a lack of re-equilibration as a result of quick precipitation as well as preferential deprotonation of isotopically light HCO_3^- ions and the incorporation of light CO_3^{2-} isotopologues into a growing carbonate mineral could account for the kinetic isotope effects observed during carbonate mineral precipitation. However, Kim *et al.*[12] have also shown that no apparent kinetic isotope effects are involved during the precipitations of inorganic aragonite under the experimental conditions of their study. A detailed description of the proposed mechanisms for these offsets can be found in McConnaughey.[16]

The causes of disequilibrium or vital effects are often systematic and can be accounted for by detailed studies of the particular genera or species in question. The aim of this study is to improve our understanding of gastropod aragonite palaeothermometry equations by calibrating the fractionation between water and biogenic carbonate (aragonite) of *Viviparus contectus* (Millet, 1813) (Fig. 1). A species of the genus *Viviparus* has been chosen specifically to complement a study on palaeoclimatic change across the Early Oligocene Glacial Maximum (Oi-1) (~33 Ma) in the Hampshire Basin, UK (51°41.570′N 1°19.003′W).

Species of the genus *Viviparus* in general colonise a wide range of habitats including rivers, streams, ponds, lakes, pools and marshes,[17] and are found in parts of North America, Australia, Asia, Africa and Europe, but do not extend to Polar Regions.[18] Its widespread distribution since the Eocene (~50 Ma) makes it an important geological proxy. Primarily, members of the genus are detritus feeders usually grazing on stones, etc., but they also have the ability to filter feed.[19] They are gill breathers and therefore are found in permanent water bodies ranging between 0 and 20 m water depths.[20] Their dependence on dissolved oxygen for respiration makes them intolerant of polluted water[21,22] and, therefore, they are rarely found in stagnant water bodies, e.g. shallow ponds, where oxygen levels are low at night or when temperatures are high.[23] For short periods of time they can exist out of water by withdrawing into their shell and sealing their aperture with the operculum.[24] Annual reproduction occurs in spring with large unevenly distributed aggradations of *Viviparus* in the littoral zone. Post-reproduction seasonal migration is common, with snails moving to deeper water in the autumn and back to shallower littoral areas in the spring.[25,26]

Figure 1. Specimen of *Viviparus contectus* collected from South Drain Canal on the Somerset Levels after cleaning with sodium hypochlorite.

EXPERIMENTAL

To achieve the aim of this study a modified version of the technique used by White *et al.*[9] in the determination of the *Lymnaea* genus specific equation, was adopted.

Field-based method

South Drain on the Somerset Levels, UK, was chosen based on the known occurrence of *V. contectus* and because large flowing water bodies (river or canal), as opposed to standing waters such as lakes, have been shown in previous studies[9] to have hydrological conditions that allow the isotope composition of the water to remain relatively constant throughout the year. South Drain Canal forms part of a man-made drainage system, initially constructed to drain the Somerset Levels for agricultural use in response to the Brue Drainage Act of 1801.[27] The sampling site is located between the villages of Chilton Polden and Burtle, where the Chilton Road crosses South Drain Canal (51°10.839′N 2°52.815′W).

During each sampling visit (approximately once per month) water samples were collected and analysed for $^{18}O/^{16}O$ ratios and the $^{13}C/^{12}C$ ratios of total dissolved organic carbon (TDIC). Temperature (±1°C), pH (±0.2) and salinity (±0.5) measurements were also measured on site.

DOI: 10.1002/rcm

Field-based *V. contectus* sample collection

A minimum of 5–10 *V. contectus* specimens were collected from the bottom sediments of the South Drain Canal (~4 m in depth) using a drag net, approximately once a month between 30/8/2007 and 13/8/2008. Upon return to the laboratory the *V. contectus* samples were ethically euthanised by cryogenesis. Their bodies were removed from the shells, sexed and when eggs/juveniles occurred these were counted. The shells were soaked overnight in dilute (2%) NaOCl to remove organic material including the periostracum. The shells were then rinsed in ultra-pure water and oven-dried at 25 °C. Using a small Dremel drill (Dremel UK, Uxbridge, UK) and a 0.4 mm tungsten carbide spade drill bit, approximately the last millimetre of shell growth was removed by milling the growth bands parallel to the aperture edge. A minimal number of growth bands were removed to produce a powdered sample at the weight required for the $^{18}O/^{16}O$ and $^{13}C/^{12}C$ ratios to be measured.

Outline of the field cage method

On 29 February 2008 at the South Drain Canal site, two cages were submerged to a depth of ~4 m, embedding approximately 5 cm of the bottom part of the cage into the canal bed sediment. The first cage consisted of a cylindrical metal structure (height 30 cm, diameter 13 cm), encased in a 15 mm^2 metal mesh. The second cage was a plastic box (height 23 cm, width 24 cm) encased in 2 mm^2 plastic mesh. Each cage contained 10 *V. contectus* specimens of varying sizes (ranging from 1.4 mm in height and 1.3 mm in width to 3.6 mm in height and 2.8 mm in width) that had been collected that day. Each specimen was numbered and the aperture (growing edge) was marked with white paint so that any subsequent growth could be identified. During each monthly sampling visit the cages were removed for inspection. Any specimens exhibiting new growth along their aperture edge were measured (using a tape measure) from the white line marking the previous location of the aperture to the present aperture edge. Samples exhibiting more than 0.5 mm of growth were taken back to the laboratory for analysis. The remaining specimens and replacements for those taken were remarked and returned to the cage. In general the smaller (spire height <2 cm) specimens (approximately 6 to 12 months old) acquired more shell growth per month than the larger specimens, which led to smaller specimens being preferentially chosen as replacements.

On return to the laboratory the specimens from the cage experiment were treated as stated for the 'field-based *V. contectus* sample collection' with an additional preparation step. A small hole (~0.3 mm in diameter) was drilled into the shell marking the position of the white paint lines, as during the removal of the residual organic material by NaOCl, the white paint was also removed. Growth while within the cage dictated the number of drill lines taken for isotopic analysis, i.e. each drill line was ca. 0.4 mm in width and therefore if growth exceeded 0.4 mm a greater number of samples could be taken. Each drill line followed the growth banding parallel to the aperture, incorporating a minimal number of growth bands without compromising sample size. In an attempt to reduce errors the drill lines were located close to the position of the white line, as this growth was secreted closest to the collection of $\delta^{18}O_{water}$ samples and temperature readings. Shell stabilisation for drilling purposes depended on the amount of growth secreted by the specimen. Infilling of the shell with resin was necessary when the growth was greater than 2–3 mm.

Two specimens that had remained within the cage from February to July 2008 and another specimen that had remained within the cage for the whole experiment (February to August 2008) were chosen to determine isotopic variation over several months of growth. To investigate whether sexual dimorphism or fecundity affects oxygen isotope fractionation the three specimens sampled were: a male (VC 8), a female containing 16 eggs (stage 1 of the embryonic development) (VC 9), and a female containing 21 juveniles (stage 3 of the embryonic development) (VC 5) (Table 5). As the mean growth achieved by the three specimens was 24 mm, infilling with resin was necessary for shell stabilisation. Each shell was infilled with blue resin so that a clear comparison between the resin and shell could be seen to prevent any resin from being incorporated into the carbonate sample. For each specimen, an average of 11 drill lines of ca. 0. 4 mm width were sampled from growth bands parallel to the aperture. As continuous monitoring was not possible, dates for the intervening samples (between the monthly collections, e.g. the white lines) were calculated by dividing the total amount of growth secreted within a specific time period, e.g. 19 mm over 42 days, giving an average daily growth rate of 0.45 mm per day. The position of the drill line was measured from the beginning of the specific sampling period (position of the white line) and was used in combination with the average growth rate to calculate an approximate date at which the growth bands encompassed by the drill line were secreted. We therefore have assumed a constant growth rate throughout any given time period.

Laboratory method

V. contectus samples were collected from South Drain Canal during the first sampling trip (August 2007) with additional specimens added during February 2008. These specimens (~10 per controlled temperature) were cultured thereafter in tanks in the laboratory at controlled temperatures (15 °C, 20 °C and 25 °C) for a period of approximately 2 months, or until each specimen had added enough new shell growth for sampling. The growing edges (aperture) of the *V. contectus* shells were marked with white paint before the specimens were added to the culturing tanks to ensure that new growth could be identified. The specimens were kept in deionised water containing 14.7 g of $MgSO_4$, 11.7 g of $NaHCO_3$, 0.48 g of KCl and 5.4 g of $CaSO_4$ (for every 60 L), to maintain suitable water quality for the gastropods to live comfortably.[28] The isotopic composition, temperature, pH and salinity of the water were measured weekly during the culturing period. Samples were collected for isotopic analysis, while temperature, pH and salinity measurements were collected using a YSI model 63, pH, Conductivity, Salinity and Temperature probe (Yellow Springs Inc., Yellow Springs, OH, USA). To minimise evaporation, particularly in the 25 °C tank, each tank was sealed with cling film causing most of the vapour to condense and be recycled back into the tank. Minimal aeration ensured that the water was well mixed and

DOI: 10.1002/rcm

oxygen levels were sufficient to sustain the gastropod specimens. Lettuce was provided as food and green algal growth was retained on the tank surfaces as an additional food source.

Oxygen and carbon isotope analysis

The collected water samples were filtered in the field through a series of filters (1.2 mm, 11 μm and 0.2 μm) to remove any particulate matter. Samples for oxygen isotope analysis were refrigerated in 30 mL Nalgene narrow-mouth low-density polyethylene (LDPE) bottles (Thermo Fisher, Rochester, NY, USA) until analysed. The waters were equilibrated with CO_2 using an Isoprep 18 device for oxygen isotope analysis with mass spectrometry performed on a SIRA isotope ratio mass spectrometer (both VG IsoGas, Middlewich, UK). For hydrogen isotope analysis an on-line Cr reduction method was used with a EuroPyrOH-3110 system (EuroVector, Milan, Italy) coupled to an Isoprime mass spectrometer (GV Instruments, Manchester, UK). Isotopic ratios ($^{18}O/^{16}O$ and $^{2}H/^{1}H$) and $\delta^{18}O$ and $\delta^{2}H$ (‰, parts per mil) are defined in relation to the international standard Vienna Standard Mean Ocean Water (VSMOW) by comparison with laboratory standards calibrated using NBS standards. The analytical precision is typically ±0.05‰ for $\delta^{18}O$ and ±1.0‰ for $\delta^{2}H$.

The total dissolved inorganic carbon (TDIC) from the water samples was precipitated in the field as $BaCO_3$ by addition of a solution of barium chloride and sodium hydroxide. In the laboratory CO_2 was generated by the reaction of the $BaCO_3$ with 100% phosphoric acid. The CO_2 was analysed for $^{13}C/^{12}C$ ratio using an Optima dual inlet mass spectrometer (VG IsoTech, Middlewich, UK). The analytical precision (1 Standard Deviation (SD)) based on laboratory standard is <0.1‰.

For the shell carbonate $^{13}C/^{12}C$ and $^{18}O/^{16}O$ measurements, approximately 30–100 μg of carbonate was analysed using the IsoPrime dual inlet mass spectrometer plus Multiprep device (GV Instruments). The analytical precision (1SD) is typically <0.07‰ for both ratios. Carbonate and TDIC isotopic ratios are reported in the per mil notation (‰) reported relative to the international standard Vienna Pee Dee Belemnite (VPDB) by comparison with laboratory standards calibrated using NBS standards. An aragonite fractionation factor (1.01034 taken from Friedman and O'Neil[29]), was applied to convert the measured isotope compositions of CO_2 generated by the reaction of aragonite with orthophosphoric acid into the isotope compositions of aragonite.

Formulation of equations

Shell $\delta^{18}O_{carb.}$ values were used in conjunction with temperature and water $\delta^{18}O$ to derive values of 1000lnα and $\Delta\delta^{18}O$ ($\delta^{18}O_{carb.} - \delta^{18}O_{water}$). This information was then plotted against 1/T (T in Kelvin) and T (°C), respectively, to give the relationships described below. The temperature dependence of the fractionation factor (α) is given by the linear relationship:

$$1000 \ln \alpha = M(1000T^{-1}) - C \quad (1)$$

where $\alpha = ((\delta^{18}O_{carb.}\ VSMOW) + 1000)/((\delta^{18}O_{water}\ VSMOW) + 1000)$

where M is the gradient of the linear trend, C is the y-axis intercept and T is the temperature in Kelvin.

The thermometry equations for both the laboratory and the field-based studies were generated by plotting the dependent variable, $\Delta\delta^{18}O$ ($\delta^{18}O_{carb.}$ (VPDB) − average $\delta^{18}O_{water}$ (VSMOW)), against the independent variable, the average recorded water temperature (°C). A linear regression was calculated to determine the relationship between the $\Delta\delta^{18}O$ and temperature, producing a thermometry equation (Eqns. (2) and (3)) in the form of:

$$\Delta\delta^{18}O = M(2S.E.) * Temp. + C(2S.E.) \quad (2)$$

This was then rearranged to give:

$$Temp.(°C) = -M(2S.E.) * \Delta\delta^{18}O + C(2S.E.) \quad (3)$$

where C is the y-axis intercept, M is the gradient of the linear trend and 2S.E. = 2 times standard error.

RESULTS

The results for the laboratory culturing experiment, field cage experiment and field collection experiment are given in Tables 1, 2 and 3, respectively.

Laboratory culturing experiment

For the duration of the laboratory experiment, the temperatures, with minor deviation from the controlled temperatures, were 15 °C mean = 15.09 °C (±0.41 °C); 20 °C mean = 19.59 °C (±0.18 °C); 25 °C mean = 24.96 °C (±0.11 °C). The measured $\delta^{18}O_{water}$ shows minimal variation from the mean, 15 °C mean = −5.23‰ (±0.15‰); 20 °C mean = −5.13‰ (±0.29‰); 25 °C mean = −4.94‰ (±0.30‰); however, deviation from the average $\delta^{18}O_{water}$ values increases with higher temperatures, suggesting some minor evaporation with increasing water temperature.

For the laboratory culturing experiment the temperature dependence of the fractionation factor (α), between 15 and 25 °C, is given by Eqn. (4):

$$1000 \ln \alpha = 8.59(\pm 0.1) * (1000T^{-1})\ 0.64(\pm 0.28) \quad (r^2 = 0.92) \quad (4)$$

where T is in Kelvin, and the relationship between $\Delta\delta^{18}O$ and temperature is given by Eqns. (5) and (6):

$$\Delta\delta^{18}O = -10.0(\pm 0.04) * Temp. + 1.98(\pm 0.72) \quad (5)$$

This rearranges to:

$$Temp.(°C) = -10.09(+1.73, -4.24) * \Delta\delta^{18}O + 20.4(\pm 7.20) \quad (Fig.\ 2(A)) \quad (6)$$

The relationship between $\Delta\delta^{18}O$ and temperature shows an excellent statistical regression ($r^2 = 0.91$).

Field experiments

In the field experiment the temperature (August 2007 to 2008) reached a maximum of 19.9 °C and a minimum of 7.4 °C, indicating a range of ~12.5 °C for the sampling period. The range in temperature between successive sampling collections was determined by calculating the difference between

DOI: 10.1002/rcm

Table 1. Laboratory culturing data (probe result and water analysis) and the results from the analysis of carbonate material from *Viviparus contectus* cultured within the laboratory culturing experiments

Mean pH	Mean Salinity (ppt)	Mean Temp. (°C)	Mean $\delta^{18}O_{water}$ (‰ VSMOW)	$\delta^{18}O_{carb.}$ (‰ VPDB)	$\Delta\delta^{18}O(\delta^{18}O_{carb.}$ ‰ (VPDB) – $\delta^{18}O_{water}$ ‰ (VSMOW))
7.62 (±0.28 std) (n = 24)	0.25 (±0.10 std) (n = 24)	15.09 (±0.41 std) (n = 24)	−5.23 (±0.15 std) (n = 2)	−4.89	+0.34
				−4.54	+0.69
				−4.84	+0.39
				−4.68	+0.55
7.51 (±0.19 std) (n = 24)	0.33 (±0.21 std) (n = 24)	19.59 (±0.18 std) (n = 24)	−5.13 (±0.29 std) (n = 2)	−5.04	+0.09
				−5.13	+0.00
				−5.37	−0.24
				−5.14	−0.01
				−5.06	+0.07
7.26 (±0.25 std) (n = 9)	0.30 (±0.00 std) (n = 9)	24.96 (±0.25 std) (n = 9)	−4.94 (±0.30 std) (n = 2)	−5.51	−0.57
				−5.26	−0.32
				−5.39	−0.45
				−5.52	−0.58
				−5.52	−0.58

Table 2. Field data (probe result and water analysis) from South Drain canal and the results from the analysis of carbonate material from *Viviparus contectus* collected from the cage experiments

Date	pH	Salinity (ppt)	Probe temp. (°C)	$\delta^{18}O_{water}$ (‰ VSMOW)	$\delta^{18}O_{carb.}$ (‰ VPDB)
03/04/2008	7.80	0.40	11.60	−5.17	−3.63
					−3.45
					−3.43
					−3.39
					−3.52
					−3.37
					−3.49
					−3.32
					−3.32
25/04/2008	8.07	0.40	13.50	−4.90	−4.00
					−3.87
					−3.62
					−3.64
					−4.26
06/06/2008	7.64	0.30	17.40	−5.24	−3.73
					−4.79
					−4.55
					−4.48
					−4.74
					−3.98
					−4.29
					−4.37
					−4.01
					−4.81
					−4.17
					−4.36
					−4.53
					−4.57
					−3.92
					−5.02
					−4.38
					−4.28
					−4.63
					−4.45
					−4.56
					−3.73
					−4.77
					−4.22
					−4.79
					−3.81
					−4.03

(*Continues*)

DOI: 10.1002/rcm

Table 2. (Continued)

Date	pH	Salinity (ppt)	Probe temp. (°C)	$\delta^{18}O_{water}$ (‰ VSMOW)	$\delta^{18}O_{carb.}$ (‰ VPDB)
					−4.02
					−4.55
					−4.49
					−4.58
					−4.70
					−4.48
					−4.69
					−4.75
					−4.51
					−4.17
03/07/2008	7.74	0.30	19.60	−5.24	−4.89
					−4.97
					−4.95
					−5.04
					−4.90
					−5.04
					−5.15
					−5.10
					−5.17
					−4.87
					−5.09
					−5.00
					−4.86
					−4.97
					−4.85
					−4.76
					−4.72
					−4.84
					−4.68
					−4.92
					−4.45
					−5.05
					−4.97
					−4.97
13/08/2008	7.33	0.30	16.90	−4.23	−3.64
					−3.66
					−3.84
					−3.64
					−3.84

the monthly probe readings. Evidence suggests that the temperature range is influenced by the length of time between temperature collections. For example, between 25/4/2008 and 6/6/2008 (42 days) the temperature was measured as 12.85°C and 15.05°C giving a ~2°C difference. Between 3/4/2008 and 25/4/2008 (22 days), however, the temperature varied between 12.00°C and 13.70°C, a difference of 1.7°C. South Drain Canal had a range of $\delta^{18}O_{water}$ over the entire sampling period of 1.94‰. The difference in the duration of time between visits also has an impact on the $\delta^{18}O_{water}$ values. For example, between 25/4/2008 and 6/6/2008 (42 days) the $\delta^{18}O_{water}$ varied between −4.80‰ and −5.67‰, a difference of 0.87‰, whereas between 3/4/2008 and 25/4/2008 (22 days) the $\delta^{18}O_{water}$ varied between −5.00‰ and −4.80‰, a difference of 0.20‰. These two parameters (temperature and $\delta^{18}O_{water}$) are important for the formulation of the thermometry equation. Owing to variability within the natural environment, the temperature and $\delta^{18}O_{water}$ are not as well constrained as those obtained for the laboratory culturing method. Production of the field-based *V. contectus* thermometry equation involved establishing average probe temperatures and $\delta^{18}O_{water}$ values between successive sampling trips (e.g. between 6/6/2008 and 3/7/2008 and between 3/7/2008 and 13/8/2008).

Field cage experiment

For the field cage experiment the temperature dependence of the fractionation factor (α), between 8.2 and 19.6°C, is given by Eqn. (7):

$$1000 \ln \alpha = 13.29(\pm 1.06) * (1000T^{-1}) - 15.35(\pm 3.69) \quad (r^2 = 0.67) \tag{7}$$

where T is in Kelvin, and the relationship between $\Delta\delta^{18}O$ and temperature is given by Eqns. (8) and (9):

$$\Delta\delta^{18}O = -0.16(\pm 0.02) * \text{Temp.} + 3.25(\pm 0.40) \tag{8}$$

This rearranges to:

$$\text{Temp.}(^{\circ}C) = -6.22(+0.86, -1.18) * \Delta\delta^{18}O + 20.75(\pm 2.47) \quad \text{(Fig. 2(B))} \tag{9}$$

The relationship between $\Delta\delta^{18}O$ and temperature shows a good statistical regression ($r^2 = 0.67$) (Fig. 2(B)).

DOI: 10.1002/rcm

Table 3. Field data (probe result and water analysis) from South Drain Canal and the results from the analysis of carbonate material from *Viviparus contectus* collected from the field

Date	pH	Salinity (ppt)	Probe temp. (°C)	$\delta^{18}O_{water}$ (‰ VSMOW)	$\delta^{18}O_{carb.}$ (‰ VPDB)
03/08/2007	7.85	0.20	19.90	−3.87	−4.04
					−4.20
					−4.15
					−3.65
31/10/2007	7.84	0.40	11.10	−4.27	−3.77
					−4.13
					−4.18
					−3.69
22/01/2008	7.60	0.30	8.20	−5.81	−3.56
					−3.15
					−3.09
					−4.31
					−5.11
					−4.77
02/09/2008	7.88	0.40	8.60	−5.33	−3.41
					−3.81
					−3.81
					−4.06
					−3.60
03/04/2008	7.80	0.40	11.60	−5.00	−3.47
					−4.44
					−3.16
					−3.18
					−3.33
25/04/2008	8.07	0.40	13.50	−4.80	−3.09
					−3.50
					−3.10
					−4.89
					−5.26
06/06/2008	7.64	0.30	17.40	−5.67	−3.94
					−5.17
					−4.80
					−4.45
					−4.46
03/07/2008	7.74	0.30	19.60	−4.80	−4.62
					−4.63
					−4.69
					−4.07
					−3.46
13/08/2008	7.33	0.30	17.10	−4.23	−3.59
					−3.65
					−3.63

Field collection

For the field collection experiment the temperature dependence of the fractionation factor (α), between 8.2 and 19.6 °C, is given by Eqn. (10):

$$1000 \ln \alpha = 9.72(\pm 1.73) * (1000 T^{-1}) - 3.01(\pm 6.04) \quad (r^2 = 0.44) \tag{10}$$

where T is in Kelvin, and the relationship between $\Delta\delta^{18}O$ and temperature is given by Eqns. (11) and (12):

$$\Delta\delta^{18}O = -0.12(\pm 0.04) * \text{Temp.} + 2.55(\pm 0.60) \tag{11}$$

This rearranges to:

$$\text{Temp.}(^{\circ}C) = -8.48(+2.22, -4.67) * \Delta\delta^{18}O + 22.00(\pm 5.15) \quad \text{(Fig. 2(C))} \tag{12}$$

The equation produced by the field collection method shows a relatively poor statistical regression ($r^2 = 0.44$) in contrast to the tank and field cage experiments (Fig. 2(C)).

Combined equation

The regression analysis indicates that the values of the gradients for all three experiments lie within 2 times the standard error of each other. Therefore, a combined correlation using all three datasets is justifiable.

For the combined dataset (laboratory, field cage and field collection) the temperature dependence of the fractionation factor (α), between 8.2 and 25.0 °C, is given by Eqn. (13):

$$1000 \ln \alpha = 9.72(\pm 1.73) * (1000 T^{-1}) - 3.01(\pm 6.04) \quad (r^2 = 0.63) \tag{13}$$

where T is in Kelvin, and the relationship between $\Delta\delta^{18}O$ and temperature is given by Eqns. (14) and (15):

$$\Delta\delta^{18}O = -0.13(\pm 0.02) * \text{Temp.} + 2.81(\pm 0.28) \tag{14}$$

DOI: 10.1002/rcm

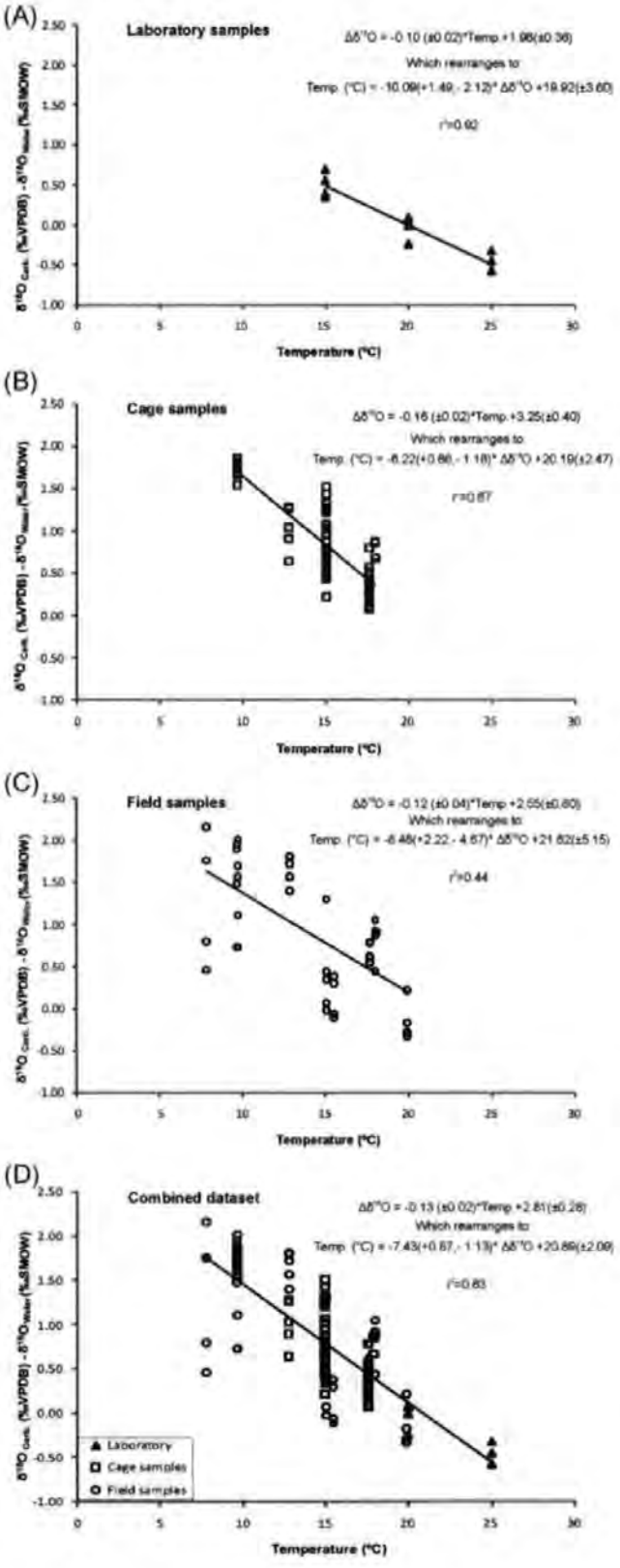

Figure 2. The relationships between temperature and $\Delta\delta^{18}O$ ($\delta^{18}O_{carb.} - \delta^{18}O_{water}$) for *Viviparus contectus* specimens from the tank experiments (A) and specimens from the cage (B) and field (C) experiments at South Drain Canal on the Somerset Levels. (D) Relationship between temperature and $\Delta\delta^{18}O$ ($\delta^{18}O_{carb.} - \delta^{18}O_{water}$) for the combined dataset (laboratory, field cage and field collection).

This rearranges to:

$$\text{Temp.}(^{\circ}\text{C}) = -7.43(+0.87, -1.13) * \Delta\delta^{18}\text{O} + 20.89(\pm 2.09) \quad \text{(Fig. 2(D))} \quad (15)$$

The relationship between $\Delta\delta^{18}O$ and temperature shows relatively good statistical regression ($r^2 = 0.63$) (Fig. 2(D)).

Temperature versus $\delta^{18}O$ water, seasonal profiles and $\delta^{13}C$ uptake

Temperature vs. $\delta^{18}O$ water

The $\delta^{18}O_{water}$ and $\delta^{2}H_{water}$ results from the analysis of water samples collected from South Drain Canal plot along a local evaporation line (LEL), which deviates away from the global meteoric water line (GMWL) (Fig. 3). The data points exhibiting the greatest deviation are not associated with the warmest temperatures nor do they systematically change with the seasonal (Fig. 4 and Table 4). Comparisons made with the monthly precipitation records from Yeovilton (51°0.529′N 2°38.275′W) (Fig. 4), the closest Meteorological Office monitoring station to our field site, illustrates that the samples deviating furthest from the GMWL were collected after a period of low average monthly precipitation (Fig. 4). In particular, reference is made to the samples collected on 29/2/2008 and 6/6/2008.

Seasonal profiles

Three *V. contectus* specimens grown within the field cage experiment were drilled at high resolution to produce a detailed record of the shell $\delta^{18}O_{carb.}$ between February and August 2008 (Fig. 5(A)). A date was attributed to each drill line by calculating the average daily growth rate, using the total growth secreted during a given sampling period (as

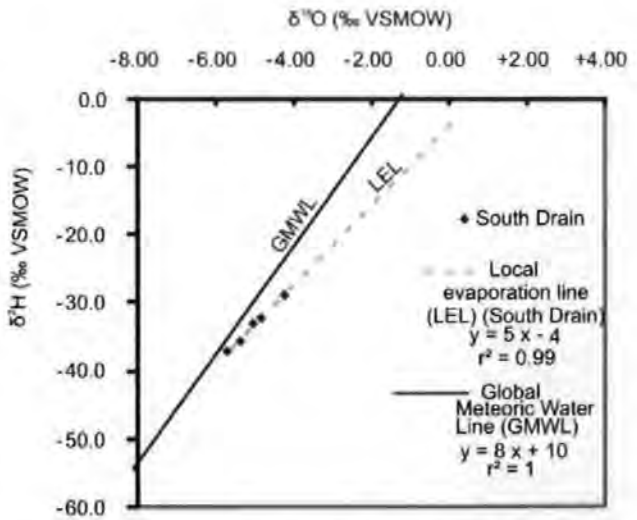

Figure 3. Comparison of the $\delta^{18}O$ (VSMOW) with the $\delta^{2}H$ (VSMOW) measured in water samples from South Drain Canal with the global meteoric water line of Craig.[39]

DOI: 10.1002/rcm

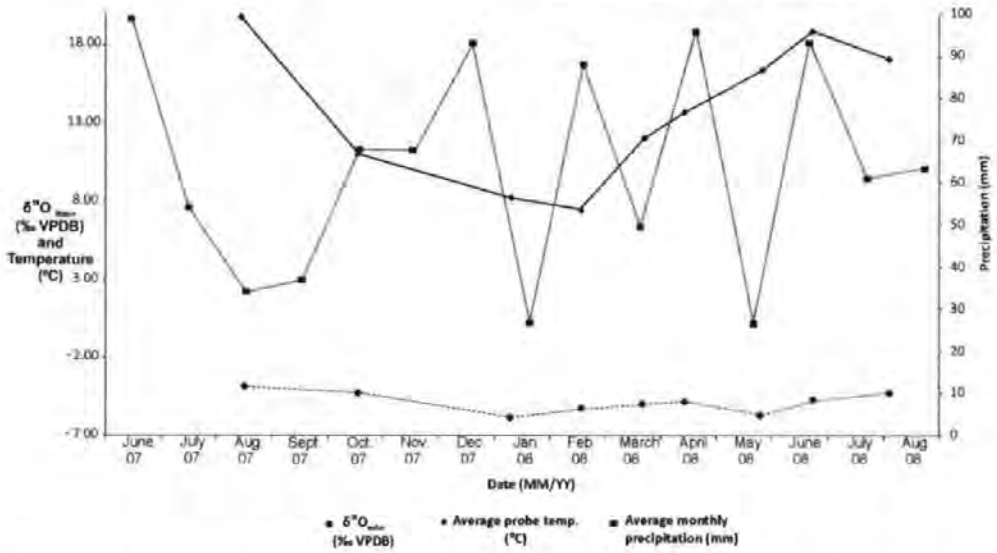

Figure 4. A comparison between the water temperatures and $\delta^{18}O$ of the canal water taken from South Drain Canal with the average monthly precipitation record from Yeovilton for 6/2007 to 9/2008.

stated in the outline of field cage methods). Due to the low resolution of the temperature and $\delta^{18}O_{water}$ data, it was not possible to determine accurate values for the individual drill lines. Therefore, the average for the time period was used.

A comparison of the $\delta^{18}O_{carb.}$ seasonality profiles from the three *V. contectus* specimens indicates that there is good isotopic reproducibility, with $\delta^{18}O_{carb.}$ co-varying throughout the experiment (Fig. 5(A)). In general the $\delta^{18}O_{carb.}$ values of the *V. contectus* profiles become progressively more negative over the duration of the experiment (−3.23‰ in February to −4.88‰ in July), indicating a total $\delta^{18}O_{carb.}$ shift of 1.65‰ between February and July 2008. However, the last two $\delta^{18}O_{carb.}$ data points of VC5 show a return to relatively positive values during August. Throughout the field cage experiment the average monthly temperatures increased from 7.40°C to 18.90°C, an overall increase of 11.50°C. The average $\delta^{18}O_{water}$ of the canal water was recorded as fluctuating between −5.57‰ and −4.51‰, a difference of 1.06‰.

Carbon ($\delta^{13}C$) uptake

Three *V. contectus* specimens grown within the field cage experiment were drilled at high resolution to produce a detailed record of the shell $\delta^{13}C_{carb.}$ between February and August 2008 (Fig. 5(B)). When the resulting $\delta^{13}C_{carb.}$ profiles from the three *V. contectus* specimens are plotted against the $\delta^{13}C_{TDIC}$ record, the observed fluctuation appear to not co-vary (Fig. 5(B)). The $\delta^{13}C$ values in the *V. contectus* specimens have an overall range of 5‰, which is significantly larger than the 3‰ range of the $\delta^{13}C_{TDIC}$. Actual values indicate that the $\delta^{13}C$ of the TDIC is within the range of the values obtained from the *V. contectus* specimens. Therefore, the sources of $\delta^{13}C$ for the secreted shell carbonate cannot be solely related to the $\delta^{13}C$ of TDIC within the water column. However, the $\delta^{13}C$ profiles of the *V. contectus* specimens show some covariance, i.e. generally increasing between February and June with a small decrease from June to August. This would suggest that the methods of uptake and/or sources of carbon influencing the final $\delta^{13}C_{carb.}$ of the shell are relatively consistent between specimens.

Table 4. $\delta^{18}O$ water, temperature and $\delta^{18}O_{carb.}$ and $\delta^{13}C_{carb.}$ for each visit to the South Drain Canal site

Location	Date (DD/MM/YY)	$\delta^{13}C_{TDIC}$ (‰ VPDB)	$\delta^{18}O_{water}$ (‰ VSMOW)	$\delta^{2}H$ (‰ VSMOW)	Temp. (°C)	$\delta^{13}C_{carb.}$ (‰ VPDB)	$\delta^{18}O_{carb.}$ (‰ VPDB)
South drain	30/08/2007		−3.87		19.90	−12.46	−3.92
South drain	31/10/2007		−4.27		11.10	−11.95	−3.85
South drain	22/01/2008		−5.81		8.20	−12.18	−3.44
South Drain	29/02/2008	−11.91	−5.33	−35.92	7.40	−12.00	−4.09
South Drain	03/04/2008	−12.90	−5.00	−33.37	12.00	−12.53	−3.66
South Drain	25/04/2008	−11.11	−4.80	−32.75	13.70	−14.57	−3.15
South Drain	06/06/2008	−14.10	−5.67	−37.48	16.40	−12.74	−4.72
South Drain	03/07/2008	−12.20	−4.80	−32.29	18.90	−11.76	−4.48
South Drain	13/08/2008	−13.50	−4.23	−29.08	17.10	−12.59	−3.59

DOI: 10.1002/rcm

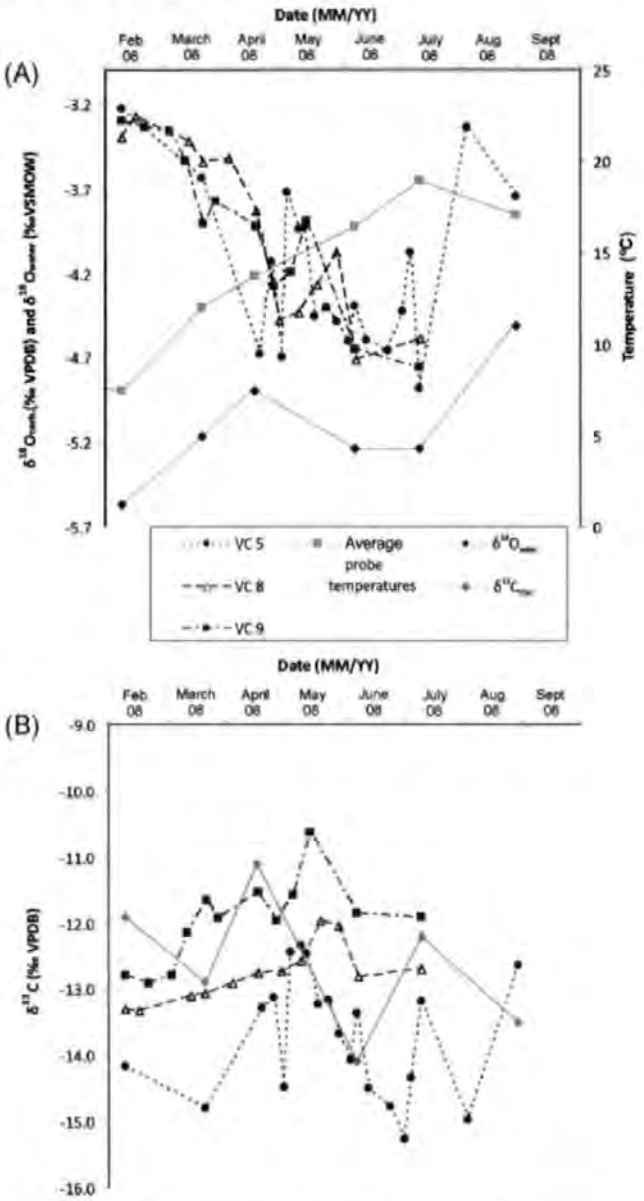

Figure 5. (A) Co-varying $\delta^{18}O_{carb.}$ relationship between the three cage specimens drilled at high resolution related to the $\delta^{18}O_{water}$ and probe temperature record from the South Drain Canal site over time. (B) Comparison of the $\delta^{13}C_{carb.}$ profiles from the three cage specimens with the $\delta^{13}C_{TDIC}$ of the water samples over time from the South Drain Canal site. For graphs A and B the open symbols for the *V. contectus* (VC) indicate that the specimen is a male and the closed symbols indicate the specimen is a female.

DISCUSSION

Issues affecting the relationship between $\delta^{18}O$ and water temperature

Laboratory culturing experiment

The linear regression ($r^2 = 0.91$) calculated for the relationship between $\Delta\delta^{18}O$ and temperature indicates that the laboratory equation is statistically the most robust of all the *V. contectus* results. This is owing to all three known variables being well constrained. However, it should be noted that the specimen growth rates were significantly slower than those within the natural environment. Specimens of a comparable size and age (e.g. those released as juveniles at the start of the experiments) in the field cage experiment secreted up to five times more carbonate per day than the laboratory specimens (Table 5). The proportion of energy allocated to growth varies with age, as a greater percentage is utilised for reproduction later in life.[30–32] Therefore, comparisons between specimens of the same age are necessary. This observed difference in growth rates could be related to a number of factors unique to the laboratory experiments including: lack of seasonal change in temperature; poor or incorrect food source; insufficient quantities of dissolved calcium carbonate; disturbance; light intensities; and pH.

Field cage experiment

The linear regression applied to determine the relationship between $\Delta\delta^{18}O$ and temperature for the field cage experiment produced a regression ($r^2 = 0.67$) that is not considered to be as statistically robust as that of the laboratory tank experiment ($r^2 = 0.92$). This is probably related to the spread of temperature and $\delta^{18}O_{water}$ data. This data could not be as well constrained owing to natural variation between sample collections. The amount of carbonate secreted by individual specimens between sampling trips was well constrained, but it was impossible to know when during the period between successive sampling trips the carbonate was secreted.

Field collection

The poor linear regression produced by the field collection experiment ($r^2 = 0.44$) was, in hindsight, inevitable. As it was not possible to determine the period of time over which the shell material that was sampled next to the aperture was secreted, it was presumed that growth had occurred at some time within the time interval between collections. As the cage experiment confirmed, differential growth rates between specimens could account for the spread of data obtained. It is probable that some specimens exhibited no carbonate secretion during the time period between sampling trips.

Combined dataset

As the linear regression output shows that the gradients of all three experiments lie within error (±2 S.E.) of each other, it is possible to combine all the datasets. A linear regression was therefore applied to the entire dataset (laboratory, field cage and field collection) in order to determine the relationship between $\Delta\delta^{18}O$ and temperature. A combined regression of 0.63 indicates a good statistical relationship between the two variables. However, this combined dataset should be treated with some caution as there is a strong overlap between the laboratory and field samples towards higher temperatures. This is probably related to how well the variables used to construct the correlations are constrained. Greater variability in the field cage and collection experiments could account for this overlap. However, it has been previously stated that the growth rates of specimens in the tank experiments were significantly lower than those from the natural environment. This slower growth rate may have influenced the oxygen isotope fractionation.

DOI: 10.1002/rcm

Table 5. Information on *Viviparus contectus* regarding the sex, whether the specimens contained eggs or juveniles and shell measurements. The measurements indicate shell secretion rates for six specimens taken from the cage experiment and six specimens from the laboratory experiments

					Shell		Aperture				
	Speciman	Tank temp. (°C)	Sex	Egg/ juveniles	Height (mm)	Width (mm)	Height (mm)	Width (mm)	Total aperture growth (mm)	Duration in Tank/Cage (days)	Growth rate per day (mm)
Cage	VC 5		Female	21 juv's	3.1	2.5	1.6	1.2	24.0	167	0.144
	VC 8		Male	—	2.5	2.0	1.3	1.1	21.0	126	0.167
	VC 9		Female	16 eggs	3.0	2.4	1.6	1.3	26.5	126	0.210
	VC 14		Male	—	1.9	1.8	1.1	0.9	3.0	110	0.027
	VC 26		Female	—	1.5	1.3	0.8	0.7	2.0	28	0.071
	VC 27		Female	—	1.5	1.4	0.9	0.8	3.0	28	0.107
Laboratory	VC 3	15	Male	—	1.7	1.5	1.0	0.8	0.9	48	0.019
	VC 7		Male	—	1.4	1.2	0.8	0.7	0.5	48	0.010
	VC 6	20	Female	—	1.3	1.3	0.9	0.8	0.9	48	0.019
	VC 3		Female	—	1.7	1.5	1.0	0.8	0.8	48	0.017
	VC 5	25	Female	—	1.8	1.6	1.1	0.9	1.2	48	0.025
	VC 6		Female	—	1.5	1.4	0.9	0.8	2.0	48	0.042

Temperature versus $\delta^{18}O$ water

Several of the $\delta^{18}O_{water}$ values obtained from samples collected from the South Drain Canal appear to have been affected by the amount of precipitation within the local area. Although it is unclear from the $\delta^{18}O$ of the canal water, some of this variation may be related to seasonal changes in the $\delta^{18}O$ of precipitation. Other influential factors are wind (e.g. high winds enhance evaporation) and humidity (high humidity would reduce evaporation); these two factors are regarded to be two of the biggest drivers of evaporation. However, there is also a land management issue. The highly managed drainage system of the Somerset Levels is likely to be responsible in part for periods of enhanced evaporation. Owing to the low elevation of the Somerset Levels, water is diverted or pumped out to sea during periods of high rainfall to prevent flooding of agricultural land. This allows a rapid recycling of water, causing the isotopic composition to be close to the GMWL. However, in periods of low rainfall, pumping ceases and water is retained to prevent the Somerset Levels from drying out. This increases the water residence times and, in turn, enables greater evaporative effects on the isotopic composition of the water. The effect of land management is, however, speculative as no data can be presented to test this hypothesis. Nevertheless, when periods of low precipitation and relatively high temperature coincide, as for the period prior to water sampling on 6/6/2008, the isotopic composition of the South Drain Canal water deviates furthest from the GMWL. This deviation does not affect the field collection and field cage data equations as these events tend to be short lived. Their effects on shell $\delta^{18}O_{carb}$ are, therefore, concealed by time averaging within the carbonate shell material, but they could be the source of some error.

Seasonality profiles

The seasonal profiles demonstrate the relationship between the $\delta^{18}O$ of the shell carbonate and water temperature, with the $\delta^{18}O$ of the shell carbonate becoming negative with increasing temperature (Fig. 5(A)). It would therefore appear that the $\delta^{18}O$ of the shell carbonate is in equilibrium with the $\delta^{18}O$ of the host water. Over the time period encompassed by the cage experiments, the temperature varied between 7 °C and 20 °C (~13 °C difference) and $\delta^{18}O_{carb}$ between −3.23‰ and −4.88‰ (1.65‰ difference) indicating a ~0.1‰ change per °C. In the majority of samples temperature appears to be the dominant factor determining $\delta^{18}O_{carb}$ of the shell carbonate. This does not, however, apply to the penultimate data point (13/8/2008) analysed for VC 5, where the isotopic composition of the water appears to have a greater influence on the $\delta^{18}O$ of the shell carbonate (Fig. 5(A)).

Does sexual dimorphism or fecundity affect the oxygen isotope fractionation?

The genus *Viviparus* has separate male and female forms, whereas many other gastropods are hermaphrodite, which could have implications for carbonate secretion. However, sex can only be determined by the snail's soft part anatomy, which could only be preserved in cases of exceptional preservation within the fossil record (we are not aware of any known for fossil *Viviparus* specimens). Sexual dimorphism also exists, with females tending to be larger than males after sexual maturity. Nevertheless, neither of these diagnostic features can easily be determined in the fossil record. Reproductive activity in modern specimens is determined by the presence of juveniles or eggs (which also will only be found in exceptionally preserved fossil specimens), which would be hard to determine in incomplete or compacted fossils or where soft part decay and transport have resulted in the loss of juveniles from the adult shell. However, the isotopic profiles of the cage specimens show that the $\delta^{18}O$ of the shell carbonate secretion does not appear to be influenced by size, sex or whether females contain eggs or juveniles (Fig. 5(A)). As these potential vital effects appear to have no influence on oxygen isotope fractionation, the *V. contectus* thermometry equation can readily be applied to the fossil record.

Factors influencing $\delta^{13}C$ values

The range of $\delta^{13}C_{carb}$ obtained from the three *V. contectus* specimens is larger than the range of $\delta^{13}C_{TDIC}$ values. However, the low sampling resolution of the $\delta^{13}C_{TDIC}$ may not provide sufficient information on the natural variability within the South Drain Canal system. Therefore, it is impossible to determine whether the shell $\delta^{13}C_{carb}$ and

DOI: 10.1002/rcm

$\delta^{13}C_{TDIC}$ are in equilibrium. Controls on the $\delta^{13}C_{TDIC}$ of the host water include changes in lake residence time, vegetation cover in the catchments and lake productivity.[14] Observations indicate a substantial increase in vegetation cover while the cage experiment was taking place. This seasonal increase in aquatic plant cover would have enriched the waters in ^{13}C, as photosynthesis preferentially uptakes ^{12}C, producing higher $\delta^{13}C_{TDIC}$. If we assume that $\delta^{13}C_{TDIC}$ is the dominant source for $\delta^{13}C_{carb}$, the generally increasing $\delta^{13}C$ of the shell carbonate for the time period encompassed by the cage experiment would represent the removal of ^{12}C by photosynthesis. However, the available data suggests that metabolised carbon and the availability of carbon as a food source has some influence on the $\delta^{13}C$ of the shell carbonate. Furthermore, most Viviparids are detritivores, preferentially filter feeding on bacteria found within detritus contained in the bottom silts and mud.[19,33] In the absence of this food source, they have retained their ability to graze on algae and macrophytes.[34] The method of feeding depends on the abundance of algal growth, diatoms or bacteria which will change seasonally. Therefore, the proportion of $\delta^{13}C_{TDIC}$ and metabolic $\delta^{13}C$ may change seasonally or be related to the species life cycle, e.g. reproduction and associated migration. *Viviparus* seasonally migrate to deeper water in the autumn and back to shallower littoral areas in the spring.[25,26] This migration may influence the food sources on offer and perhaps provide a valid reason for this genus retaining a variety of feeding mechanisms. Finally, during spring the energetic cost of reproduction is greater for males than for females,[35] as females continue to feed during copulation where males do not. This would result in low growth rates during this period and therefore may not affect the $\delta^{13}C_{carb}$ of the shell.

Interestingly, the $\delta^{13}C$ values of shell carbonate from the tank experiments are similar to $\delta^{13}C_{TDIC}$ values measured from the field and field cage specimens. It was observed that the *V. contectus* specimens preferred to graze the tank sides, which were rapidly colonised by green algae, whereas they were rarely observed filter feeding or grazing on the provided food source (lettuce). It is probable that the green algal layers on the tank walls were seeded by propagules attached to the gastropod shells when initially introduced to the tanks. The $\delta^{13}C$ of TDIC, and in turn of the algae, may have been influenced by the addition of $NaHCO_3$, maintaining the TDIC values similar to those of the natural environment.

Although there is insufficient evidence to reach a sound conclusion on whether the shell $\delta^{13}C_{carb}$ and $\delta^{13}C_{TDIC}$ are in equilibrium, there is indirect evidence to suggest that carbon equilibrium may exist. Covariance between the $\delta^{13}C_{carb}$ profiles of the *V. contectus* specimens would suggest that the carbon incorporated into the shell was not substantially derived from metabolic carbon, but from the $\delta^{13}C_{TDIC}$ of the canal water.[5] McConnaughey *et al.*[36] also noted that fully aquatic, gill-breathing gastropods (such as *V. contectus*) produced shells with $\delta^{13}C$ values similar to $\delta^{13}C_{TDIC}$. They suggest that the CO_2:O_2 values are much higher in aquatic systems, resulting in greater amounts of environmental carbon being incorporated into their skeletons compared with air-breathing species. This assumes that CO_2 accompanies O_2 during exchange within the gills. Fritz and Poplawski[6] showed that aquatic gastropods reared under differing TDIC conditions had $\delta^{13}C$ values that closely resembled the isotopic composition of the TDIC rather than the food they ingested. However, the range of $\delta^{13}C$ values obtained from the shell carbonate and TDIC implies that metabolic carbon has a greater influence.

Equation comparison

In order to validate the use of the combined *V. contectus* thermometry equation a comparison was made with already established palaeothermomerty equations (Fig. 6). Our combined equation shows good agreement in the absolute magnitude of the oxygen isotope fractionation, particularly at higher temperatures, compared with the laboratory study of White *et al.*[9] and the field samples of Grossman and Ku.[7] Deviation in the cooler temperatures can be attributed to the data obtained from the field collection experiment. This portion of the data has a larger associated error due to poor constraints on temperature, $\delta^{18}O$ of the canal water and growth of the specimens. Care must also be taken when comparing this study with others due to possible difference in the fractionation factors used to produce these equations. To be fully compatible, the same aragonitic fractionation factor must have been used in all three studies. Both White *et al.*[9] and Grossman and Ku[7] provide no information on the value of the aragonite fractionation factor that they used.

Nevertheless, *V. contectus* appears to show no strong species-specific vital effects. This study appears to be in good agreement with other studies of isotope fractionation between biogenic aragonite and water covering a wide range of phyla, e.g. marine and freshwater fish otoliths, gastropoda, scaphopoda, foraminifera, bivalves, etc. (e.g.[7,9,37,38]). This would imply that any of the aragonitic equations (this study, White *et al.*[9] or Grossman and Ku[7]) could be applied to fossil specimens of the genus *Viviparus*. However, we would strongly recommend that our combined thermometry equation be used if fossil specimens of the genus *Viviparus* can be identified and if the $\delta^{18}O$ of the host water can be determined.

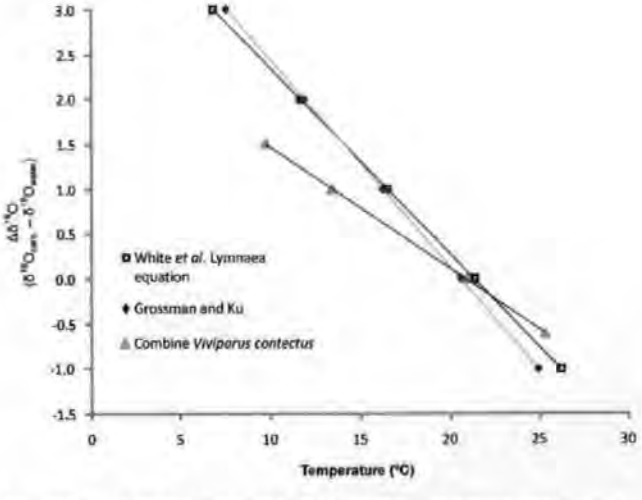

Figure 6. Graph showing the *V. contectus* equations in comparison with the White *et al.*[9] Lymnaea equation and the Grossman and Ku[7] general aragonite equation. The solid lines represent the temperature range used in the determination of the linear regression.

DOI: 10.1002/rcm

CONCLUSIONS

The results from this study indicate that *V. contectus* does not exhibit any significant species-specific vital effects when secreting shell carbonate. This species also appears to precipitate its shell in oxygen isotopic equilibrium with the host water, as the equation produced is similar within error to previously published aragonitic equations. This confirms that this species is capable of recording the combined signal of the temperature and the oxygen isotope composition of the host water. The isotope signal of the secreted shell carbonate is dominated by temperature when the $\delta^{18}O$ of the host water remains relatively constant, as indicated by the laboratory experiment and cage specimens. Seasonal isotopic profiles indicate that the uptake of $\delta^{18}O$ during shell secretion is not influenced by size, sex or whether females contain eggs or juveniles.

Acknowledgements

For assistance with field collection we are grateful to Charu Sharma, Timothy Kearsey and Laura Domingo Martinez. For help with setting up of culturing tanks, we would like to thank the Ecology technicians at Plymouth University. For their help and assistance in the analysis of isotopic samples, we would also like to thank the technical staff at NIGL. Finally, we would like to thank Jim Marshall and one anonymous reviewer whose comments greatly improved this manuscript.

REFERENCES

1. Andreasson FP, Schmitz B. *GSA Bulletin* 2001; **113**: 774.
2. Grimes ST, Hooker JJ, Collinson ME, Mattey DP. *Geology* 2005; **33**: 189.
3. Kobashi T, Grossman EL, Yancey TE, Dockery DT. *GSA* 2001; **29**: 983.
4. Harzhauser M, Latal C, Piller WE. *Palaeogeography, Palaeoclimatology, Palaeoecology* 2007; **249**: 335.
5. Jones MD, Leng MJ, Eastwood WJ, Keen DH, Turney CSM. *The Holocene* 2002; **12**: 629. DOI: 10.1191/0959683602HL564rr.
6. Fritz P, Poplawski S. *Earth Planet. Sci. Lett.* 1974; **24**: 91.
7. Grossman EL, Ku TL. *Chem. Geol.* 1986; **59**: 59.
8. Leng MJ, Lamb AL, Lamb HF, Telford RJ. *J. Paleolimnol.* 1999; **21**: 97.
9. White RMP, Dennis PF, Atkinson TC. *Rapid Commun. Mass Spectrom.* 1999; **13**: 1242.
10. Shanahan TM, Pigati JS, Dettman DL. *Quade Geochim. Cosmochim. Acta* 2005; **69**: 3949. DOI: 10.1016/j.gca.2005.03.049.
11. Kim ST, Hillaire-Marcel C, Mucci A. *Geochim. Cosmochim. Acta* 2006; **70**: 5790. DOI: 10.1016/j.gca.2006.08.003.
12. Kim ST, O'Neil JR, Hillaire-Marcel C, Mucci A. *Geochim. Cosmochim. Acta* 2007; **71**: 4704. DOI: 10.1016/j.gca.2007.04.019.
13. Chacko T, Deines P. *Geochim. Cosmochim. Acta* 2008; **72**: 3642. DOI: 10.1016/j.gca.2008.06.001.
14. Leng MJ, Lamb AL, Heaton THE, Marshall JD, Wolfe BB, Jones MD, Holmes JA, Arrowsmith C. In *Isotopes in Palaeoenvironmental Research*, Leng MJ (ed). Springer: The Netherlands, 2005; 147.
15. Zeebe RE. *Geochim. Cosmochim. Acta* 1999; **63**: 2001.
16. McConnaughey TA. *Coral Reefs* 2003; **22**: 316.
17. Boycott AE. *J. Anim. Ecol.* 1936; **5**: 116.
18. Fretter V, Graham A. *J. Molluscan Stud.* 1978; **44**: 107.
19. Cook PM. *Proc. Malacological Society of London* 1949; **27**: 265.
20. Boss KJ. On the evolution of gastropods in ancient lakes. In *Pulmonates: Sytematics, Evolution and Ecology*, Fretter V, Peake J (eds). Academic Press: New York, 1978; 385–428.
21. Snails (Mollusca: Gastropoda). In *Pollution Ecology of Freshwater Invertebrates*, Harman WN (ed). Academic Press: New York, 1974; 275–312.
22. Strayer D. Freshwater mollusca. In *Freshwater Macroinvertebrates of Northeastern North America*, Peckarsky BL, Frassinet PR, Penton MA, Conklin DJ (eds). Cornell University Press: New York, 1990; 335–372.
23. Jokinen EH. *The Freshwater Snails of Connecticut Bulletin* 1983; **109**: 83.
24. Prashad B. *Memoirs of the Indian Museum* 1928; **VIII**: 153.
25. Jokinen EH. *Nautilus* 1982; **96**: 89.
26. Cheatum ER. *Trans. Am. Micro Soc.* 1934; **53**: 348.
27. Dunning R. *A History of the County of Somerset: The Poldens and the Levels, vol.* **8**: Victoria County History. 2004; 1.
28. Rundle SD, Spicer IJ, Coleman RA, Vosper J, Soane J. *Proc. R. Soc. Lond. B*, (Suppl.). 2004; **271**: S67. DOI: 10.1098/rsbl.2003.0106
29. Friedman I, O'Neil JR. Compilation of stable isotope fractionation factors of geochemical interest. In *Data of Geochemistry* (6th edn). Geological Survey, 1977; Professional Paper 440-KK.
30. Browne RA, Russell-Hunter WD. *Oecologia* 1978; **37**: 23.
31. Tashiro JS. *Am. Midland Naturalist* 1982; **107**: 133.
32. Russell-Hunter WD, Buckley DE. Actuarial bioenergetics of nonmarine molluscan productivity. In *The Mollusca*, vol. **6**, Wilbur KM (ed). Academic Press: Orlando, NewYork, London, 1983; 464–503.
33. Studier EH, Pace GL. *Comp. Biochem. Physiol. A: Mol. Integr. Physiol.* 1978; **59**: 199.
34. Dillon RT. *The Ecology of Freshwater Molluscs*. Cambridge University Press: Cambridge, 2000.
35. Ribi G, Katoh M. *Ethol. Ecol. Evolution* 1998; **10**: 383.
36. McConnaughey TA, Burdett J, Welhan JF, Paul CK. *Geochim. Cosmochim. Acta* 1997; **61**: 611.
37. Patterson WP, Smith GR, Lohmann KC. Climate Change in Continental Records, Geophysical Monograph, 1993; 78.
38. Epstein S, Buchsbaum R, Lowenstam H, Urey HC. *Geol. Soc. Am. Bull.* 1953; **64**: 1315.
39. Craig H. *Science* 1961; **133**: 1833.